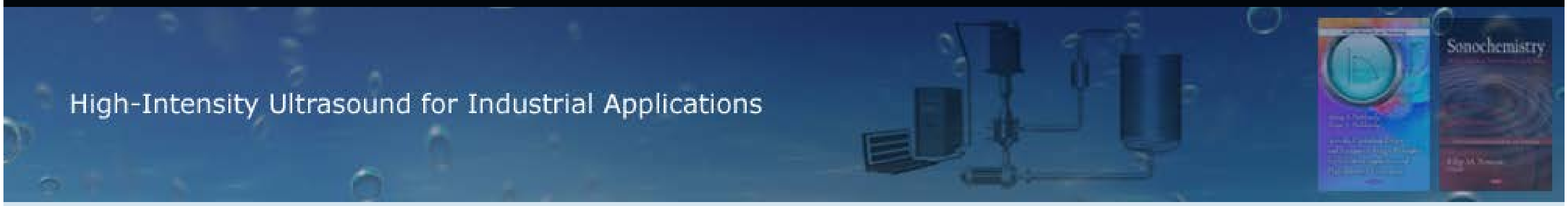

NANOCRYSTALLIZATION FOR IMPROVED DRUG DELIVERY

BACKGROUND

Up to 40% of currently available drug substances and up to 70% of those under investigation by the pharmaceutical industry exhibit poor water solubility, leading to reduced bioavailability and increased potential of adverse effects. Furthermore, fears of problems with future launch preclude many otherwise promising water-insoluble compounds from being taken beyond early R&D stages. Particle size reduction down to the nano-scale (nanocrystallization) has been shown to increase the bioavailability and reduce the required dose frequency, thereby improving patient compliance and decreasing drug side-effects.

PRODUCTION WITH HIGH-AMPLITUDE ULTRASOUND

Industrial Sonomechanics, LLC (ISM), offers bench and industrial-scale high-power ultrasonic processors for the production of nanosized drug crystals. This procedure may be called top-down ultrasonic nanocrystallization, nanomilling, wet milling, particle size reduction or nanosizing, among other names. ISM's processors are based on patented Barbell Horn Ultrasonic Technology (BHUT), which, as explained below, makes it possible to directly implement laboratory accomplishments in a production environment, guaranteeing reproducible and predictable results at any scale.

The process of ultrasonic top-down nanocrystallization requires extremely high ultrasonic amplitudes to be applied to particle suspensions producing extreme shear forces. The shear forces are the result of intense ultrasonic cavitation, which creates violently and asymmetrically imploding vacuum bubbles and causes micro-jets that break up the original drug particles down to the nano-size range. However, prior to the introduction of BHUT, none of the existing ultrasonic liquid processors could generate the required high amplitudes on the industrial scale.

Why ISM's Ultrasonic Technology?

Conventional high-power ultrasonic technology inherently forces all processes to run either at a small scale and high amplitude or a large scale and low amplitude, which is why commercial implementation of high-power ultrasound has been limited to processes for which low-amplitudes are sufficient (cleaning, simple deagglomeration, mixing, macro-emulsification, etc.). ISM has successfully overcome this limitation by developing BHUT, which permits constructing industrial-scale ultrasonic processors able to operate at extremely high amplitudes. The processors are directly scalable and can be used in the commercial production of high-quality drug nanocrystals for the pharmaceutical industry. Our equipment is compact and relatively low-cost, needs little technical support, includes very few wetted parts, generally requires no special pre-treatment of precursors, and is potentially self-sterilizing due to antibacterial properties of high-intensity ultrasound.

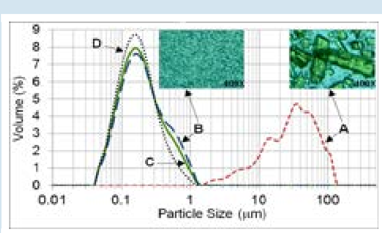

Sample	Processing	Rate (ml/min)	d(vol;0.1) (µm)	d(vol;0.5) (µm)	d(vol;0.9) (µm)
A	NONE	NA	8.090	33.29	82.71
B	CH	0.84	0.088	0.203	0.625
C	FBH	4.2	0.085	0.191	0.554
D	C, filtered	4.2	0.083	0.176	0.421

Examples of Produced Drug Nanocrystals

The experiments were conducted using ISM's 1200 W bench-scale flow-through ultrasonic processor equipped with a piezoelectric transducer, flow-through reactor chamber and either a Common Horn (CH) with the output tip diameter of 15.7 mm or a Full-wave Barbell Horn (FBH) with the output tip diameter of 35 mm. A 100 ml beaker, used in conjunction with the CH, was placed into an ice bath. The FBH was used with a water-cooled jacketed 500 ml beaker. Both horns operated at the ultrasonic amplitude of 100 μ_{pp}. Nifedipine was chosen as the model drug for this study because it has very poor water solubility and is composed of hard, difficult to fracture crystals.

Nifedipine powder was stirred into aqueous solution of HPMC surfactant. The initial mixture (sample **A**) was split into a 50 ml and a 250 ml volumes, which were processed for 90 min using the CH (sample **B**) and the FBH (sample **C**), resulting in processing rates of 0.84 ml/min and 4.2 ml/min, respectively. A portion of sample **C** was passed through a 450 nm filter (sample **D**). The data demonstrates that high-intensity ultrasound exposure yields very small nifedipine nanocrystals, with d(vol;0.5)<200 nm. FBH permitted processing 5 times more material per unit of time than CH, demonstrating direct scalability of the BHUT-based nanocrystallization process. No pre-processing of precursor materials was required. The obtained nanosuspension was able to pass through the 450 nm filter almost unperturbed, which is essential for the post-processing effectiveness, resulting in efficient decontamination and sterilization.

Ultrasound is a simple and effective technique for producing drug nanocrystals. With the use of BHUT, the process is directly scalable, making it possible to implement laboratory accomplishments in an industrial production environment.

The data presented above was collected in collaboration with Allied Innovative Systems, LLC (ALLIS).

Sitemap Contact Us

Home About ISM Technology Services Ultrasonic Systems Applications Technical Resources

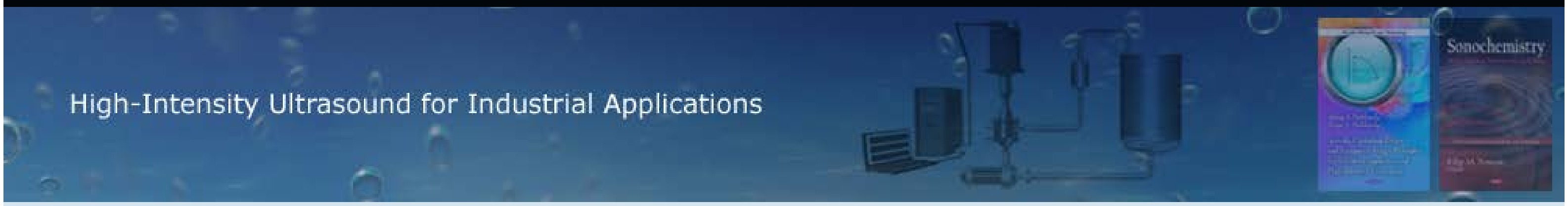

Home → Applications

APPLICATIONS

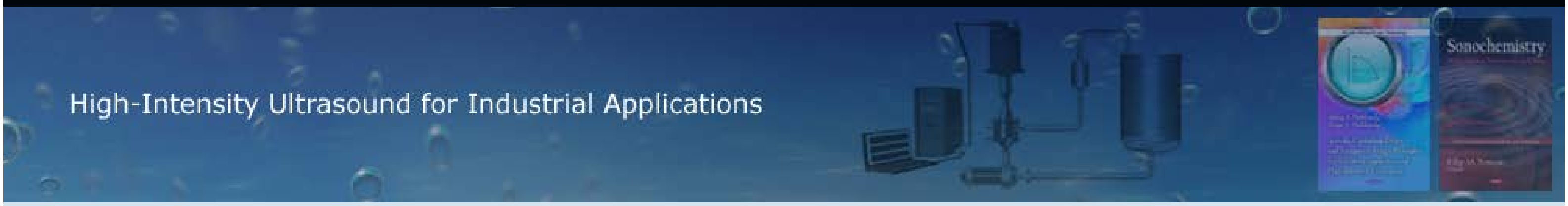

PHARMACEUTICAL

BACKGROUND

Pharmaceutical companies are under constant pressure to develop new, more effective drug formulations and improve their existing products. At the same time, there is continuous struggle in the industry to maintain commercial viability and reduce time-to-market. It is now generally recognized that nanocrystal, nanoemulsion and liposome-based formulations utilized as drug delivery platforms can provide very effective novel therapies and enhance existing product lines, while reducing costs and improving safety margins.

PRODUCTION WITH HIGH-AMPLITUDE ULTRASOUND

The formation of nanocrystals, nanoemulsions and liposomes requires intense shear forces and significant energy deposition in order to break the original particles down to the nanometer scale. Industrial Sonomechanics, LLC (ISM), offers bench and industrial-scale high-power ultrasonic processors for the production of nanocrystals, nanoemulsions and liposomes. The processors are based on our patented Barbell Horn Ultrasonic Technology (BHUT), which, as explained below, makes it possible to directly implement laboratory accomplishments in a production environment, guaranteeing reproducible and predictable results at any scale.

Very high ultrasonic vibration amplitudes are required for efficient particle size reduction. The necessary shear forces are created by ultrasonic cavitation, which produces violently and asymmetrically imploding vacuum bubbles and causes micro-jets that disperse and break up the particles down to the nanometer scale. Known for many decades, this effect of high-amplitude ultrasound has been extensively studied and successfully used in laboratory-scale research. However, prior to the introduction of BHUT, none of the existing ultrasonic liquid processors could generate the required amplitudes on the industrial scale. Commercial implementation of high-power ultrasound has, therefore, been limited to processes for which low-amplitudes are sufficient (cleaning, simple deagglomeration, mixing, macro-emulsification, etc.).

WHY ISM ULTRASONIC TECHNOLOGY?

Conventional high-power ultrasonic technology inherently forces all processes to run either at a small scale and high amplitude or a large scale and low amplitude. ISM has successfully overcome this limitation by developing BHUT, which permits constructing industrial-scale ultrasonic processors able to operate at extremely high amplitudes. The processors are directly scalable and can be used in the commercial production of high-quality nanocrystals, nanoemulsions and liposomes for the pharmaceutical industry. Our equipment is compact and relatively low-cost, needs little technical support, includes very few wetted parts, generally requires no special pre-treatment of precursors, and is potentially self-sterilizing due to antibacterial properties of high-intensity ultrasound.

Please follow the links at the top right of this page for specific examples of pharmaceutical nanomaterials produced using our high-power ultrasonic processors.

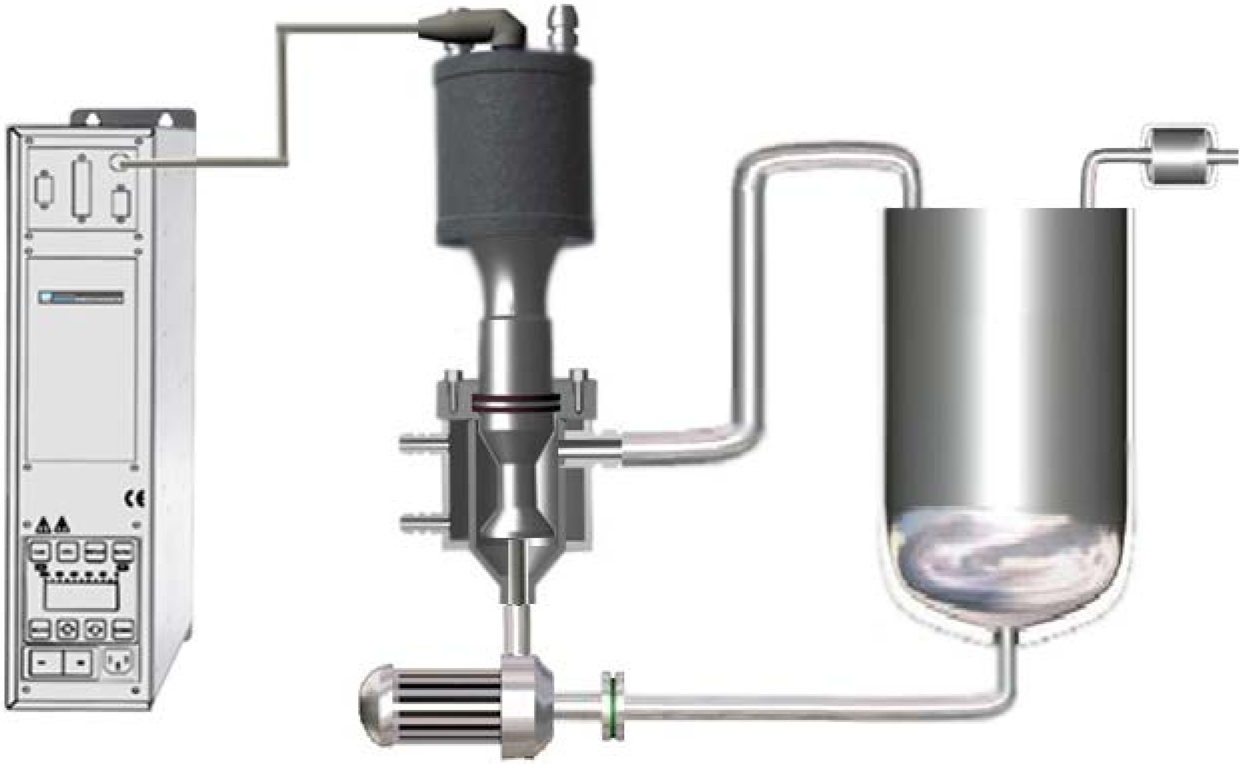

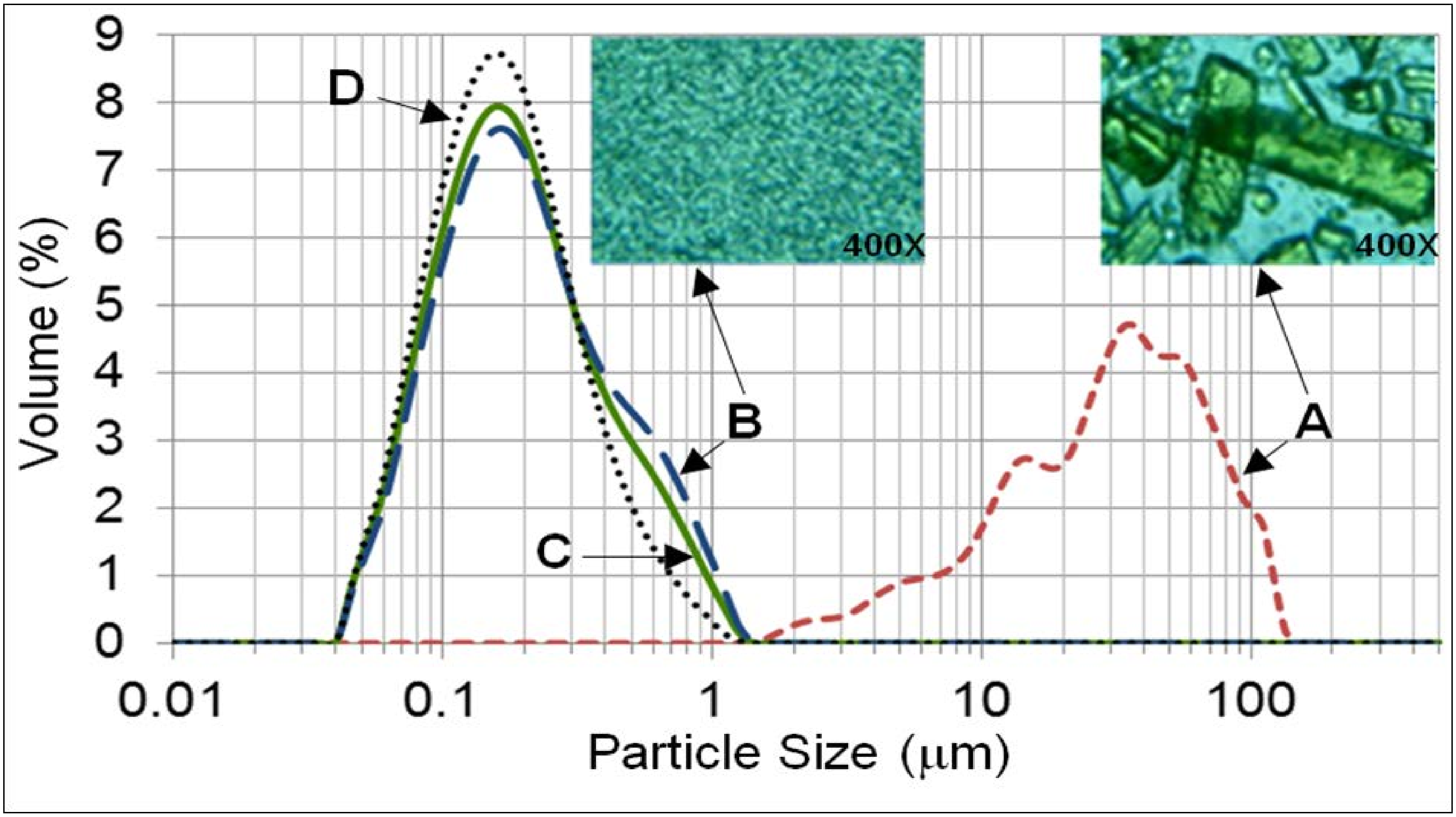

Volume (%)
Particle Size (μm)
0.01
0.1
1
10
100
0
1
2
3
4
5
6
7
8
9
A
B
C
D
400X
400X

Sample	Processing	Rate (ml/min)	d(vol;0.1) (μm)	d(vol;0.5) (μm)	d(vol;0.9) (μm)
A	NONE	NA	8.090	33.29	82.71
B	CH	0.84	0.088	0.203	0.625
C	FBH	4.2	0.085	0.191	0.554
D	**C**, filtered	4.2	0.083	0.176	0.421

Sitemap Contact Us

Home | About ISM | Technology | Services | Ultrasonic Systems | Applications | Technical Resources

- **ULTRASONIC SYSTEMS**
- **PROCESS CONSULTING**

ISM offers bench and commercial-scale ultrasonic liquid processors, homogenizers, wet milling systems and sonochemical reactors able to provide very high ultrasonic cavitation intensities and processing rates. Application examples include: production of nanoemulsions, nanocrystals and wax nanoparticles for pharmaceutical, cosmetic, food, ink, paint, coating, wood treatment, metalworking, nanocomposite, pesticide, and fuel industries, extraction of oil from algae, production of biofuels, crude oil desulphurization, degassing, cell disruption, polymer and epoxy processing, and more.

High ultrasonic amplitudes able to generate intense acoustic cavitation are required for most processes. Unlike conventional ultrasonic devices, ISM's patented Barbell horn-based ultrasonic systems make it possible to produce extremely high ultrasonic amplitudes at any scale, from laboratory to industrial, guaranteeing reproducible results after scale-up. Our experienced consultants will be glad to help optimize your process and implement it in your production environment.


Ultrasonic Dispersion of Carbon Black in Water, 750 ml Batch


Ultrasonic Degassing of Heavy Industrial Gear Oil


Ultrasonic Removal of Air Bubbles from Epoxy Resin

Ultrasonic Cavitation in Water Produced by FBH, tip Ø = 75 mm

479 W 146 Street, Ground Floor, New York, NY 10031 - 1.646.580.HORN (1.646.580.4676)

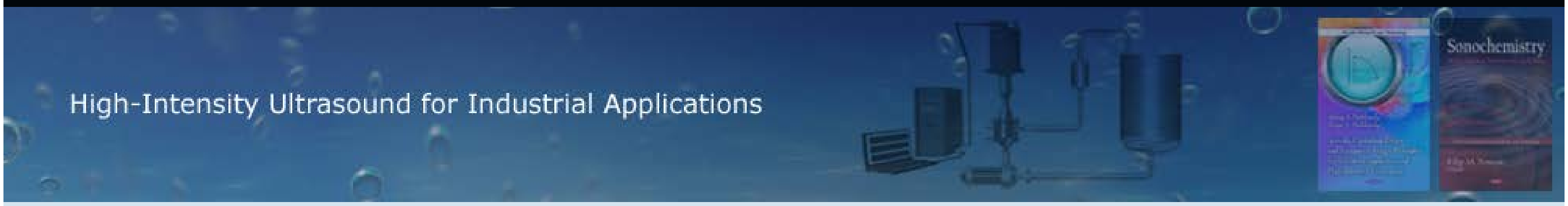

ULTRASONIC SYSTEMS

- High-Efficiency Ultrasonic Liquid Processors
  - 1200 W Processor with Air-Cooled Transducer
  - 2400 W Processor with Air-Cooled Transducer
- Special-Request Ultrasonic Liquid Processors
  - 1000 W Processor with Water-Cooled Transducer
  - 2000 W Processor with Water-Cooled Transducer

OVERVIEW

Industrial Sonomechanics, LLC, (ISM) offers bench and commercial-scale ultrasonic liquid processors (also known as ultrasonic homogenizers and sonochemical reactors) able to provide very high ultrasonic amplitudes and cavitation intensities. Application examples include: production of nanoemulsions, nanocrystals and wax nanoparticles for pharmaceutical, cosmetic, food, ink, paint, coating, wood treatment, metalworking, nanocomposite, pesticide, and fuel industries, extraction of oil from algae, production of biofuels, crude oil desulphurization, degassing, cell disruption, polymer and epoxy processing, and more.

ISM's ultrasonic processors are based on Barbell Horn Ultrasonic Technology (BHUT), which makes it possible to implement high-amplitude ultrasound on any scale, form laboratory to industrial, guaranteeing reproducible and predictable results. The processors utilize patented ultrasonic reactor chambers and provide very uniform ultrasonic treatment with no bypass.

HIGH-EFFICIENCY ULTRASONIC LIQUID PROCESSORS

1200 W Processor with Air-Cooled Transducer

1200 W bench-scale ultrasonic processor system is designed for batch and flow-through process investigations and small-scale production. The system operates at the frequency of approximately 20 kHz. Barbell horns used in this system have output tip diameters of up to 35 mm and can provide stable operation at output amplitudes up to 120 microns in aqueous loads at a normal pressure, corresponding to acoustic power intensities up to 80 W/cm^2. This gives investigators a wide range of experimental conditions to determine optimal parameters for even the most challenging ultrasonic processes. The system can be used for small-scale production.

2400 W Processor with Air-Cooled Transducer

2400 W industrial-scale ultrasonic processor system is designed for high-volume continuous-mode commercial production. The system operates at the frequency of approximately 20 kHz. Barbell horns used in this system have large output tip diameters (Ø) and provide very high output amplitudes (A) and output power densities (Pd). For example, for FBH-type horns the following combinations are possible (water up to the nodal point, at 1 bar and 25 ºC):

Ø = 50 mm, A = 120 microns, Pd = 80 W/cm^2;
Ø = 60 mm, A = 85 microns, Pd = 55 W/cm^2;
Ø = 70 mm, A = 60 microns, Pd = 35 W/cm^2.

Other types of Barbell horns can be used as well. These amplitudes and power densities are extremely high and are unprecedented for industrial-scale systems, which are commonly restricted to ultrasonic amplitudes below 25 microns and power densities below 10 W/cm^2. ISM's Barbell Horn Ultrasonic Technology (BHUT) utilized in this processor makes it possible to implement even the most challenging ultrasonic processes in the commercial environment.

SPECIAL-REQUEST ULTRASONIC LIQUID PROCESSORS

1000 W Processor with Water-Cooled Transducer

1000 W (output power) bench-top water-cooled ultrasonic system is a "special request" unit, designed for batch and flow-through process investigations and small-scale production. The system operates at the frequency of approximately 22 kHz. FBH-type Barbell horns used in this system have output tip diameters up to 35 mm and can provide stable operation at output amplitudes up to 75 microns in aqueous loads at a normal pressure, corresponding to acoustic power intensities up to 50 W/cm^2. The system is based on a water-cooled magnetostrictive transducer.

2000 W Processor with Water-Cooled Transducer

2000 W (output power) industrial water-cooled ultrasonic system is a "special request" unit, designed for flow-through or batch production on a commercial scale. The system operates at the frequency of approximately 18 kHz. FBH-type Barbell horns used in this system have output tip diameters of 60 mm, with larger diameters (up to 75 mm) available upon request. These horns can provide stable operation at output amplitudes up to 85 microns in aqueous loads at a normal pressure, corresponding to acoustic power intensities up to 55 W/cm^2. The system is able to directly reproduce any laboratory or bench-scale process optimization study in a commercial production environment and is based on a water-cooled magnetostrictive transducer.

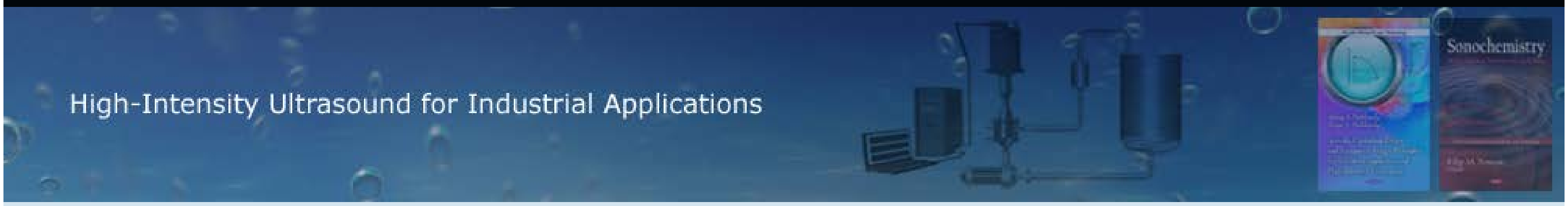

INTELLECTUAL PROPERTY

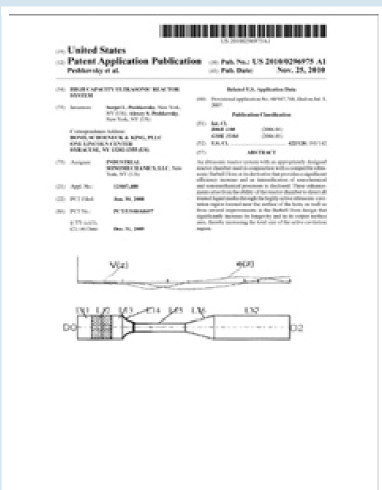

HIGH CAPACITY ULTRASONIC REACTOR SYSTEM

International Application No.: PCT/US2008/068697, International Filing Date: 30.06.2008
Sergei Peshkovsky, Alexey Peshkovsky

Abstract

An ultrasonic reactor system with an appropriately designed reactor chamber used in conjunction with a compatible ultrasonic Barbell Horn or its derivative that provides a significant efficiency increase and an intensification of sonochemical and sonomechanical processes is disclosed. These enhancements arise from the ability of the reactor chamber to direct all treated liquid media through the highly active ultrasonic cavitation region located near the surface of the horn, as well as from several improvements in the Barbell Horn design that significantly increase its longevity and in its output surface area, thereby increasing the total size of the active cavitation region.

Complete document is available in PDF format:

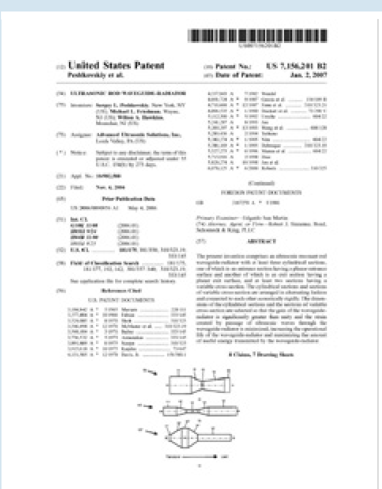

ULTRASONIC ROD WAVEGUIDE-RADIATOR

United States Patent #7,156,201, January 2, 2007
Sergey Peshkovskiy, Michael Friedman, Wilton Hawkins

Abstract

The present invention comprises an ultrasonic resonant rod waveguide-radiator with at least three cylindrical sections, one of which is an entrance section having a planar entrance surface and another of which is an exit section having a planar exit surface, and at least two sections having a variable cross-section. The cylindrical sections and sections of variable cross-section are arranged in alternating fashion and connected to each other acoustically rigidly. The dimensions of the cylindrical sections and the sections of variable cross-section are selected so that the gain of the waveguide-radiator is significantly greater than unity and the strain created by passage of ultrasonic waves through the waveguide-radiator is minimized, increasing the operational life of the waveguide-radiator and maximizing the amount of useful energy transmitted by the waveguide-radiator.

Complete document is available in PDF format:

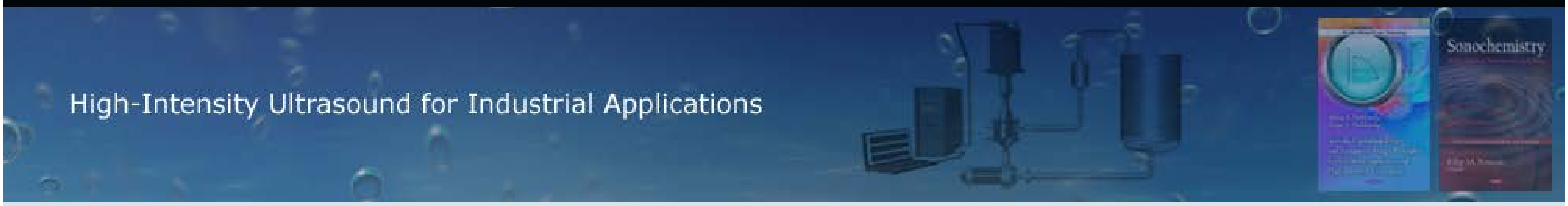

BARBELL HORN ULTRASONIC TECHNOLOGY

INTRODUCTION TO BARBELL HORN ULTRASONIC TECHNOLOGY

Industrial Sonomechanics , LLC (ISM), specializes in high-capacity commercial-scale ultrasonic homogenizers adapted to many industrial processes. In addition, ISM provides laboratory and bench-scale ultrasonic systems which can be used to study processes before they are scaled up or for semi-industrial scale production. As described below, several unique features of ISM's patented Barbell Horn Ultrasonic Technology (BHUT) make it possible to directly transfer what can be accomplished in the laboratory to the plant floor, guaranteeing reproducible and predictable results at any scale.

Advantages of High Ultrasonic Amplitudes

Liquids exposed to high-intensity ultrasound undergo ultrasonic cavitation, which produces violently and asymmetrically imploding bubbles and causes micro-jets that create extreme mechanical shear forces. These forces are responsible for the well-known ability of ultrasound to tremendously facilitate many physical and chemical processes. Ultrasonic amplitudes on the order of 100 microns peak-to-peak (below, "microns") are commonly necessary in order to take full advantage of this effect. At low amplitudes (below about 50 microns), the intensity of ultrasonic cavitation is insufficient for many processes. For example, such processes as nano-crystallization, nano-emulsification, deagglomeration, extraction, as well as many others, are inefficient or do not occur at low amplitudes. In order to produce sufficient cavitation intensity, ultrasonic transducers (sometimes also called "converters") are equipped with high-gain acoustic horns (sometimes also called "sonotrodes" or, together with transducers, "probes"), which amplify the vibration amplitudes generated by the transducers and deliver the ultrasonic energy to working liquids.

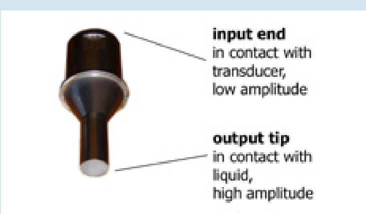

Converging Horns - Main Limitation of Conventional Ultrasonic Technology

Conventional ultrasonic systems utilize acoustic horns that converge in the output direction and are restricted to having small output tip diameters in order to provide high amplitudes. Converging horns are excellent for studying processes on a laboratory scale, but they make it impossible to transfer the processes to an industrial scale. Process scale-up requires switching to horns with larger output tip diameters, able to output the ultrasonic energy into larger volumes of working liquids while still maintaining high amplitudes. If, however, the output tip diameter of a conventional horn is increased, its maximum vibration amplitude necessarily becomes significantly lower.

For example, ultrasonic amplitudes on the order of 100 microns can only be reached by conventional horns when their output tip diameters do not exceed about 25 mm (laboratory scale). Conventional horns with output tip diameters of 50 mm and above (industrial scale) operate at maximum amplitude of about 25 microns, irrespective of the specified system power. Conventional ultrasonic technology, therefore, does not permit to directly transfer high-amplitude ultrasonic processes from laboratory to industrial scale, which is why numerous successful laboratory studies have never been implemented in industrial production.

Barbell Horns - Scalable High-Amplitude Ultrasound

Barbell horns, developed by ISM, are able to amplify ultrasonic amplitudes while retaining large output diameters. Barbell horns utilized in our industrial 2400 W systems can have output diameters as large as 75 mm and produce extremely high ultrasonic amplitudes, exceeding 100 microns. Our 1200 W systems designed for process optimization and medium-scale production feature Barbell horns with output tip diameters up to 35 mm, which are also able to output ultrasonic amplitudes exceeding 100 microns. Thus, Barbell horns make it possible to directly reproduce any laboratory or bench-scale process optimization study in a commercial production environment. Since the scale-up is accomplished without changing any of the optimized parameters, including the amplitude, the process is guaranteed to generate the same reproducible results on the plant floor as it does in the laboratory.

Because system productivity depends on the size of the active cavitation zone created under a horn, which is proportional to the area of the horn's output surface, productivity rates in Barbell horn-based

systems can be orders of magnitude higher than those achieved with conventional ultrasonic devices.

Different Types of Available Babell Horns - Shapes Adapted to Each Application

Barbell horns are available in different shapes and sizes. Besides Full-wave Barbell horns of the type shown above, specialized Half-wave Barbell horns and Open Barbell horns (Full and Half-wave) are available. These recently introduced horns are smaller and lighter that Full-wave Barbell horns and have shapes that, when incorporated into appropriately designed reactor chambers, ensure that no working liquid bypasses the active cavitation zone. These horns are, therefore, preferred for the tasks involving high-intensity flow-through ultrasonic processing, such as deagglomeration of solid particles, nanoemulsification and the production micronized waxes, where uniform exposure to ultrasound and the resulting narrow particle size distributions are essential. Different types of available ultrasonic horns are described here.

Sitemap Contact Us

Home About ISM Technology Services Ultrasonic Systems Applications Technical Resources

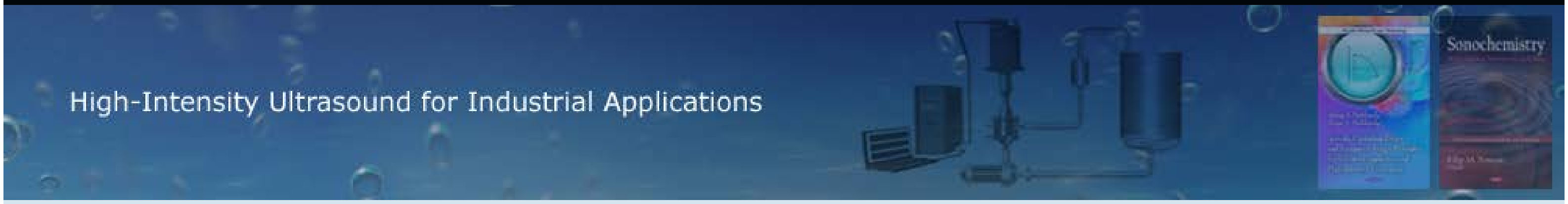

Home → Technology → Ultrasonic Liquid Processor Systems

ULTRASONIC LIQUID PROCESSOR SYSTEMS

OVERVIEW

Industrial Sonomechanics, LLC, (ISM) offers bench and commercial-scale ultrasonic liquid processors (also known as ultrasonic homogenizers and sonochemical reactors) able to provide very high ultrasonic amplitudes and cavitation intensities. Application examples include: production of nanoemulsions, nanocrystals and wax nanoparticles for pharmaceutical, cosmetic, food, ink, paint, coating, wood treatment, metalworking, nanocomposite, pesticide, and fuel industries, extraction of oil from algae, production of biofuels, crude oil desulphurization, degassing, cell disruption, polymer and epoxy processing, and more.

ISM's ultrasonic processors are based on Barbell Horn Ultrasonic Technology (BHUT), which makes it possible to implement high-amplitude ultrasound on any scale, form laboratory to industrial, guaranteeing reproducible and predictable results. The processors utilize patented ultrasonic reactor chambers and provide very uniform ultrasonic treatment with no bypass.

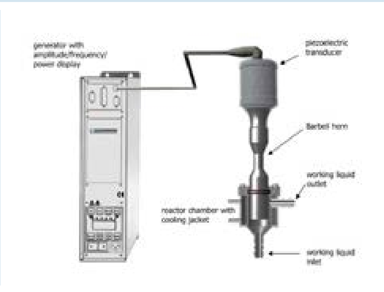

1200 W Processor with Air-Cooled Transducer

1200 W bench-scale ultrasonic processor system is designed for batch and flow-through process investigations and small-scale production. The system operates at the frequency of approximately 20 kHz. Barbell horns used in this system have output tip diameters of up to 35 mm and can provide stable operation at output amplitudes up to 120 microns peak-to-peak (below, microns) in aqueous loads at a normal pressure, corresponding to acoustic power intensities up to 80 W/cm^2. This gives investigators a wide range of experimental conditions to determine optimal parameters for even the most challenging ultrasonic processes. The system can be used for small-scale production.

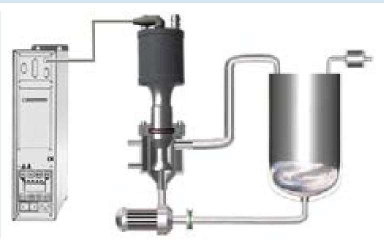

2400 W Processor with Air-Cooled Transducer

2400 W industrial-scale ultrasonic processor system is designed for high-volume continuous-mode commercial production. The system operates at the frequency of approximately 20 kHz. Barbell horns used in this system have large output tip diameters (Ø) and provide very high output amplitudes (A) and output power densities (Pd). For example, for FBH-type horns the following combinations are possible (water up to the nodal point, at 1 bar and 25 ºC):

Ø = 50 mm, A = 120 microns, Pd = 80 W/cm^2;
Ø = 60 mm, A = 85 microns, Pd = 55 W/cm^2;
Ø = 70 mm, A = 60 microns, Pd = 35 W/cm^2.

Other types of Barbell horns can be used as well. These amplitudes and power densities are extremely high and are unprecedented for industrial-scale systems, which are commonly restricted to ultrasonic amplitudes below 25 microns and power densities below 10 W/cm^2. ISM's Barbell Horn Ultrasonic Technology (BHUT) utilized in this processor makes it possible to implement even the most challenging ultrasonic processes in the commercial environment.

1000 W Processor with Water-Cooled Transducer

1000 W (output power) bench-top water-cooled ultrasonic system is a "special request" unit, designed for batch and flow-through process investigations and small-scale production. The system operates at the frequency of approximately 22 kHz. FBH-type Barbell horns used in this system have output tip diameters up to 35 mm and can provide stable operation at output amplitudes up to 75 microns in aqueous loads at a normal pressure, corresponding to acoustic power intensities up to 50 W/cm^2. The system is based on a water-cooled magnetostrictive transducer.

2000 W Processor with Water-Cooled Transducer

2000 W (output power) industrial water-cooled ultrasonic system is a "special request" unit, designed for flow-through or batch production on a commercial scale. The system operates at the frequency of approximately 18 kHz. FBH-type Barbell horns used in this system have output tip diameters of 60 mm, with larger diameters (up to 75 mm) available upon request. These horns can provide stable operation at output amplitudes up to 85 microns in aqueous loads at a normal pressure, corresponding to acoustic power intensities up to 55 W/cm^2. The system is able to directly reproduce any laboratory or bench-scale process optimization study in a commercial production environment and is based on a water-cooled magnetostrictive transducer.

The Ultrasonic Systems' design corresponds to the International Patent Application PCT/US2008/068697, "High capacity ultrasonic reactor system". The incorporated Barbell horn design corresponds to the US Patent 7,156,201, "Ultrasonic rod waveguide-radiator".

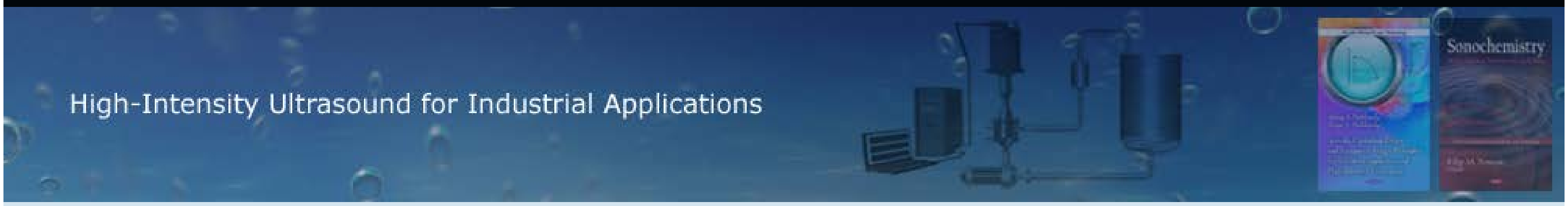

1200 W PROCESSOR WITH AIR-COOLED TRANSDUCER

SYSTEM OVERVIEW

Industrial Sonomechanics (ISM)’ 1200 W bench-top ultrasonic processor system is designed for batch and flow-through process investigations and small-scale production. The system operates at the frequency of approximately 20 kHz. Barbell horns used in this system can have output tip diameters of up to 35 mm and provide stable operation at output amplitudes up to 120 microns in aqueous loads at a normal pressure, corresponding to acoustic power intensities up to 80 W/cm^2. This gives investigators a wide range of possible experimental conditions to determine optimal parameters for even the most challenging ultrasonic processes. When optimal process conditions are established, the same system can be used for medium-scale production. The process can also be transferred to commercial scale utilizing ISM’s 2400 W industrial-scale ultrasonic processor system.

Batch Mode System Schematic

Schematic of the 1200 W ultrasonic system is illustrated in its batch processing configuration. Ultrasonic generator excites vibrations in the piezoelectric transducer, which are subsequently amplified by the Full-wave Barbell horn. The horn delivers the ultrasonic energy to the liquid, contained in the beaker. The liquid may be cooled using an ice bath or a water-cooled jacketed beaker.

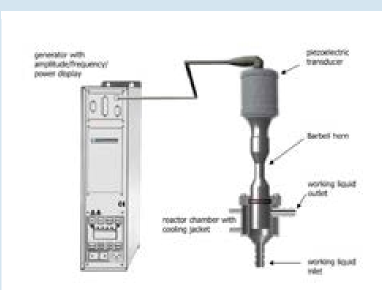

Flow-Through Mode System Schematic

Schematic of the 1200 W ultrasonic system is illustrated in its flow-through configuration. Ultrasonic electric generator, controlled form the front panel excites vibrations in the piezoelectric transducer, which are subsequently amplified by the Full-wave Barbell horn. The horn delivers the ultrasonic energy to the liquid, flowing through the reactor chamber. The reactor chamber may include a cooling/heating jacket. The working liquid inlet and outlet valves may be designed to enable adjustable, pressurized flow through the ultrasonic reactor chamber. The system can be configured to operate under pressures of up to 3 atmospheres.

WARNING: The piezoelectric transducer must be cooled with forced air, supplied through an air-hose connection at the top (not shown in this schematic). The air must be filtered, dry and not warmer than 30 degrees C (86 degrees F). The air flow rate must be at least 0.5 m^3/min (18 cfm). Operating the unit without the cooling air may irreversibly damage the transducer and is strictly prohibited.

The Ultrasonic System design corresponds to the International Patent Application PCT/US2008/068697, "High capacity ultrasonic reactor system“. The incorporated Barbell horn design corresponds to the US Patent 7,156,201, "Ultrasonic rod waveguide-radiator”.

Generator and Transducer-Horn Assemblies

Photographs are presented of: 1 – 1200 kW ultrasonic generator, 2 - piezoelectric transducer assembled with a Full-wave Barbell horn, 3 - piezoelectric transducer assembled with a Half-wave

Barbell horn, 4 - piezoelectric transducer assembled with a conventional horn.

Examples of Available Horns and Reactor Chambers

Photographs of several types of horns and reactor chambers are presented. 1 – Full-wave Barbell horn with upper node attachment flange (works with reactor chamber #5; also used for medium-size batch processes), 2 – Full-wave Barbell horn with lower node attachment flange (works with reactor chamber #6; also used for medium-size batch processes), 3 – Half-wave Barbell horn (works with reactor chamber #6; also used for medium-size batch processes), 4 – conventional converging horn (for small-size batch studies), 5 - long reactor chamber (works with Barbell horn #1), 6 - short reactor chamber (works with Barbell horns #2 and #3).

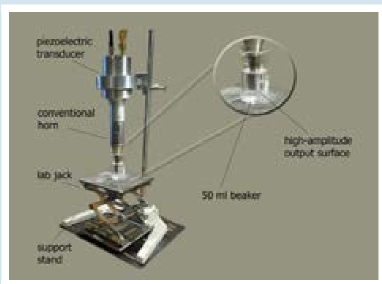

Setup Configuration 1

Batch configuration with a conventional converging horn (CH) is illustrated. Small batch studies may be carried out using the setup illustrated in this example. Typical processing volumes are 10 – 100 ml. The working liquid inside the beaker may be cooled by using an ice bath. Alternatively, a jacketed beaker equipped with a water cooling jacket may be used.

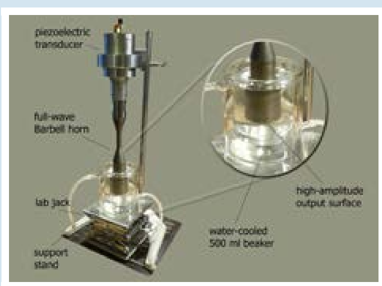

Setup Configuration 2

Batch configuration with a Full-wave Barbell horn (FBH) is illustrated. Medium batch studies and processes may be carried out using this setup. Typical processing volumes are 200 – 1000 ml, however, up to 20 liters processing volume is possible if independent batch mixing is provided. Using a beaker equipped with a water cooling jacket is recommended in order to cool the working liquid. This setup is recommended when high amplitudes (on the order of 100 microns) and/or homogeneous exposure intensities are required.

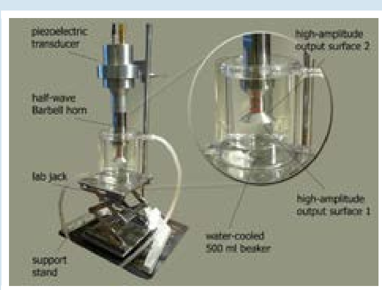

Setup Configuration 3

Batch configuration with a Half-wave Barbell horn (HBH) is illustrated. Medium batch studies and processes may be carried out using this setup. Typical processing volumes are 400 – 2000 ml, however, up to 20 liters processing volume is possible if independent batch mixing is provided. Using a beaker equipped with a water cooling jacket is recommended in order to cool the working liquid.

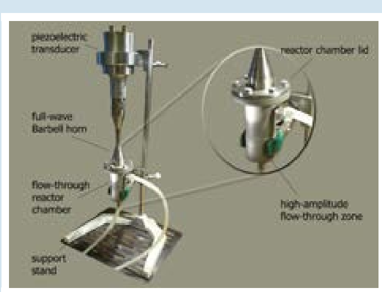

Setup Configuration 4

Flow-through configuration with a Full-wave Barbell horn (FBH) is illustrated. Flow-through studies and processes may be carried out using this setup at the productivity rates of 50 – 5000 ml/min, depending on the process. A heat exchanger (not shown) is commonly used in conjunction with this setup, however, jacketed water-cooled reactor chambers are available if additional cooling is desired. This setup is recommended when high amplitudes (up to about 120 microns) are required.

Setup Configuration 5

This configuration is commonly preferred for flow-though processes requiring high productivity rates

and is based on Half-wave Barbell horns (HBH). Flow-through studies and processes may be carried out using this setup at the productivity rates of 100 – 10000 ml/min, depending on the process. A heat exchanger (not shown) is typically used in conjunction with this setup, however, jacketed water-cooled reactor chambers are available if additional cooling is desired. This high-productivity setup is recommended when amplitudes on the order of 90 microns and homogeneous exposure intensities are required.

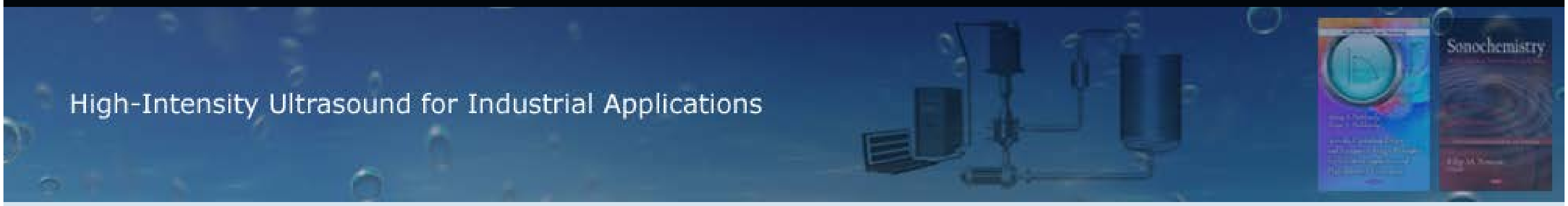

ULTRASONIC TRANSDUCERS

Ultrasonic transducers are devices used to convert electric energy coming from an ultrasonic generator into mechanical energy in the form of ultrasonic vibrations. Two main types of ultrasonic transducers are utilized in ISM's ultrasonic liquid processors: piezoelectric and magnetostrictive.

High-Power Piezoelectric Transducers

ISM's 1200 W bench-scale ultrasonic processor system used for batch and flow-through process investigations and small-scale production, and 2400 W industrial-scale ultrasonic processor system designed for high-volume continuous-mode commercial production are based on high-power piezoelectric transducers. The main advantage of these devices is high efficiency (up to 95%). Piezoelectric transducers are high-voltage driven and air cooled. They can become irreversibly damaged if overheated, which is why it is important to cool them well by setting up a good airflow. These devices are smaller and lighter than magnetostrictive transducers and are easier to setup and drive. The frequency of operation is approximately 20 kHz.

High-Power Magnetostrictive Transducers

ISM's 1000 W (output power) bench-top water-cooled ultrasonic system designed for batch and flow-through process investigations and small-scale production, and 2000 W (output power) industrial water-cooled ultrasonic system used for flow-through or batch production on a commercial scale are based on high-power magnetostrictive transducers. These devices are constructed from high-strength metallic alloys and permit reaching very high levels of acoustic power intensity. The main disadvantage of magnetostrictive transducers is their low efficiency (below 50%), which is why they must be liquid-cooled. These devices are used in special cases, for example in hazardous environments, such as chemical factories or refineries. They can be built without any high-power cable connections, thereby eliminating the possibility of creating a spark inside a failed connector. In addition, since the magnetostrictive transducers are water-cooled, the risk of introducing a hazardous gas into its internal area is eliminated. The frequency of operation is approximately 18 or 22 kHz.

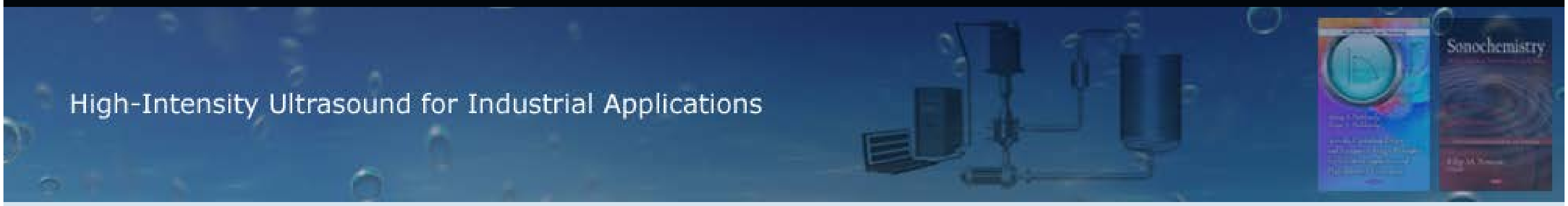

FLOW-THROUGH REACTOR CHAMBERS

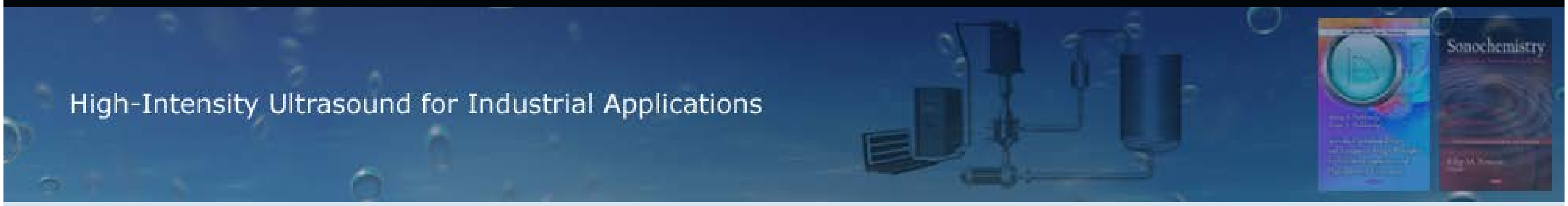

Home → Technology → Ultrasonic Horn Designs and Properties

ULTRASONIC HORN DESIGNS AND PROPERTIES

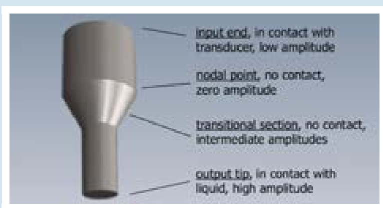

Conventional Horn

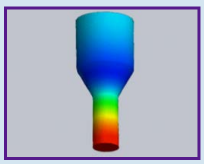

Conventional horns (CH series) are suitable for small-scale process investigations. Able to provide very high ultrasonic amplitudes and power densities, these horns cannot deliver significant amounts of total power to liquids because their output tips are small, which limits cavitation zone volumes they are able to generate. These horns, therefore, are not appropriate for commercial-scale liquid processing, but are recommended for process data collection prior to scale-up.

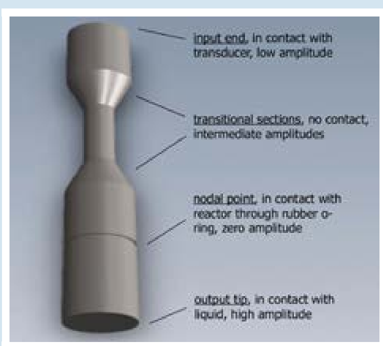

Full-Wave Barbell Horn

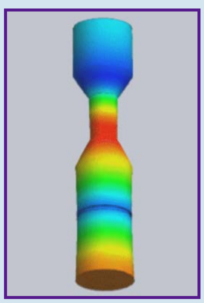

Process scale-up requires switching to horns with larger output tip diameters, able to output the ultrasonic energy into greater volumes of working liquids while still maintaining high amplitudes. Full-wave Barbell horns (FBH series) are appropriate for large-scale batch and flow-through liquid processing and investigations. These devices can have large output tip diameters (up to about 75 mm) and are able to generate very high ultrasonic amplitudes and power densities, creating large cavitation zones and delivering substantial amounts of power to liquids. When inserted up to their lower nodal point, these horns produce one major cavitation zone under the output tip. Downward liquid streaming in the cavitation zone helps mixing the liquids during batch mode operation.

Scaling up processes with full-wave Barbell horns leads to an increase in liquid processing capacity approximately proportional to (Dfbh/Dch)^2, where Dfbh and Dch are the FBH (after the scale-up) and CH (before the scale-up) output tip diameters, respectively. For example, if conventional ultrasonic horn has an output tip diameter of 13 mm and the full-wave Barbell horn operating at the same amplitude has an output tip diameter of 65 mm, the productivity-rate increase factor after the scale-up will be 25.

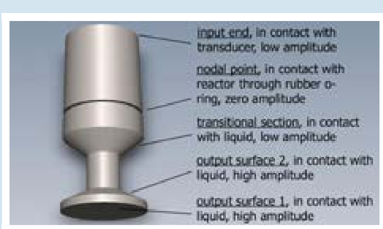

Half-Wave Barbell Horn

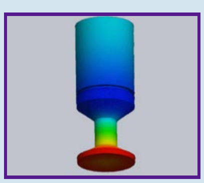

Half-wave Barbell horns (HBH series) are ideal for industrial-scale flow-through liquid processing. These devices can have large output tip diameters and generate high ultrasonic amplitudes and power densities, creating large cavitation zones and delivering very high power to liquids. These horns produce two major cavitation zones (under and above the output section) ensuring that no liquid is able to bypass the active treatment zone as it flows through the reactor chamber.

HBH devices generate both downward and upward liquid streaming, which helps mixing the liquids inside a batch or flow-through reactor. HBH devices are smaller than FBH devices, making it possible to design more compact systems. The cumulative cavitation area produced by these horns is very large (approximately double of that produced by an FBH). Scaling up processes with half-wave Barbell horns leads to an increase in liquid processing capacity approximately proportional to 2(Dhbh/Dch)^2, where Dhbh and Dch are the HBH (after the scale-up) and CH (before the scale-up) output tip diameters, respectively. For example, if conventional ultrasonic horn has an output tip diameter of 13 mm and the half-wave Barbell horn operating at the same amplitude has an output tip diameter of 65 mm, the productivity-rate increase factor after the scale-up will be approximately 50.

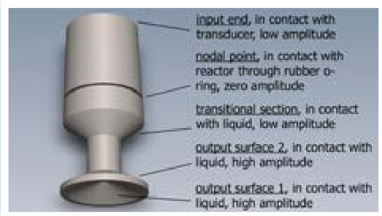

Half-Wave Barbell Horn with an Opening

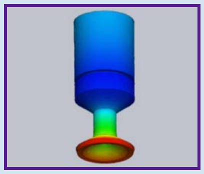

Half-wave Barbell horns with an opening (HBHO series) are the right choice for industrial-scale flow-through liquid processing where extremely high power deposition is required. These devices can have large-diameter output sections and generate high ultrasonic amplitudes and power densities, creating very large cavitation zones and delivering extremely high power to liquids. The output surface areas of these devices are further increased by hollow regions in their output sections.

These horns produce two major cavitation zones (under/inside and above the output section) ensuring that no liquid is able to bypass the active treatment zone as it flows through the reactor chamber. The lower zone experiences an additional effect of cavitation focusing, due to concentric expansion-contraction which occurs simultaneously with the longitudinal motion of the output section. HBHO devices generate both downward and upward liquid streaming, which helps mixing the liquids inside a batch or flow-through reactor. Scaling up processes with HBHO devices leads to an increase in liquid processing capacity, which depends on the shape and size of the hollow section and is greater than 2(Dhbho/Dch)^2, where Dhbho and Dch are the HBHO (after the scale-up) and CH (before the scale-up) output tip diameters, respectively. For example, if conventional ultrasonic horn has an output tip diameter of 13 mm and the half-wave Barbell horn with an opening operating at the same amplitude has an output tip diameter of 65 mm, the productivity-rate increase factor after the scale-up will be greater than 50.

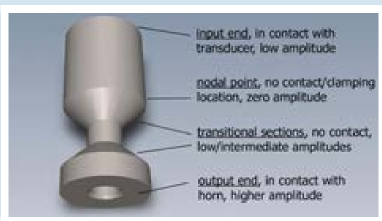

Half-Wave Barbell Booster

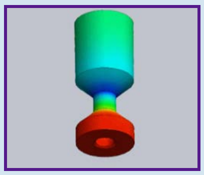

Half-wave Barbell boosters (HBB series) are connected between a transducer and a horn to modify the horn's effective gain factor (amplify or reduce). The HBB device's gain (when used as an amplifier, as shown on the left) or reduction (when connected in the opposite direction) factor should be multiplied by the horn's gain factor to obtain the resulting assembly's gain factor. HBB devices can also be used as assembly length extenders and to provide additional clamping support.

It is important to point out that in order for an FBH, HBH or HBHO device to permit direct process scale-up, during which the ultrasonic amplitude and other parameters are maintained while the liquid processing capacity is increased, it is necessary to make sure that the power to be delivered to the working liquid is made available by the processor's generator and transducer. For example, a CH with an output tip diameter of 13 mm, operating at the amplitude of 90 microns in water at atmospheric pressure and 25 deg.C outputs approximately 80 W of ultrasonic power. An FBH with a 35 mm output tip diameter operating at the same amplitude will draw approximately 580 W. An FBH with a 65 mm output tip diameter will draw approximately 2,000 W. These power values are approximately doubled for HBH devices and more than doubled for HBHO devices.

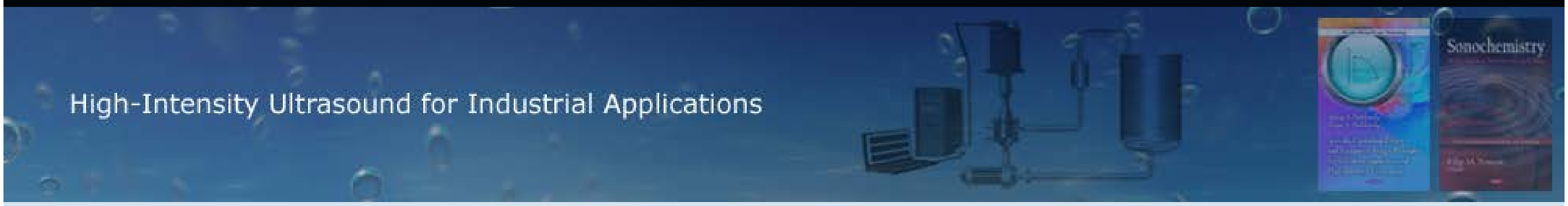

CONTACTS

Full Name

Address

Company

Phone

E-mail

Make your request here

Industrial Sonomechanics LLC

479 W 146 Street, Ground Floor
New York, NY 10031
1.646.580.HORN (1.646.580.4676)

E-mail: contact@sonomechanics.com

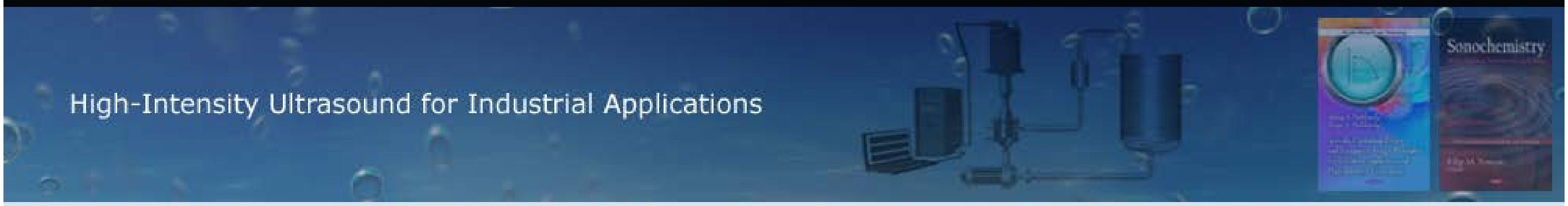

ABOUT ISM

ISM offers high-intensity ultrasonic liquid processors, ultrasonic homogenizers, sonochemical reactors and ultrasonic wet milling systems. Our equipment can be used for the production of nanoparticles (nanoemulsions, nanocrystals and nano-sized wax particles), extraction of oil from algae, production of biofuels, crude oil desulphurization, liquid degassing, cell disruption, polymer and epoxy processing, adhesive thinning, mixing, and many other processes. We serve the pharmaceutical, cosmetic, food, ink, paint, coating, wood treatment, metalworking, nanocomposite, pesticide, fuel, wood product and many other industries.

High ultrasonic amplitudes able to generate intense acoustic cavitation are required for most processes. Unlike conventional ultrasonic devices, ISM's patented Barbell horn-based ultrasonic systems make it possible to produce extremely high ultrasonic amplitudes at any scale, from laboratory to industrial, guaranteeing reproducible results after scale-up. Our experienced consultants will be glad to help optimize your process and implement it in your production environment.

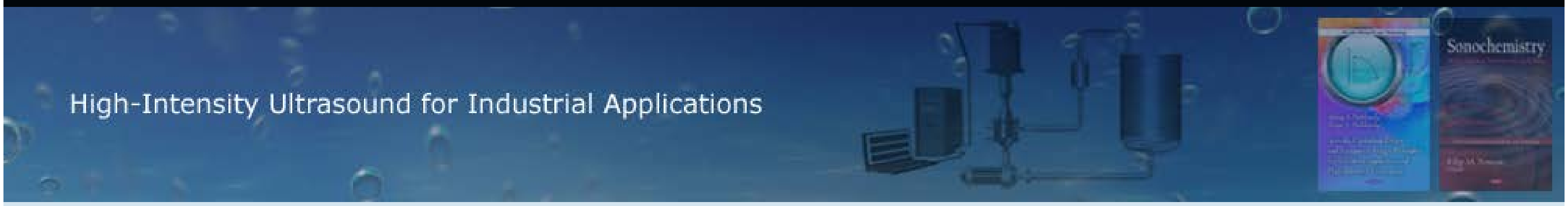
High-Intensity Ultrasound for Industrial Applications
Sonochemistry

TECHNOLOGY

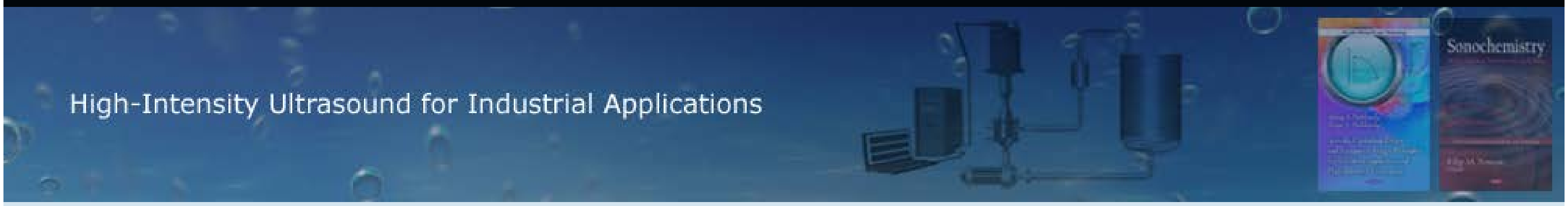
High-Intensity Ultrasound for Industrial Applications
Sonochemistry

SERVICES

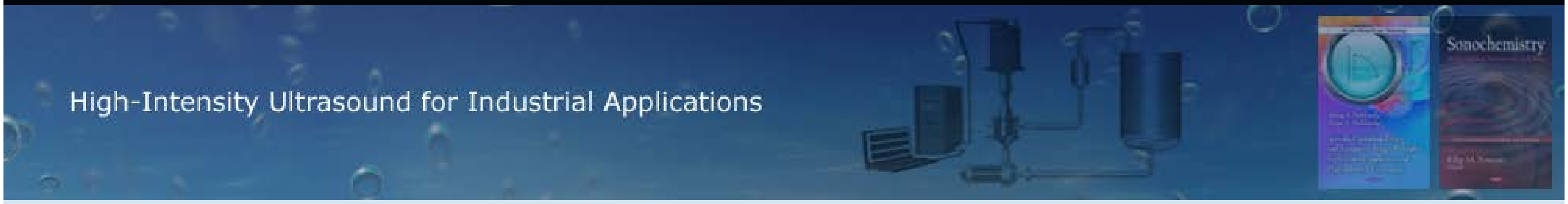

Home → Technical Resources

TECHNICAL RESOURCES

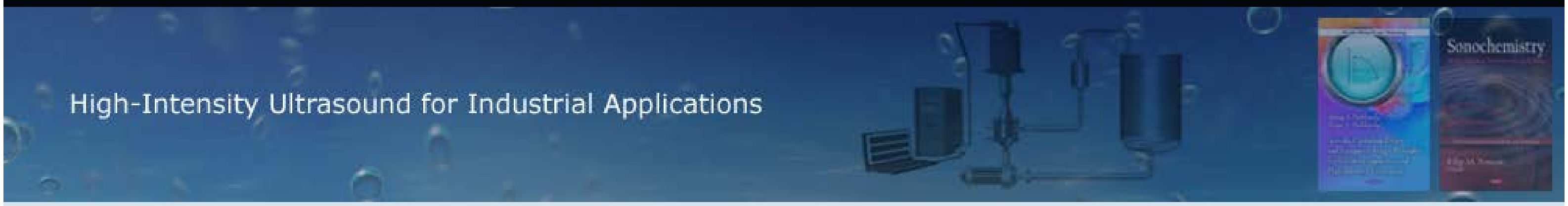

Home → Sitemap

SITEMAP

- Home
- About ISM
  - Introduction to ISM
    - A High-Intensity Industrial Ultrasound Company
    - An Active R&D Firm
    - Ultrasonic Process Consulting Company
  - Our Team
  - Company News
- Technology
  - Barbell Horn Ultrasonic Technology
  - Ultrasonic Liquid Processor Systems
  - Ultrasonic Horn Designs and Properties
  - Ultrasonic Transducers
  - Flow-Through Reactor Chambers
- Services
  - Overview of Process Optimization and Scale-up Services
  - Service Project Example - Translucent Nanoemulsion for Food Industry
- Ultrasonic Systems
  - High-Efficiency Ultrasonic Liquid Processors
    - 1200 W Processor with Air-Cooled Transducer
    - 2400 W Processor with Air-Cooled Transducer
  - Special-Request Ultrasonic Liquid Processors
    - 1000 W Processor with Water-Cooled Transducer
    - 2000 W Processor with Water-Cooled Transducer
- Applications
  - Pharmaceutical
    - Nanocrystallization for Improved Drug Delivery
    - Nanoemulsions Used for Parenteral Nutrition
    - Drug-Carrier Liposomes and Nanoemulsions
  - Cosmetic and Dermatological
    - Translucent Oil-in-Water Nanoemulsions
  - Extraction and Transesterification of Mircoalgal Oil
- Technical Resources
  - Videos
  - Intellectual Property
  - Books
  - Peer-Reviewed Publications
  - Downloads

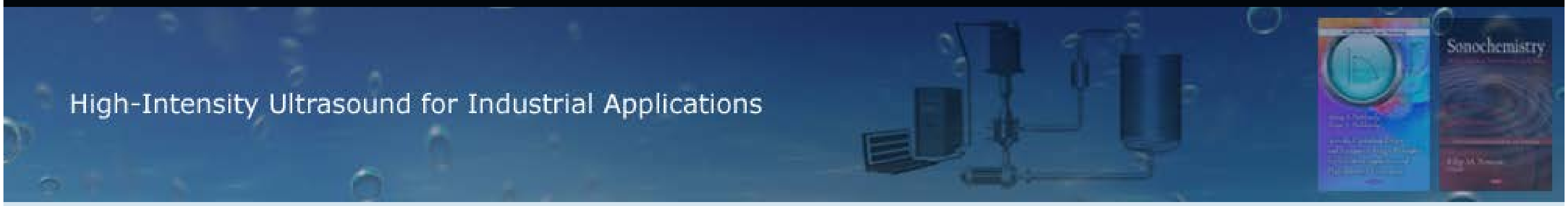

NANOEMULSIONS USED FOR PARENTERAL NUTRITION

BACKGROUND

Lipid nanosized emulsions (nanoemulsions) are complex, kinetically stable oil-in-water dispersions, homogenized with the aid of one or several surfactants (emulsifiers). In clinical practice, one major application of lipid nanoemulsions is parenteral nutrition, with such products as Intralipid® used for patients who are unable to get nutrition via an oral diet.

Traditional nanoemulsions used for parenteral nutrition are made of safflower and/or soybean oils using egg-derived phospholipids as emulsifiers. These nanoemulsions are known as long-chain triglyceride emulsions and are composed of omega-6 polyunsaturated fatty acids (linoleic and linolenic acids) and long-chain non-essential saturated fatty acids. New types of lipid nanoemulsions used for parenteral nutrition consist of physical mixtures of soybean or safflower oil with oils that are rich in medium-chain triglycerides, such as olive and coconut oils and/or omega-3 long-chain polyunsaturated fatty acids found in fish oil. These lipid formulations have clinical benefits over traditional soybean and safflower nanoemulsions and offer improvements in stability and safety when combined in new multi-chamber bags. Omega-3 fatty acids laden nanoemulsions made from fish oil are likely to be increasingly used not only for nutrition, but also for the modification of biological and pathological processes.

Two parameters are measured to check toxicity and physical stability of nanoemulsions: 1) lipid globule mean droplet size (MDS) and 2) particle size distribution (PSD). United States Pharmacopeia (USP) adopted Chapter 729, entitled “Globule Size Distribution in Lipid Injectable Emulsions”, which sets two physical limits for nanoemulsions used for parenteral nutrition: 1) MDS < 500 nanometers (nm); 2) percent of lipid globules > 5 microns (um) or $PFAT_5$ < 0.05%. This is of great significance for infusion safety: higher amounts (> 0.05%) of outsized (> 5 um) lipid droplets are associated with instability; moreover, intravenously administered lipid droplets exceeding 5 um have been shown to cause adverse effects, in particular emboli in the lungs.

PRODUCTION WITH HIGH-AMPLITUDE ULTRASOUND

Industrial Sonomechanics, LLC (ISM), offers bench and industrial-scale high-power ultrasonic processors for the production of nanoemulsions. The processors are based on our patented Barbell Horn Ultrasonic Technology (BHUT), which, as explained below, makes it possible to directly implement laboratory accomplishments in a production environment, guaranteeing reproducible and predictable results at any scale.

High ultrasonic vibration amplitudes are required for efficient oil droplet size reduction. The necessary shear forces are created by ultrasonic cavitation, which produces violently and asymmetrically imploding vacuum bubbles and causes micro-jets that disperse and break up the droplets down to the nanometer scale. Known for many decades, this effect of high-amplitude ultrasound has been extensively studied and successfully used in laboratory-scale research. However, prior to the introduction of BHUT, none of the existing ultrasonic liquid processors could generate the required amplitudes on the industrial scale. Commercial implementation of high-power ultrasound has, therefore, been limited to processes for which low-amplitudes are sufficient (cleaning, simple deagglomeration, mixing, macro-emulsification, etc.).

Why ISM's Ultrasonic Technology?

Conventional high-power ultrasonic technology inherently forces all processes to run either at a small scale and high amplitude or a large scale and low amplitude. ISM has successfully overcome this limitation by developing BHUT, which permits constructing industrial-scale ultrasonic processors able to operate at extremely high amplitudes. The processors are directly scalable and can be used in the commercial production of high-quality nanoemulsions for the pharmaceutical industry. Our equipment is compact and relatively low-cost, needs little technical support, includes very few wetted parts, generally requires no special pre-treatment of precursors, and is potentially self-sterilizing due to antibacterial properties of high-intensity ultrasound.

Examples of Intralipid-Type Nanoemulsions Produced Using ISM's Ultrasonic

Number of passes	Ultrasonic amplitude (μ_{pp})	SLS, MDS (nm)	DLS, MDS (nm)	$PFAT_5$ (%)
1	75	319.7		
3	75	308.7		
5	75	200.2	199.23	0.024
5	25		527.7	0.364

Table 1. $PFAT_5$ is percentage (volume-weighted) of oil droplets > 5 µm, determined by LE/SPOS, MDS is mean droplet size (intensity-weighted) determined by Static (SLS) and Dynamic Light Scattering (DLS). Color coding refers to pass and fail, according to USP recommendations.

Technology

Intralipid-type nanoemulsion consisting of soybean oil (10%), L-a-Phosphatilylcholine, Type IV-S (1.2%), glycerol (2.25%) and water (86.55%) was prepared using Industrial Sonomechanics' (ISM) 1200 W bench-scale flow-through ultrasonic processor, equipped with a piezoelectric transducer, flow-through reactor chamber and Full-wave Barbell Horn (FBH) operating at the ultrasonic amplitude of 75 microns. The results are presented on the left. The obtained Intralipid-type nanoemulsion's quality exceeds USP standards. It should be emphasized that decreasing the ultrasonic amplitude to 25 microns (as in conventional industrial ultrasonic systems) results in a significant increase of MDS and PFAT5, both of which are well outside of the acceptable levels. This result clearly shows that ultrasonic amplitude plays a crucial role in the process of preparing high-quality nanoemulsions and justifies the importance of being able to scale up without sacrificing the amplitude.

The data presented above was collected in collaboration with Allied Innovative Systems, LLC (ALLIS).

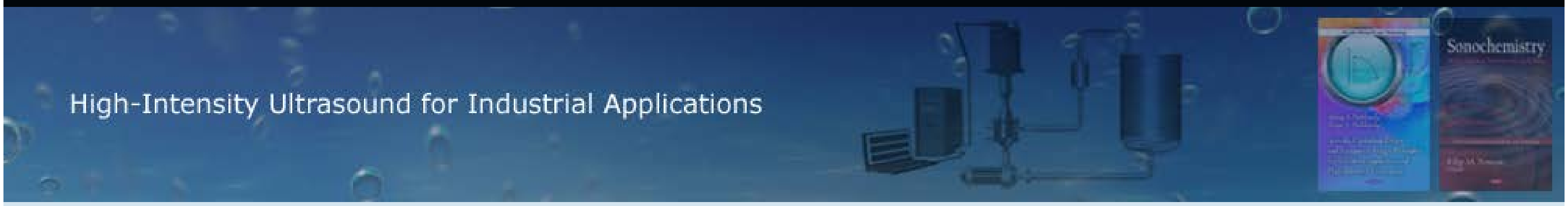

DRUG-CARRIER LIPOSOMES AND NANOEMULSIONS

BACKGROUND

Liposomes are spherical, self-closed structures formed by one or several concentric lipid bilayers with an aqueous phase inside and in between the lipid bilayers, having droplet diameters from about 50 to 5000 nm. Some attractive properties of liposomes include their biocompatibility and ability to entrap water-soluble (hydrophilic) pharmaceutical agents in their internal water compartment and water-insoluble (hydrophobic) pharmaceuticals in their membrane. There are approximately a dozen liposomal drugs currently on the market, including anticancer agent doxorubicin, in both polyethylene glycol (PEG) liposomes (Doxil) and in non-pegylated liposomes (Myocet). This agent is used widely off-label and is approved for the treatment of solid tumors in patients with breast-carcinoma metastases.

Lipid nanosized emulsions or nanoemulsions are complex, kinetically stable oil-in-water dispersions, homogenized with the aid of an emulsifier. In clinical practice, there are two major applications of lipid nanoemulsions: 1) parenteral nutrition and 2) colloidal drug carriers.

Lipid nanoemulsions are widely used as drug carriers because they easily incorporate lipophilic bioactive compounds, stabilize bioactive compounds that tend to undergo hydrolysis, and reduce side effects of potent drugs. Additionally, lipid nanoemulsions are biodegradable and can be produced on a large scale using ISM's ultrasonic processors. Furthermore, nanoemulsions can be administered by almost all available routes including parenteral, ocular, nasal, oral, topical, and even aerosilization to the lungs. Examples of commercially available drugs encapsulated into nanoemulsions include Diprivan (Propofol) from AstraZeneca, Etomidat-Lipuro (Etomidate) from B. Braun Melsungen, Lipotalon (Limethason, Dexamethasone Palmitate) from Merckle, Restasis (Cyclosporin A) from Allergan, and Gengraf (Cyclosporin A) and Norvir (Ritonavir) both from Abbott.

Two parameters are measured to check toxicity and physical stability of liposomes and nanoemulsions: 1) mean droplet size (MDS) and 2) particle size distribution (PSD). United States Pharmacopeia (USP) adopted Chapter 729, entitled “Globule Size Distribution in Lipid Injectable Emulsions”, which sets two physical limits for nanoemulsions: 1) MDS < 500 nanometers (nm); 2) percent of lipid globules > 5 microns (um) or $PFAT_5$ < 0.05%. This is of great significance for infusion safety: higher amounts (> 0.05%) of outsized (> 5 um) lipid droplets are associated with instability; moreover, intravenously administered lipid droplets exceeding 5 um have been shown to cause adverse effects, in particular emboli in the lungs.

PRODUCTION WITH HIGH-AMPLITUDE ULTRASOUND

The formation of nanoemulsions and liposomes requires intense shear forces and significant energy deposition in order to break the original particles down to the nanometer scale. Industrial Sonomechanics, LLC (ISM), offers bench and industrial-scale high-power ultrasonic processors for the production of nanoemulsions and liposomes. The processors are based on our patented Barbell Horn Ultrasonic Technology (BHUT), which, as explained below, makes it possible to directly implement laboratory accomplishments in a production environment, guaranteeing reproducible and predictable results at any scale.

High ultrasonic amplitudes are required for efficient nanoemulsion and nanoliposome production. The necessary shear forces are created by ultrasonic cavitation, which produces violently and asymmetrically imploding vacuum bubbles and causes micro-jets that disperse and break up the original oil droplets and liposomes down to the nanometer scale. Known for many decades, this effect of high-amplitude ultrasound has been extensively studied and successfully used in laboratory-scale research. However, prior to the introduction of BHUT, none of the existing ultrasonic liquid processors could generate the required amplitudes on the industrial scale. Commercial implementation of high-power ultrasound has, therefore, been limited to processes for which low-amplitudes are sufficient (cleaning, simple deagglomeration, mixing, macro-emulsification, etc.).

Why ISM's Ultrasonic Technology?

Conventional high-power ultrasonic technology inherently forces all processes to run either at a small scale and high amplitude or a large scale and low amplitude. ISM has successfully overcome this

limitation by developing BHUT, which permits constructing industrial-scale ultrasonic processors able to operate at extremely high amplitudes. The processors are directly scalable and can be used in the commercial production of high-quality drug-containing nanoemulsions and liposomes for the pharmaceutical industry. Our equipment is compact and relatively low-cost, needs little technical support, includes very few wetted parts, generally requires no special pre-treatment of precursors, and is potentially self-sterilizing due to antibacterial properties of high-intensity ultrasound.

Sample type	SLS, MDS (nm)	DLS, MDS (nm)	$PFAT_5$ (%)
Emulsion 1	215	190	0.007
Emulsion 1+ ZnPC	210	177	0.001
Emulsion 2	60		
Emulsion 2+ ZnPC	84	70	0.026
Liposomes	101		

$PFAT_5$ is the percentage (volume-weighted) of oil droplets > 5 µm, determined by LE/SPOS, MDS is the mean droplet size (intensity-weighted) determined by Static (SLS) and Dynamic Light Scattering (DLS).

Examples of Drug-Containing Nanoemulsions and Liposomes Produced by High-Intensity Ultrasound

The table on the left demonstrates that nanoemulsions and liposomes prepared using our ultrasonic technology are effective for the delivery of one of the most promising hydrophobic drugs widely used for the treatment of a variety of solid tumors, Zn-Phtalocyanine (ZnPC). The following nanoemulsion and liposome systems were prepared using Industrial Sonomechanics' (ISM) 1200 W bench-scale flow-through ultrasonic processor equipped with a piezoelectric transducer, flow-through reactor chamber and Full-wave Barbell Horn (FBH) operating at the ultrasonic amplitude of 75 microns: 1) Emulsion 1 (Intralipid-type emulsion): soybean oil-in-water nanoemulsion consisting of soybean oil (10%), L-a-Phosphatilylcholine, Type IV-S (1.2%), glycerol (2.25%), water (86.55%) 2) Emulsion 2: soybean oil-in-water nanoemulsion consisting of Soybean oil (10%), Tween 80 (8.7%), Span 80 (1.3%), water (80%)); 3) Liposomes: L-a-Phosphatilylcholine, Type IV-S (2.4%), phosphate buffer saline (97.6%). We also prepared Emulsions 1 and 2 containing 0.05 mg/ml ZnPC with and without preliminary dissolution of ZnPC in ethanol (final ethanol concentration did not exceed 2%). In this case, either ZnPC powder or its ethanol solution was added to the oil phase. In order to examine the effect of filtration on the size of the droplets, Emulsion 2 was also filtered using a 0.45 mm filter.

As can be seen from the table, all parameters of the prepared nanoemulsions and liposomes are well within USP requirements. Other most significant results obtained for Emulsions 1, 2 and Liposomes include: 1) The addition of ethanol to Emulsions 1 and 2 does not significantly change the droplet size; 2) The droplet sizes for filtered (through a 0.45 mm filter) and unfiltered Emulsion 2 are practically the same; 3) The absorbance and fluorescence spectra obtained for ZnPC-containing Emulsions 1 and 2 coincide with those for solutions of ZnPC in pure soybean oil; 4) Absorbance and fluorescence spectroscopy measurements showed that the ZnPC incorporation coefficient is close to 100% (results were confirmed by scanning electronic images showing no ZnPC crystals in the water phase).

The data presented above was collected in collaboration with Allied Innovative Systems, LLC (ALLIS).

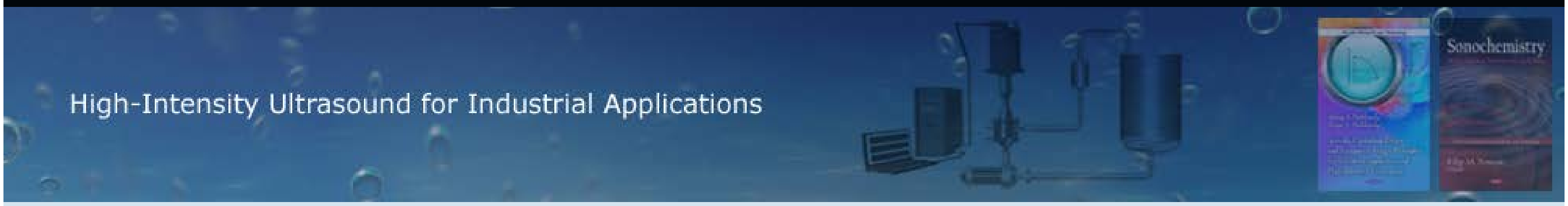

2400 W PROCESSOR WITH AIR-COOLED TRANSDUCER

SYSTEM OVERVIEW

Industrial Sonomechanics (ISM)' 2400 W industrial-scale ultrasonic processor system is designed for high-volume continuous-mode commercial production. The system operates at the frequency of approximately 20 kHz. Barbell horns used in this system have large output tip diameters (Ø) and provide very high output amplitudes (A) and output power densities (Pd). For example, for FBH-type horns the following combinations are possible (water up to the nodal point, at 1 bar and 25 ºC):

Ø = 50 mm, A = 120 microns, Pd = 80 W/cm^2;
Ø = 60 mm, A = 85 microns, Pd = 55 W/cm^2;
Ø = 70 mm, A = 60 microns, Pd = 35 W/cm^2.

Other types of Barbell horns can be used as well. These amplitudes and power densities are extremely high and are unprecedented for industrial-scale systems, which are commonly restricted to ultrasonic amplitudes below 25 microns and power densities below 10 W/cm^2. ISM's Barbell Horn Ultrasonic Technology (BHUT) utilized in this processor makes it possible to implement even the most challenging ultrasonic processes in the commercial environment.

Batch Mode System Schematic

Schematic of the 2400 W ultrasonic processor system is illustrated in its batch processing configuration. Ultrasonic generator excites vibrations in the piezoelectric transducer, which are subsequently amplified by the Full-wave Barbell horn. The horn delivers the ultrasonic energy to the liquid, contained in the beaker. The liquid may be cooled using an ice bath or a water-cooled jacketed beaker.

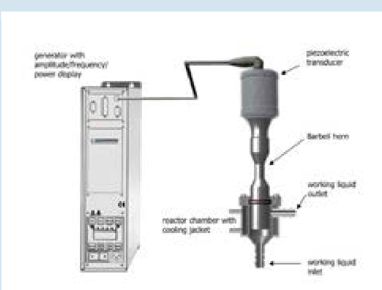

Flow-Through Mode System Schematic

Schematic of the 2400 W ultrasonic processor system is illustrated in its flow-through configuration. 2500 W ultrasonic electric generator, controlled form the front panel excites vibrations in the piezoelectric transducer (maximum output power - 2400 W), which are subsequently amplified by the Full-wave Barbell horn. The horn delivers the ultrasonic energy to the liquid, flowing through the reactor chamber. The reactor chamber may include a cooling/heating jacket. The working liquid inlet and outlet valves may be designed to enable adjustable, pressurized flow through the ultrasonic reactor chamber. The system can be configured to operate under pressures of up to 3 atmospheres.

WARNING: The piezoelectric transducer must be cooled with forced air, supplied through an air-hose connection at the top (not shown in this schematic). The air must be filtered, dry and not warmer than 30 degrees C (86 degrees F). The air flow rate must be at least 0.5 m^3/min (18 cfm). Operating the unit without the cooling air may irreversibly damage the transducer and is strictly prohibited.

The Ultrasonic System design corresponds to the International Patent Application PCT/US2008/068697, "High capacity ultrasonic reactor system". The incorporated Barbell horn design corresponds to the US Patent 7,156,201, "Ultrasonic rod waveguide-radiator".

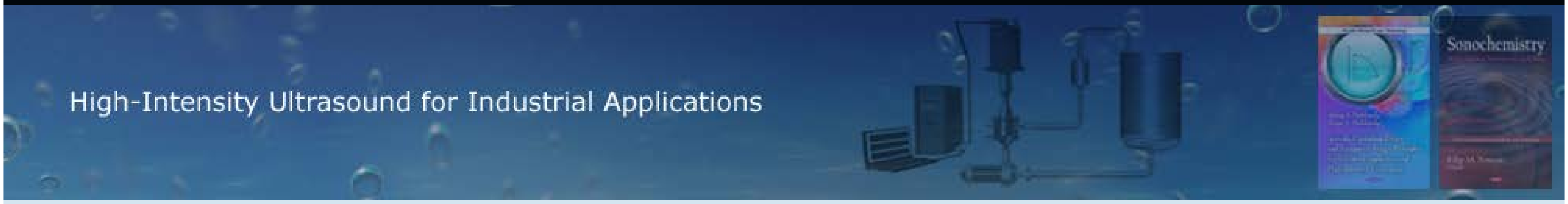

1000 W PROCESSOR WITH WATER-COOLED TRANSDUCER

SYSTEM DESCRIPTION

Industrial Sonomechanics (ISM)' 1000 W (output power) bench-top water-cooled ultrasonic system is a "special request" unit, designed for batch and flow-through process investigations and semi-industrial scale production. The system operates at the frequency of approximately 22 kHz. FBH-type Barbell horns used in this system have output tip diameters up to 35 mm and can provide stable operation at output amplitudes up to 75 microns in aqueous loads at a normal pressure, corresponding to acoustic power intensities up to 50 W/cm^2. This gives investigators a wide range of possible experimental conditions to determine optimal parameters for even the most challenging ultrasonic processes. When optimal process conditions are established, the same system can be used for production on a semi-industrial scale. The system is based on a water-cooled magnetostrictive transducer, which offers several advantages, as described below.

System Schematic

1000 W flow-through ultrasonic reactor system in its most common configuration is illustrated on the left. Ultrasonic generator, controlled form the front panel interface or (optional) from a computer running Generator Control software, excites vibrations in the magnetostrictive transducer, which are subsequently amplified by the Full-wave Barbell horn. The horn delivers the ultrasonic energy to the liquid, flowing through the reactor chamber. The reactor chamber may include a cooling/heating jacket. The working liquid inlet and outlet valves may be designed to enable adjustable, pressurized (if needed) flow through the ultrasonic reactor chamber (optional). The system can be designed to operate under static pressures of up to 3 atmospheres.

The processor can be configured for the use in hazardous environments, such as chemical factories or refineries, by incorporating the following protective features into its magnetostrictive transducer and ultrasonic generator:

1. The transducer can be built without any high-power cable connections. In this configuration, the Teflon-insulated wire wound around its magnetostrictive element continues uninterrupted from the unit all the way to the generator, thereby eliminating any possibility of creating a spark inside a failed connector. In addition, since the magnetostrictive transducer is water-cooled, any possibility of introducing a hazardous gas into its internal area is eliminated.
2. Two methods of protection may be employed for the ultrasonic generator: a) since the generator can be fully monitored and controlled by a computer, it may be kept out of the hazardous area altogether; b) the generator may be designed to be water-cooled, which means that it will not depend on the external air for heat removal. The generator's enclosure can, therefore, be sealed and/or pressurized with an inert gas, eliminating the possibility of introducing external air (possibly with hazardous gasses) into its internal area.

Maximum flow rate through the processor is approximately 2,500 liter/h (11 gpm). The system design corresponds to the International Patent Application PCT/US2008/068697, "High capacity ultrasonic reactor system". The incorporated Barbell horn design corresponds to the US Patent 7,156,201, "Ultrasonic rod waveguide-radiator".

Assemblies for Flow-through and Batch Processes

Photographs are presented of: **1** - 2000 W ultrasonic generator, **2** - magnetostrictive transducer (maximum output power - 1000 W) assembled with Full-wave Barbell horn and reactor chamber (for flow-through process studies and semi-industrial scale production), **3** - magnetostrictive transducer assembled with Full-wave Barbell horn (for batch experiments).
Besides Full-wave Barbell horns (FBH) of the type shown on the left, specialized Half-wave Barbell horns (HBH) and Half-wave Barbell horns with an Opening (HBHO) are available. These horns are shorter and lighter than Full-wave Barbell horns and have shapes that, when incorporated into appropriately designed reactor chambers, ensure that no working liquid bypasses the active cavitation zone. These horns are frequently preferred for the tasks involving high-intensity flow-through

ultrasonic processing, such as dispersion and deagglomeration of solid particles, nanoemulsification and the production micronized waxes, where uniform exposure to ultrasound and the resulting narrow particle size distributions are essential.

Examples of Available Horns and Reactor Chambers

Photographs of several types of horns and reactor chambers are presented. **1** – Full-wave Barbell horn with an upper-node attachment flange (works with reactor chamber **5**; also used for medium-size batch studies), **2** – Full-wave Barbell horn with a lower-node attachment flange (works with reactor chamber **6**; also used for medium-size batch studies), **3** – Half-wave Barbell horn (works with reactor chamber **6**; also used for medium-size batch studies), **4** – Conventional converging horn (works with reactor chamber **6**; also used for small-size batch studies), **5** - long reactor chamber (works with Full-wave Barbell horn **1**), **6** - short reactor chamber (works with Barbell horns **2** and **3** as well as with horn **4**).

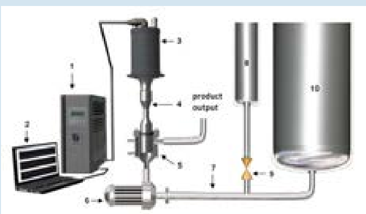

Common Setup Example 1

A common setup of the 1000 W ultrasonic system is shown, where: **1** - ultrasonic generator; **2** – computer running Generator Control software, **3** - magnetostrictive transducer; **4** - Full-wave Barbell horn; **5** – flow-through reactor chamber; **6** – pump; **7** - pipeline; **8** – tank for supplying additional components; **9** – valve; **10** – main liquid supply tank. This setup may be used for such processes as biodiesel production, nano-emulsification, oil extraction, solid particle dispersing, etc. The product may be collected from the **product output** line or re-circulated into the main liquid supply tank, **10**.

Common Setup Example 2

Medium batch (150 - 2000 ml) studies and processes may be carried out using this setup. The flow-through reactor chamber is replaced by a beaker. Ultrasonic generator, **1**, excites vibrations in the magnetostrictive transducer, **2**, which are subsequently amplified using the Full-wave Barbell horn, **3**, and delivered to the working liquid contained in the beaker, **4**. If desired, the ultrasonic generator may be programmed and the data may be recorded by a computer, **5**, running Generator Control software. The working liquid inside the beaker may be cooled by using an ice bath. Using narrow (about 50 – 60 mm in diameter) 500 ml beakers and liquid batch volumes of 150 - 250 ml is recommended for best performance.

CHALLENGING PROCESS SETUP EXAMPLES

The following two examples illustrate setup arrangements that can be used for especially challenging processes, such as the production of translucent nanoemulsions with dispersed phase droplet diameters below 100 nanometers. These processes frequently require longer ultrasound exposure times, which may be achieved by reducing liquid flow rates through the reactor, passing the liquid several times through the system (Example 3) or utilizing several in-series reactors (Example 4).

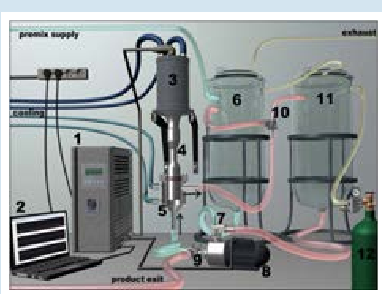

Common Setup Example 3

Schematic is illustrated of a setup appropriate for challenging processes, such as the production of translucent nanoemulsions in which the dispersed phase droplet sizes must be below 100 nanometers. Coarse pre-emulsion (premix) is initially supplied through the "premix supply" line into vessel, **6**. Ultrasonic generator, **1**, controlled by computer, **2**, excites mechanical vibrations in magnetostrictive transducer, **3**, which are amplified by Full-wave Barbell horn, **4**. Pass 1: liquid is drawn from the bottom of vessel, **6**, through valve, **7**, by pump, **8**, which then pushes it into reactor, **5**, through valve, **9**. From there it is deposited into vessel, **11**, through valve, **10**. Pass 2: liquid is drawn from the bottom of vessel, **11**, through valve, **7**, by pump, **8**, which then pushes it into reactor, **5**, through valve, **9**. From there it is deposited into vessel, **6**, through valve, **10**. The process repeats itself for as many passes as needed, and when it is finished, the resulting product comes out through valve, **7**, pump, **8**, and valve, **9**, out of "product exit" line. Nitrogen gas, **12**, maintains inert atmosphere and provides the necessary static pressure.

Common Setup Example 4

Diagram of a translucent nanoemulsion production process is shown in this example, which utilizes a multiple series ultrasonic reactor setup. Oil and aqueous phases are brought together in appropriate

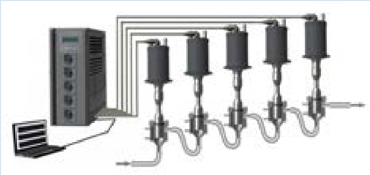

proportions and are sequentially pumped through multiple ultrasonic reactors, each incorporating a magnetostrictive transducer and a Full-wave Barbell horn.

Sitemap Contact Us

Home About ISM Technology Services Ultrasonic Systems Applications Technical Resources

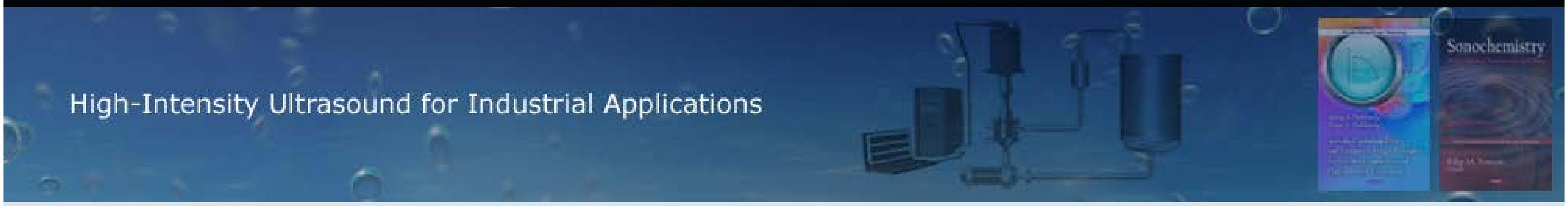

Home → Ultrasonic Systems → High-Efficiency Ultrasonic Liquid Processors

HIGH-EFFICIENCY ULTRASONIC LIQUID PROCESSORS

OVERVIEW

Industrial Sonomechanics, LLC, (ISM) offers bench and commercial-scale ultrasonic liquid processors (ultrasonic homogenizers) able to provide very high ultrasonic amplitudes and cavitation intensities. Application examples include: production of nanoemulsions, nanocrystals and wax nanoparticles for pharmaceutical, cosmetic, food, ink, paint, coating, wood treatment, metalworking, nanocomposite, pesticide, and fuel industries, extraction of oil from algae, production of biofuels, crude oil desulphurization, degassing, cell disruption, polymer and epoxy processing, and more.

ISM's ultrasonic processors are based on Barbell Horn Ultrasonic Technology (BHUT), which makes it possible to implement high-amplitude ultrasound on any scale, form laboratory to industrial, guaranteeing reproducible and predictable results. The processors utilize patented ultrasonic reactor chambers and provide very uniform ultrasonic treatment with no bypass.

1200 W Processor with Air-Cooled Transducer

1200 W bench-scale ultrasonic processor system is designed for batch and flow-through process investigations and small-scale production. The system operates at the frequency of approximately 20 kHz. Barbell horns used in this system have output tip diameters of up to 35 mm and can provide stable operation at output amplitudes up to 120 microns peak-to-peak (below, microns) in aqueous loads at a normal pressure, corresponding to acoustic power intensities up to 80 W/cm^2. This gives investigators a wide range of experimental conditions to determine optimal parameters for even the most challenging ultrasonic processes. The system can be used for small-scale production.

2400 W Processor with Air-Cooled Transducer

2400 W industrial-scale ultrasonic processor system is designed for high-volume continuous-mode commercial production. The system operates at the frequency of approximately 20 kHz. Barbell horns used in this system have large output tip diameters (Ø) and provide very high output amplitudes (A) and output power densities (Pd). For example, for FBH-type horns the following combinations are possible (water up to the nodal point, at 1 bar and 25 ºC):

Ø = 50 mm, A = 120 microns, Pd = 80 W/cm^2;
Ø = 60 mm, A = 85 microns, Pd = 55 W/cm^2;
Ø = 70 mm, A = 60 microns, Pd = 35 W/cm^2.

Other types of Barbell horns can be used as well. These amplitudes and power densities are extremely high and are unprecedented for industrial-scale systems, which are commonly restricted to ultrasonic amplitudes below 25 microns and power densities below 10 W/cm^2. ISM's Barbell Horn Ultrasonic Technology (BHUT) utilized in this processor makes it possible to implement even the most challenging ultrasonic processes in the commercial environment.

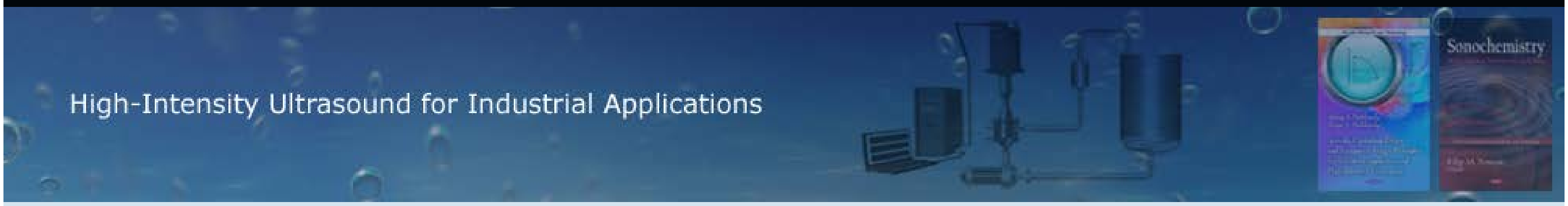

SPECIAL-REQUEST ULTRASONIC LIQUID PROCESSORS

OVERVIEW

Industrial Sonomechanics, LLC, (ISM) offers bench and commercial-scale ultrasonic liquid processors (ultrasonic homogenizers) able to provide very high ultrasonic amplitudes and cavitation intensities. Application examples include: production of nanoemulsions, nanocrystals and wax nanoparticles for pharmaceutical, cosmetic, food, ink, paint, coating, wood treatment, metalworking, nanocomposite, pesticide, and fuel industries, extraction of oil from algae, production of biofuels, crude oil desulphurization, degassing, cell disruption, polymer and epoxy processing, and more.

ISM's ultrasonic processors are based on Barbell Horn Ultrasonic Technology (BHUT), which makes it possible to implement high-amplitude ultrasound on any scale, form laboratory to industrial, guaranteeing reproducible and predictable results. The processors utilize patented ultrasonic reactor chambers and provide very uniform ultrasonic treatment with no bypass.

1000 W Processor with Water-Cooled Transducer

1000 W (output power) bench-top water-cooled ultrasonic system is a "special request" unit, designed for batch and flow-through process investigations and small-scale production. The system operates at the frequency of approximately 22 kHz. FBH-type Barbell horns used in this system have output tip diameters up to 35 mm and can provide stable operation at output amplitudes up to 75 microns in aqueous loads at a normal pressure, corresponding to acoustic power intensities up to 50 W/cm^2. The system is based on a water-cooled magnetostrictive transducer.

2000 W Processor with Water-Cooled Transducer

2000 W (output power) industrial water-cooled ultrasonic system is a "special request" unit, designed for flow-through or batch production on a commercial scale. The system operates at the frequency of approximately 18 kHz. FBH-type Barbell horns used in this system have output tip diameters of 60 mm, with larger diameters (up to 75 mm) available upon request. These horns can provide stable operation at output amplitudes up to 85 microns in aqueous loads at a normal pressure, corresponding to acoustic power intensities up to 55 W/cm^2. The system is able to directly reproduce any laboratory or bench-scale process optimization study in a commercial production environment and is based on a water-cooled magnetostrictive transducer.

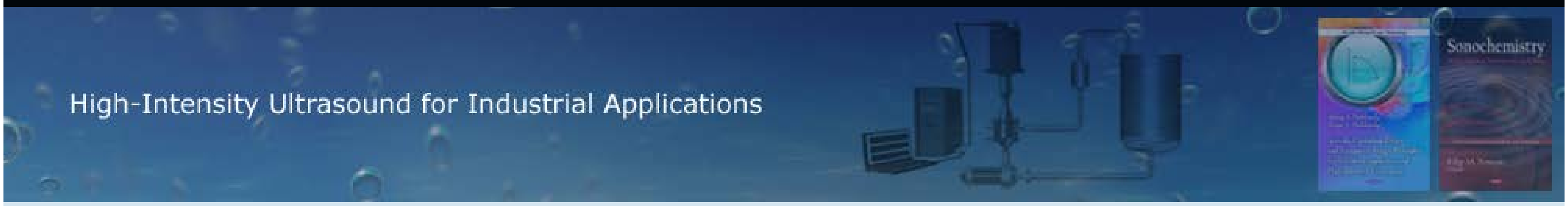

2000 W PROCESSOR WITH WATER-COOLED TRANSDUCER

SYSTEM DESCRIPTION

Industrial Sonomechanics (ISM)' 2000 W (output power) ultrasonic liquid processor system is a "special request" unit, designed for flow-through or batch production on a commercial scale. The system operates at the frequency of approximately 18 kHz. FBH-type Barbell horns used in this system have output tip diameters of 60 mm, with larger diameters (up to 75 mm) available upon request. These horns can provide stable operation at output amplitudes up to 85 microns in aqueous loads at a normal pressure, corresponding to acoustic power intensities up to 55 W/cm^2. The system is able to directly reproduce any laboratory or bench-scale process optimization study in a commercial production environment. Since the scale-up from lab/bench to commercial size can be accomplished without changing any of the optimized parameters, including the amplitude, the process is guaranteed to generate the same reproducible results on the plant floor as it did in the laboratory. The system is based on a water-cooled magnetostrictive transducer, which offers several advantages, as described below.

System Schematic

2000 W flow-through ultrasonic reactor system in its most common configuration is illustrated on the left. Ultrasonic generator, controlled form the front panel interface or (optional) from a computer running Generator Control software, excites vibrations in the magnetostrictive transducer, which are subsequently amplified by the Full-wave Barbell horn. The horn delivers the ultrasonic energy to the liquid, flowing through the reactor chamber. The reactor chamber may include a cooling/heating jacket. The working liquid inlet and outlet valves may be designed to enable adjustable, pressurized (if needed) flow through the ultrasonic reactor chamber (optional). The system can be designed to operate under static pressures of up to 3 atmospheres.

The processor can be configured for use in hazardous environments, such as chemical factories or refineries, by incorporating the following protective features into its magnetostrictive transducer and ultrasonic generator:

1. The transducer can be built without any high-power cable connections. In this configuration, the Teflon-insulated wire wound around its magnetostrictive element continues uninterrupted from the unit all the way to the generator, thereby eliminating any possibility of creating a spark inside a failed connector. In addition, since the unit is water-cooled, any possibility of introducing a hazardous gas into its internal area is eliminated.
2. Two methods of protection may be employed for the ultrasonic generator: a) since generator can be fully monitored and controlled by a computer, it may be kept out of the hazardous area altogether; b) the generator may be designed to be water-cooled, which means that it will not depend on the external air for heat removal. The generator's enclosure can, therefore, be sealed and/or pressurized with an inert gas, eliminating the possibility of introducing external air (possibly with hazardous gasses) into its internal area.

Maximum flow rate through the processor is approximately 10,000 liters/hour (44 gpm). The system design corresponds to the International Patent Application PCT/US2008/068697, "High capacity ultrasonic reactor system". The incorporated Barbell horn design corresponds to the US Patent 7,156,201, "Ultrasonic rod waveguide-radiator".

Photographs of System Components

Photographs are presented of: **1** - magnetostrictive transducer assembled with Full-wave Barbell horn, **2** - magnetostrictive transducer assembled with Full-wave Barbell horn and reactor chamber without a cooling jacket, **3** - Full-wave Barbell horn, **4** – reactor chamber with cooling jacket, **5** – magnetostrictive transducer.

Besides Full-wave Barbell horns (FBH) of the type shown on the left, specialized Half-wave Barbell horns (HBH) and Half-wave Barbell horns with an Opening (HBHO) are available. These horns are shorter and lighter than Full-wave Barbell horns and have shapes that, when incorporated into appropriately designed reactor chambers, ensure that no working liquid bypasses the active cavitation zone.

Half-wave and Barbell horns with an Opening are frequently preferred for the tasks involving high-intensity flow-through ultrasonic processing, such as dispersion and deagglomeration of solid particles, nanoemulsification and the production micronized waxes, where uniform exposure to ultrasound and the resulting narrow particle size distributions are essential. Different types of Barbell horns are described in detail on another page.

Photograph of a Common System Setup

Photograph of a common system setup is presented, where: **1** – 5000 W ultrasonic generator, **2** - magnetostrictive transducer (maximum output power - 2000 W), **3** - Barbell horn and reactor chamber, **4** – liquid pump, **5** – liquid storage tank.

This arrangement is simple and commonly used for processes that require recirculation of the working liquid through the reactor. It is similar to setups in Schematics 1 and 3 illustrated below, but differs from Schematic 1 in that there is no tank for supplying additional components (assuming that the premixing of components is carried out elsewhere) and from Schematic 3 in that it allows the product after each pass to mix with the precursor liquid in the tank. This setup s appropriate for many processes, such as mixing, extraction, homogenization, sonochemstry, and the production of nano-emulsions and nano-dispersions with narrow particle size distributions.

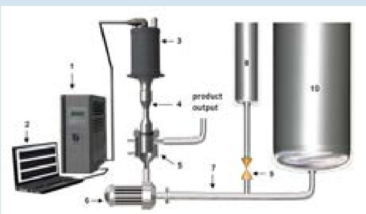

Common Setup Schematic 1

A common setup of the 2000 W ultrasonic system is shown, where: **1** - 5000 W ultrasonic generator; **2** – computer running Generator Control software, **3** - magnetostrictive transducer (maximum output power - 2000 W); **4** - Full-wave Barbell horn; **5** – flow-through reactor chamber; **6** – pump; **7** - pipeline; **8** – tank for supplying additional components; **9** – valve; **10** – main liquid supply tank. This setup may be used for such processes as biodiesel production, nano-emulsification, oil extraction, solid particle dispersing, etc. The product may be collected from the **product output** line or re-circulated into the main liquid supply tank, **10**.

Common Setup Schematic 2

Large batch (1 - 20 liters) processes may be carried out using the setup illustrated in this schematic. The flow-through reactor chamber is replaced by a batch container. The working liquid may be cooled by using a batch container equipped with a water cooling jacket. Ultrasonic generator, **1**, excites vibrations in the magnetostrictive transducer, **2**, which are subsequently amplified using the Full-wave Barbell horn, **3**, and delivered to the working liquid in the batch container, **4**. If desired, the ultrasonic generator may be programmed and the data may be recorded by a computer, **5**, running Generator Control software. This setup may be used for such processes as biodiesel production, nano-emulsification, oil extraction, solid particle dispersing, etc.

CHALLENGING PROCESS SETUP SCHEMATICS

The following two schematics illustrate setup arrangements that can be used for especially challenging processes, such as the production of translucent nanoemulsions with dispersed phase droplet diameters below 100 nanometers. These processes frequently require longer ultrasound exposure times, which may be achieved by reducing liquid flow rates through the reactor, passing the liquid several times through the system (Schematic 3) or utilizing several in-series reactors (Schematic 4).

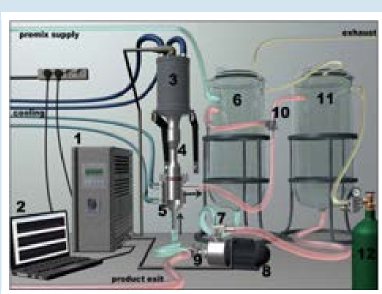

Common Setup Schematic 3

Schematic is illustrated of a setup appropriate for challenging processes, such as the production of translucent nanoemulsions in which the dispersed phase droplet sizes must be below 100 nanometers. Coarse pre-emulsion (premix) is initially supplied through the "premix supply" line into vessel, **6**. Ultrasonic generator, **1**, controlled by computer, **2**, excites mechanical vibrations in magnetostrictive transducer, **3**, which are amplified by Full-wave Barbell horn, **4**. Pass 1: liquid is drawn from the bottom of vessel, **6**, through valve, **7**, by pump, **8**, which then pushes it into reactor, **5**, through valve, **9**. From there it is deposited into vessel, **11**, through valve, **10**. Pass 2: liquid is drawn from the bottom of vessel, **11**, through valve, **7**, by pump, **8**, which then pushes it into reactor, **5**, through valve, **9**. From there it is deposited into vessel, **6**, through valve, **10**. The process repeats itself for as many passes as needed, and when it is finished, the resulting product comes out through valve, **7**, pump, **8**, and valve, **9**, out of "product exit" line. Nitrogen gas, **12**, maintains inert atmosphere and provides the necessary static pressure.

Common Setup Schematic 4

Diagram of a translucent nanoemulsion production process is shown in this example, which utilizes a multiple series ultrasonic reactor setup. Oil and aqueous phases are brought together in appropriate proportions and are sequentially pumped through multiple ultrasonic reactors, each incorporating a

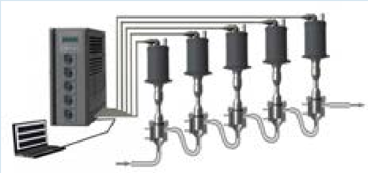

magnetostrictive transducer and a Full-wave Barbell horn.

US 20100296975A1

(19) **United States**
(12) **Patent Application Publication**
(10) **Pub. No.: US 2010/0296975 A1**
(43) **Pub. Date: Nov. 25, 2010**
Peshkovsky et al.

(54) **HIGH CAPACITY ULTRASONIC REACTOR SYSTEM**

(75) Inventors: **Sergei L. Peshkovsky**, New York, NY (US); **Alexey S. Peshkovsky**, New York, NY (US)

Correspondence Address:
BOND, SCHOENECK & KING, PLLC
ONE LINCOLN CENTER
SYRACUSE, NY 13202-1355 (US)

(73) Assignee: **INDUSTRIAL SONOMECHANICS, LLC**, New York, NY (US)

(21) Appl. No.: **12/667,480**

(22) PCT Filed: **Jun. 30, 2008**

(86) PCT No.: **PCT/US08/68697**

§ 371 (c)(1), (2), (4) Date: **Dec. 31, 2009**

Related U.S. Application Data

(60) Provisional application No. 60/947,768, filed on Jul. 3, 2007.

Publication Classification

(51) **Int. Cl.**
B06B 1/00 (2006.01)
G10K 15/04 (2006.01)

(52) **U.S. Cl.** **422/128**; 181/142

(57) **ABSTRACT**

An ultrasonic reactor system with an appropriately designed reactor chamber used in conjunction with a compatible ultrasonic Barbell Horn or its derivative that provides a significant efficiency increase and an intensification of sonochemical and sonomechanical processes is disclosed. These enhancements arise from the ability of the reactor chamber to direct all treated liquid media through the highly active ultrasonic cavitation region located near the surface of the horn, as well as from several improvements in the Barbell Horn design that significantly increase its longevity and in its output surface area, thereby increasing the total size of the active cavitation region.

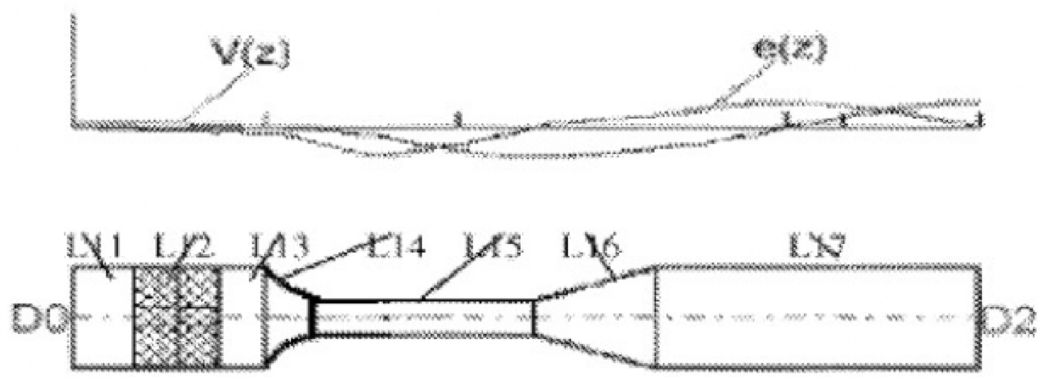

US007156201B2

(12) **United States Patent**
Peshkovskiy et al.

(10) **Patent No.: US 7,156,201 B2**
(45) **Date of Patent: Jan. 2, 2007**

(54) **ULTRASONIC ROD WAVEGUIDE-RADIATOR**

(75) Inventors: **Sergey L. Peshkovskiy**, New York, NY (US); **Michael L. Friedman**, Wayne, NJ (US); **Wilton A. Hawkins**, Montclair, NJ (US)

(73) Assignee: **Advanced Ultrasonic Solutions, Inc.**, Lords Valley, PA (US)

(*) Notice: Subject to any disclaimer, the term of this patent is extended or adjusted under 35 U.S.C. 154(b) by 273 days.

(21) Appl. No.: **10/982,588**

(22) Filed: **Nov. 4, 2004**

(65) **Prior Publication Data**

US 2006/0090956 A1 May 4, 2006

(51) **Int. Cl.**

G10K 11/08	(2006.01)
H03H 9/24	(2006.01)
H04B 11/00	(2006.01)
H03H 9/25	(2006.01)

(52) **U.S. Cl.** **181/175**; 381/338; 310/323.19; 333/145

(58) **Field of Classification Search** 181/175, 181/177, 192, 142; 381/337–340; 310/323.19; 333/145

See application file for complete search history.

(56) **References Cited**

U.S. PATENT DOCUMENTS

3,184,842	A *	5/1965	Maropis	228/111
3,277,404	A *	10/1966	Fabian	333/145
3,524,085	A *	8/1970	Shoh	310/325
3,546,498	A *	12/1970	McMaster et al.	310/323.19
3,568,104	A *	3/1971	Bailey	333/145
3,736,532	A *	5/1973	Armenakas	333/145
3,891,869	A *	6/1975	Scarpa	310/325
3,915,018	A *	10/1975	Karplus	73/647
4,131,505	A *	12/1978	Davis, Jr.	156/580.1
4,337,843	A	7/1982	Wendel	
4,691,724	A *	9/1987	Garcia et al.	134/169 R
4,710,668	A *	12/1987	Fima et al.	310/323.21
4,896,535	A *	1/1990	Duckart et al.	73/290 V
5,112,300	A *	5/1992	Ureche	604/22
5,241,287	A	8/1993	Jen	
5,269,297	A *	12/1993	Weng et al.	606/128
5,289,436	A	2/1994	Terhune	
5,380,274	A *	1/1995	Nita	604/22
5,386,169	A *	1/1995	Dubruque	310/323.19
5,527,273	A *	6/1996	Manna et al.	604/22
5,713,916	A	2/1998	Dias	
5,828,274	A	10/1998	Jen et al.	
6,078,125	A *	6/2000	Roberts	310/325

(Continued)

FOREIGN PATENT DOCUMENTS

GB	2167270	A *	5/1986

Primary Examiner—Edgardo San Martin
(74) *Attorney, Agent, or Firm*—Robert J. Sinnema; Bond, Schoeneck & King, PLLC

(57) **ABSTRACT**

The present invention comprises an ultrasonic resonant rod waveguide-radiator with at least three cylindrical sections, one of which is an entrance section having a planar entrance surface and another of which is an exit section having a planar exit surface, and at least two sections having a variable cross-section. The cylindrical sections and sections of variable cross-section are arranged in alternating fashion and connected to each other acoustically rigidly. The dimensions of the cylindrical sections and the sections of variable cross-section are selected so that the gain of the waveguide-radiator is significantly greater than unity and the strain created by passage of ultrasonic waves through the waveguide-radiator is minimized, increasing the operational life of the waveguide-radiator and maximizing the amount of useful energy transmitted by the waveguide-radiator.

8 Claims, 7 Drawing Sheets

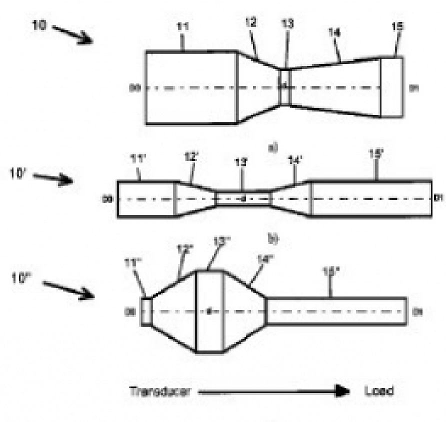

US 20100296975A1

(19) United States

(12) Patent Application Publication

Peshkovsky et al.

(10) Pub. No.: US 2010/0296975 A1

(43) Pub. Date: Nov. 25, 2010

(54) HIGH CAPACITY ULTRASONIC REACTOR SYSTEM

(75) Inventors: **Sergei L. Peshkovsky**, New York, NY (US); **Alexey S. Peshkovsky**, New York, NY (US)

Correspondence Address:
BOND, SCHOENECK & KING, PLLC
ONE LINCOLN CENTER
SYRACUSE, NY 13202-1355 (US)

(73) Assignee: **INDUSTRIAL SONOMECHANICS, LLC**, New York, NY (US)

(21) Appl. No.: **12/667,480**

(22) PCT Filed: **Jun. 30, 2008**

(86) PCT No.: **PCT/US08/68697**

§ 371 (c)(1),
(2), (4) Date: **Dec. 31, 2009**

Related U.S. Application Data

(60) Provisional application No. 60/947,768, filed on Jul. 3, 2007.

Publication Classification

(51) **Int. Cl.**
B06B 1/00 (2006.01)
G10K 15/04 (2006.01)

(52) **U.S. Cl.** **422/128**; 181/142

(57) **ABSTRACT**

An ultrasonic reactor system with an appropriately designed reactor chamber used in conjunction with a compatible ultrasonic Barbell Horn or its derivative that provides a significant efficiency increase and an intensification of sonochemical and sonomechanical processes is disclosed. These enhancements arise from the ability of the reactor chamber to direct all treated liquid media through the highly active ultrasonic cavitation region located near the surface of the horn, as well as from several improvements in the Barbell Horn design that significantly increase its longevity and in its output surface area, thereby increasing the total size of the active cavitation region.

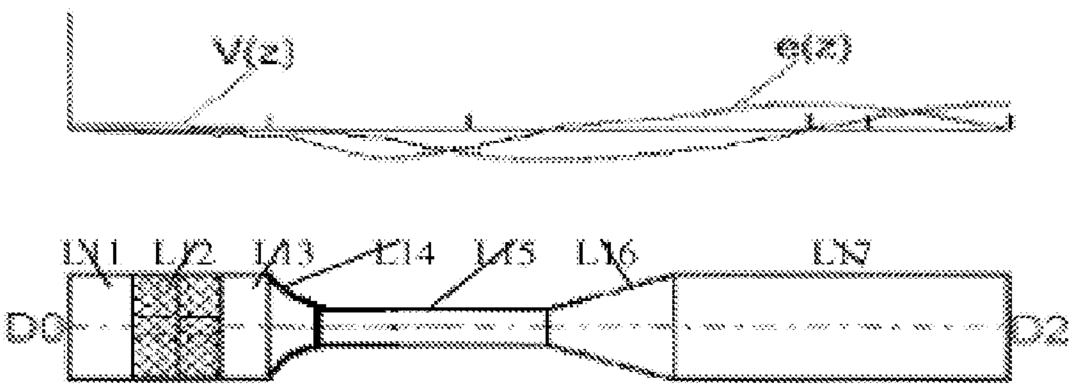

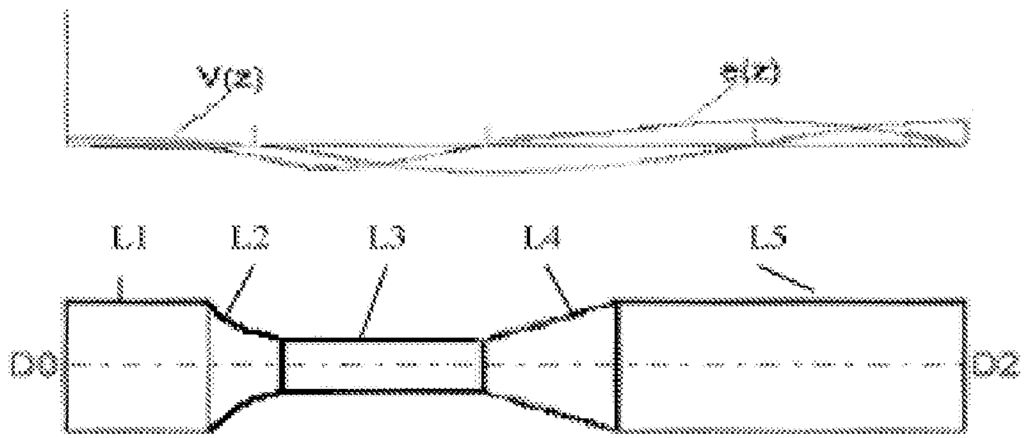

Figure 1

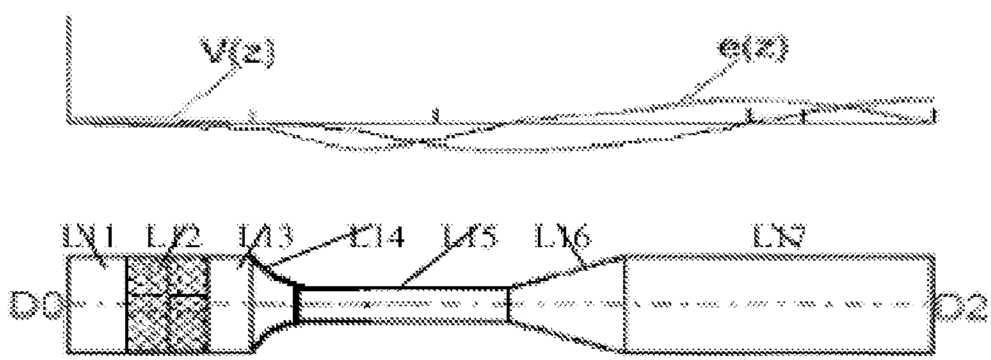

Figure 2

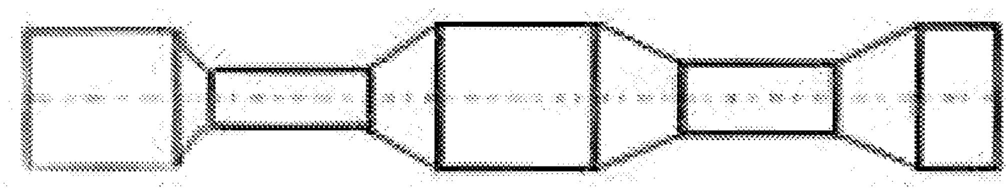

Figure 3

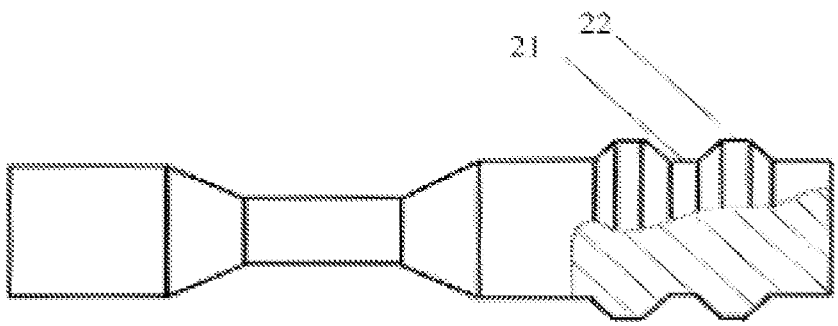

Figure 4

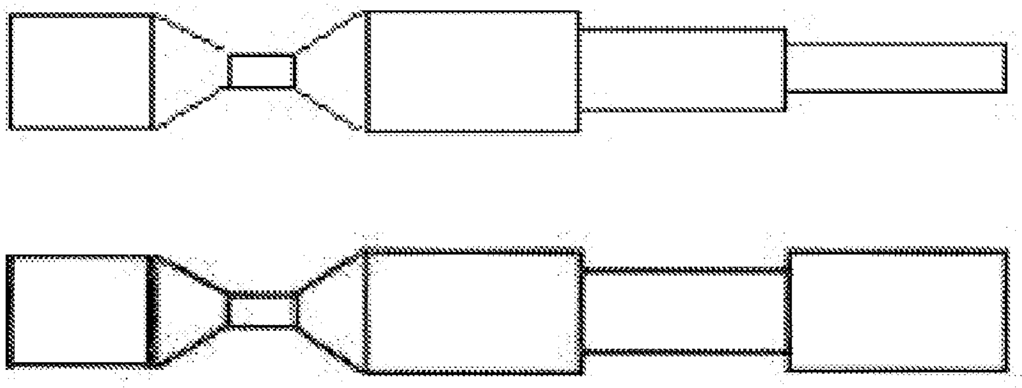

Figure 5

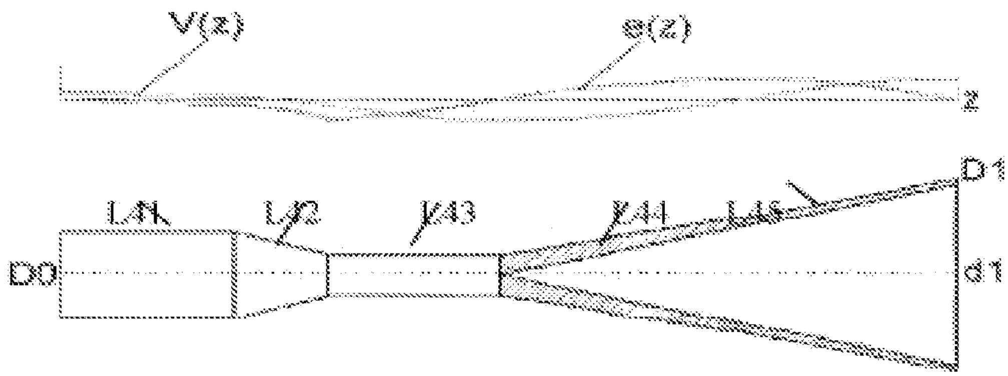

Figure 6

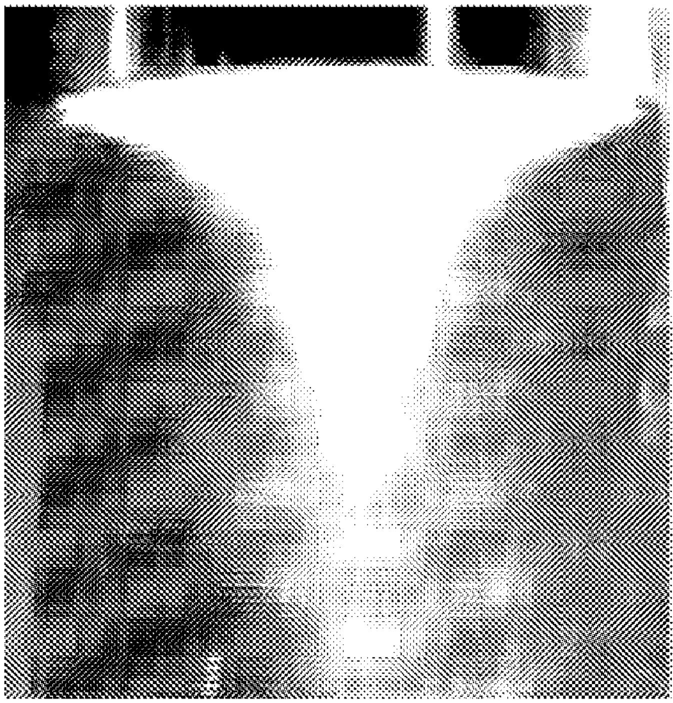

Figure 7

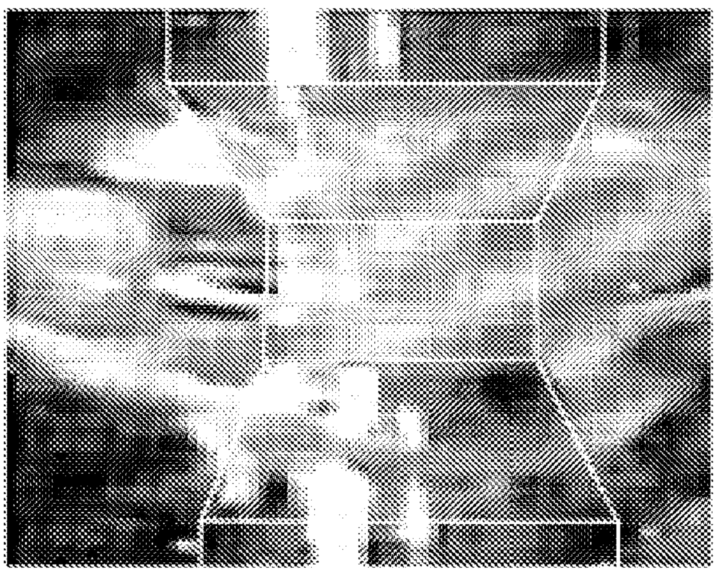

Figure 8

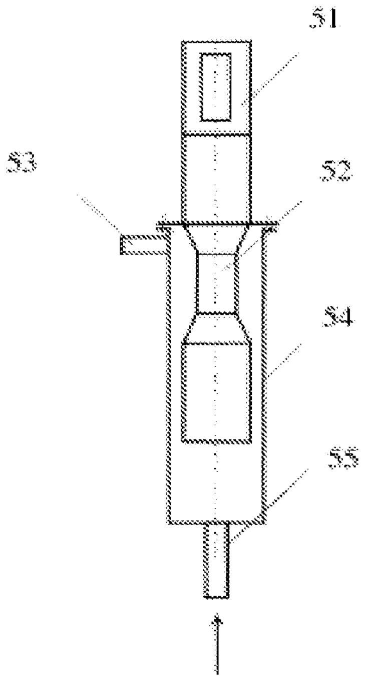

Figure 9

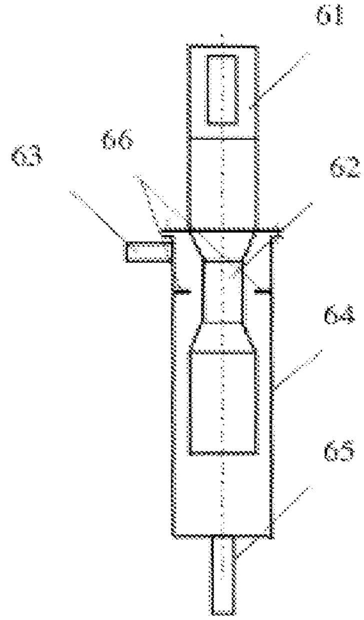

Figure 10

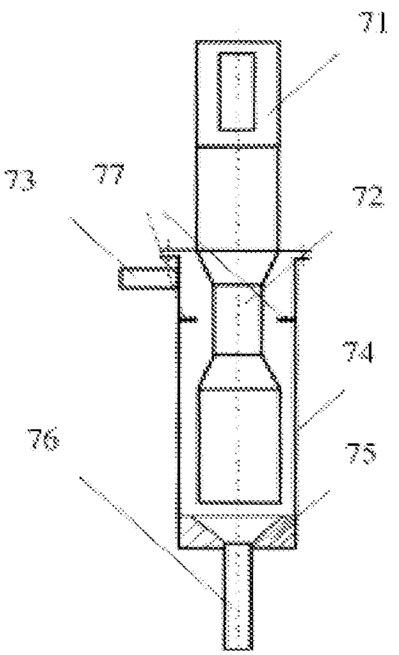

Figure 11

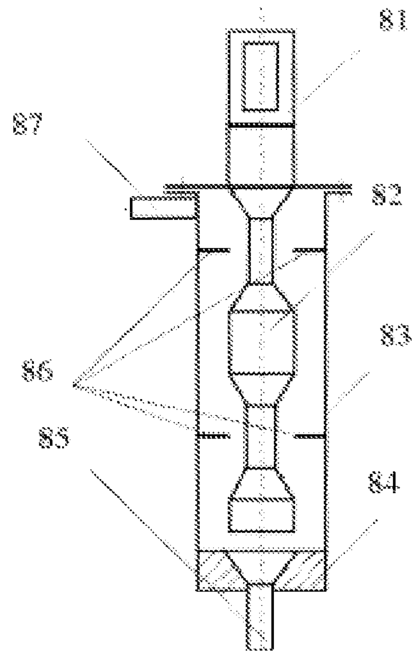

Figure 12

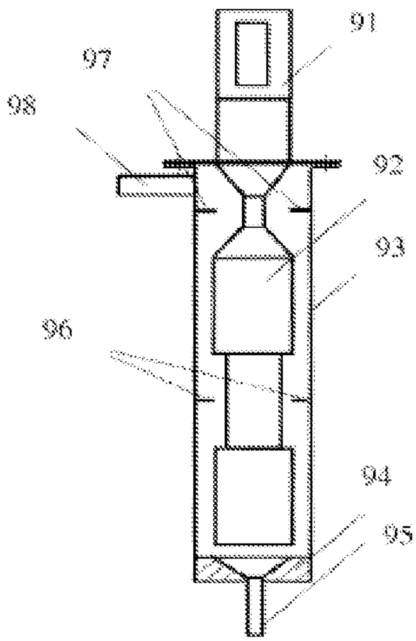

Figure 13

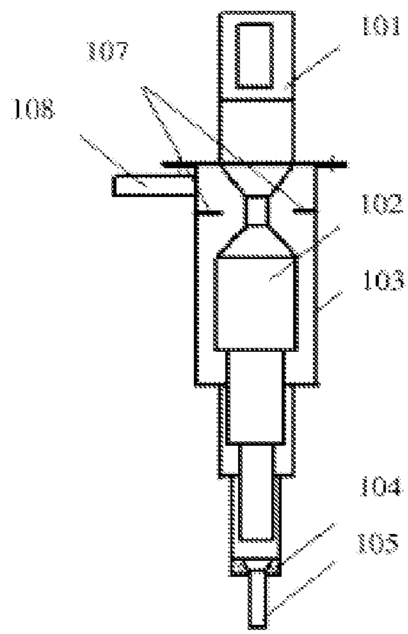

Figure 14

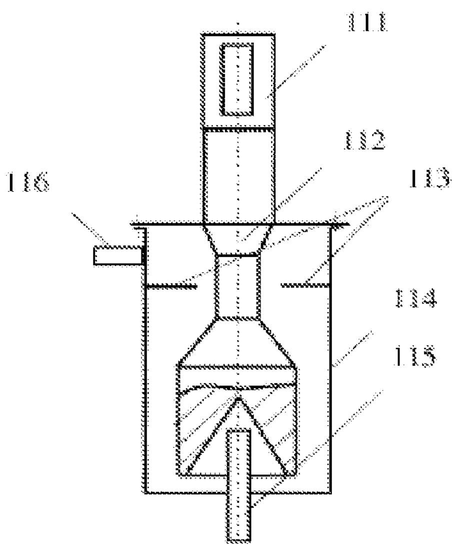

Figure 15

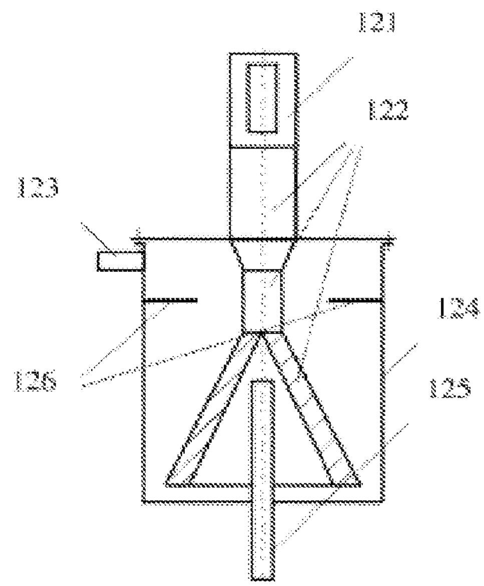

Figure 16

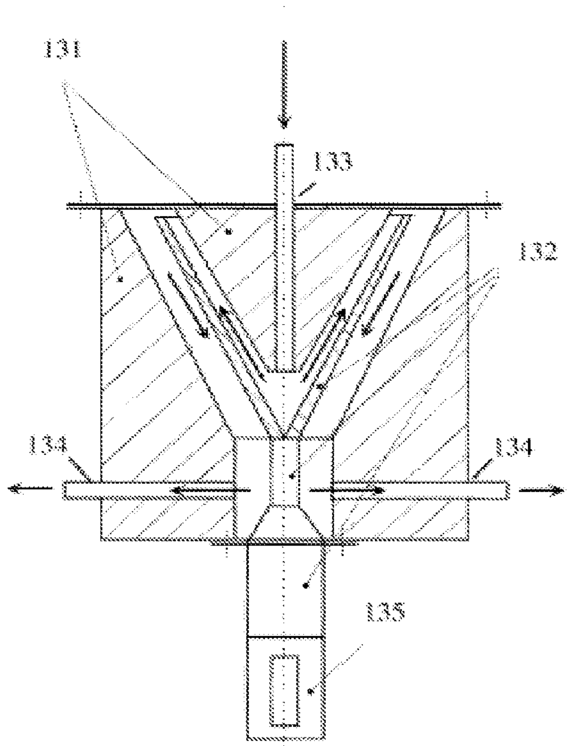

Figure 17

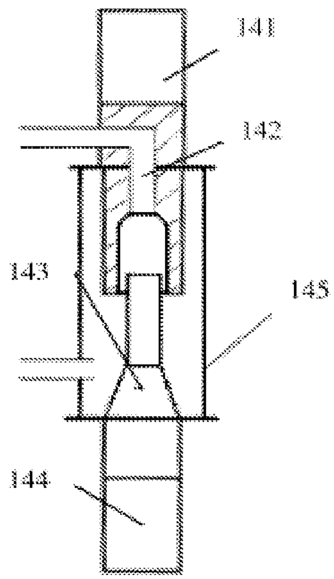

Figure 18

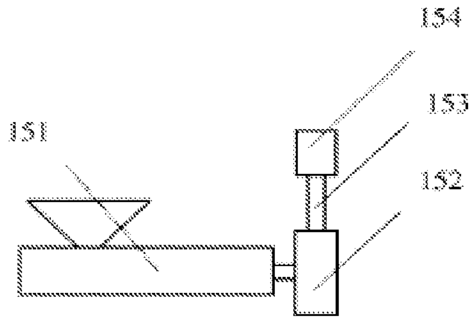

Figure 19

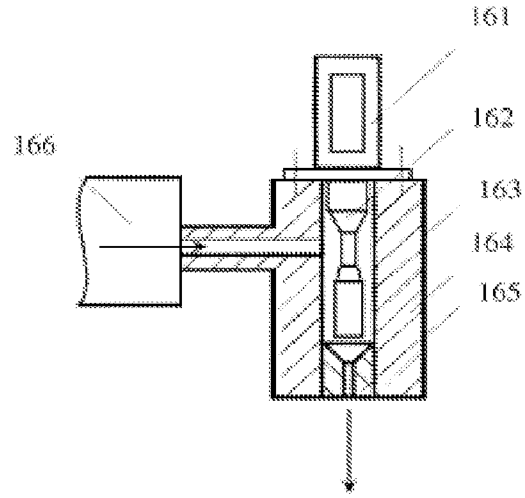

Figure 20

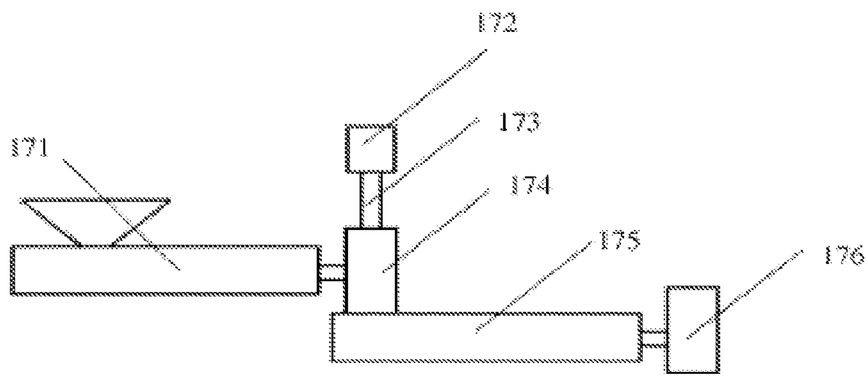

Figure 21

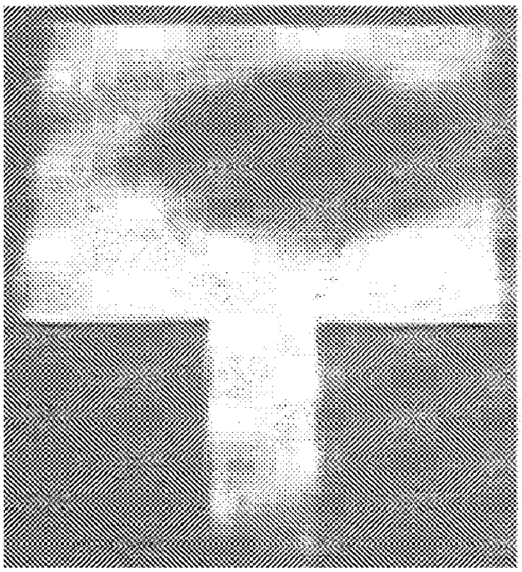

Figure 22

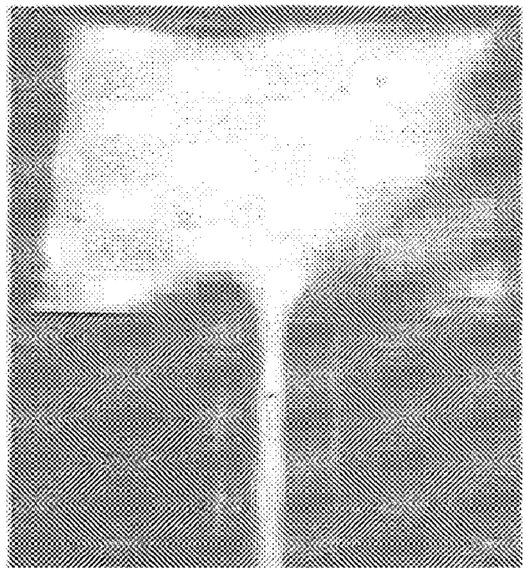

Figure 23

HIGH CAPACITY ULTRASONIC REACTOR SYSTEM

CROSS-REFERENCE TO RELATED APPLICATION

[0001] The present application claims priority to PCT Number PCT/US2008/068697 which claims priority to U.S. Provisional Application No. 60/947,768, filed Jul. 3, 2007.

BACKGROUND OF THE INVENTION

[0002] 1. Field of the Invention

[0003] The present invention relates to the field of ultrasonic equipment and, more specifically, systems for the transmission of acoustic energy into liquid media during acoustic cavitation-based sonochemical and sonomechanical processes.

[0004] 2. Description of the Related Art

[0005] Advantages of using ultrasonically induced acoustic cavitation to carry out technological processes in liquids are well documented, for example, in the following references: K. S. Suslick, Sonochemistry, Science 247, pp. 1439-1445 (1990); T. J. Mason, Practical Sonochemistry, A User's Guide to Applications in Chemistry and Chemical Engineering, Ellis Norwood Publishers, West Sussex, England (1991), hereby incorporated by reference.

[0006] In the prior art ultrasonic systems designed for industrial sonochemical and sonomechanical processes, the liquid commonly is subjected to ultrasonic treatment as it flows through a reactor. The latter commonly consists of a reactor chamber incorporating an ultrasonic waveguide radiator (horn) connected to an electro-acoustical transducer. The horn is used to amplify the transducer's vibration amplitude, which is necessary because the vibration amplitude of the transducer itself is not sufficient for most industrial processes. Such ultrasonic reactor systems are described, for example, in U.S. Published Patent Application No. 2006/0196915, U.S. Published Patent Application No. 2005/0274600 and U.S. Pat. No. 7,157,058, hereby incorporated by reference.

[0007] All of the abovementioned systems possess an important common drawback, which restricts their ability to create powerful ultrasonic cavitation fields and limits their production capacity. This drawback stems from the fact that the acoustic horns used in the prior art generally have tapered shapes, such as conical, exponential, catenoidal, stepped, or more complex, converging in the direction of the load. While these horns may have high gain factors and permit significantly increasing vibration amplitudes, the increase occurs always at the expense of the output surface areas, which become small as a result. Therefore, while converging horns are capable of increasing the specific acoustic power (or vibration amplitude at a given ultrasonic frequency) radiated by a transducer into a load quite effectively, they do not permit achieving significant levels of total radiated acoustic power. The total power provided by a generator and a transducer is, therefore, not efficiently transmitted into the liquid (reflected back). Consequentially, sonochemical reactors based on these horns are effective only on the laboratory scale. Success of industrial applications of such systems is limited. Additionally, in the design of the abovementioned ultrasonic reactors, the size and shape of the cavitation field itself is not taken into account, which further lowers their efficiency.

[0008] In the work by G. Cervant, J.-L. Laborde, et al., "Spatio-Temporal Dynamics of Cavitation Bubble Clouds in a Low Frequency Reactor," Ultrasonic Sonochemistry 8 (2001), 163-174, hereby incorporated by reference, a theoretical study describing the shape, size and position of the cavitation field formed under an ultrasonic radiator is described in detail. In the article by A. Moussatov, R Mettin, C. Granger et all "Evolution of Acoustic Cavitation Structures Near Larger Emitting Surface", WCU 2003, Paris, Sep. 7-10, 2003, hereby incorporated by reference, a similar experimental study was conducted. The results show that during operation of an acoustic horn, a stable well developed cavitation filed only starts to form when the following two necessary conditions are fulfilled: (1) specific intensity of the ultrasonic energy radiated into liquid exceeds 8 W/cm^2 (for water) and (2) the output diameter of the radiator's cross section is on the order of the acoustic wavelength, λ, in the original supplied liquid load (before cavitation has started). In other words, the radiator should transmit a planar acoustic wave into the liquid. In this case, the cavitation field starts to become stable and takes the shape of an upside-down circular cone. It is important to also point out that such stable cavitation field at the described conditions has maximum possible geometrical size. Therefore, only if such stable cavitation field can be established in an ultrasonic reactor will the productivity be maximized and will the optimal stability and the operational quality be reached. The exact size of the cavitation field formed under an ultrasonic radiator was not, however, obtained in the abovementioned studies. Additionally, cavitation formed near the lateral surface of the radiator was not studied.

[0009] Deposition of at least 8 W/cm^2 (for water) of specific acoustic power requires the amplitudes of vibration velocity of the output surface of an acoustic horn to exceed 112 cm/sec (rms) (oscillatory amplitudes exceeding 25 microns peak-to-peak at 20 kHz). Since most materials used to make ultrasonic transducers cannot themselves provide such amplitudes, ultrasonic horns must be utilized, having gain factors of at least 3. Even higher horn gain factors are preferred because most sonochemical or sonomechanical processes require amplitudes that are much greater than this threshold value. Since the speed of sound in most liquids of interest, such as water, oils, alcohols, etc, is on the order of 1500 msec, λ in those liquids at the common working ultrasonic frequencies of 18-22 kHz is about 65-75 mm. As mentioned above, it is necessary that the diameter of the output surface of the horn be close to λ in the liquid load. Consequentially, only the horns that provide high output oscillatory amplitudes (high gain factors) and have large output surface areas simultaneously are truly appropriate for the use in efficient high-capacity industrial ultrasonic reactor systems for sonomechanical and sonochemical processes. None of the common converging horns are, therefore, appropriate.

[0010] A prior art "Barbell Horn" design, U.S. Pat. No. 7,156,201, hereby incorporated by reference, circumvents the abovementioned limitation of converging horns to a large degree, being able to provide high output oscillatory amplitudes (high gain factors) and large output surface areas simultaneously. In the same prior art, a modified version of the Barbell Horn is also introduced, which may be called "Long Barbell Horn." This horn has a very large lateral radiation surface and is also convenient for the use in the efficient high-capacity industrial ultrasonic reactor systems.

[0011] The prior art "Barbell Horn", its derivatives as well as the related ultrasonic reactor designs, however, are subject to some important limitations. U.S. Pat. No. 7,156,201 provides a system of equations that is suitable only for the calculation of the Barbell Horns with cone-shaped transitional sections (parts of the horns that have changing cross-sections). Additionally, a restriction exists in the description and in the claims of the same prior art, requiring that the length of any transitional section be equal or greater than Log(N)/k, where $k=\omega/C$ is the wave number for the transitional section, N is the ratio of the diameters of the thick and the thin cylindrical sections that are adjacent to the transitional section, w is the angular vibration frequency, C is the sound velocity in the horn material at the transitional section (with phase velocity dispersion taken into account). This restriction came from the fact that the specified length of the transitional section is critical from the standpoint of the passage of a longitudinal acoustic wave. Such selection of the length of the transitional section was thought to be necessary to decrease the degree of dynamical strain and stress along the section length and thus to increase the operational life of the waveguide-radiator. The design principles and the calculation method for the horns which are free from this restriction were not available and are not provided in the prior art.

[0012] Additionally, the only ultrasonic reactor designs mentioned in the prior art are those based on the Barbell Horns equipped with additional resonance elements, such as vibrating disks, spheres, helical surfaces, etc. All these additional elements significantly complicate the construction of the Barbell Horns, introduce additional mechanical connections and, therefore, reduce life span and reliability. It is also clear that utilizing the Barbell Horns or any of their modified versions in a non-restricted or an incorrectly restricted volume (reactor chamber) leads to an inefficient process, since not all liquid is put through the well developed cavitation field zone and/or the optimal treatment time in the cavitation field is not reached.

[0013] Therefore, to be able to maximize the effect of the ultrasonic cavitation treatment on a liquid load (pure liquid, liquid mixture, liquid emulsion, suspension of solid particles in a liquid, polymer melts, etc.), a well defined need exists to develop: 1) improved Barbell Horn designs, free from the abovementioned limitations and 2) improved ultrasonic reactor designs in which a Barbell Horn (of a novel design introduced in this invention or of a design described in the prior art) is correctly placed inside a flow-through (or stationary) volume (also called reactor chamber, flow cell, etc.).

BRIEF SUMMARY OF THE INVENTION

[0014] It is therefore a principal object and advantage of the present invention to provide a high-capacity ultrasonic reactor system that increases the total amount of acoustic energy radiated into a liquid medium by the ultrasonic reactor system.

[0015] It is an additional object and advantage of the present invention to provide a high-capacity ultrasonic reactor system that increases the available radiation surface and the uniformity of the distribution of acoustic energy throughout the volume of an ultrasonic reactor system.

[0016] It is a further object and advantage of the present invention to provide a high-capacity ultrasonic reactor system that increases the intensity of acoustic energy radiated into the liquid medium of an ultrasonic reactor system.

[0017] It is another object and advantage of the present invention to provide a high-capacity ultrasonic reactor system that maximizes the transfer efficiency of the ultrasonic generator's electric energy into the acoustic energy radiated into the liquid medium.

[0018] It is an additional object and advantage of the present invention to provide a high-capacity ultrasonic reactor system that improves the quality of operation and to increase the operational lifespan of the ultrasonic horn incorporated in the ultrasonic reactor system.

[0019] It is a further object and advantage of the present invention to provide a high-capacity ultrasonic reactor system that maximizes the production capacity of the ultrasonic reactor system.

[0020] In accordance with the foregoing objects and advantages, the present invention provides several novel designs of Barbell Horns and further provides several novel ultrasonic reactor systems with appropriately designed reaction chambers used in conjunction with compatible ultrasonic Barbell Horns. The use of these novel ultrasonic reactor system designs significantly increases the efficiency of the systems and greatly intensifies the sonochemical and sonomechanical processes. These enhancements occur primarily due to the resulting ability to direct all treated liquid media through the highly active cavitation region located near the surface of the Barbell Horns, as well as due to the improvements in the horn designs providing significant increase in their output surface areas and, therefore, increasing the size of the active cavitation regions, while increasing their longevity by drastically improving the associated strain and stress distributions.

[0021] In the first embodiment of the present invention a novel Barbell Horn design is introduced, in which the first transitional section is short (shorter than the value Log(N)/k) and has a catenoidal shape (referred to herein as the Catenoidal Barbell Horn).

[0022] In the second embodiment of the present invention a novel Transducer-Barbell Horn Assembly design is introduced, in which the first transitional section is short and has a catenoidal shape (referred to herein as the Catenoidal Transducer-Barbell Horn Assembly).

[0023] In the third embodiment of the present invention a novel Long Barbell Horn design is introduced, in which the first (and, optionally, the second) transitional section is short and has a catenoidal shape. Additionally, piezoelectric annular transducers may be incorporated close to the nodal locations of this horn (referred to herein as the Catenoidal Long Transducer-Barbell Horn Assembly).

[0024] In the fourth embodiment of the present invention a novel Barbell Horn design is introduced, in which the output cylindrical section has a series of specially positioned grooves and protrusions (referred to herein as the Patterned Barbell Horn). The first transitional section of this horn may have any of the shapes described in U.S. Pat. No. 7,156,201 or a short catenoidal shape as described in the present invention. Additionally, piezoelectric annular transducers may be incorporated close to the nodal locations of this horn (referred to herein as the Patterned Transducer-Barbell Horn Assembly).

[0025] In the fifth embodiment of the present invention a novel Barbell Horn design is introduced, in which additional radiating cylindrical sections of different diameters are incorporated (referred to herein as the Extended Barbell Horn). The first transitional section of this horn may have any of the shapes described in U.S. Pat. No. 7,156,201 or a short catenoidal shape as described in the present invention. Additionally, piezoelectric annular transducers may be incorporated close to the nodal locations of this horn (referred to herein as the Extended Transducer-Barbell Horn Assembly).

[0026] In the sixth embodiment of the present invention a novel Barbell Horn design is introduced, in which a hollow region in one or two last sections (the last output section and the section adjacent to it) exists, called the short or the long hollow region, respectively. The first transitional section of this horn may have any of the shapes described in U.S. Pat. No. 7,156,201 or a short catenoidal shape as described in the present invention. Additionally, piezoelectric annular transducers may be incorporated close to the nodal locations of this horn (referred to herein as the Hollow Transducer-Barbell Horn Assembly).

[0027] In all of the subsequent embodiments of the present invention, the novel ultrasonic reactor designs are based on Barbell Devices (Barbell Horns or Transducer-Barbell Horn Assemblies). In some of the embodiments, the novel ultrasonic reactor designs are based on the prior art Barbell Devices, which are the Barbell Horn, the Long Barbell Horn or the corresponding Transducer-Barbell Horn Assemblies with long first transitional sections. In other embodiments, the novel designs of the Barbell Devices (Catenoidal Barbell Horn, Catenoidal Long Barbell Horn, Patterned Barbell Horn, Extended Barbell Horn, Hollow Barbell Horn or the corresponding Transducer-Barbell Horn Assemblies) are used as a basis of the novel complementary ultrasonic reactor designs.

[0028] In all of the subsequent embodiments of the present invention, the utilized Barbell Device has an output diameter that is close to the acoustic wavelength, λ, in a given liquid before cavitation at a given ultrasonic frequency.

[0029] In all of the subsequent embodiments of the present invention, the specific radiated acoustic power is not less than 10 W/cm^2.

[0030] In all of the subsequent embodiments of the present invention, a Barbell Device is incorporated into a reaction chamber

[0031] In the seventh embodiment of the present invention the distance between the radiating surface of the horn and the bottom of the reactor chamber is close to the acoustic wavelength, λ, in a given liquid at a given ultrasonic frequency, the volume of liquid in the active cavitation field is close to $\lambda^3/4$, and the reactor chamber is attached to the Barbell Device, such as the Barbell Horn, Catenoidal Barbell Horn, Patterned Barbell Horn or the any of the corresponding Transducer Barbell Horn Assemblies, with a hermetically tight connection at a node of its acoustic vibrations.

[0032] In the eighth embodiment of the present invention, a circular reflection surface is attached to an internal wall of the flow-through reactor chamber, which directs the entire flow of the liquid through the additional cavitation field formed near the lateral surface of the Barbell Device at its narrow part.

[0033] In the ninth embodiment of the present invention, the Barbell Device is inserted into a reactor chamber, which at the bottom has an upside-down circular cone insert with an opening at the top containing a liquid inlet/outlet valve. The height of this cone and the diameter of its base are close to λ, its volume—to $\lambda^3/4$. The abovementioned circular reflection surface may also be used in conjunction with this embodiment.

[0034] In the tenth embodiment of the present invention, the ultrasonic flow-through reactor incorporates a Long Barbell Horn, a Catenoidal Long Barbell Horn or a corresponding Long Transducer Barbell Horn Assembly. The abovementioned circular reflection surface(s) and the upside-down circular cone insert may also be used in conjunction with this embodiment.

[0035] In the eleventh embodiment of the present invention, the ultrasonic flow-through reactor incorporates an Extended Barbell Horn (or Extended Transducer Barbell Horn Assembly). The abovementioned circular reflection surface(s) and the upside-down circular cone insert may also be used in conjunction with this embodiment.

[0036] In the twelfth embodiment of the present invention, the ultrasonic flow-through reactor incorporates a different version of the Extended Barbell Horn (or Extended Transducer Barbell Horn Assembly). The abovementioned circular reflection surface(s) and the upside-down circular cone insert may also be used in conjunction with this embodiment.

[0037] In the thirteenth embodiment of the present invention, the ultrasonic flow-through reactor incorporates a Hollow Barbell Horn (or Hollow Transducer Barbell Horn Assembly), with a short hollow region (in its output section only). The liquid is supplied near the top of the hollow region into the cavitation field formed inside the hollow region.

[0038] In the fourteenth embodiment of the present invention, the ultrasonic flow-through reactor incorporates a Hollow Barbell Horn (or Hollow Transducer Barbell Horn Assembly), which incorporates a long hollow region (in the last output section and the section adjacent to it). The liquid is supplied near the top of the hollow region into the cavitation field formed inside the hollow region.

[0039] In the fifteenth embodiment of the present invention, the ultrasonic flow-through reactor incorporates a Hollow Barbell Horn (or Hollow Transducer Barbell Horn Assembly), which incorporates a long hollow region. The reactor chamber is modified such that all liquid is directed into the highest intensity cavitation zone. An upside-down position of this reactor is preferably utilized. The liquid is supplied near the top of the hollow region into the cavitation field formed inside the hollow region.

[0040] In the sixteenth embodiment of the present invention, the ultrasonic flow-through reactor incorporates a Hollow Barbell Horn (or Hollow Transducer Barbell Horn Assembly) with a short or long hollow region and a generic horn of an arbitrary design. The horns are arranged such that the generic horn fits inside the Hollow Barbell Horn (or Hollow Transducer Barbell Horn Assembly). The horns are operated in-phase, thereby increasing the cavitation field intensity.

[0041] In the seventeenth embodiment of the present invention, the ultrasonic flow-through reactor is designed to be suitable for processing high-viscosity viscoelastic liquids, such as polymer melts. Polymer melt is supplied from the polymer extruder into the heated reactor at the narrow region of the Barbell Device, such that the upper cylindrical element of the Barbell Device, which is inserted into the reactor body on a sliding sealed connection with minimal gap. The shaping device of the reactor has an entrance region in the shape of an upside-down circular cone. Cascade extrusion arrangements are also possible to use in conjunction with this embodiment.

[0042] In the eighteenth embodiment of the present invention, the ultrasonic flow-through reactor is designed to be suitable for the processing of chemically aggressive liquids, extremely high-purity compounds, as well as for operation in electromagnetic, magnetic, electric, microwave, etc, fields in which the use of metallic objects is undesirable or impossible. Ultrasonic radiation in such a reactor is performed using a Barbell Device (possibly with an additional acoustically rigidly connected waveguide-radiator) made from a nonmetallic material, such as technical corundium material, Al_2O_3, (for example, sapphire, leucosapphire, ruby, etc.)

BRIEF DESCRIPTION OF THE DRAWINGS

[0043] The present invention will be more fully understood and appreciated by reading the following Detailed Description in conjunction with the accompanying drawings, in which:

[0044] FIG. **1** is a Catenoidal Barbell Horn according to one embodiment of the present invention.

[0045] FIG. **2** is a Catenoidal Transducer Barbell Horn Assembly according to another embodiment of the present invention.

[0046] FIG. **3** is a Catenoidal Long Barbell Horn (or Catenoidal Long Transducer Barbell Horn Assembly) according to another embodiment of the present invention.

[0047] FIG. **4** is a Patterned Barbell Horn (or Patterned Transducer Barbell Horn Assembly) according to another embodiment of the present invention.

[0048] FIG. **5** is two versions of an Extended Barbell Horn (or Extended Transducer Barbell Horn Assembly) according to another embodiment of the present invention.

[0049] FIG. **6** is a Hollow Barbell Horn (or Hollow Transducer Barbell Horn Assembly) according to another embodiment of the present invention.

[0050] FIG. **7** is a photograph of a well-developed stable cavitation field created in water under the output radiating surface of a Barbell Device.

[0051] FIG. **8** is a photograph of a stable cavitation field created in water near the lateral surface of a Barbell Device.

[0052] FIG. **9** is a flow-through ultrasonic reactor based on a Barbell Device, such as the Barbell Horn, Catenoidal Barbell Horn, Patterned Barbell Horn or the any of the corresponding Transducer Barbell Horn Assemblies, according to another embodiment of the present invention.

[0053] FIG. **10** is a flow-through ultrasonic reactor based on a Barbell Device, such as the Barbell Horn, Catenoidal Barbell Horn, Patterned Barbell Horn or the any of the corresponding Transducer Barbell Horn Assemblies, according to another embodiment of the present invention.

[0054] FIG. **11** is a flow-through ultrasonic reactor based on a Barbell Device, such as the Barbell Horn, Catenoidal Barbell Horn, Patterned Barbell Horn or the any of the corresponding Transducer Barbell Horn Assemblies, according to another embodiment of the present invention.

[0055] FIG. **12** is a flow-through ultrasonic reactor based on a Long Barbell Horn, a Catenoidal Long Barbell Horn or a corresponding Long Transducer Barbell Horn Assembly, according to another embodiment of the present invention.

[0056] FIG. **13** is a flow-through ultrasonic reactor based on an Extended Barbell Horn (or Extended Transducer Barbell Horn Assembly), according to another embodiment of the present invention.

[0057] FIG. **14** is a flow-through ultrasonic reactor based on another version of an Extended Barbell Horn (or Extended Transducer Barbell Horn Assembly), according to another embodiment of the present invention.

[0058] FIG. **15** is a flow-through ultrasonic reactor based on a Hollow Barbell Horn (or Hollow Transducer Barbell Horn Assembly) with a short internal hollow region according to another embodiment of the present invention.

[0059] FIG. **16** is a flow-through ultrasonic reactor based on a Hollow Barbell Horn (or Hollow Transducer Barbell Horn Assembly) with a long internal hollow region according to another embodiment of the present invention.

[0060] FIG. **17** is another version of a flow-through ultrasonic reactor based on a Hollow Barbell Horn (or Hollow Transducer Barbell Horn Assembly) with a long internal hollow region according to another embodiment of the present invention.

[0061] FIG. **18** is a flow-through ultrasonic reactor based on a Hollow Barbell Horn (or Hollow Transducer Barbell Horn Assembly) with a short or a long internal hollow region and a generic horn operating in-phase according to another embodiment of the present invention.

[0062] FIG. **19** is a schematic of a device for treatment of high-viscosity polymer melts with high-intensity ultrasound according to another embodiment of the present invention.

[0063] FIG. **20** is an expanded view of a flow-through ultrasonic reactor for treatment of high-viscosity polymer melts with high-intensity ultrasound according to another embodiment of the present invention.

[0064] FIG. **21** is a schematic of a device for the treatment of high-viscosity polymer melts with high-intensity ultrasound based on the principle of cascade extrusion according to another embodiment of the present invention.

[0065] FIG. **22** is a photograph of a cavitation field formed in static high-viscosity polymer melt formed under the output radiating surface of a Barbell Device.

[0066] FIG. **23** is a photograph of a cavitation field formed in high-viscosity polymer melt flowing through a transparent shaping channel, formed under the output radiating surface of a Barbell Device.

DETAILED DESCRIPTION OF THE INVENTION

Embodiment 1

Catenoidal Barbell Horn

[0067] U.S. Pat. No. 7,156,201 provides a system of equations that is suitable only for calculating the Barbell Horns (or Transducer Barbell Horn Assemblies) with cone-shaped transitional sections (parts of the horns that have changing cross-sections). Additionally, a restriction exists in the description and in the claims of the same prior art, requiring that the length of any transitional section be equal or greater than Log(N)/k, where $k=\omega/C$ is the wave number, N is the ratio of the diameters of the thick and the thin cylindrical sections that are adjacent to the transitional section, w is the angular vibration frequency, C is the sound velocity in the horn material at the transitional section (with phase velocity dispersion taken into account). This restriction came from the fact that the specified length of the transitional section is critical from the standpoint of the passage of a longitudinal acoustic wave. Such selection of the length of the transitional section was thought to be necessary to decrease the degree of dynamical strain and stress along the section length and thus to increase the operational life of the waveguide-radiator. The design principles and the calculation method for the horns which are free from this restriction were not available and are not provided in the prior art.

[0068] In the present invention it has been determined that when the cross-section of the transitional section changes according to a more complex pattern, such as the catenoidal law, the degree of dynamical strain and stress along the section length does not reach dangerous levels even when the section is shorter than the abovementioned restriction. This stems from the fact that when the transitional section's cross-sectional diameter changes according to the catenoidal law, a very smooth transition into the surface of the adjacent cylindrical section is always achieved. The transitional section length values corresponding to the condition L<Log(N)/k, where the operator Log is a natural logarithm, are critical with respect to the value of k, which becomes imaginary for the exponential transitional section shapes. For the catenoidal transitional section shapes, the value k becomes imaginary at lower values of L, specifically L<Arch(N)/k, where the operator ch is a hyperbolic cosign. Since in this case the value of k=i|k| is imaginary, the equations provided in U.S. Pat. No. 7,156,201 can be also used for the calculations of the Barbell Horns with catenoidal transitional sections if the trigonometric functions are replaced by the hyperbolic functions. Using such calculations it is possible to construct a Catenoidal Barbell Horn that has a significantly shorter transitional section than Log(N)/k without high dynamical stains and/or stresses.

[0069] The following example provides clarification of the abovementioned theoretical explanation. Catenoidal Barbell Horn was calculated for the operation frequency of 20 kHz, having catenoidal first transitional section of the length significantly smaller than the value Log(N)/k. FIG. **1** shows a Catenoidal Barbell Horn according to the first embodiment of the present invention, where V(z)—distribution of the amplitude of vibration velocity along the horn length, e(z)—distribution of the deformation along the horn length, with lengths L**1**-L**5** representing the lengths of the corresponding horn elements, respectively. In a preferred embodiment, the Catenoidal Barbell Horn has the following lengths: L**1**=54.33 mm, L**2**=20.61 mm, L**3**=54.33 mm, L**4**=41.22 mm, L**5**=106.71 mm, Gain=5.16, D**0**=D**2**=50 mm, Freq=20 kHz, and is made from 2024 aluminum. It can be seen from the figure that although the transitional section L**2** is significantly shorter than Log(N)/k, the deformation change along the horn is smooth and continuous, without any dangerous discontinuities associated with high degrees of strain and stress. The calculated horn was constructed and tested, showing excellent correlation of its properties with those predicted in the calculations.

Embodiment 2

Catenoidal Transducer-Barbell Horn Assembly

[0070] Barbell Horn incorporating an active acoustic transducer for converting electric energy into acoustic energy was described in U.S. Pat. No. 7,156,201. In this device, piezoelectric annular transducers are situated in the Barbell Horn close to the node locations, and, because the utilized Barbell Horn has a gain factor greater than unity, the amplitude of the vibrations at the output end of the assembly is much higher than the amplitude of the vibrations of the piezoelectric annular transducers themselves.

[0071] The first transitional section of this device, however, was limited to having a conical shape and the length equal or greater than the value Log(N)/k (Conical Transducer-Barbell Horn Assembly). In the present invention, a Catenoidal Transducer-Barbell Horn Assembly is introduced, having catenoidal first transitional section of the length significantly smaller than the value Log(N)/k. FIG. **2** shows this assembly along with the distributions of the amplitude of vibration velocity, V(z), and deformation, e(z), along the assembly's length, with L**11**-L**17**—indicating the lengths of the corresponding assembly elements, respectively. In a preferred embodiment, the Catenoidal Transducer-Barbell Horn Assembly has the following dimensions: L**11**=17.96 mm, L**12**=32.00 mm, L**13**=12.3 mm, L**14**=20.6 mm, L**15**=49.46 mm, L**16**=41.22 mm, L**17**=106.71 mm, G=6.07, D**0**=D**2**=50 mm, d=20 mm, F=20 kHz, and is made from 2024 aluminum and APC 841 ceramic (APC International Ltd., USA). The drawing shows that although the transitional section L**4** is significantly shorter than Log(N)/k, the deformation change along the assembly is smooth and continuous, without any dangerous discontinuities associated with high degrees of strain and stress. The calculated assembly was constructed and tested, showing excellent correlation of its properties to those predicted in the calculations.

Embodiment 3

Catenoidal Long Barbell Horn (Catenoidal Long Transducer-Barbell Horn Assembly)

[0072] A modification of the Barbell Horn was described in U.S. Pat. No. 7,156,201, in which radiation occurs also from the side surface. The horn is made in the form of alternating cylindrical sections and sections of variable cross-section. The surfaces of the sections of variable cross-section have components of the amplitude of vibrations that are directed perpendicular to the horn's main axis. In addition, the lengths of the horn sections are calculated in such a way that the components of the vibration amplitude of the sections of variable cross-section that are directed along the waveguide axis are oriented toward each other. In this manner, a strong lateral radiation of the waveguide-radiator is achieved. Since there are no theoretical limitations on the total length of the horn, the total area of its side radiating surface can be arbitrarily large corresponding to an arbitrarily large amount of the total acoustic energy radiated into a liquid. The first transitional section of this device, however, was limited to having a conical shape and the length equal or greater than the value Log(N)/k. In the present invention, a Catenoidal Long Barbell Horn is introduced, having catenoidal first transitional section of the length significantly shorter than the value Log(N)/k, as shown in FIG. **3**. Additionally, piezoelectric annular transducers may be incorporated close to the nodal locations of this horn converting it into a Catenoidal Long Transducer-Barbell Horn Assembly.

Embodiment 4

Patterned Barbell Horn (Patterned Transducer-Barbell Horn Assembly)

[0073] To increase the total radiating surface of a Barbell Horn and, therefore, to achieve an increase in the total radiated energy, additional radiating elements, such as resonant plates and spheres may be used, such as described in U.S. Pat. No. 7,156,201. The elements may be acoustically rigidly connected to the horn using welding, soldering or threaded connections. However, because the elements are not machined as integral parts of the horns, but are attached afterwards, the resulting horns have "weak spots" at the connections and could break at high vibration amplitudes during which they undergo significant sign-changing deformations.

[0074] In the present invention, a Barbell Horn design is introduced incorporating additional radiating elements, which are machined as integral parts of the horn, as shown in FIG. **4**. The output cylindrical section of the device is given a series of specially positioned grooves **21**, and protrusions **22**, which may be horizontal (orthogonal to the main horn axis) or be arranged as intersecting right-hand and left-hand screw threads positioned at an angle to the main horn axis. This system of grooves and protrusions permits significantly increasing total radiated acoustic energy from the side surface of the device and enhances the ultrasonic effect on the liquid load as it moves inside the reactor chamber. The first transitional section of this horn may have any of the shapes described in U.S. Pat. No. 7,156,201 or a short catenoidal shape as described in the present invention. Additionally, piezoelectric annular transducers may be incorporated close to the nodal locations of this horn converting it into a Patterned Transducer-Barbell Horn Assembly.

Embodiment 5

Extended Barbell Horn (Extended Transducer-Barbell Horn Assembly)

[0075] To increase the total radiating surface of a Barbell Horn and, therefore, to achieve an increase in the total radiated energy, additional radiating cylindrical sections of different diameters may be incorporated, preferably machined as integral parts of the horn as seen in FIG. **5**. This horn has additional radiating surfaces orthogonal to its main axis, formed due to the differences in the diameters of the cylindrical sections, which are mainly responsible for the increased radiation of acoustic energy. The first transitional section of this horn may have any of the shapes described in U.S. Pat. No. 7,156,201 or a short catenoidal shape as described in the present invention. Additionally, piezoelectric annular transducers may be incorporated close to the nodal locations of the horn converting it into an Extended Transducer-Barbell Horn Assembly.

Embodiment 6

Hollow Barbell Horn (Hollow Transducer-Barbell Horn Assembly)

[0076] From the theory of acoustics, it follows that the cross-sectional diameter of any ultrasonic horn is required to be smaller than approximately $\lambda/4$, where λ is the ultrasound wavelength in the horn material. This, however, relates only to the "live" cross-section, or that actually filled with horn material. If a part of the cross-section is formed by a hollow region, that part should not be included in this restriction. This important condition permits calculating a Barbell Horn with a short hollow region in its last output section or a long hollow region in its last output section and the section adjacent to it, as shown in FIG. **6**, where V(z)—distribution of the amplitude of vibration velocity along the horn length, e(z)—distribution of the deformation along the horn length, with L**41**-L**45** indicating the lengths of the corresponding horn elements, respectively. It is important to point out that in this case the total diameter of the output section of the horn may be much greater than $\lambda/4$ even at a high gain factor. The main radiating surface of the horn during its operation in a liquid load, therefore, becomes the cumulative side surface of its hollow region, including both the outside and the inside surfaces, since both are positioned at a significant angle to the main horn axis and, therefore, have large longitudinal vibration components. The cumulative radiating surface of this horn and, therefore, its total radiated acoustic energy may be much greater than those of a common Barbell Horn. The longevity and reliability of this horn is also very high because it is machined as one integral unit. The first transitional section of this horn may have any of the shapes described in U.S. Pat. No. 7,156,201 or a short catenoidal shape as described in the present invention. Additionally, piezoelectric annular transducers may be incorporated close to the nodal locations of the horn converting it into a Hollow Transducer-Barbell Horn Assembly.

[0077] FIG. **7** is an experimentally obtained photograph of a well developed stable cavitation field created in an unrestricted volume of water under the output radiating surface of a Barbell Device, having the following operational parameters: output surface diameter—65 mm, ultrasound frequency—18 kHz, specific acoustic power—20 W/cm^2.

[0078] FIG. **8** is an experimentally obtained photograph of a stable cavitation field created in an unrestricted volume of water near the lateral surface of a Barbell Device (marked with a white line), having the following operational parameters: output surface diameter—65 mm, ultrasound frequency—18 kHz, specific acoustic power—20 W/cm^2.

Embodiment 7

Ultrasonic Reactor Based on a Barbell Device, Such as the Barbell Horn, Catenoidal Barbell Horn, Patterned Barbell Horn or the any of the Corresponding Transducer Barbell Horn Assemblies

[0079] Referring to FIG. **9**, there is seen a flow-through ultrasonic reactor based on a Barbell Device, such as the Barbell Horn, Catenoidal Barbell Horn, Patterned Barbell Horn or the any of the corresponding Transducer Barbell Horn Assemblies, according to the seventh embodiment of the present invention. The reactor comprises an electro-acoustical transducer **51**, a Barbell Device **52**, a valve **53**, a reactor chamber **54**, and a valve **55**.

Embodiment 8

Ultrasonic Reactor Based on a Barbell Device, Such as the Barbell Horn, Catenoidal Barbell Horn, Patterned Barbell Horn or the any of the Corresponding Transducer Barbell Horn Assemblies

[0080] FIG. **10** is a flow-through ultrasonic reactor based on a Barbell Device, such as the Barbell Horn, Catenoidal Barbell Horn, Patterned Barbell Horn or the any of the corresponding Transducer Barbell Horn Assemblies, according to the eighth embodiment of the present invention. The reactor is equipped with a circular reflection surface and comprises an electro-acoustical transducer **61**, a Barbell Device **62**, a valve **63**, a reactor chamber **64**, a valve **65**, and a circular reflection surface **66**.

Embodiment 9

Ultrasonic Reactor Based on a Barbell Device, Such as the Barbell Horn, Catenoidal Barbell Horn, Patterned Barbell Horn or the any of the Corresponding Transducer Barbell Horn Assemblies

[0081] FIG. **11** is a flow-through ultrasonic reactor based on a Barbell Device, such as the Barbell Horn, Catenoidal Barbell Horn, Patterned Barbell Horn or the any of the corresponding Transducer Barbell Horn Assemblies, according to the ninth embodiment of the present invention. The reactor is equipped with a circular reflection surface and an insert at the bottom, shaped as an upside-down circular cone, and comprises an electro-acoustical transducer **71**, a Barbell Horn **72**, a valve **73**, a reactor chamber **74**, an upside-down circular cone insert **75**, a valve **76**, and a circular reflection surface **77**.

[0082] Experimental Results Illustrating the Embodiments 7-9

[0083] It is well known that during acoustic cavitation the acoustic energy is practically completely absorbed by the liquid load in the active cavitation zone and that the acoustic cavitation itself is the mechanism that converts the absorbed acoustic energy into heat. Therefore, the effectiveness and the degree of the technological activity of a given ultrasonic apparatus can be judged by the amount of heat deposited in the cavitation zone during its operation. In other words, maximization and optimization of the active zone volume and the intensity of cavitation in a given ultrasonic reactor leads to maximization and optimization of the technological effects obtained during operation of the reactor.

[0084] A series of experiments are presented below, in which the above-mentioned considerations are used to evaluate the seventh through ninth embodiments of the present invention. The liquid load utilized in these experiments was tap water settled during a 24 hour period. The amount of heat produced due to the acoustic energy absorbed by the liquid load was measured by a direct calorimetry method, as described in the following references: S. L. Peshkovsky, A. S. Peshkovsky, Ultrason. Sonochem. 14 (2007) 314 and S. L. Peshkovsky, A. S. Peshkovsky, Ultrason. Sonochem. 15 (2008) 618.

[0085] According to the equations provided in U.S. Pat. No. 7,156,201 and in the publication, S. L. Peshkovsky, A. S. Peshkovsky, Ultrason. Sonochem. 14 (2007) 314, a titanium alloy Barbell Horn was calculated and constructed having the following main parameters: output tip diameter—65 mm, output tip surface—33.2 cm^2, output vibration amplitude—70 microns peak-to-peak, frequency of ultrasonic vibration—20 kHz, output tip oscillation velocity—314 cm/sec (rms). Three reactor chamber types were also constructed for the experiments, corresponding to the seventh through ninth embodiments of the present invention (FIGS. **9-11**). All three reactor chambers were equipped with thermo-isolated walls with incorporated heat sensors. The distance between the output tip of the Barbell Horn and the bottom of the reactor chamber (or the top of the cone insert used in the ninth embodiment shown in FIG. **11**) was 70 mm. Vibration amplitude was maintained constant during the experiments.

[0086] Experiment 1: Liquid load (settled tap water) was placed in the reactor chamber according to the seventh embodiment of the present invention, such that the surface of the water was approximately 20 mm above the output tip of the Barbell Horn. The measured acoustical power deposited into the water during operation of the reactor was 996 W. In this case the cavitation zone was formed almost entirely at the output tip of the horn, as shown in FIG. **7**.

[0087] Experiment 2: Liquid load (settled tap water) was placed in the reactor chamber according to the eighth embodiment of the present invention, such that the surface of the water reached the outlet valve. The reactor chamber was, therefore, filled with the liquid completely. The measured acoustical power deposited into the water during operation of the reactor was 1295 W. The increase in the absorbed acoustic energy compared to Experiment 1 was due to the presence of an additional upper cavitation zone in the narrow part of the Barbell Horn, as shown in FIG. **8**.

[0088] Experiment 3: Liquid load (settled tap water) was placed in the reactor chamber according to the ninth embodiment of the present invention, such that the surface of the water reached the outlet valve. The reactor chamber was, therefore, filled with the liquid completely. The measured acoustical power deposited into the water during operation of the reactor was 1554 W. The increase in the absorbed acoustic energy compared to Experiment 2 was due to the presence of a cone insert at the bottom of the reactor chamber, which optimized the volume and the shape of the main cavitation zone at the output tip the Barbell Horn.

Embodiment 10

Ultrasonic Reactor Based on a Long Barbell Device, Such as the Long Barbell Horn, Catenoidal Long Barbell Horn or a Corresponding Long Barbell Horn Assembly

[0089] FIG. **12** is a flow-through ultrasonic reactor based on a Long Barbell Device, such as the Long Barbell Horn, Catenoidal Long Barbell Horn or a corresponding Long Barbell Horn Assembly, according to the tenth embodiment of the present invention. The reactor is equipped with two circular reflection surfaces and an insert at the bottom, shaped as an upside-down circular cone. The reactor comprises an electro-acoustical transducer **81**, a Long Barbell Device **82**, a reactor chamber **83**, an upside-down circular cone insert **84**, a valve **85**, circular reflection surfaces **86**, and a valve **87**.

Embodiments 11 and 12

Two Versions of Ultrasonic Reactors Based on Extended Barbell Horns or the Extended Transducer Barbell Horn Assemblies

[0090] FIGS. **13** and **14** are two versions of flow-through ultrasonic reactors based on Extended Barbell Horns or the Extended Transducer Barbell Horn Assemblies, according to the eleventh and twelfth embodiments of the present invention. The reactors are equipped with circular reflection surfaces and inserts at the bottom, shaped as upside-down circular cones. The reactor of FIG. **13** comprises an electro-acoustical transducer **91**, an Extended Barbell Horn or Extended Transducer Barbell Horn Assembly **92**, a reactor chamber **93**, an upside-down circular cone insert **94**, a valve **95**, a first circular reflection surface **96**, a second circular reflection surface **97**, and a valve **98**. The reactor of FIG. **14** comprises an electro-acoustical transducer **101**, an Extended Barbell Horn or Extended Transducer Barbell Horn Assembly **102**, a reactor chamber **103**, an upside-down circular cone insert **104**, a valve **105**, a circular reflection surface **107**, and a valve **108**.

Embodiments 13, 14 and 15

Ultrasonic Reactors Based on Hollow Barbell Horns or Hollow Transducer Barbell Horn Assemblies

[0091] FIG. **15** is a flow-through ultrasonic reactor based on a Hollow Barbell Horn or a Hollow Transducer Barbell Horn Assembly with a short internal hollow region, according to the thirteenth embodiment of the present invention. The length of the hollow region is smaller or equal to the length of the cylindrical output element of the device. The reactor comprises an electro-acoustical transducer **111**, a Hollow Barbell Horn or Hollow Transducer Barbell Horn Assembly **112**, a circular reflection surface **113**, a reactor chamber **114**, a valve **115**, and a valve **116**. The liquid load is supplied near the top of the hollow region into the cavitation field formed inside the hollow region.

[0092] Experimental Results Illustrating the Embodiment 13

[0093] A titanium alloy Hollow Barbell Horn with a short internal hollow region was calculated and constructed according to the equations given in U.S. Pat. No. 7,156,201 and in the publication S. L. Peshkovsky, A. S. Peshkovsky, Ultrason. Sonochem. 14 (2007) 314. The internal hollow region of the horn was a straight circular cone with a sharp tip. The constructed horn had the following parameters: Outside output diameter—60 mm, inside output diameter-50 mm, depth of the internal hollow region—60 mm, output vibration amplitude—70 microns peak-to-peak, ultrasonic frequency—20 kHz, output oscillation velocity—314 cm/sec (rms). The total surface area of the internal hollow region was 51 cm^2.

[0094] Liquid load (settled tap water) was placed in the reactor chamber, according to the thirteenth embodiment of the present invention, such that the surface of the water reached the outlet valve. The reactor chamber was, therefore, filled with the liquid completely. The reactor chamber was equipped with thermo-isolated walls with an incorporated heat sensor. The measured acoustical power deposited into the water during operation of the reactor was 1709 W. This example shows that the use of the Hollow Barbell Horn in an appropriate ultrasonic reactor chamber permits achieving an additional increase in the acoustic energy deposited in the active cavitation zone in the reactor chamber, thereby increasing technological effectiveness of the reactor.

[0095] FIG. **16** is a flow-through ultrasonic reactor based on a Hollow Barbell Horn with a long internal hollow region, according to the fourteenth embodiment of the present invention. The length of the hollow region is smaller or equal to the combined lengths of the cylindrical output element of the horn and its adjacent element with variable cross-section. The reactor comprises a electro-acoustical transducer **121**, a Hollow Barbell Horn or Hollow Transducer Barbell Horn Assembly **122**, a valve **123**, a reactor chamber **124**, a valve **125**, and a circular reflection surface **126**. The liquid is supplied near the top of the hollow region into the cavitation field formed inside the hollow region.

[0096] FIG. **17** is another version of a flow-through ultrasonic reactor based on a Hollow Barbell Horn or a Hollow Transducer Barbell Horn Assembly with a long internal hollow region, according to the fifteenth embodiment of the present invention. The reactor chamber is modified such that all liquid is directed into the highest intensity cavitation zone. An upside-down positioning of the reactor is preferably utilized. The reactor comprises a reactor chamber **131**, a Hollow Barbell Horn or Hollow Transducer Barbell Horn Assembly **132**, a valve **133**, a valve **134**, and an electro-acoustical transducer **135**. The liquid is supplied near the top of the hollow region into the cavitation field formed inside the hollow region.

Embodiment 16

Ultrasonic Reactor Based on a Hollow Barbell Horn or a Hollow Transducer Barbell Horn Assembly and a Generic Ultrasonic Horn of an Arbitrary Design

[0097] FIG. **18** is a flow-through ultrasonic reactor based on a Hollow Barbell Horn (or Hollow Transducer Barbell Horn Assembly) and a generic horn of arbitrary design, according to the sixteenth embodiment of the present invention, where the reactor comprises electro-acoustical transducer **141** and **144**, a Hollow Barbell Horn or Hollow Transducer Barbell Horn Assembly **142**, a generic ultrasonic horn **143**, and a reactor chamber **145**. The horns are arranged such that the generic horn fits inside the Hollow Barbell Horn (or Hollow Transducer Barbell Horn Assembly). The horns are operated in-phase, thereby increasing the cavitation field intensity.

Embodiment 17

Ultrasonic Extruder for Polymer Melts Processing

[0098] It is generally thought that acoustic cavitation can only occur in low viscosity liquids. Consequentially, the prior art studies of the cavitation effects on high-molecular compounds (such as polymers) are restricted to those conducted in low-viscosity solutions of such compounds. Many of such studies show that ultrasonic cavitation causes significant physical and chemical transformations in such polymers, which can be very useful for their processing. These studies, however, are mostly of academic interest because processing of weak polymer solutions is very technologically inefficient. Industrial impact of such studies, therefore, was severely limited.

[0099] One publication (M. L. Friedman and S. L. Peshkovsky, Molding of Polymers under Conditions of Vibration Effects, Advances in Polymer Science, Polymer Processing, NY, 1990, p 41-79), incorporated herein by reference, however, shows experimental evidence that visco-elastic fluids, such as polymer melts with viscosity on the order of 10^6 Pa*s, can also undergo cavitation, as a result of which clouds of active cavitation regions are created. This phenomenon is related to the presence of not only the high viscosity, but also the elasticity in these compounds. FIG. **22** and FIG. **23** show photographs of such cavitation cloud regions in the stationary and the flowing melt of polyisobutylene, respectively. Based of these observations, in the present invention it has been determined that an appropriately designed polymer extruder with and suitable ultrasonic reactor equipped with a Barbell Horn can be very useful for the polymer processing industry.

[0100] FIG. **19** is a schematic of an Ultrasonic Extruder for the treatment of high-viscosity polymer melts with high-intensity ultrasound, according to the seventeenth embodiment of the present invention. The Ultrasonic Extruder comprises a polymer extruder **151**, a reactor chamber **152**, a Barbell Device **153**, and an electro-acoustical transducer **154**.

[0101] FIG. **20** is an expanded view of a flow-through ultrasonic reactor head for an ultrasonic extruder **160**, comprising an electro-acoustical transducer **161**, a Barbell Device **162**, a heating element **163**, a reactor chamber **164**, a shaping head **165**, and a polymer extruder body **166**. Polymer melt from extruder **160** is directed under pressure into the ultrasonic reactor head equipped with a temperature control unit. In the ultrasonic reactor head, the polymer melt flows into the spacing between the shaping head and the Barbell Device, where it becomes exposed to ultrasonic vibrations excited by an electro-acoustical transducer. During high-intensity ultrasonic treatment, the physical/chemical properties of the polymers change, along with their molecular structures. Various chemical reactions, copolymerization, devulcanization, side chain aggregation and other modifications may take place.

[0102] FIG. **21** is a schematic of a device for treatment of high-viscosity polymer melts with high-intensity ultrasound, based on the principle of cascade extrusion. The reactor comprises a first polymer extruder **171**, an electro-acoustical transducer **172**, a Barbell Device **173**, a reactor chamber **174**, a second polymer extruder **175**, and a shaping head **176**.

Embodiment 18

Ultrasonic Reactor Based on a Nonmetallic Barbell Device

[0103] In the eighteenth embodiment of the present invention, the ultrasonic flow-through reactor is designed to be suitable for the processing of chemically aggressive liquids, extremely high-purity compounds, as well as for operation in electromagnetic, magnetic, electric, microwave, etc, fields in which the use of metallic objects is undesirable or impossible. Ultrasonic radiation in such a reactor is performed using a Barbell Device (possibly with an additional acoustically rigidly connected waveguide-radiator) made from a nonmetallic material, such as technical corundium material, Al_2O_3, (for example, sapphire, leucosapphire, ruby, etc.).

What is claimed is:

1. An ultrasonic waveguide-radiator having a total length formed from a predetermined material, comprising:

a first cylindrical section having a first diameter and a first length, and including an entrance surface having an entrance cross-sectional area;

a first transitional section acoustically coupled to the first cylindrical section and having a catenoidal shape decreasing from a first diameter to a second diameter over a first transitional length;

a second cylindrical section acoustically coupled to the first transitional section and having a second diameter and a second length;

a second transitional section acoustically coupled to the second cylindrical section and having a second variable cross-section and a second transitional length;

a third cylindrical section acoustically coupled to the second transitional section and having a third diameter and a third length, and including an exit surface having an exit cross-sectional area;

wherein the total length is equal to a multiple of one-half of the acoustic wavelength in the predetermined material accounting for phase velocity dispersion;

wherein the length of said first transitional section is less than the value of Log(N)/k, where N is the ratio of the first and second diameters of the first and second cylindrical sections, respectively, and k is the wave number representing the angular frequency of ultrasonic vibrations divided by the speed of sound in the predetermined material.

2. The waveguide-radiator of claim **1**, wherein the third cylindrical section is patterned.

3. The waveguide-radiator of claim **1**, further comprising a stepped extension having at least a fourth cylindrical section having a fourth diameter acoustically coupled to the third cylindrical section.

4. The waveguide-radiator of claim **1**, further comprising at least a third transitional section acoustically coupled to said third cylindrical section and at least a fourth cylindrical section acoustically coupled to the third transitional section.

5. The waveguide-radiator of claim **1**, wherein said waveguide-radiator comprises a non-metal material.

6. The waveguide-radiator of claim **1**, further comprising a non-metal rod acoustically coupled to the exit surface of the third cylindrical section.

7. An ultrasonic waveguide-radiator having an exit surface and total length formed from a predetermined material, comprising:

a first cylindrical section having a first diameter and a first length, and including an entrance surface having an entrance cross-sectional area;

a first transitional section acoustically coupled to the first cylindrical section and having a first variable cross-section and a first transitional length;

a second cylindrical section acoustically coupled to the first transitional section and having a second diameter and a second length;

a second transitional section acoustically coupled to the second cylindrical section and having a second variable cross-section and a second transitional length;

a third section acoustically coupled to the second transitional section and having a third length;

wherein said third section includes a hollow portion that extends from a first internal diameter to a second internal diameter that is different than the first internal diameter;

wherein the total length is equal to a multiple of one-half of the acoustic wavelength in the predetermined material accounting for phase velocity dispersion.

8. The ultrasonic waveguide-radiator of claim **7**, wherein said second transitional section includes a second hollow portion that extends from a third internal diameter to a fourth internal diameter that is different than the third internal diameter.

9. An ultrasonic waveguide-radiator having an exit surface and total length formed from a predetermined material, comprising:

a first cylindrical section having a first diameter and a first length, and including an entrance surface having an entrance cross-sectional area;

a first transitional section acoustically coupled to the first cylindrical section and having a first variable cross-section and a first transitional length;

a second cylindrical section acoustically coupled to the first transitional section and having a second diameter and a second length;

a second transitional section acoustically coupled to the second cylindrical section and having a second variable cross-section and a second transitional length;

a third cylindrical section acoustically coupled to the second transitional section and having a third diameter and a third length;

a stepped extension acoustically coupled to the third cylindrical section and having at least a fourth cylindrical section having a fourth diameter that is at least fifty percent of the third diameter;

wherein the total length is equal to a multiple of one-half of the acoustic wavelength in the predetermined material accounting for phase velocity dispersion;

wherein the length of said first transitional section is no less than the value of Log(N)/k, where N is the ratio of the first and second diameters of the first and second cylindrical sections, respectively, and k is the wave number representing the angular frequency of ultrasonic vibrations divided by the speed of sound in the predetermined material.

10. An ultrasonic reactor, comprising:

a chamber having an inlet and an outlet and a top and a bottom and including a working fluid having an acoustic wavelength;

an ultrasonic waveguide-radiator positioned in the chamber having an exit surface and a total length formed from a predetermined material, wherein the waveguide-radiator comprises:

a first cylindrical section having a first diameter and a first length, and including an entrance surface having an entrance cross-sectional area;

a first transitional section acoustically coupled to the first cylindrical section and having a first variable cross-section and a first transitional length;

a second cylindrical section acoustically coupled to the first transitional section and having a second diameter and a second length;

a second transitional section acoustically coupled to the second cylindrical section and having a second transitional length; and

a third section acoustically coupled to the second transitional section and having a third length;

wherein the total length is equal to a multiple of one-half of the acoustic wavelength in the predetermined material accounting for phase velocity dispersion.

11. The reactor of claim **10**, wherein said chamber further comprises at least one reflector surface positioned in the chamber adjacent to said second cylindrical section.

12. The reactor of claim **10**, wherein said chamber further comprises:

a conical zone positioned in said chamber adjacent to said exit surface;

wherein the height of the conical zone and the diameter of the base of the conical zone are about the acoustic wavelength in the working fluid, the volume of the conical zone is about one quarter of the cube of the acoustic wavelength in the working fluid, and the inlet or the outlet is positioned at the top of the conical zone.

13. The reactor of claim **10**, wherein said third cylindrical section is at least partially hollow and the reactor further comprises a second radiator positioned in said chamber and extending into the hollow portion cylindrical section of the first radiator.

14. An ultrasonic waveguide-radiator having a total length formed from a predetermined material, comprising:

a first cylindrical section having a first diameter and a first length, and including an entrance surface having an entrance cross-sectional area;

a first transitional section acoustically coupled to the first cylindrical section that decreases from a first diameter to a second diameter over a first transitional length;

a second cylindrical section acoustically coupled to the first transitional section and having a second diameter and a second length;

a second transitional section acoustically coupled to the second cylindrical section and having a second variable cross-section and a second transitional length;

a third cylindrical section acoustically coupled to the second transitional section and having a third diameter and a third length, and including an exit surface having an exit cross-sectional area;

wherein the total length is equal to a multiple of one-half of the acoustic wavelength in the predetermined material accounting for phase velocity dispersion; and

wherein the length of said first transitional section is less than the value of Log(N)/k, where N is the ratio of the first and second diameters of the first and second cylindrical sections, respectively, and k is the wave number representing the angular frequency of ultrasonic vibrations divided by the speed of sound in the predetermined material.

* * * * *

US007156201B2

(12) United States Patent
Peshkovskiy et al.

(10) Patent No.: US 7,156,201 B2
(45) Date of Patent: Jan. 2, 2007

(54) **ULTRASONIC ROD WAVEGUIDE-RADIATOR**

(75) Inventors: **Sergey L. Peshkovskiy**, New York, NY (US); **Michael L. Friedman**, Wayne, NJ (US); **Wilton A. Hawkins**, Montclair, NJ (US)

(73) Assignee: **Advanced Ultrasonic Solutions, Inc.**, Lords Valley, PA (US)

(*) Notice: Subject to any disclaimer, the term of this patent is extended or adjusted under 35 U.S.C. 154(b) by 273 days.

(21) Appl. No.: **10/982,588**

(22) Filed: **Nov. 4, 2004**

(65) **Prior Publication Data**

US 2006/0090956 A1 May 4, 2006

(51) **Int. Cl.**
G10K 11/08 (2006.01)
H03H 9/24 (2006.01)
H04B 11/00 (2006.01)
H03H 9/25 (2006.01)

(52) **U.S. Cl.** **181/175**; 381/338; 310/323.19; 333/145

(58) **Field of Classification Search** 181/175, 181/177, 192, 142; 381/337–340; 310/323.19; 333/145
See application file for complete search history.

(56) **References Cited**

U.S. PATENT DOCUMENTS

3,184,842	A	*	5/1965	Maropis	228/111
3,277,404	A	*	10/1966	Fabian	333/145
3,524,085	A	*	8/1970	Shoh	310/325
3,546,498	A	*	12/1970	McMaster et al.	310/323.19
3,568,104	A	*	3/1971	Bailey	333/145
3,736,532	A	*	5/1973	Armenakas	333/145
3,891,869	A	*	6/1975	Scarpa	310/325
3,915,018	A	*	10/1975	Karplus	73/647
4,131,505	A	*	12/1978	Davis, Jr.	156/580.1
4,337,843	A		7/1982	Wendel	
4,691,724	A	*	9/1987	Garcia et al.	134/169 R
4,710,668	A	*	12/1987	Fima et al.	310/323.21
4,896,535	A	*	1/1990	Duckart et al.	73/290 V
5,112,300	A	*	5/1992	Ureche	604/22
5,241,287	A		8/1993	Jen	
5,269,297	A	*	12/1993	Weng et al.	606/128
5,289,436	A		2/1994	Terhune	
5,380,274	A	*	1/1995	Nita	604/22
5,386,169	A	*	1/1995	Dubruque	310/323.19
5,527,273	A	*	6/1996	Manna et al.	604/22
5,713,916	A		2/1998	Dias	
5,828,274	A		10/1998	Jen et al.	
6,078,125	A	*	6/2000	Roberts	310/325

(Continued)

FOREIGN PATENT DOCUMENTS

GB 2167270 A * 5/1986

Primary Examiner—Edgardo San Martin
(74) *Attorney, Agent, or Firm*—Robert J. Sinnema; Bond, Schoeneck & King, PLLC

(57) **ABSTRACT**

The present invention comprises an ultrasonic resonant rod waveguide-radiator with at least three cylindrical sections, one of which is an entrance section having a planar entrance surface and another of which is an exit section having a planar exit surface, and at least two sections having a variable cross-section. The cylindrical sections and sections of variable cross-section are arranged in alternating fashion and connected to each other acoustically rigidly. The dimensions of the cylindrical sections and the sections of variable cross-section are selected so that the gain of the waveguide-radiator is significantly greater than unity and the strain created by passage of ultrasonic waves through the waveguide-radiator is minimized, increasing the operational life of the waveguide-radiator and maximizing the amount of useful energy transmitted by the waveguide-radiator.

8 Claims, 7 Drawing Sheets

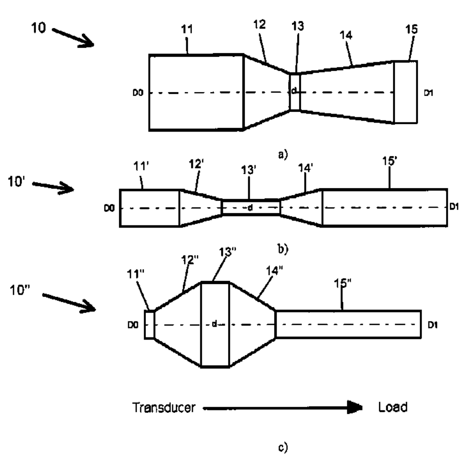

U.S. PATENT DOCUMENTS

6,400,648 B1 6/2002 Heijnsdijk et al.
6,837,445 B1 * 1/2005 Tsai 239/102.2
6,841,921 B1 * 1/2005 Stegelmann 310/323.19
7,002,283 B1 * 2/2006 Li et al. 310/325
2004/0127926 A1 7/2004 Beaupre

* cited by examiner

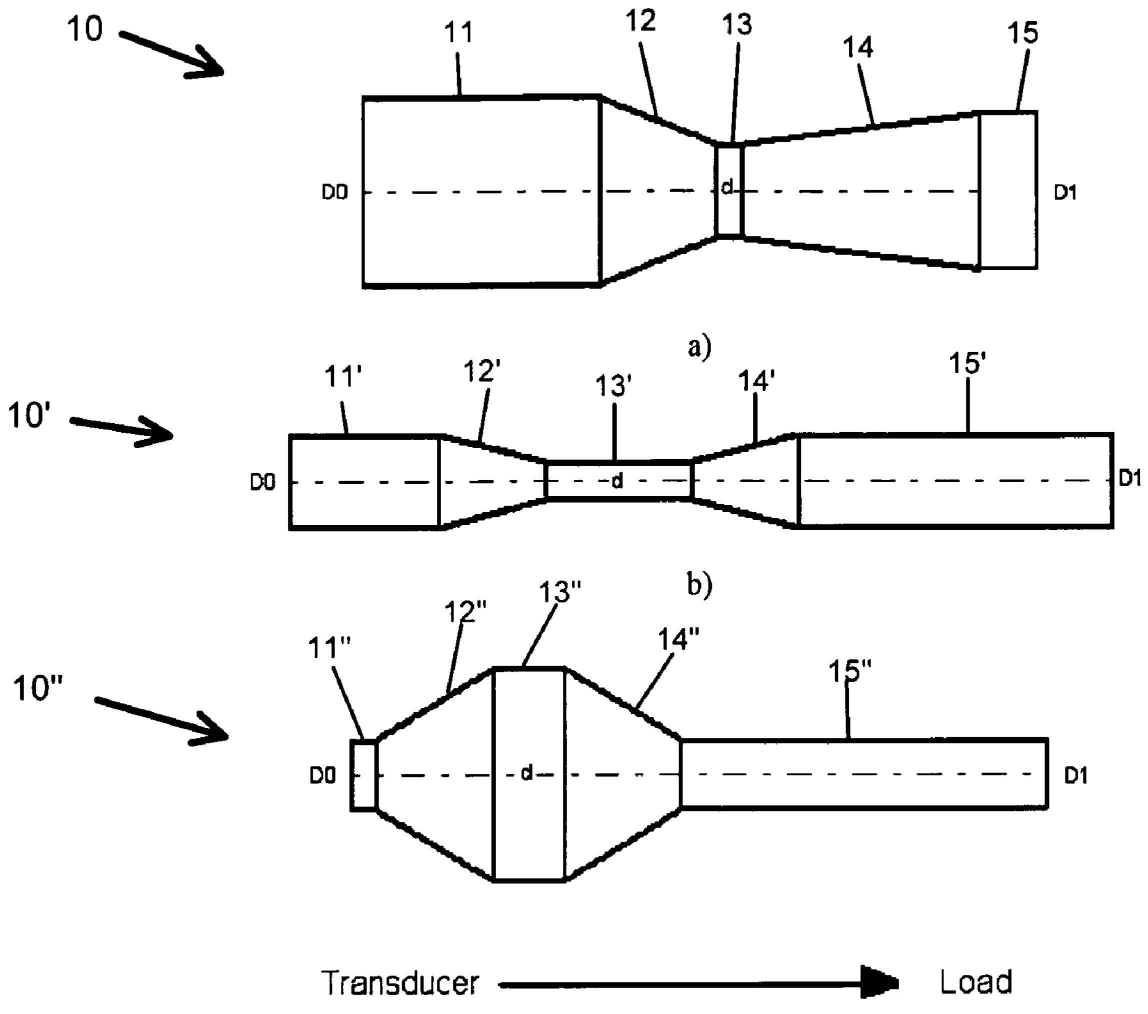
10
11
12
13
14
15
D0
d
D1
a)
10'
11'
12'
13'
14'
15'
D0
d
D1
b)
10"
11"
12"
13"
14"
15"
D0
d
D1
Transducer
Load

c)

Fig. 1

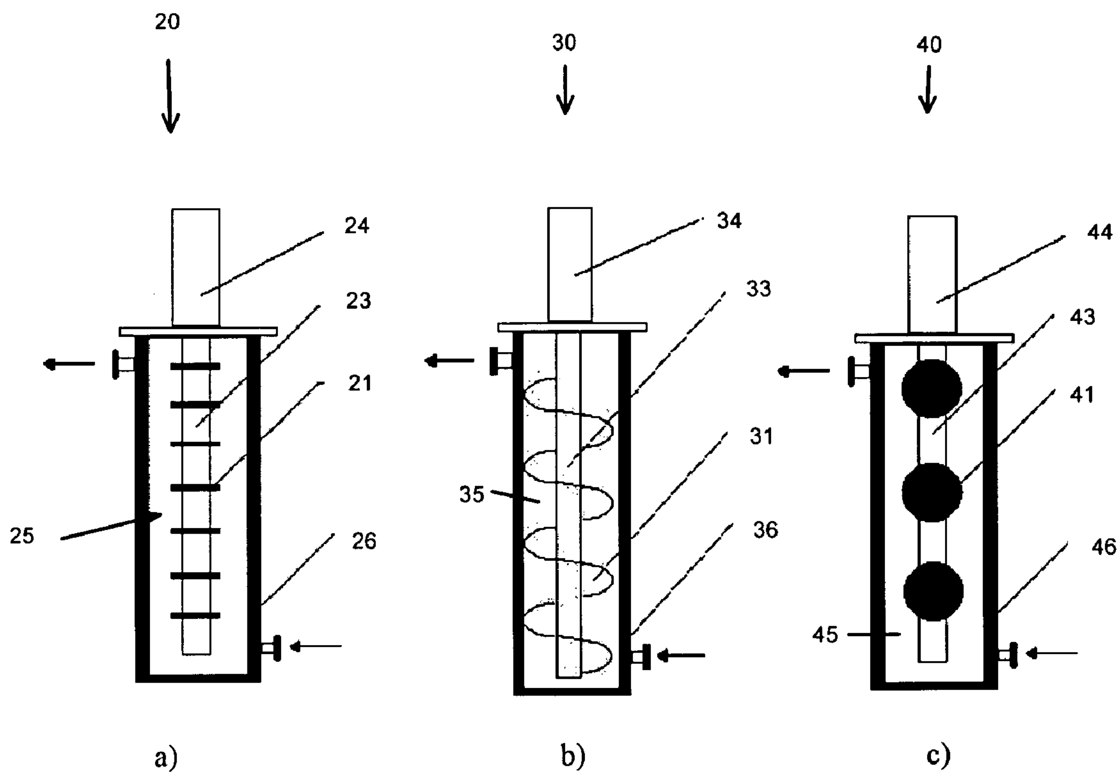

Fig. 2

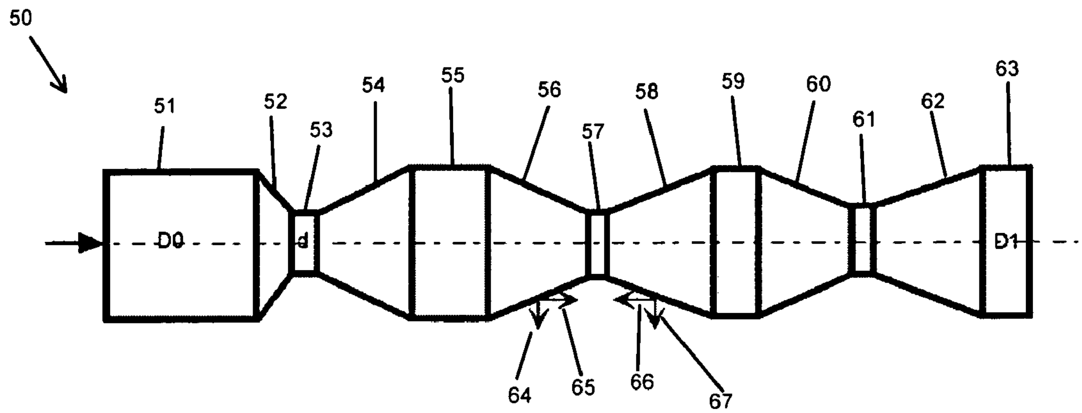
50
51
52
53
54
55
56
57
58
59
60
61
62
63
D0
d
D1
64
65
66
67

Fig. 3

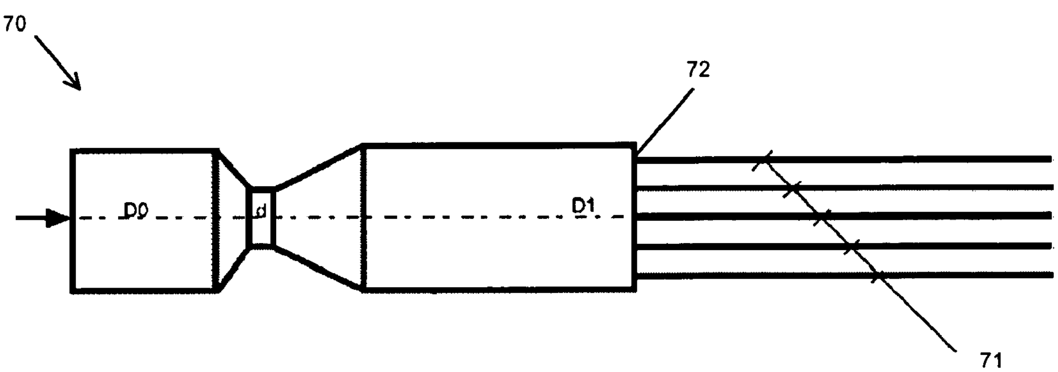
70
72
D0
d
D1
71

Fig. 4

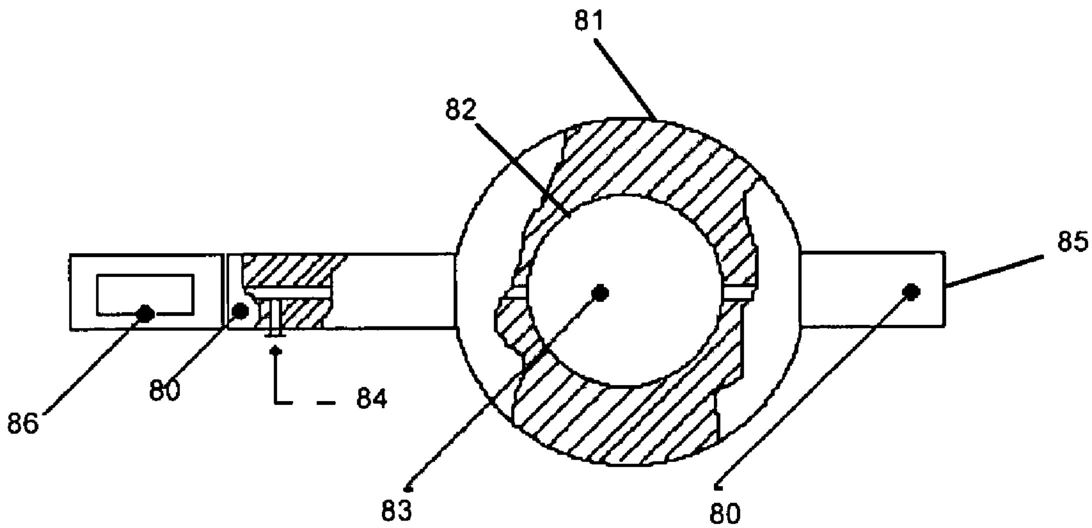

Fig. 5

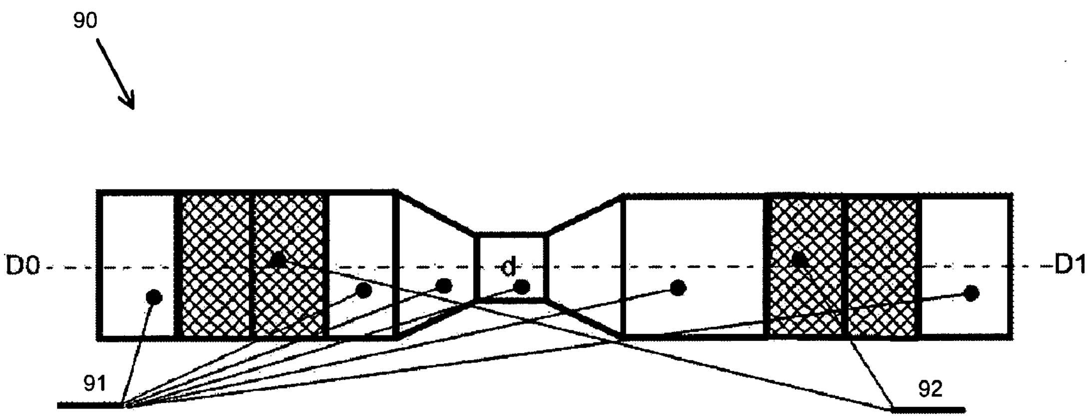

Fig. 6

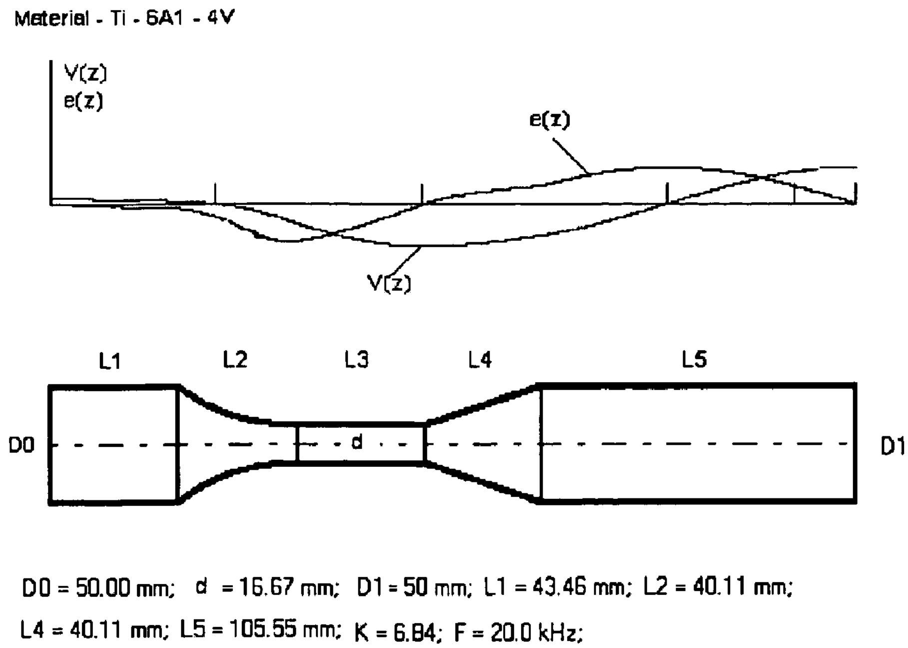
Material - Ti - 6A1 - 4V
V(z)
e(z)
e(z)
V(z)
L1
L2
L3
L4
L5
D0
d
D1
D0 = 50.00 mm; d = 16.67 mm; D1 = 50 mm; L1 = 43.46 mm; L2 = 40.11 mm;
L4 = 40.11 mm; L5 = 105.55 mm; K = 6.84; F = 20.0 kHz;

Fig. 7

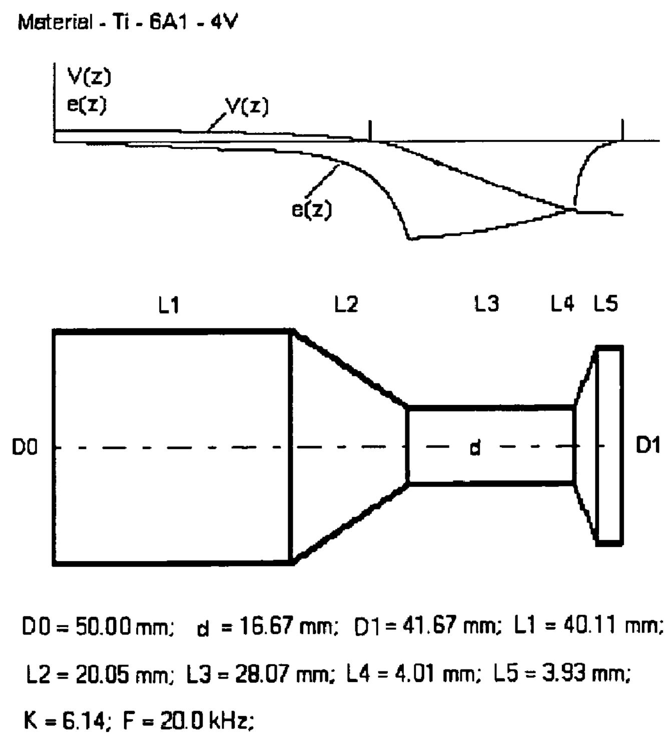
Material - Ti - 6A1 - 4V
V(z)
e(z)
V(z)
e(z)
L1
L2
L3
L4
L5
D0
d
D1
D0 = 50.00 mm; d = 16.67 mm; D1 = 41.67 mm; L1 = 40.11 mm;
L2 = 20.05 mm; L3 = 28.07 mm; L4 = 4.01 mm; L5 = 3.93 mm;
K = 6.14; F = 20.0 kHz;

Fig. 8

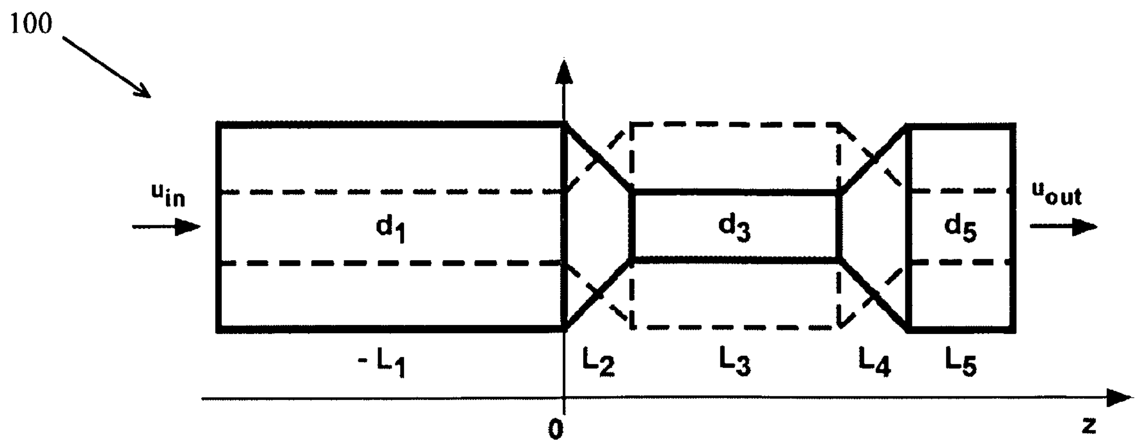

Fig. 9

ULTRASONIC ROD WAVEGUIDE-RADIATOR

BACKGROUND OF THE INVENTION

1. Field of the Invention

The present invention relates to the field of ultrasonic equipment and can be used in different technological devices for the transmission of acoustic energy into an acoustic load, for example, in heat and mass transfer processes, plastic welding, metal treatment, etc.

2. Description of Prior Art

Acoustic energy is usually transmitted into an acoustic load (liquid, polymeric or hard material) using an ultrasonic waveguide-radiator connected to an electro-acoustic transducer (magnetostrictive or piezoelectric). The tasks of the waveguide-radiator are to increase the amplitude of the transducer vibrations A up to the level necessary in a given technology, to match the energy of a transducer to an acoustic load, to uniformly distribute radiated acoustic energy throughout the volume of the medium being treated, and/or to facilitate reliable fastening of cutting and other tools to the waveguide radiator. Matching the energy of the transducer to the acoustic load means the development of a waveguide-radiator design that provides transmission of maximum acoustic power from the transducer into the load.

It is known that specific acoustic power radiated by a waveguide into an acoustic load, for instance into a liquid, is equal to $w=0.5\ \rho C\omega^2 A^2$ [Wt/sq.m]. Here ρ is the density of liquid, C is the speed of sound in liquid, ω is the frequency of ultrasonic vibrations, and A is the amplitude of ultrasonic vibrations. The total acoustic power radiated into liquid is equal to $W=wS$ [Wt]. Here S is the area of the radiating surface of the waveguide-radiator. Thus, it is evident that an increase in the total radiated acoustic power at constant load and frequency can be achieved by increasing either of the following two factors: the amplitude of output vibrations of the waveguide-radiator or the area of the waveguide-radiator's radiating surface. The amplitude of output vibrations cannot be increased above a certain level that corresponds to the fatigue strength of the waveguide-radiator material. Increasing amplitude above this level causes the waveguide-radiator to break down. Furthermore, a considerable increase in the amplitude of vibrations is not always justified from the technological point of view. It is also possible to increase the exit diameter of a rod waveguide-radiator up to a certain level that is equal to about $\lambda/4$ (where λ is the wavelength of ultrasound waves in the material of a thin-rod waveguide-radiator). When the waveguide-radiator exit diameter is larger than this value, radiation via the waveguide-radiator's side surfaces begins to have a strong effect, and calculation of the waveguide's acoustic properties becomes difficult to predict. Nevertheless, increasing the waveguide-radiator exit diameter up to a value close to $\lambda/4$ gives an opportunity to increase the radiated power by several times.

The closest device in its essence to the present invention is a known ultrasonic rod waveguide-radiator that has a shape converging (tapering) to a load. The shape of such a waveguide-radiator is determined by the fact that its gain factor of the amplitude of ultrasonic vibrations in the direction of an acoustic load must be higher than unity. To increase the radiating surface, a converging waveguide radiator is provided at the radiating exit end with a section in the form of a thin disk or plate having a large diameter, usually close to the waveguide-radiator entrance diameter. The presence of a short transition section of arbitrary shape between the waveguide radiator and the plate at its radiating end is also possible. This section is designed to increase the area of the exit radiating surface and consequently the acoustic energy radiated into a load.

Such a waveguide-radiator with a plate or disk at the end has substantial disadvantages. First, at a small value of the ratio of the length and diameter of the specified section (usually less than 0.5), instead of the axial (longitudinal) mode of vibrations which must occur in the body of the waveguide-radiator, vibrations of more complex modes (for instance, offaxial mode) arise in it (for example, flexural vibrations). This leads to a disruption of the regime of the operation of the entire waveguide-radiator. Its natural resonance frequency changes and, as a consequence, additional experimental fitting of geometrical dimensions is required. Thus, a direct acoustic calculation of the waveguide-radiator as a waveguide of longitudinal waves becomes inaccurate. This manifests itself particularly clearly at high vibration amplitudes of the specified section of the waveguide-radiator. Second, the length of the specified exit section is small as compared with its diameter and, therefore, in this section the degree of strain (and, as a consequence, stress) along the section length is high, which substantially decreases the operational life span of such a waveguide-radiator at high amplitude.

3. Objects and Advantages

It is therefore a principal object and advantage of the present invention to provide a waveguide-radiator that is free from the drawbacks enumerated above, having an exit diameter close to the entrance diameter, and a gain factor much higher than unity, and having the following objectives:

1. To improve the quality of operation and to increase the operational life of a wave guide-radiator.

2. To increase the acoustic energy radiated into a load by a waveguide-radiator.

3. To increase the reliability of fastening various cutting and other tools on the waveguide radiator.

4. To increase the available radiation surface and the uniformity of the distribution of acoustic energy throughout the volume of an ultrasonic reactor.

5. To conduct ultrasonic treatment of the internal surfaces of thin extended channels and tubes.

6. To increase the intensity of acoustic radiation in the working medium of an ultrasonic reactor.

7. To increase the efficiency of conversion of electric energy of an ultrasonic generator into acoustic energy radiated into a load.

SUMMARY OF THE INVENTION

In accordance with the foregoing objects and advantages, the present invention provides an ultrasonic resonant rod waveguide-radiator with at least three cylindrical sections, one of which is an entrance section having a planar entrance surface and another of which is an exit section having a planar exit surface, and at least two sections having a variable cross-section. The cylindrical sections and sections of variable cross-section are arranged in alternating fashion and connected to each other acoustically rigidly. As described herein, the dimensions of the sections are selected so that the exit surface and entrance surface are approximately equal, the length of the sections of variable cross-section is determined according to a specified formula, and the sum of the length of the exit section and the adjacent section is 30% or more of the total length of the waveguide radiator.

BRIEF DESCRIPTION OF THE DRAWINGS

The present invention will be more fully understood and appreciated by reading the following Detailed Description in conjunction with the accompanying drawings, in which:

FIG. **1** depicts side elevation views of a waveguide-radiator according to three embodiments of the present invention.

FIG. **2** depicts sectional side elevation views of a waveguide-radiator according to three other embodiment of the present invention.

FIG. **3** is a side elevation view of a waveguide-radiator according to another embodiment of the present invention.

FIG. **4** is side elevation view of a waveguide-radiator according to another embodiment of the present invention.

FIG. **5** is a partial sectional side elevation view of a waveguide-radiator according to another embodiment of the present invention.

FIG. **6** is side elevation view of a waveguide-radiator according to another embodiment of the present invention.

FIG. **7** is a graph depicting the amplitude and strain of a wave passing through a waveguide-radiator according to the present invention.

FIG. **8** is a graph plotting the amplitude and strain of a wave passing through a waveguide-radiator according to the prior art.

FIG. **9** is a side elevation view of a waveguide-radiator according to an embodiment of the present invention.

DETAILED DESCRIPTION

Referring now to the drawings, wherein like reference numerals refer to like parts throughout, there is seen in FIG. **1** a waveguide-radiator **10**, **10'**, **10"** according to the present invention. The improvement of the quality of operation and an increase in the operational life of a waveguide-radiator are achieved through the use of a waveguide-radiator shown in FIG. **1**. The waveguide-radiator consists of five sections **11**–**15**, **11'**–**15'**, **11"**–**15"** in a combination of cylindrical sections **11**, **13**, **15**, **11'**, **13'**, **15'**, **11"**, **13"**, **15"** and sections of variable cross-section **12**, **14**, **12'**, **14'**, **12"**, **14"**, all made of metal. The cylindrical sections and variable cross-section sections alternate in series and are acoustically rigidly connected between themselves. The geometrical dimensions of these sections are selected using a known method of acoustic calculation (Rayleigh equation) in such a way that their total length is equal to the value that is a multiple of half the length of an acoustic wave in the waveguide-radiator material, taking into account a geometrical sound dispersion. That is, the waveguide-radiator must be resonant and also provide a gain factor of the amplitude of vibrations in the direction of an acoustic load significantly higher than unity. The waveguide-radiator sections of variable cross-section have a particular shape: conical, exponential or catenoidal. The lengths of the sections of variable cross-section are approximately equal between themselves and are equal to or more than the following value: (LogN)/k. Here $k=\omega/C$ is the wave number, N is the ratio of the diameters of thick and thin cylindrical sections that are adjacent to the section of variable cross-section. It is known that the specified length of a section of variable cross-section is critical from the standpoint of the passage of a longitudinal acoustic wave. Such selection of the length and shape of a section of variable cross-section allows one to decrease considerably the degree of dynamical strain along the section length and thus to increase the operational life of the waveguide-radiator. Furthermore, because the relation of the length to the diameter of the section is very large, the deformations in perpendicular direction (non-axial modes) are miniscule and the strain is practically an axial one, causing the longitudinal mode of an acoustic wave to be maintained along the entire length of the waveguide radiator. At its exit section, complex modes of vibrations (for instance, bending ones), as in the case of a waveguide according to the prior art, do not arise. In this case, even at very high output amplitudes close to maximum allowable values for the radiator material, the operational life of a waveguide-radiator according to the present invention is several years.

An increase in the total acoustic power radiated into a load is achieved through a special acoustic calculation based on the Rayleigh equation and the design of such a waveguide-radiator whose exit section has a relatively large area of cross-section at the gain factor of the waveguide-radiator much higher than unity. The gain factor of the waveguide-radiator can be much higher than unity, in spite of the diameter D**1** of its exit section **15**, **15'**, **15"** is close to the diameter D**0** of its entrance section **11**, **11'**, **11"**. (See FIGS. **1**A, **1**B, **1**C.)

Incorporating an exit cylindrical section **15**, **15'**, **15"** (FIGS. **1**A, **1**B, **1**C) having a large diameter facilitates easy connection to the waveguide-radiator of different devices that provide a generally uniform acoustic treatment of large volumes and surfaces. A large diameter exit section of the waveguide-radiator, when combined with large amplitude vibrations also facilitates easy connection to the waveguide-radiator of different cutting and other tools used in ultrasonic surgery and treatment of hard materials.

FIG. **2**A shows an ultrasonic device **20**, inside of which the specified waveguide-radiator is placed. Resonant thin plates **21** fastened acoustically rigidly to the waveguide-radiator body are positioned at a certain distance from one another on the extended exit section **23** of the waveguide-radiator. The waveguide-radiator is connected to an acoustic transducer **24** and increases the vibration amplitude of the latter. Longitudinal vibrations of the extended exit section **23** of the waveguide-radiator are converted into the flexural vibrations of resonant plates interacting with a liquid acoustic load **25** situated in a reactor **26**. In this way, the present invention achieves uniform treatment of a large volume of liquid with high-intensity ultrasound.

FIG. **2**B shows an ultrasonic device **30**, inside of which the specified waveguide-radiator with an extended exit section **33** is also placed. The extended exit section **33** of the waveguide-radiator is provided with a thin plate **31** fixed on its side surface in a helical fashion in such a way that the radiating surfaces of the plate **31** are positioned at an acute angle to the axis of the rod waveguide **33**. The waveguide-radiator is connected to an acoustic transducer **34** and increases the vibration amplitude of the latter. Longitudinal vibrations of the extended exit section **33** of the waveguide-radiator are converted into the flexural vibrations of the specified thin plate **31** interacting with a liquid acoustic load **35** situated in a reactor **36**. In this way, the present invention achieves uniform treatment of a large volume of liquid with high-intensity ultrasound.

FIG. **2**C shows an ultrasonic device **40**, inside of which the specified waveguide-radiator with an extended exit section **43** is also placed. The extended exit section of the waveguide-radiator is provided with several resonant spheres **41** that are acoustically rigidly connected to the waveguide radiator. The waveguide-radiator is connected to an acoustic transducer **44** and increases the vibration amplitude of the latter. Longitudinal vibrations of the extended exit section of the waveguide-radiator are converted into the radial vibrations of the specified spheres interacting with a liquid acoustic load **45** situated in a reactor **46**. In this way, the present invention achieves uniform treatment of a large volume of liquid with high-intensity ultrasound.

It should be noted that the total area of radiating plates, helical side plate and radiating spheres is very large and thus overcomes the theoretical limitations of previous waveguide designs, and therefore produces a maximum increase in the total acoustic power radiated into a liquid.

As set forth above, conventional ultrasonic rod waveguide-radiators have a theoretical limitation on their diameter, which does not allow the radiated energy to be considerably increased by increasing the device's diameter. To overcome this limitation, a modification of the disclosed waveguide-radiator shown in FIG. **3** was developed. In the given modification of the disclosed waveguide-radiator **50**, radiation occurs from its side surface that is made in the form of alternating cylindrical sections (**51**, **53**, **55**, **57**, **59**, **61**, **63**) and sections of variable cross-section (**52**, **54**, **56**, **58**, **60**, **62**). The surfaces of the sections of variable cross-section have components **64**, **67** of the amplitude of vibrations that are directed perpendicular to the waveguide-radiator axis. In addition, the lengths of the waveguide radiator sections are calculated in such a way that the components **65**, **66** of the vibration amplitude of the sections of variable cross-section that are directed along the waveguide axis are oriented toward each other. In this manner, a strong lateral radiation of the waveguide-radiator is achieved. Since there are no theoretical limitations on the waveguide-radiator length, the total area of its side radiating surface can be large. The total acoustic energy radiated into a liquid can be also substantially increased over the prior art.

In ultrasonic practice there are cases when ultrasonic treatment must be conducted inside narrow long tubes, channels or slots. For such cases, the following modification of the specified waveguide-radiator **70** can be used. See FIG. **4**. One or several long flexible rods **71** whose ratio of length to diameter is significantly greater than 100 are connected acoustically rigidly to the transverse exit surface **72** of the waveguide-radiator **70**. During the operation of the ultrasonic waveguide radiator, longitudinal ultrasonic vibrations of large amplitude are transmitted to the specified flexible rods also in the longitudinal direction. It is known that at a certain critical amplitude of longitudinal vibrations a long rod loses its mechanical stability and begins to vibrate in a bending mode. Therefore its side surface also becomes a source of ultrasonic radiation into a liquid, and this radiation can be used for technological purposes inside narrow extended channels, into which the rod is introduced, for example, for the cleaning of their walls.

It was stated above that because of limitations on the fatigue strength of a metal, there is an upper limit to the amplitude of the vibrations of a waveguide-radiator, at which the waveguide-radiator rapidly breaks down mechanically and its operational life sharply decreases. This phenomenon also limits the possibility of increasing the acoustic power radiated into a load using a conventional waveguide. To overcome this basic obstacle and to increase further the acoustic energy radiated into a load, the following modification of a waveguide-radiator according to the present invention was developed. As shown in FIG. **5**, a waveguide radiator **80** according to the present invention has an ultrasonic reactor **81** arranged immediately inside the waveguide-radiator **80** in the form of a hollow resonant sphere **82** acoustically rigidly connected to it and being an integral part of it. The resonant sphere **82** is filled with a working liquid or gas (acoustic load) **83**. The waveguide radiator also includes an inlet **84** and outlet **85** for the acoustic load **83**, and is connected to a transducer **86**. The acoustic parameters of the resonant sphere **82** are selected such that the focus of the acoustic field inside the sphere is located in its geometric center. Thus, in the geometric center of the sphere a very high amplitude of vibrations in a load can be achieved due to concentration of the vibrations in a converging acoustic wave.

Another embodiment of a waveguide-radiator **90** according to the present invention is shown in FIG. **6**. According to other embodiments of the present invention, the waveguide-radiator is passive. That is, it does not have inside itself an active acoustic transducer for converting electric energy into acoustic energy. According to the present embodiment of the invention, the waveguide-radiator **90** also performs an active function, the conversion of electric energy into acoustic energy. Acoustic calculation of the geometrical parameters of the waveguide radiator in the given case is carried out taking into account not only the passive properties of the cylindrical sections and sections of variable cross-section all comprised of standard waveguide-radiator material **91**, but also the active properties of piezoelectric annular transducers **92** connected acoustically rigidly to the waveguide-radiator. Piezoelectric annular transducers **92** are situated in the waveguide-radiator cross-sections close to nodal cross-sections. Because the number of nodal cross-sections of the specified waveguide-radiator can be greater than one, the number of the pairs of piezoelectric rings **92** can also be increased manifold in comparison with known piezoelectric transducers. Thus, the total power of the waveguide-radiator also increases manifold. In addition, because an active waveguide-radiator according to this embodiment has a gain factor greater than unity, the amplitude of the vibrations at its exit end is much higher than the amplitude of the vibrations of the piezoelectric annular transducers themselves.

For calculation of a waveguide-radiator according to the present invention, the following initial parameters are taken. The waveguide-radiator material is titanium (Ti-6AL-4V), the operating frequency F=20 kHz, the gain factor of the amplitude of vibrations $K \approx 6$, and the entrance and exit diameters of the waveguide-radiator are approximately equal. The ratio of the total length of the waveguide radiator sections L**4**+L**5** to its exit diameter is about 3:1.

FIG. **7** shows the following calculated parameters for a resonant waveguide-radiator: diameters D**0**, d, D**1**; lengths of cylindrical sections L**1**, L**3**, L**5**; lengths of the sections of variable cross section L**2**, L**4**. Besides, FIG. **7** shows the plots of the distribution of the vibration amplitudes V(z) and strain e(z) along the waveguide-radiator length, which were also obtained as a result of calculation.

In order to allow the comparison of the results of calculation of the specified waveguide-radiator with analogous calculated data for a conventional waveguide (so called spool horn), FIG. **8** is given. The ratio of the total length of the conventional waveguide sections L**4**+L**5** to its exit diameter is about 0.2:1.

From comparison of FIG. **7** and FIG. **8** it is seen that the course of the distribution of strain e(z) along the length of the conventional waveguide shown in FIG. **8** has a discontinuous, polygonal character, which is indicative of high values of the strain and stress gradients in the conventional waveguide body. At the same time, the course of analogous curve e(z) for the waveguide-radiator according to the present invention has a smooth character without sharp bends and kinks. This points to the absence of considerable gradients of strain and stresses in the body of the waveguide radiator according to the present invention. The absence of high local gradients of mechanical stresses in the body of the disclosed waveguide-radiator provides a considerable increase in the limit of its fatigue strength and, as a consequence, its expected operational life in comparison with the conventional waveguide at equal parameters and conditions of their operation.

On the basis of the data given in FIG. **7** and FIG. **8**, the disclosed waveguide-radiator shown in FIG. **7** and the conventional waveguide shown in FIG. **8** were manufactured and tested. Tests were carried out at equal amplitudes of vibrations at the exit ends of the waveguides and being 150 μm peak-to-peak. The acoustic load was tap water. The results of tests showed the following:

1. The disclosed waveguide-radiator (FIG. **7**) had an actual resonance frequency that corresponded closely with the predicted one and an actual gain factor that corresponded closely with the predicted one. It operates stably. Moreover, the disclosed waveguide was tested for 6 (six) month of continuous work without failure; after this time the tests were stopped.

2. The conventional waveguide (FIG. **8**) operated unstably. The actual waveguide resonance frequency differed from the predicted one (which was calculated in advance). The exit section L**5** had a considerable bending mode of vibrations. It was necessary to conduct an incremental tuning of this waveguide to obtain its resonance length. Only after such tuning was it possible to test the waveguide. The operating time of the conventional waveguide after its additional tuning was about 6 days, at which point it suffered mechanical failure.

The theory of acoustic waveguide-radiators is based on the problem of longitudinal vibrations of multi-section rods that have cylindrical sections and sections of variable cross-section. We will consider only waveguide-radiators of axially symmetric shape. Other types of waveguide-radiators (for example, wedge-shaped) can be considered in the analogous way.

We assume that during the passage of the stress waves through a waveguide-radiator, the wave front remains plane, while the stresses are uniformly distributed over the waveguide-radiator's cross-section. This assumption limits us to the consideration of only thin waveguide-radiators, whose resonance length significantly exceeds their diameter. The scheme and the designation of parameters for an exemplary five-section rod waveguide-radiator are given in FIG. **9**, which depicts a rod waveguide-radiator **100** having five sections of length L_N and diameter d_N, where N is the number of the section. Two possible situations are presented: a waveguide-radiator for which $d_1/d_3>1$ is shown by the solid line; a waveguide-radiator for which $d_1/d_3<1$ is shown by the dotted line. In the approximation used, the problem is considered in one dimension, and it is limited to the consideration of sections with variable cross-section of only conical shape. For steady-state mode, the Rayleigh equation of vibrations for displacements u takes the following:

$$u'' + \frac{1}{S}S'u' + k^2u = 0. \tag{1}$$

Here: k=ω/C is the wave number, ω=2πf is the angular frequency of vibrations, and f is the frequency of vibrations.

The solution of equation (1) for the waveguide-radiator sections can be written as:

$$u_1=A_1 \cos kz+B_1 \sin kz \quad -L_1<z<0$$

$$u_2=F(A_2 \cos kz+B_2 \sin kz) \quad 0<z<L_2$$

$$u_3=A_3 \cos kz+B_3 \sin kz \quad L_2<z<L_2+L_3$$

$$u_4=F(A_4 \cos kz+B_4 \sin kz) \quad L_2+L_3<z<L_2+L_3+L_4$$

$$u_5=A_5 \cos kz+B_5 \sin kz \quad L_2+L_3+L_4<z<L_2+L_3+L_4+L_5$$

Then, using the boundary conditions for the waveguide-radiator sections, we obtain the system of equations for displacements u and strains u'.

At $z=-L_1$, $u_1=u_{in}$, $ES_1u'_1=-F_{in}$, $F_{in}=0$

$$A_1 \cos kL_1-B_1 \sin kL_1=u_{in};$$

$$EkS_1(A_1 \sin kL_1+B_1 \cos kL_1)=-F_{in}.$$

At z=0, $u_2=u_1$, $u'_2=u'_1$.

$$FA_2=A_1;$$

$$F'A_2+FB_2k=kB_1;$$

$$\alpha=(d_1-d_3)/L_2d_1;$$

$$F=2/d_1;\ F'=F\alpha.$$

At $z=L_2$, $u_3=u_2$, $u'_3=u'_2$.

$$A_3 \cos kL_2+B_3 \sin kL_2=F(A_2 \cos kL_2+B_2 \sin kL_2);$$

$$-kA_3 \sin kL_2+kB_3 \cos kL_2=(F'B_2-FkA_2)\sin kL_2+(F'A_2FkB_2)\cos kL_2;$$

$$\alpha=(d_1-d_3)/L_2d_1;$$

$$F=2/d_3;\ F'=-F/(L_2-1/\alpha).$$

At $z=L_2+L_3$, $u_4=u_3$, $u'_4=u'_3$.

$$F[A_4 \cos k(L_2+L_3)+B_4 \sin k(L_2+L_3)]=A_3 \cos k(L_2+L_3);$$

$$(F'B_4-FkA_4)\sin k(L_2+L_3)+(F'A_4+FkB_4)\cos k(L_2+L_3)==-kA_3 \sin k(L_2+L_3)+kB_3 \cos k(L_2+L_3);$$

$$\alpha=(d_3-d_5)/L_4d_3;$$

$$F=2/d_3;\ F'=F\alpha.$$

At $z=L_2+L_3+L_4$, $u_5=u_4$, $u'_5=u'_4$.

$$A_5 \cos k(L_2+L_3+L_4)+B_5 \sin k(L_2+L_3+L_4)==F[A_4 \cos k(L_2+L_3+L_4)+B_4 \sin k(L_2+L_3+L_4)];$$

$$-kA_5 \sin k(L_2+L_3+L_4)+kB_5 \cos k(L_2+L_3+L_4)==(F'B_4-FkA_4)\sin k(L_2+L_3+L_4)+(F'A_4+FkB_4)\cos k(L_2+L_3+L_4);$$

$$\alpha=(d_3-d_5)/L_4d_3;$$

$$F=2/d_5;\ F'=-F/(L_4-1/\alpha).$$

At $z=L_2+L_3+L_4+L_5$, $u_5=u_{out}$, $u'_5=0$.

$$A_5 \cos k(L_2+L_3+L_4+L_5)+B_5 \sin k(L_2+L_3+L_4+L_5)=U_{out};$$

$$-A_5 \sin k(L_2+L_3+L_4+L_5)+B_5 \cos k(L_2+L_3+L_4+L_5)=0$$

The waveguide-radiator gain factor equals:

$$K = \left|\frac{u_{out}}{u_{in}}\right| = \left|\frac{A_5 \cos k(L_2 + L_3 + L_4 + L_5) + B_5 \sin k(L_2 + L_3 + L_4 + L_5)}{A_1 \cos kL_1 - B_1 \sin kL_1}\right|$$

Here: $F=2/d_n$, d_n is the diameter of the corresponding cylindrical section of the waveguide-radiator, A_n and B_n are the constant coefficients for the corresponding sections of the waveguide-radiator, L_n is the length of the corresponding section of the waveguide-radiator, n is the order number of the waveguide-radiator section, α is the cone index of the waveguide-radiator section with variable cross-section, u_{in} and u_{out} are the amplitudes of displacements at the waveguide-radiator input and output, respectively. The boundary conditions for a force acting on the waveguide-radiator input $F_{in}=0$ and strains $u'_5=0$ at the waveguide-radiator output in this system of equations indicate that the waveguide-radiator has a resonance total length and does not have an acoustic load. From the system of equations (3), one can obtain all necessary characteristics of a five-section waveguide-radiator: lengths and diameters of sections, gain factor, and distribution of vibration amplitudes and strains along the length. From this system of equations, it is also easy to obtain solutions for waveguide-radiators of any type with conical sections (from single-section to five-section waveguide-radiators). Thus, the given system of equations is the most general one. Waveguide-radiators with other shapes of the sections of variable cross-section (for example, with exponential or catenoidal sections) can be considered exactly in the analogous way, taking into account the variation of sound velocity in such sections.

While there has been illustrated and described what are at present considered to be preferred and alternate embodiments of the present invention, it should be understood and appreciated that modifications may be made by those skilled in the art, and that the appended claims encompass all such modifications that fall within the full spirit and scope of the present invention.

What is claimed is:

1. An ultrasonic resonant rod waveguide-radiator having a defined length, an entrance surface and an exit surface, comprising: at least three cylindrical sections, including a first cylindrical section comprising the radiator's entrance surface and a second cylindrical section comprising the radiator's exit surface; at least two sections of variable cross-section;

wherein said at least three cylindrical sections and said at least two sections of variable cross-section are arrayed in alternating positions and acoustically rigidly connected together; wherein the ratio of the cross-sectional areas of the exit surface and the entrance surface is approximately 1:1; wherein the waveguide-radiator's total length is equal to a multiple of half the length of an acoustic wave in the waveguide-radiator material, taking into account a geometrical dispersion; wherein the length of each of said at least two section of variable cross-section is no less than the value of Log(N)/k, where N is the ratio of diameters of the cylindrical sections adjacent to said section of variable cross-section and where k is the wave number, which is equal to ω /C where ω is the frequency of ultrasonic vibrations and C is the speed of sound in liquid;

wherein the sum of the length of the second cylindrical section and the length of the section of variable cross-section adjacent to said second cylindrical section is at least 30% of the total length of the waveguide-radiator.

2. The ultrasonic resonant rod waveguide-radiator of claim **1** further comprising resonant plates fastened acoustically rigidly to said second cylindrical section for vibrating at a bending mode.

3. The ultrasonic resonant rod waveguide-radiator of claim **1** further comprising resonant spheres fastened acoustically rigidly to said second cylindrical section for vibrating in a radial mode.

4. The ultrasonic resonant rod waveguide-radiator of claim **1** further comprising a thin plate fastened acoustically rigidly to said second cylindrical section and positioned on said second cylindrical section's side surface in a helix in such a way that the radiating surfaces of the plate are at an acute angle with the axis of the waveguide-radiator.

5. The ultrasonic resonant rod waveguide-radiator of claim **1**, wherein said cylindrical sections and said sections of variable cross-section are selected such that the main flux of acoustic radiation into a load additionally is directed through the side surfaces of said waveguide-radiator's second cylindrical section.

6. The ultrasonic resonant rod waveguide-radiator of claim **1** further comprising flexible long waveguides rigidly connected to the exit surface of said waveguide-radiator, said flexible waveguides capable of being excited by said waveguide-radiator's vibration amplitude causing such that said flexible waveguides lose mechanical stability.

7. The ultrasonic resonant rod waveguide-radiator of claim **1** further comprising an ultrasonic reactor having a working medium, said reactor situated within the waveguide radiator and said reactor comprising a hollow resonant sphere acoustically rigidly connected to said waveguide-radiator and being an integral part of said waveguide-radiator.

8. The ultrasonic resonant rod waveguide-radiator of claim **1** further comprising an even number of annular piezoelectric elements situated on said cylindrical sections, for converting electric energy into acoustic energy.

* * * * *


input end
in contact with
transducer,
low amplitude
output tip
in contact with
liquid,
high amplitude

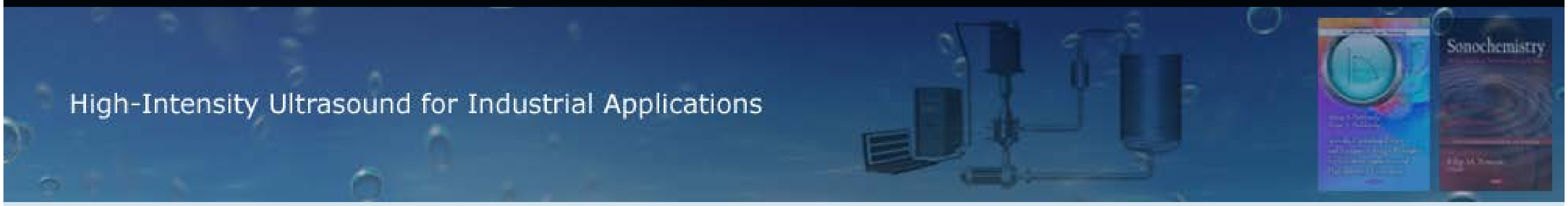

INTRODUCTION TO ISM

WHAT IS ISM?

ISM is a research and development, equipment design and process consulting firm, specializing in high-power ultrasonics. Our mission is to help businesses optimize their ultrasound-assisted processes and subsequently implement them in commercial-scale production. ISM offers high-intensity ultrasonic homogenizers for such industrial processes as the manufacture of nanocrystals, nanoemulsions, nanosuspensions in viscous liquids, micronized waxes, as well as for oil extraction, cell disruption, degassing, deagglomeration and many more.

INDUSTRIES/APPLICATIONS

- Pharmaceutical
- Cosmetics
- Food
- Pigments for inks, paints, coatings and varnishes
- Wood treatment
- Metalworking fluids
- Chemicals, including petrochemicals
- Alternative fuels
- Plastics, rubber, and epoxy processing

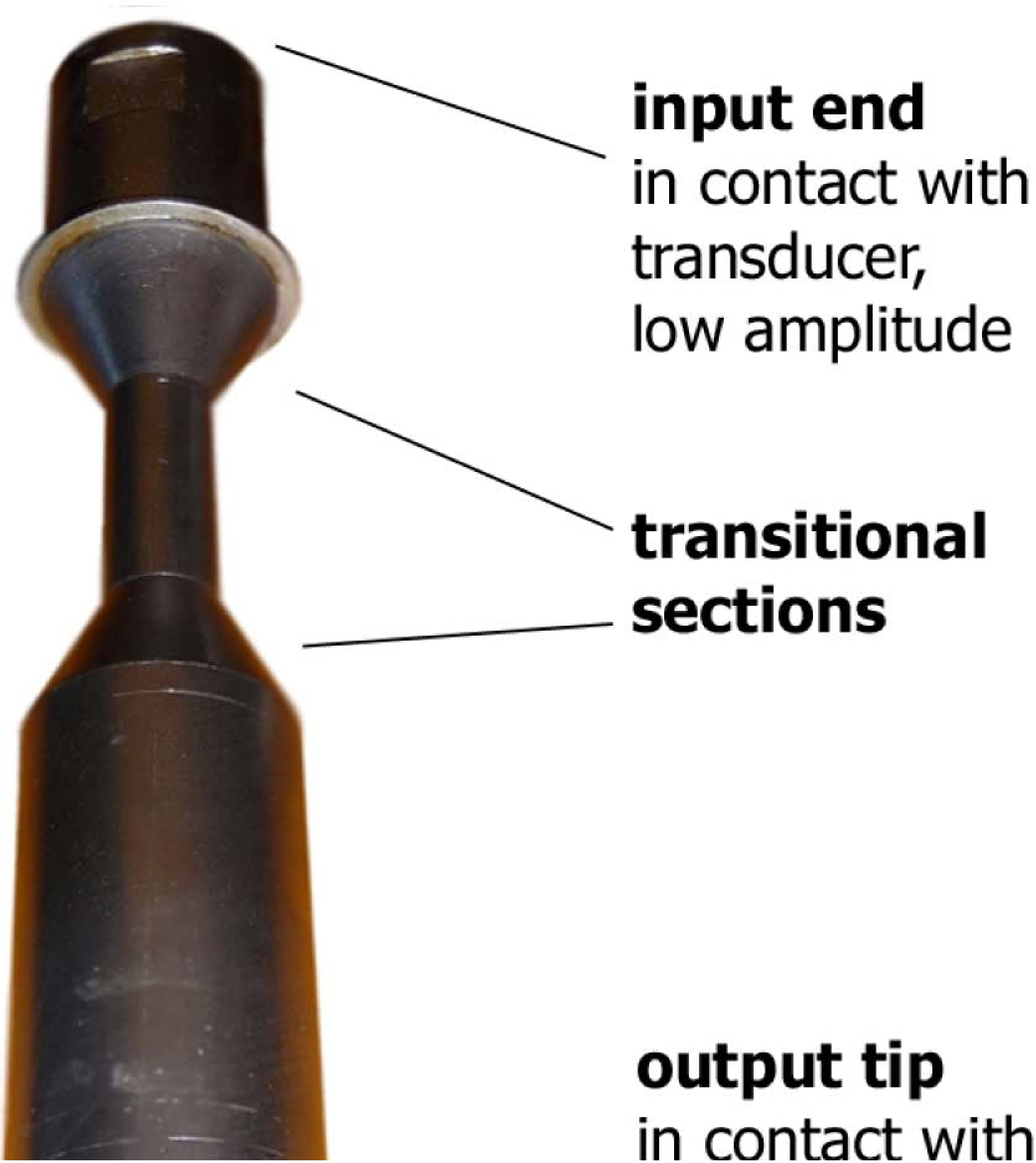
input end
in contact with
transducer,
low amplitude
transitional
sections
output tip
in contact with


liquid,
high amplitude

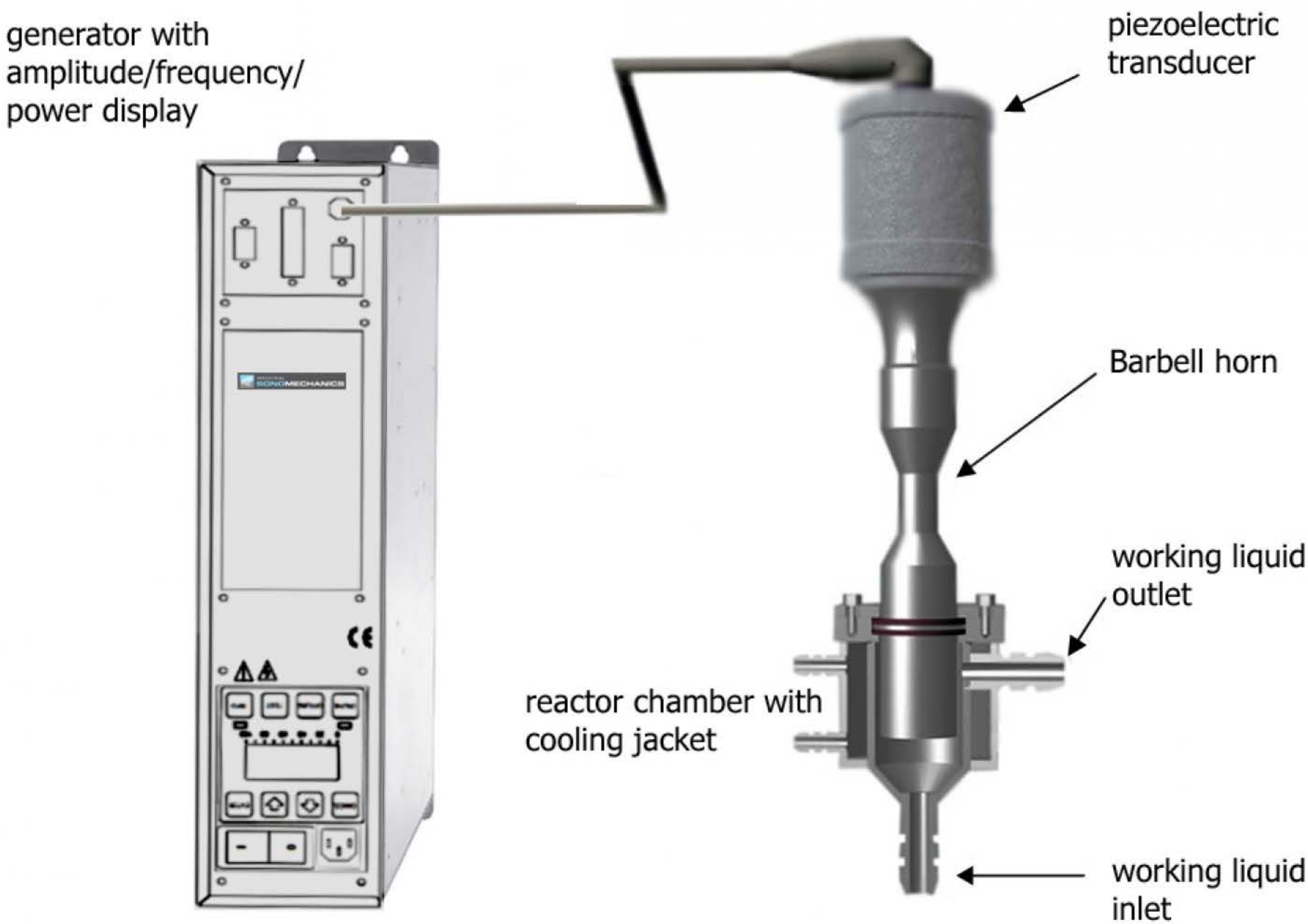
generator with
amplitude/frequency/
power display
piezoelectric
transducer
Barbell horn
working liquid
outlet
reactor chamber with
cooling jacket
working liquid
inlet


1
2
3
4
5

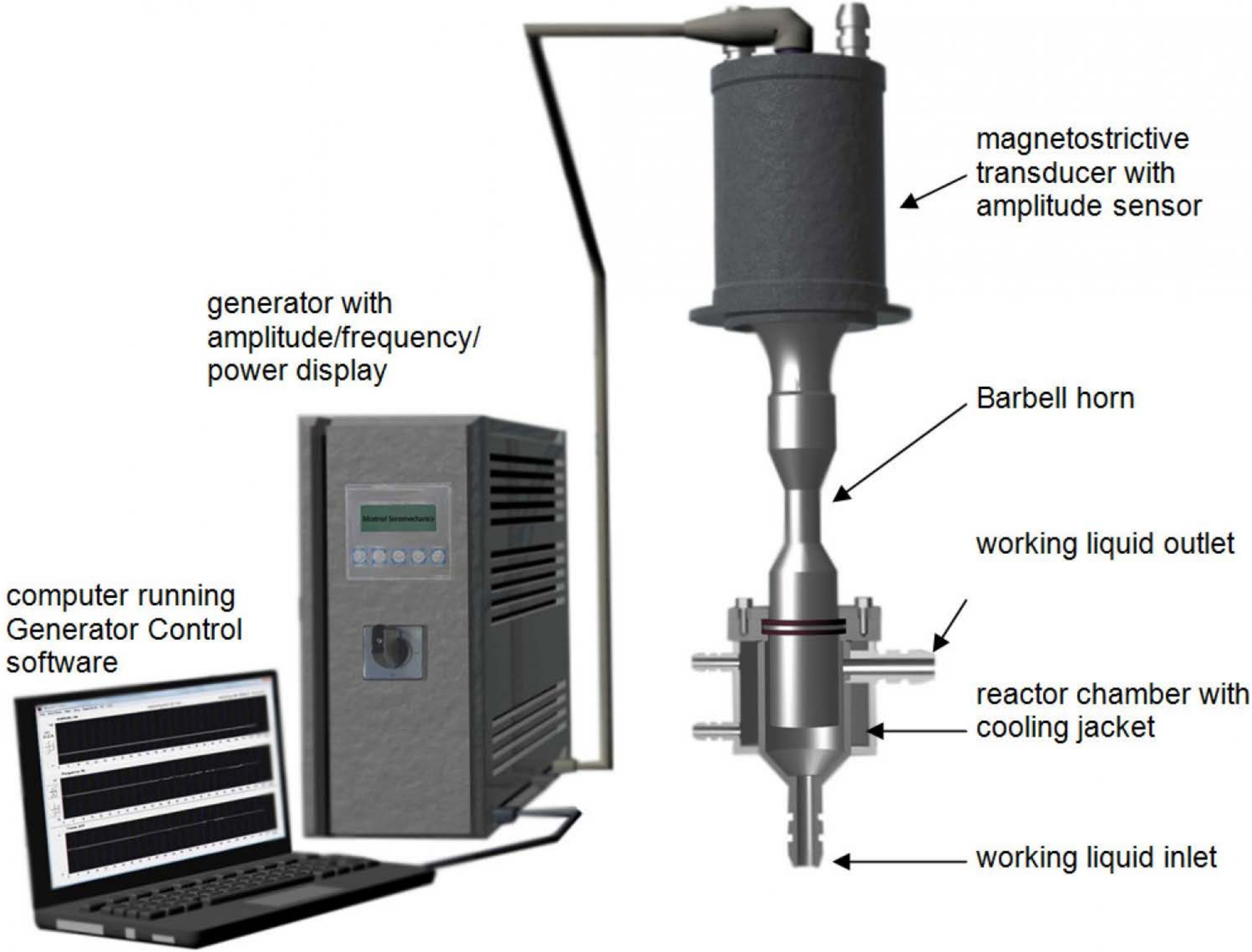
magnetostrictive transducer with amplitude sensor
generator with amplitude/frequency/ power display
Barbell horn
working liquid outlet
computer running Generator Control software
reactor chamber with cooling jacket
working liquid inlet

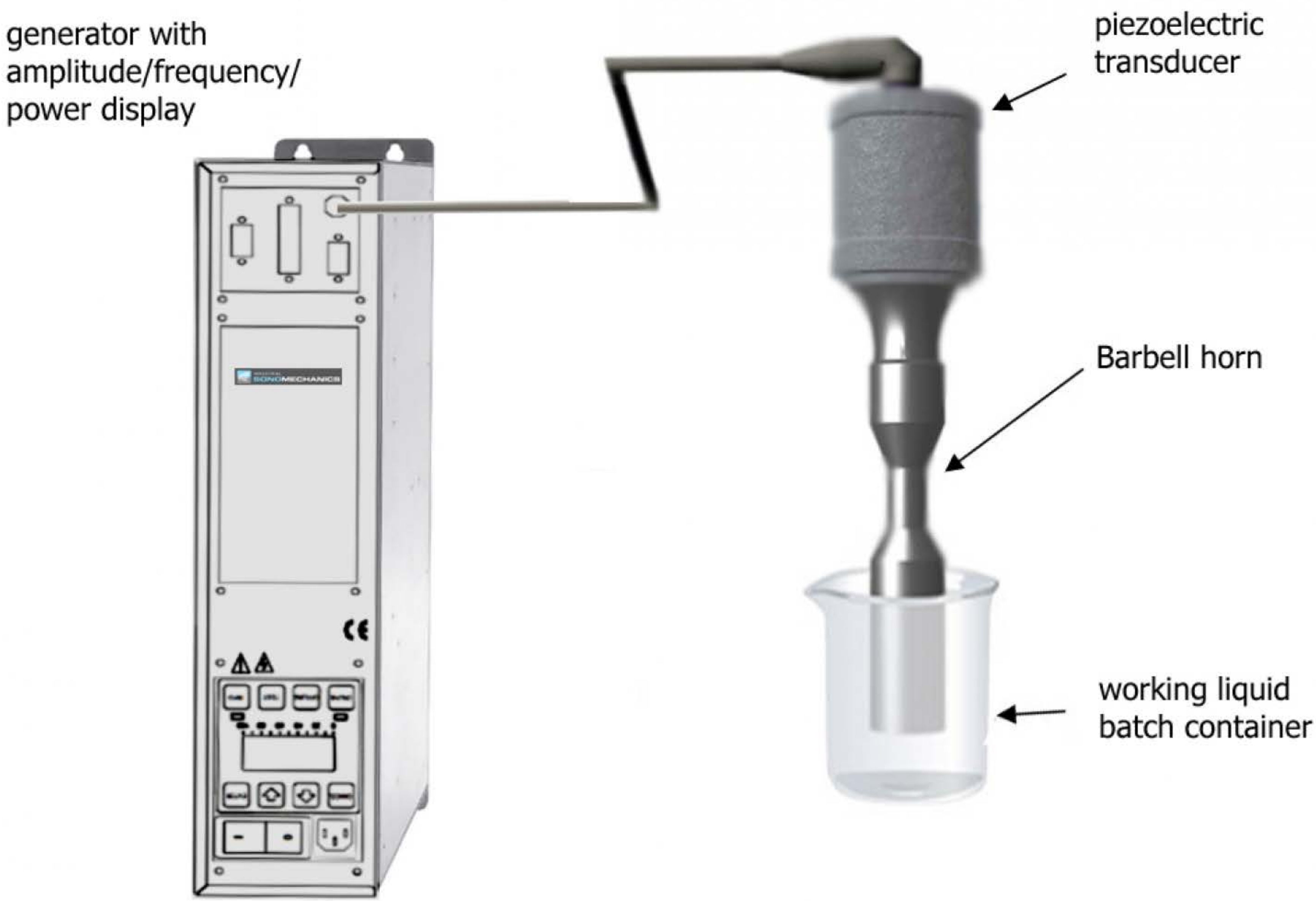
generator with
amplitude/frequency/
power display
piezoelectric
transducer
Barbell horn
working liquid
batch container
CE

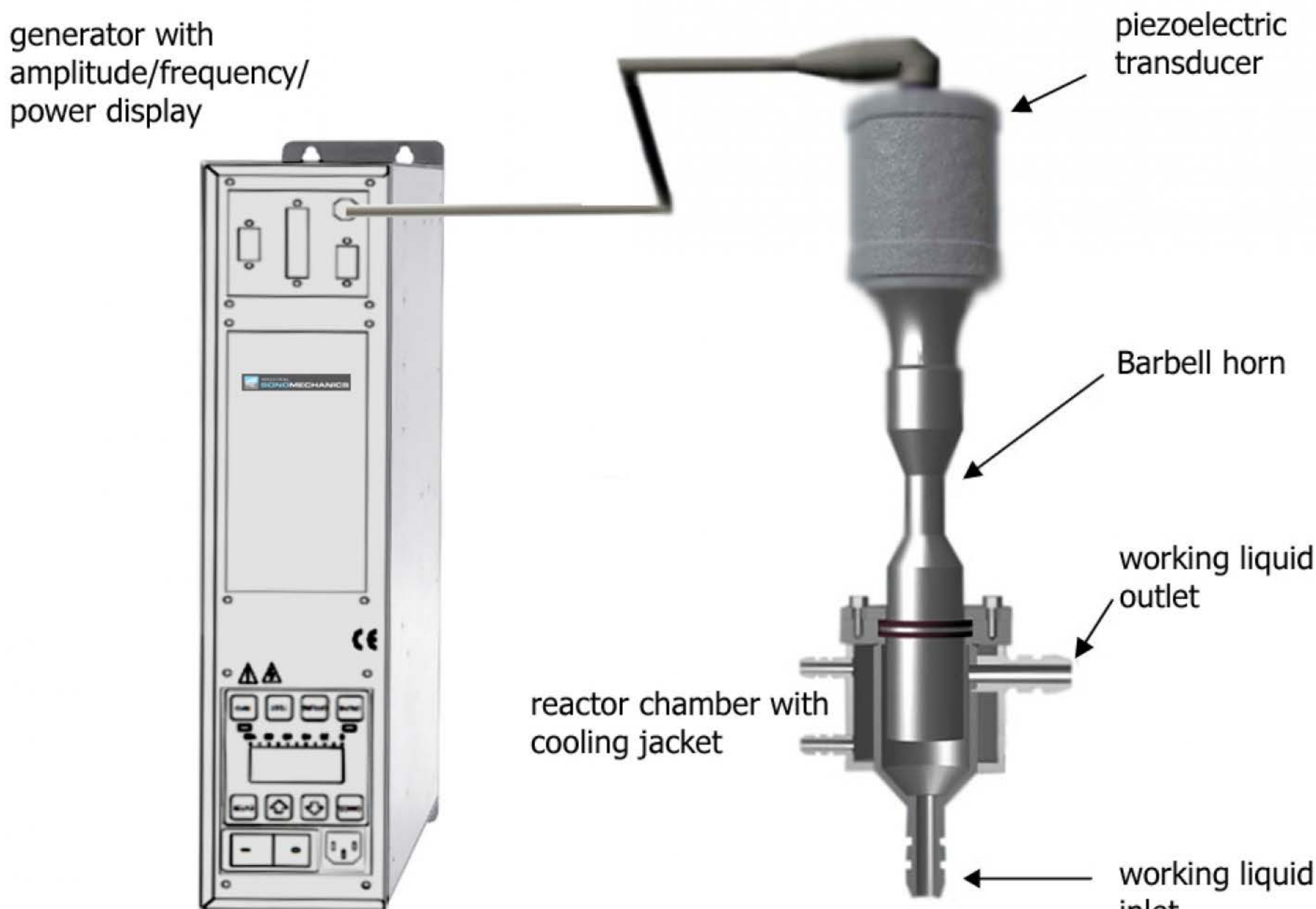
generator with
amplitude/frequency/
power display
piezoelectric
transducer
Barbell horn
working liquid
outlet
reactor chamber with
cooling jacket
working liquid
inlet

1

2

3

4


1
2
3
4
5
6

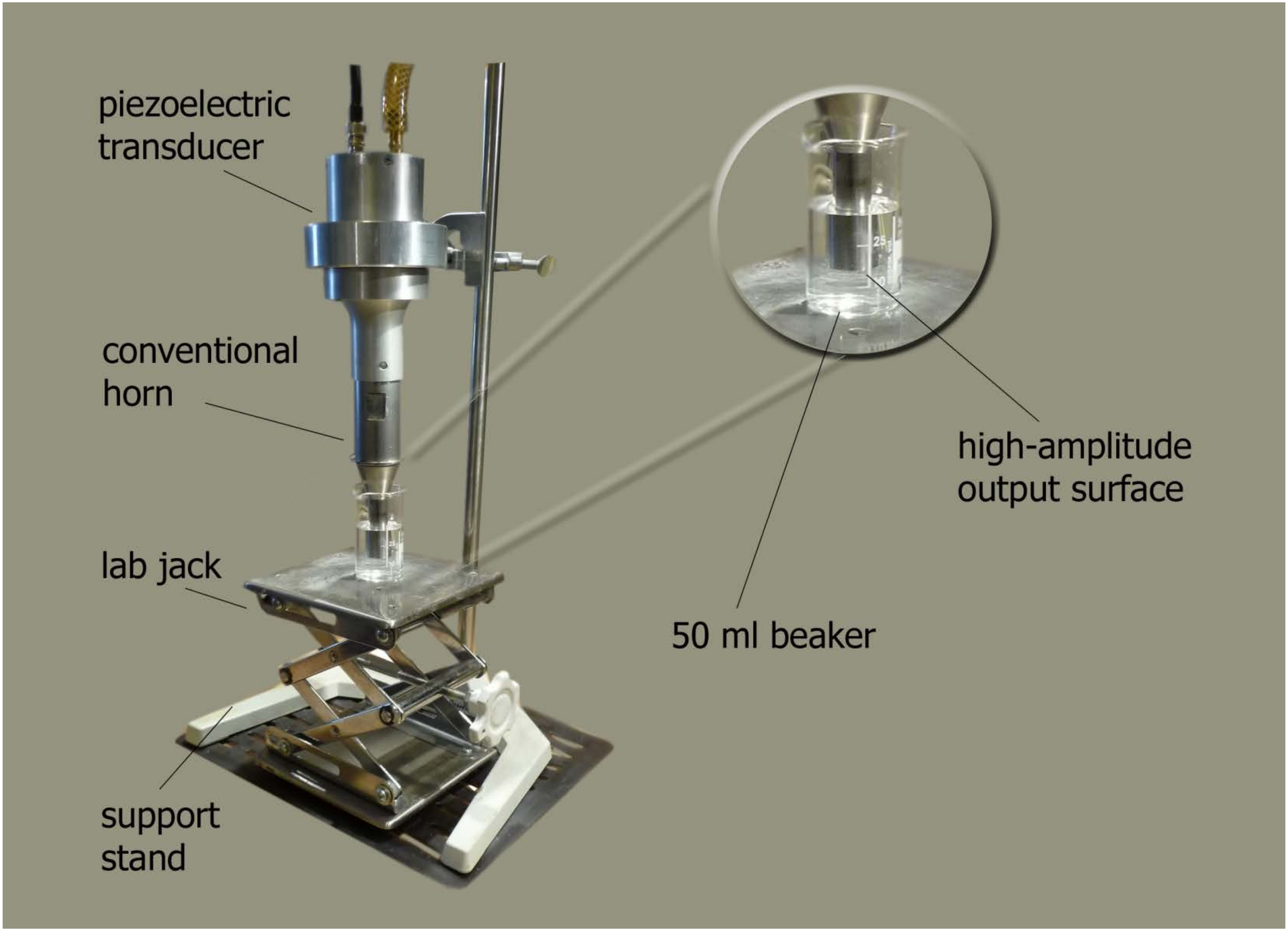
piezoelectric
transducer
conventional
horn
lab jack
support
stand
high-amplitude
output surface
50 ml beaker

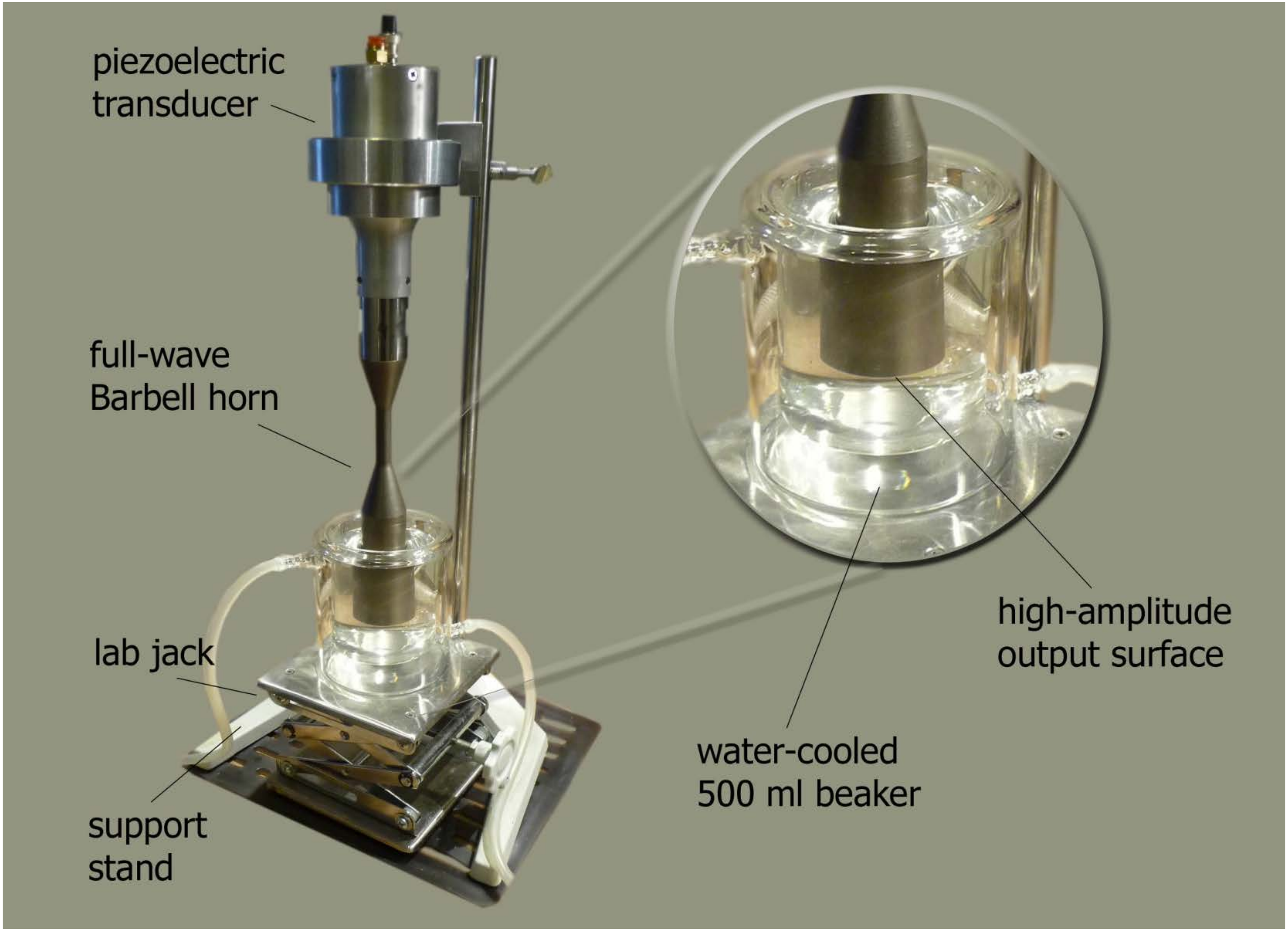
piezoelectric
transducer
full-wave
Barbell horn
lab jack
support
stand
high-amplitude
output surface
water-cooled
500 ml beaker

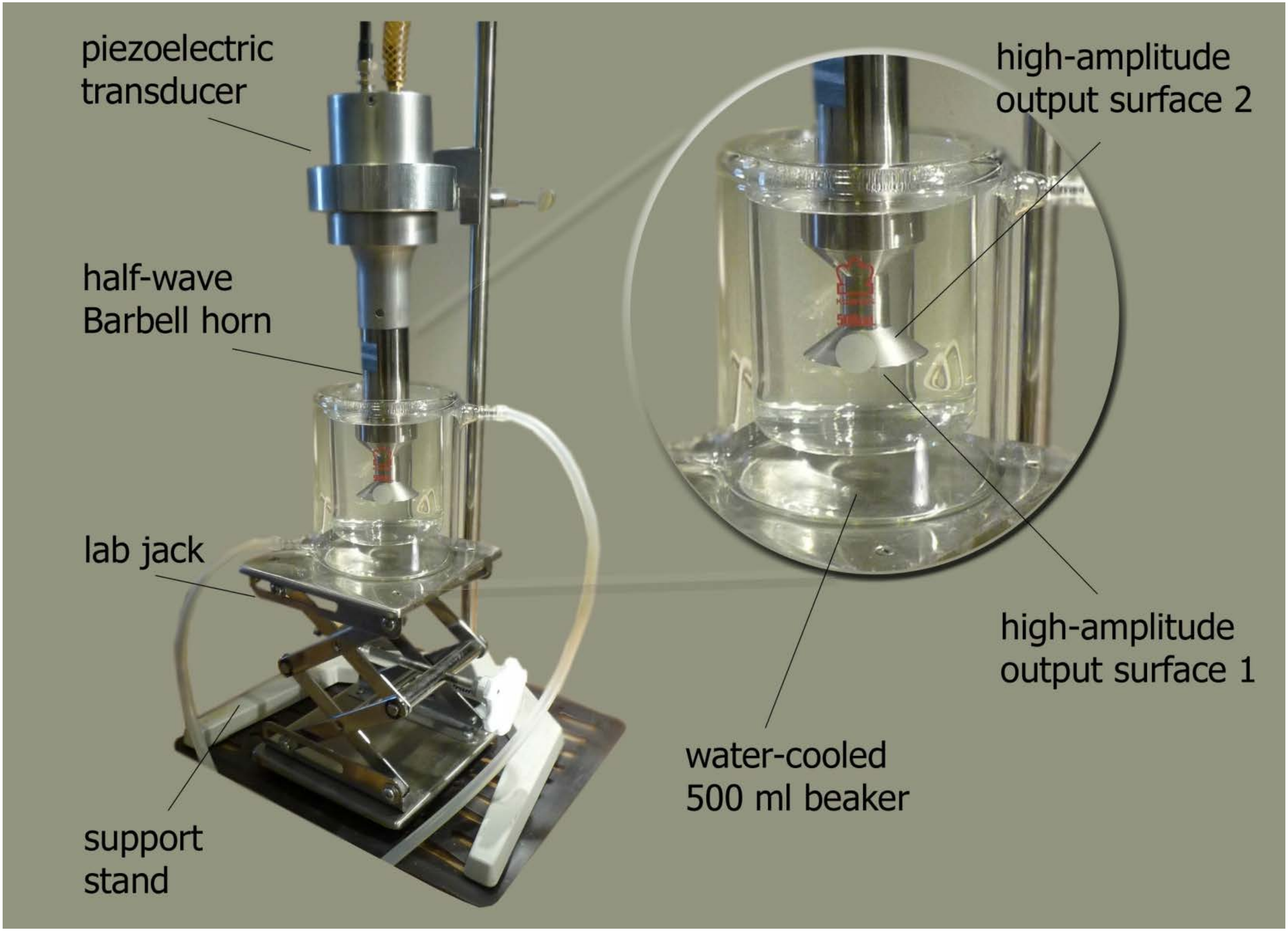
piezoelectric transducer
half-wave Barbell horn
lab jack
support stand
high-amplitude output surface 2
high-amplitude output surface 1
water-cooled 500 ml beaker

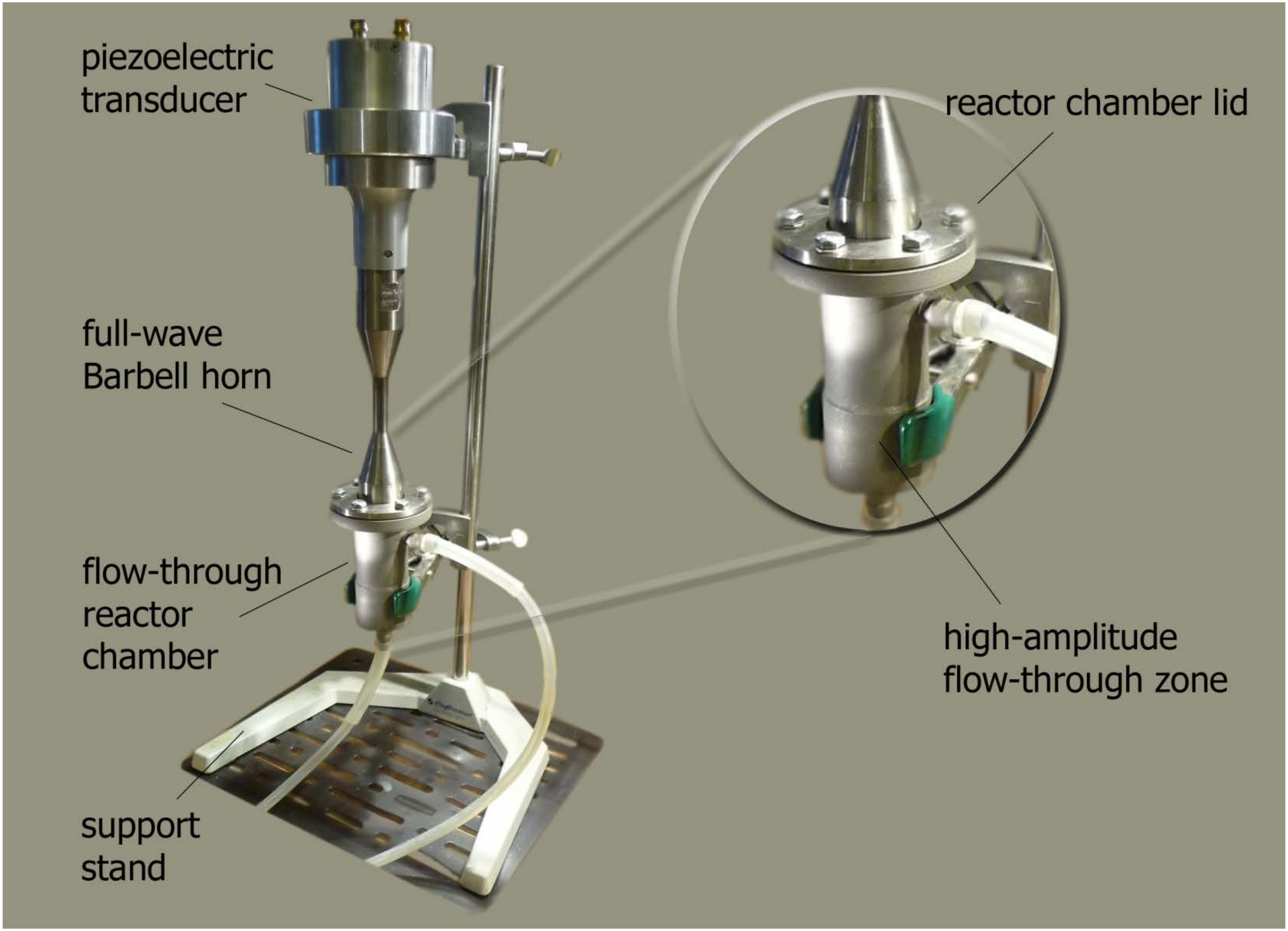
piezoelectric transducer
reactor chamber lid
full-wave Barbell horn
flow-through reactor chamber
high-amplitude flow-through zone
support stand

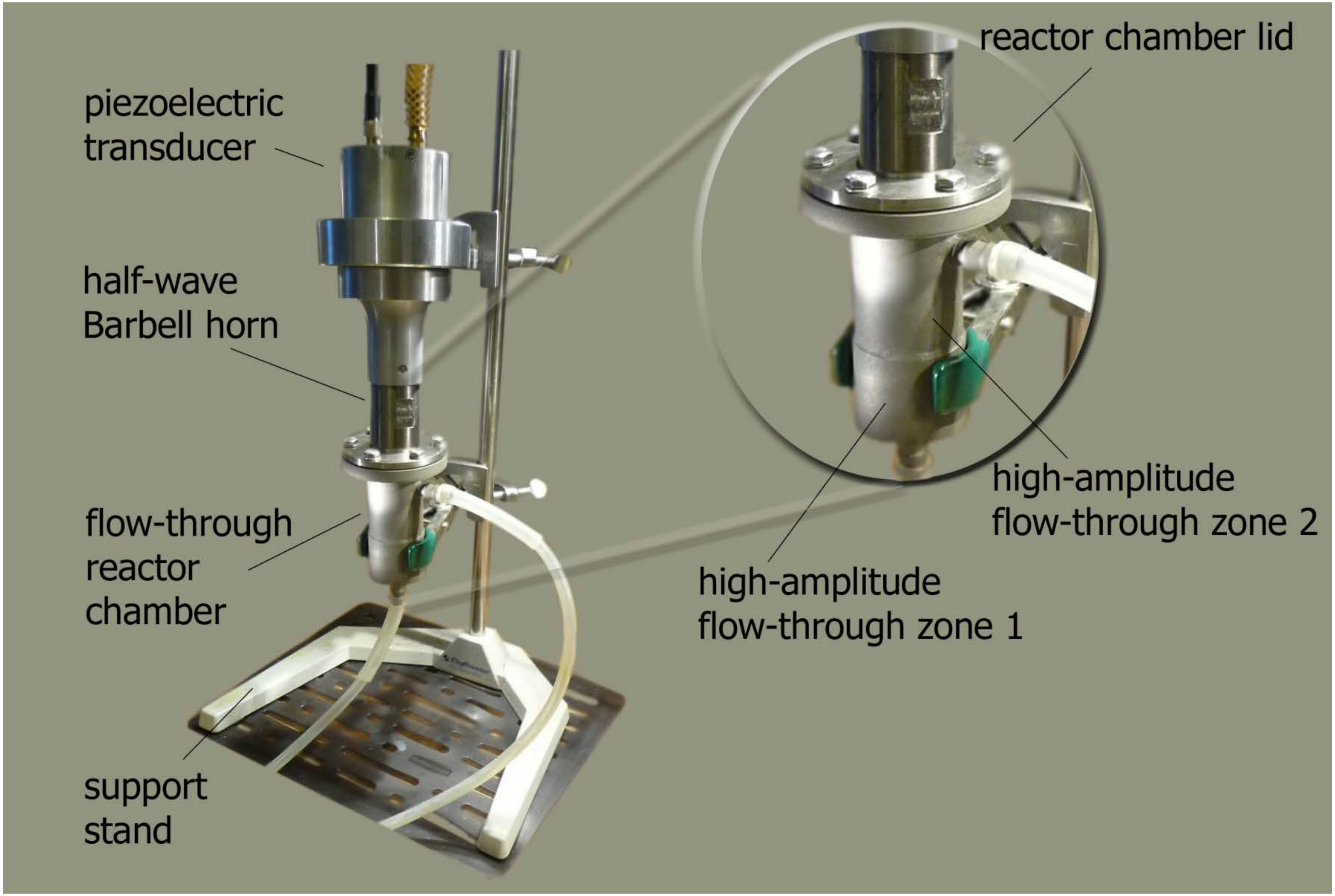
piezoelectric
transducer
half-wave
Barbell horn
flow-through
reactor
chamber
support
stand
reactor chamber lid
high-amplitude
flow-through zone 2
high-amplitude
flow-through zone 1


www.sonomechanics.com
SONOMECHANICS

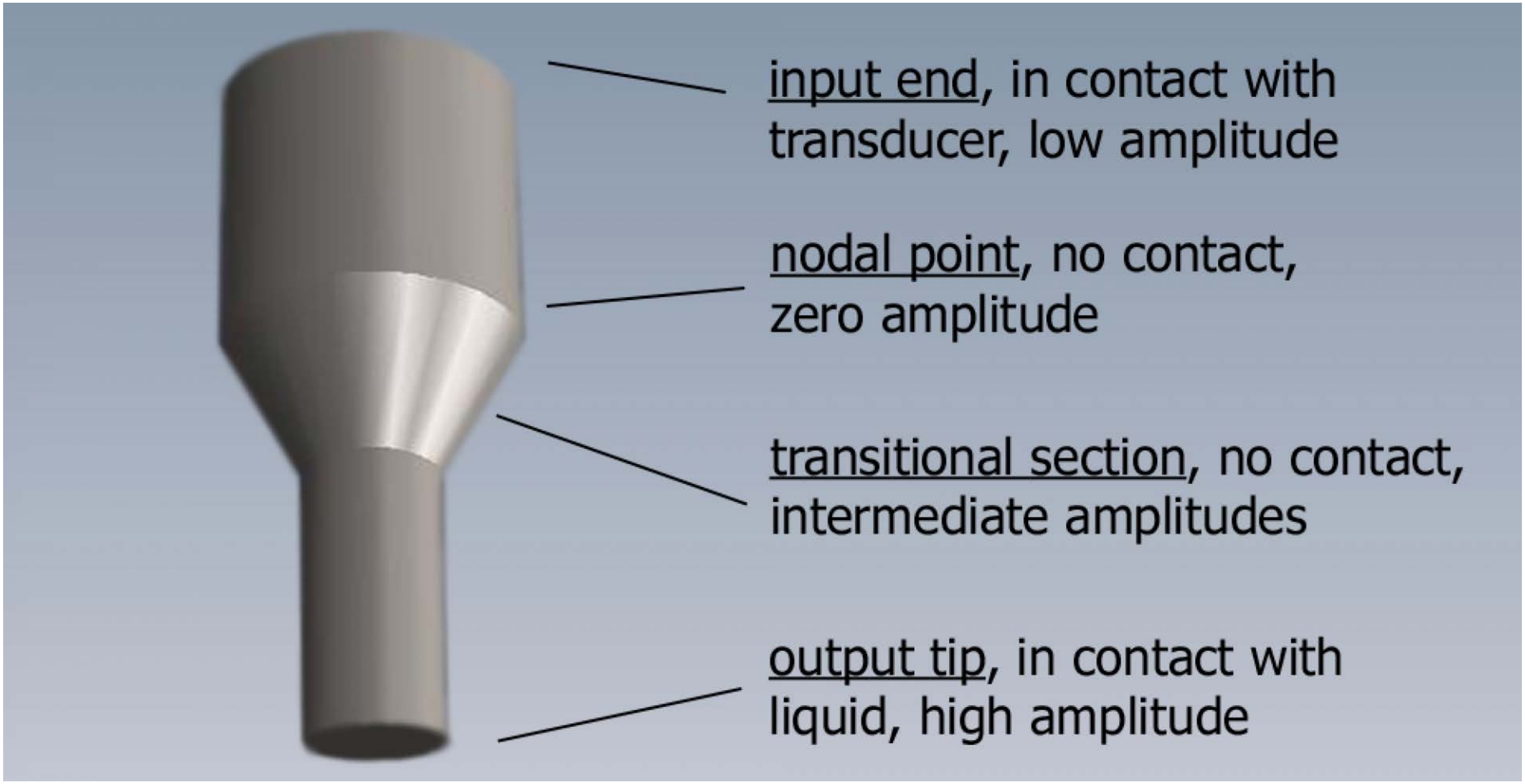
input end, in contact with transducer, low amplitude
nodal point, no contact, zero amplitude
transitional section, no contact, intermediate amplitudes
output tip, in contact with liquid, high amplitude

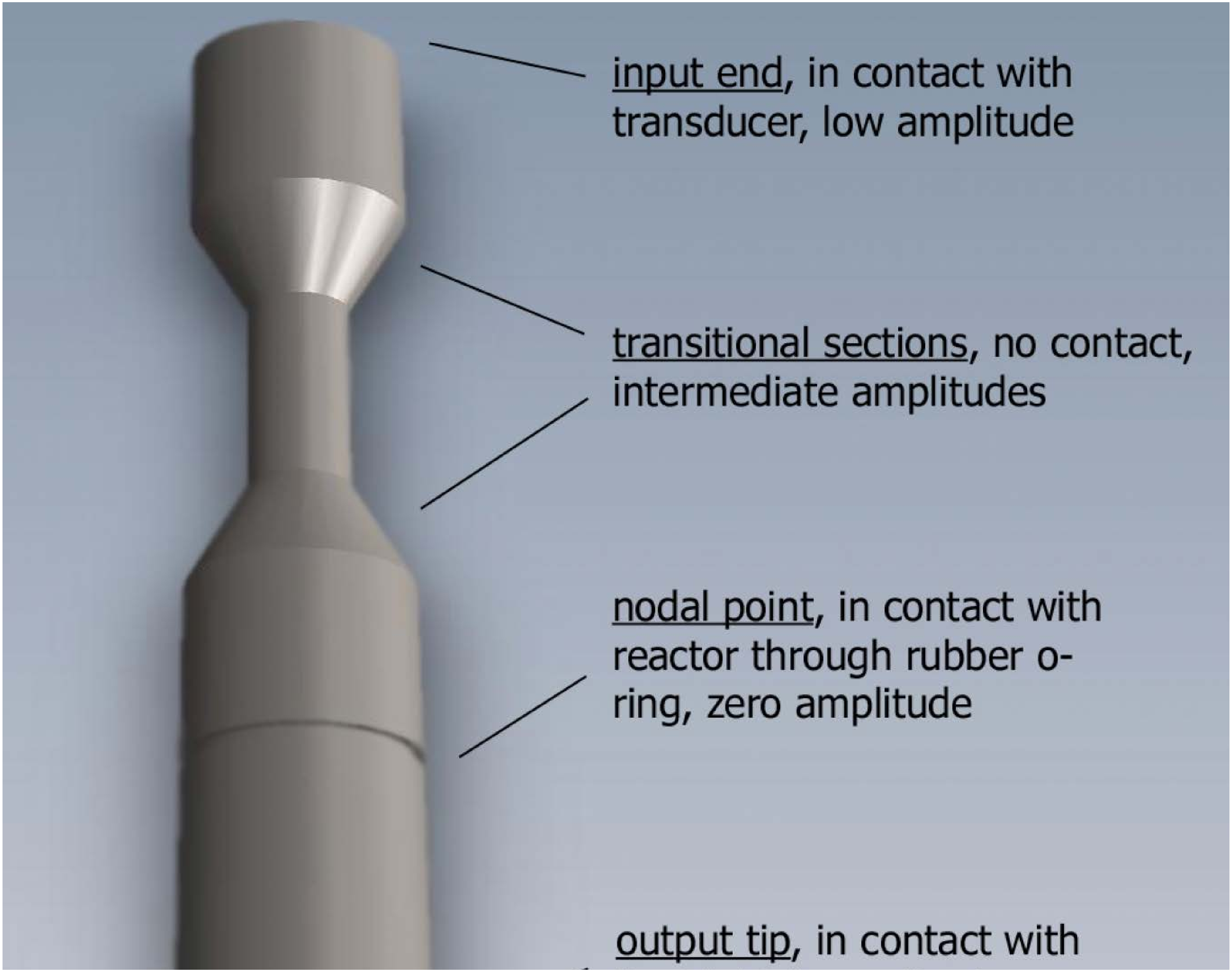
input end, in contact with transducer, low amplitude
transitional sections, no contact, intermediate amplitudes
nodal point, in contact with reactor through rubber o-ring, zero amplitude
output tip, in contact with

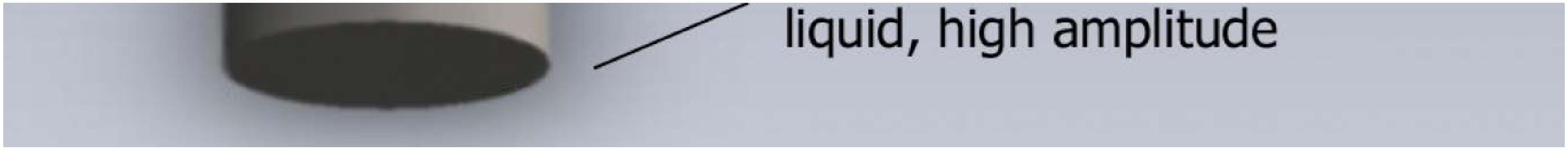
liquid, high amplitude

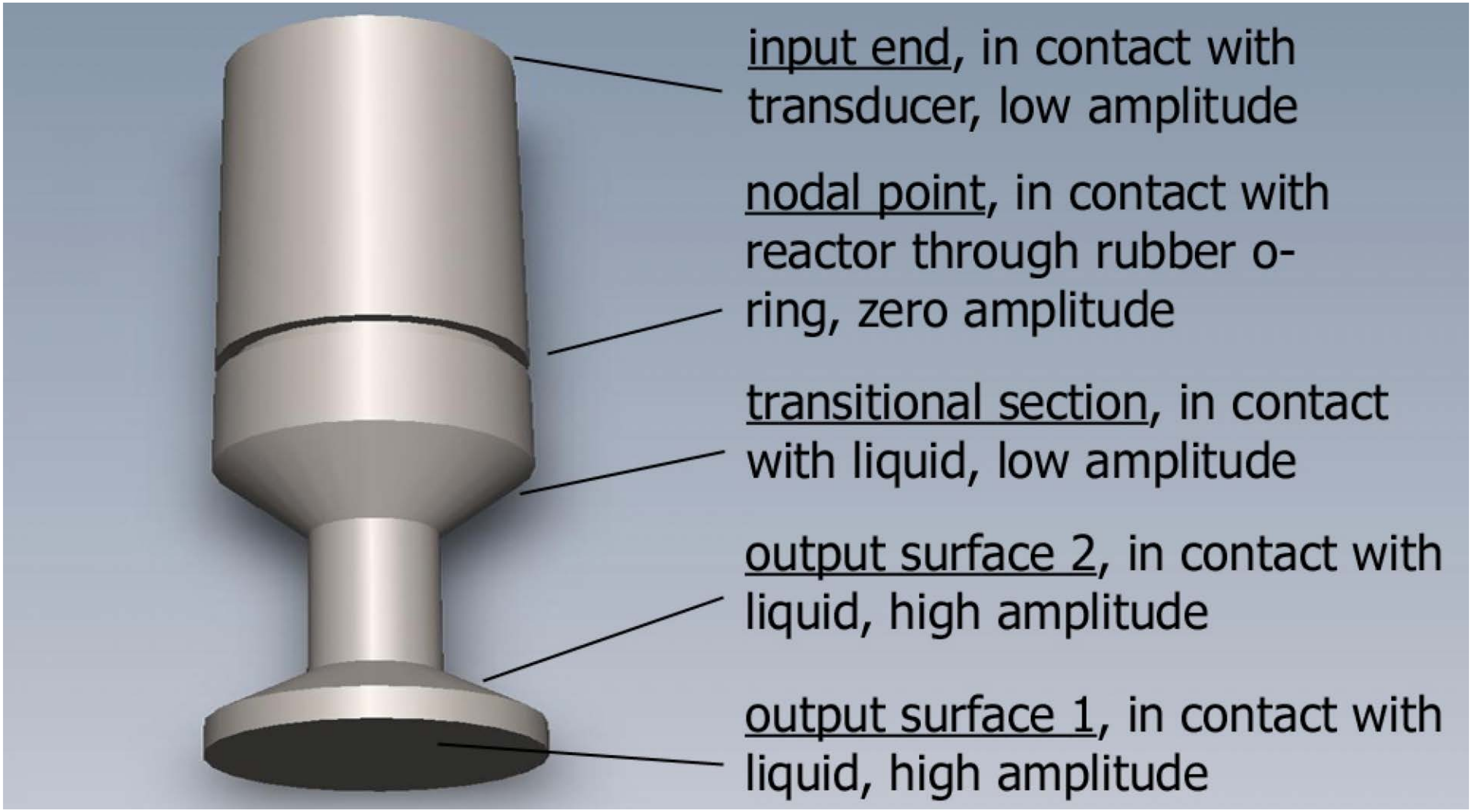
input end, in contact with transducer, low amplitude
nodal point, in contact with reactor through rubber o-ring, zero amplitude
transitional section, in contact with liquid, low amplitude
output surface 2, in contact with liquid, high amplitude
output surface 1, in contact with liquid, high amplitude

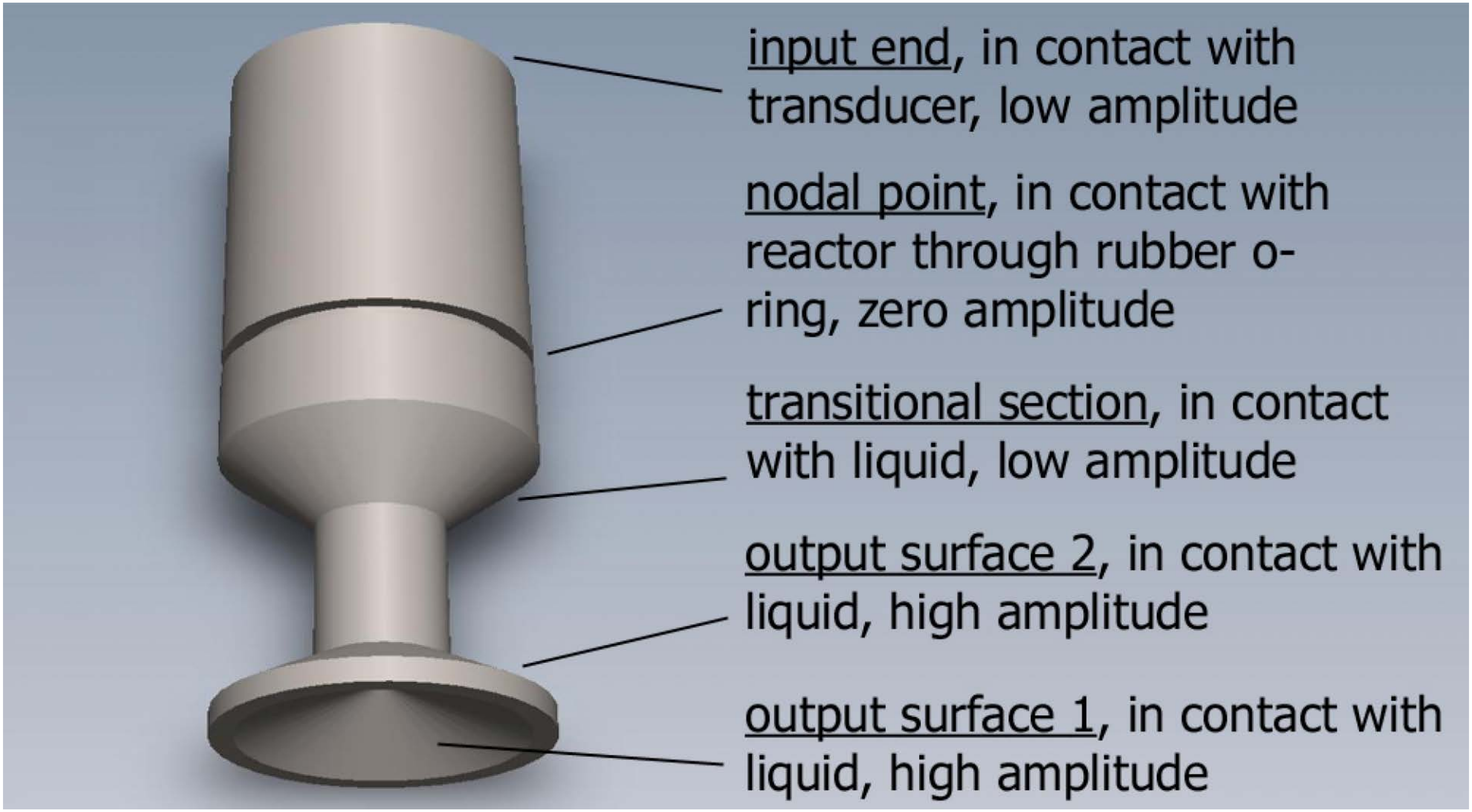
input end, in contact with transducer, low amplitude
nodal point, in contact with reactor through rubber o-ring, zero amplitude
transitional section, in contact with liquid, low amplitude
output surface 2, in contact with liquid, high amplitude
output surface 1, in contact with liquid, high amplitude

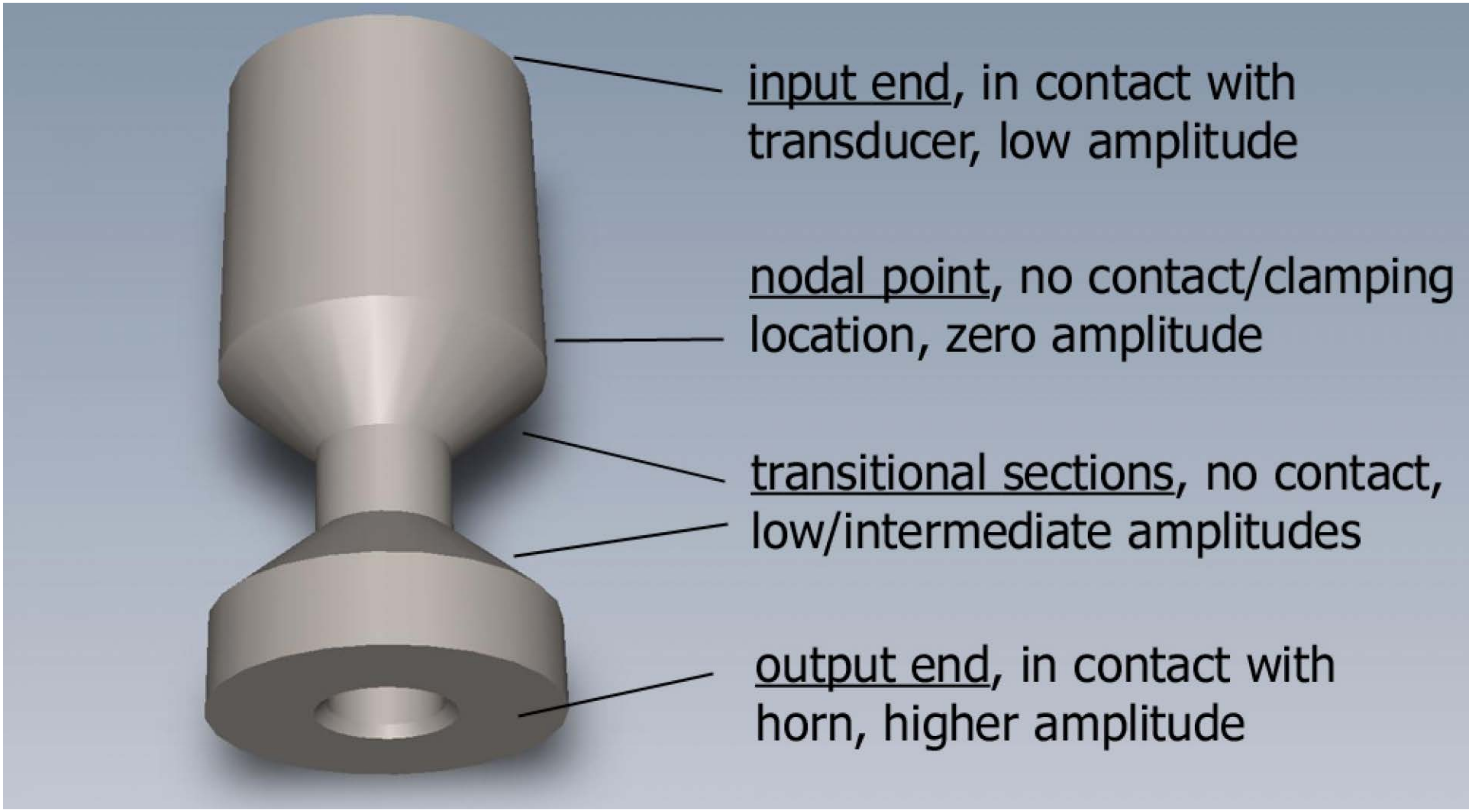
input end, in contact with
transducer, low amplitude
nodal point, no contact/clamping
location, zero amplitude
transitional sections, no contact,
low/intermediate amplitudes
output end, in contact with
horn, higher amplitude

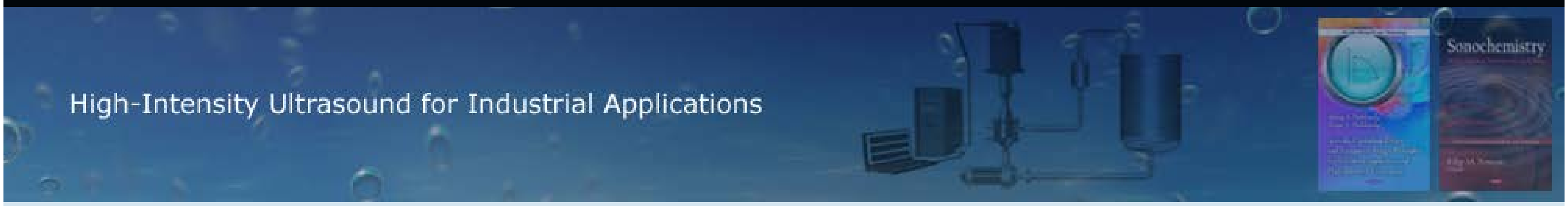

A HIGH-INTENSITY INDUSTRIAL ULTRASOUND COMPANY

Commercia-Scale High-Intensity Ultrasound

ISM is a high-intensity industrial ultrasound company. High-intensity (high amplitude) ultrasound is still mainly thought of as a laboratory technique, incapable of being efficiently implemented in commercial production. The reason for this reputation is that in order for most ultrasound-assisted processes to be efficient, it is necessary to generate ultrasonic amplitudes of at least 70 - 100 microns. Several ultrasound companies offer *laboratory* processors able to produce such amplitudes. However, these companies' *industrial* ultrasonic processors cannot generate amplitudes greater than about 25 microns, irrespective of the specified system power, which can be quite high for some companies. The difference between ultrasonic cavitation generated at the amplitudes of 30 and 100 microns is substantial, as shown in the video on the left.

One analogy of a high-power, low-amplitude approach would be trying to cook eggs in a very large pot, in which the water can only be warmed, but not boiled (analogy of low amplitude). The total power deposition into the process of warming a lot of water can be very high, but the desired effect will not be achieved. The proper procedure for designing an industrial egg boiling process would be to maximize the amount of water and eggs in the pot, but only under the condition that the boiling temperture of water can actually be reached (analogy of high amplitude).

The fact that conventional ultrasonic technology does not permit increasing ultrasonic processor sizes to the industrial scale without drastically lowering ultrasonic amplitudes is the reason why scale-up has always led to unavoidable reduction of cavitation intensities and significant losses in product quality.

ISM's ultrasonic processors are free from this limitation. With the use of our patented Barbell Horn Ultrasonic Technology (BHUT), we are able to generate extremely high ultrasonic cavitation intensities at any scale, directly implementing laboratory accomplishments in a production environment.

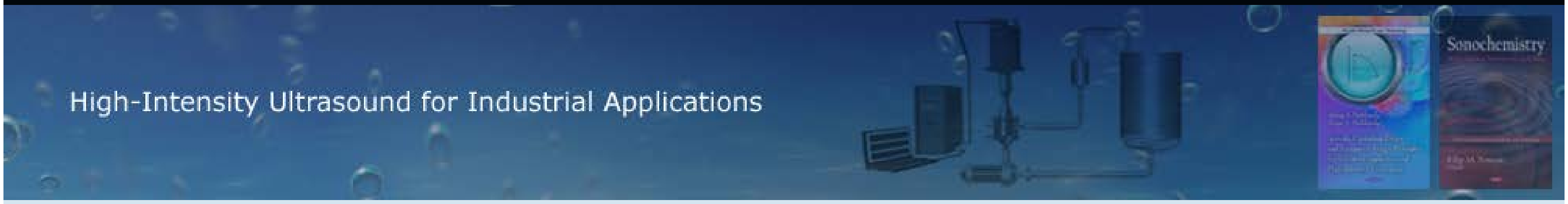

AN ACTIVE R&D FIRM

ISM constantly conducts research and development, aimed both at improving its ultrasonic technology and at applying the technology to different applications. Examples of our R&D activities in both fields are presented below:

ULTRASONIC INSTRUMENTATION DEVELOPMENT

ISM is developing a specialized piezoelectric transducer, capable of providing an unprecedented combination of output characteristics – output power up to 5 kW, ultrasonic amplitudes up to 30 microns (without an ultrasonic horn) and the output end diameter of 60 mm. This transducer will be designed to work in combination with Barbell horns, which will then be able to produce extremely high amplitudes, creating extremely intense ultrasonic cavitation in large volumes of liquid. The abovementioned features will be achieved by incorporating piezoelectric rings into a Full-wave Barbell Horn (FBH) structure, thereby producing a transducer/Barbell horn hybrid.

An extremely powerful Half-wave Barbell horn with an Opening (HBHO) will be constructed and tested in conjunction with this transducer. HBHO has a larger output surface than any other Barbell horn of similar diameter and can provide very high ultrasonic amplitudes. The device will be designed to create “acoustic focusing” by umbrella-like expansion-contraction of its output section, potentially leading to “super-cavitation”, potentially resulting in fundamentally new sonochemical and sonophysical effects.

ULTRASONIC TECHNOLOGY APPLICATIONS DEVELOPMENT

ISM is engaged in active research in multiple areas of ultrasonic technology application. Examples of our ongoing projects include: designing ultrasonic nano-particle production processes for the pharmaceutical and cosmetics industries, improving the properties of formaldehyde-free adhesives used in MDF and particle board production, developing the process of simultaneous extraction and transesterification of microalgal oil for inexpensive biofuel synthesis, optimizing metalworking fluid formulations, creating highly UV resistant pigment nano-dispersions used in coatings, sunscreens and printer inks, investigating methods to make superior-quality wax emulsions, designing ways to efficiently degas liquids, and studying the effects of high-intensity ultrasound on molten resins.

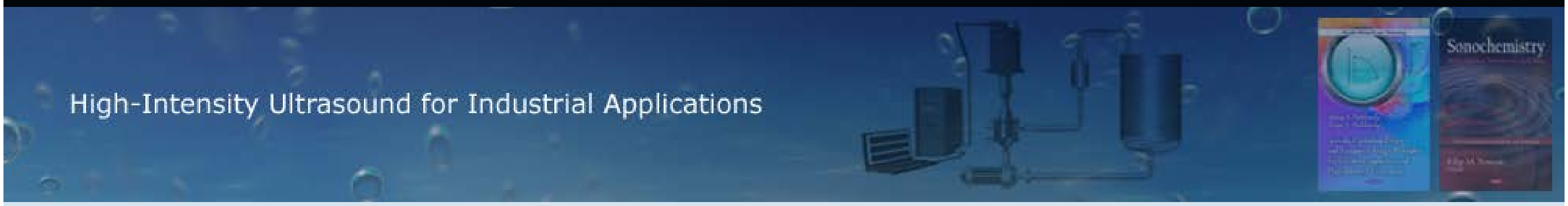

ULTRASONIC PROCESS CONSULTING COMPANY

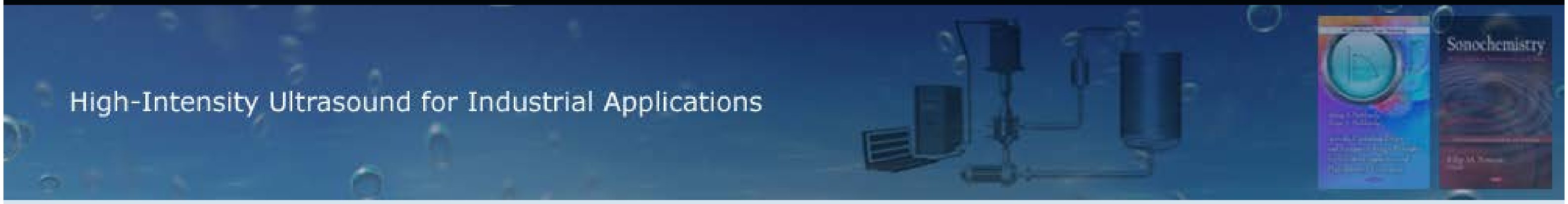

OUR TEAM

BOARD OF DIRECTORS

Alexey Peshkovsky, Ph.D. - President

Dr. A. Peshkovsky is co-founder and President of ISM. He is responsible for setting the overall strategic direction for the company and oversees applications development. Dr. A. Peshkovsky received his B.A. in Chemistry from the University of Pennsylvania and his M.S. and Ph.D. in Physical Chemistry from Columbia University. His professional experience includes over 15 years as a manager, investigator and product developer in both the academic and industrial sectors, mainly focusing on instrumentation design and applications development. Dr. A. Peshkovsky also teaches environmental chemistry at The New School and serves as a grant reviewer for the Environmental Protection Agency and as a manuscript reviewer for several scientific journals. Dr. A. Peshkovsky is the author of over 30 scientific papers, patents and presentations as well as two books.

Sergei Peshkovsky, Ph.D. - Technical Director

Dr. S. Peshkovsky is co-founder and Technical Director of ISM. He oversees product development and leads the company's R&D. Dr. S. Peshkovsky holds an M.S. and a Ph.D. from Moscow Institute of Chemical Engineering in Power Ultrasonics and is a prominent scientist in the field of ultrasound theory and engineering. He is the creator of Barbell Horn Ultrasonic Technology, which is key to industrial implementation of high-power ultrasound and is central to ISM. During his 40-year career Dr. S. Peshkovsky has achieved remarkable international recognition as one of the leading scientists in the field of acoustic cavitation physics and ultrasonic engineering, in which he has patented more than 20 discoveries and inventions, written over 50 publications and published several books.

Jeffrey Meyer - Commercial Director

Mr. J. Meyer is Commercial Director of ISM. He is responsible for defining the company's overall commercial strategy. Mr. J. Meyer holds a B.S. in Economics from Bowling Green State University and an M.B.A. in Marketing and International Business from Wright State University, and is functionally trained in global supply chain operations, marketing, and business development. Having worked around the globe, in China, India and Mexico, Mr. J. Meyer has proven experience in technology transfer, strategic alliance creation, mergers and acquisitions, and supply chain management.

BOARD OF ADVISORS

Ilya A. Volfson, M.D. - Advisor

Dr. I. Volfson holds a B.A. from the University of Pennsylvania and an M.D. from Albany Medical College. He has completed 2 years of General Surgery and 4 years of Urology residency at UMDNJ-NJ Medical School as well as a highly prestigious fellowship in Endourology, Laparoscopy and Robotic Surgery at Hackensack University Medical Center, accredited by the American Endourological Society.

Dr. Volfson is Board Certified by American Board of Urology and is a fellow of the American College of Surgeons. Dr. Volfson is a practicing urologist at Delaware County Division of Academic Urology and a Chief of Division of Urology at Taylor Hospital, Ridley Park, P.A.

Simon Bystryak, Ph.D. - Advisor

Dr. S. Bystryak holds a Ph.D. from the Institute of Chemical Physics, Russian Academy of Sciences. He has extensive experience in developing and implementing new biomedical technologies, and has developed, validated and marketed five new technologies in the field of life sciences. Dr. S. Bystryak's focus is on preparation and characterization of various polymer, surfactant and colloid systems such as nanocrystals, nanoemulsions, liposomes, latex and protein particles by using ultrasound, fluorescence, confocal fluorescence microscopy, light scattering, potentiometry and conductometry techniques, NMR and microcalorimetry. Dr. S. Bystryak is President of Allied Innovative Systems - an R&D company engaged in the development of new technologies in the field of biochemical and biomedical assays and reagents.

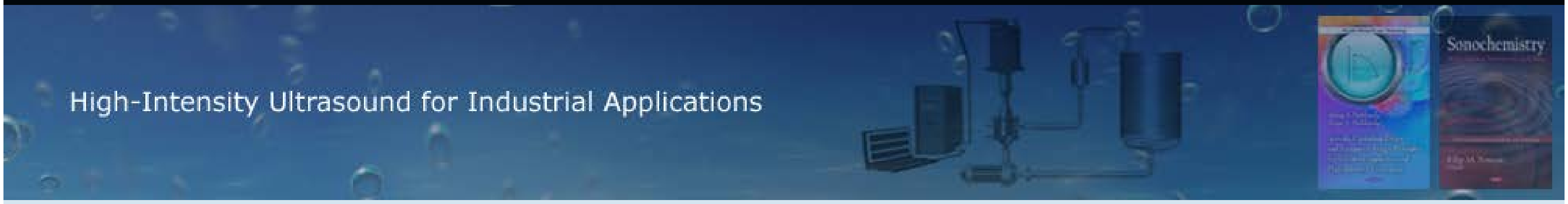

COMPANY NEWS

November 13, 2008 - SulphCo Extends Technology Transfer Agreement with Industrial Sonomechanics

HOUSTON, Nov. 13 /PRNewswire/ -- SulphCo, Inc. SUF (the "Company" or "SulphCo") announced today that it has exercised its option to extend the term of the license agreement (the "License Agreement") dated November 9, 2007 with Industrial Sonomechanics, LLC ("ISM") covering ISM's patented ultrasound horn and reactor technology. The term has been extended to the date on which the ISM patents expire. Under the terms of the License Agreement, ISM granted SulphCo exclusive worldwide rights to use its patented ultrasound horn and reactor technology for ultrasound upgrading of crude oil and crude oil fractions. Pursuant to the terms of the License Agreement, SulphCo will issue 50,000 restricted shares of the Company's common stock. All other terms of the License Agreement remain unchanged.

"We are pleased to continue our relationship with ISM as an important member of the SulphCo team and, by the exercise of this option, we will continue to maintain access to their cutting edge probe and reactor chamber technology," said Dr. Larry D. Ryan, CEO of SulphCo. ISM is a U.S.-based company formed in 2006 to commercialize its patented high-power ultrasonics technology, which was developed by its founders during several decades of research in Russia. ISM specializes in very high capacity industrial ultrasonic reactor systems, which incorporate powerful ultrasonic horns capable of simultaneously providing high output vibration amplitudes and large output diameters.

August 25, 2008 - Märkisches Werk joins forces with Industrial Sonomechanics

Märkisches Werk (MWH) has joined forces with Industrial Sonomechanics, LLC (ISM) to bring ISM's unique high-intensity high volume ultrasound technology to industrial customers. MWH and ISM have signed agreements, under which ISM has granted non-exclusive worldwide rights to MWH to use its patented ultrasound horn and reactor technology and will provide consultation services to support R&D efforts undertaken by MWH in multiple application areas. MWH is a leading manufacturer and technology development company located in central Germany. In operation for 150 years, MWH can draw upon a long and rich history of successful innovations. The company has a wide array of in-house manufacturing capabilities, the newest manufacturing technology and a strong engineering and development department.

November 15, 2007 - SulphCo Executes Technology Transfer Agreement With Industrial Sonomechanics

HOUSTON, Nov. 15 /PRNewswire-FirstCall/ -- SulphCo(R), Inc. SUF (the "Company") announced today that it has entered into an agreement with Industrial Sonomechanics, LLC ("ISM"), under which ISM has granted exclusive worldwide rights to the Company to use its patented ultrasound horn and reactor technology for ultrasound upgrading of crude oil and crude oil fractions. In return, ISM will receive license fees, consulting fees, warrants to purchase 50,000 shares of SulphCo(R) common stock and, should the Company exercise its option to extend the agreement, a grant of 50,000 restricted shares of SulphCo(R) common stock. The ISM probe design embodies state of the art technology, a unique combination of prodigious power output and high energy efficiency.

"We are pleased to welcome ISM as an important member of the SulphCo(R) team and are excited about their cutting edge technology," said Dr. Larry Ryan, CEO of SulphCo(R). ISM is a U.S. based company formed in 2006 to commercialize its patented high-power ultrasonics technology, which was developed by the company's founders during several decades of research in Russia. The company specializes in very high capacity industrial ultrasonic reactor systems, which incorporate powerful ultrasonic horns capable of simultaneously providing high output vibration amplitudes and large output diameters. "This unique combination of features," said ISM President Alexey Peshkovsky, "is ideally suited to SulphCo's(R) Sonocracking(TM) process, which requires high ultrasonic vibration amplitudes to efficiently alter the molecular structure of the crude oil and crude oil fractions and large output diameters to maximize productivity."

Several experimental prototypes of the ISM probe design were manufactured for SulphCo(R) by MWH in Germany. In a head to head laboratory comparison, the ISM probe generated more than three times the amplitude in horn surface movement than the SulphCo(R) Series II probe design and, as reported earlier, in successive test runs in Fujairah on a medium crude (32.9 API, 1.6% sulphur by content) the new ISM experimental probe achieved a reduction in sulphur by content more than two and one half times greater than that produced by the SulphCo(R) Series II probe.

"While these preliminary results are encouraging, bear in mind that the ISM probes are first generation prototypes and further work will be required to develop the kind of consistent performance necessary for commercial applications," said Dr Ryan. "But we are very pleased with the initial results and believe this technology is a perfect fit for our Sonocracking(TM) technology. By the same token, we will continue to utilize and refine the SulphCo(R) Series II probe design in parallel, as that design has also produced significant API shifts and sulphur reduction in initial testing in Fujairah."

In another development, before the resumption of testing in Europe, the ISM probe was upgraded to incorporate a SulphCo(R) engineered modification allowing real time feedback measuring the energy released from the probe surface into the reaction chamber, a feature not present in earlier probe designs. "This is an invaluable tool in our ongoing efforts to optimize this process," noted Dr. Ryan. "Real time feedback will allow us to 'tune' the ultrasound probe characteristics for a given crude oil by constantly adjusting power and frequency to maintain uniform energy output into the reactor chamber."

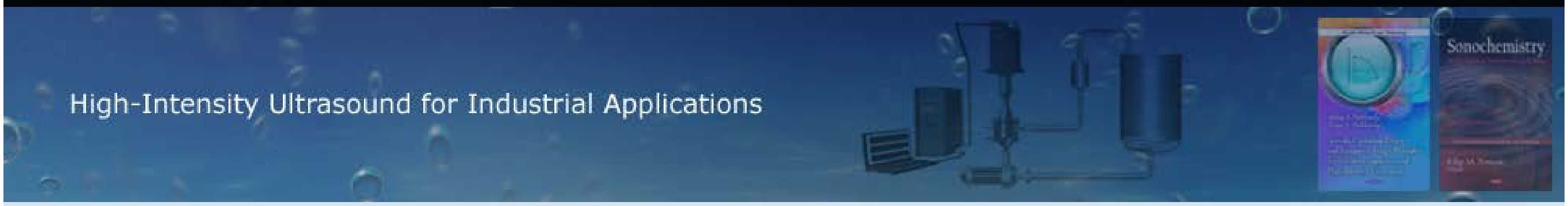

OVERVIEW OF PROCESS OPTIMIZATION AND SCALE-UP SERVICES

It is quite often the case that companies are interested in the benefits that ultrasound provides, but do not have the technical experience and/or equipment to test the efficacy of ultrasound on a unique process or substrate. ISM is capable of providing testing, measuring, and results dissemination services, in addition to advising its clients on the process improvement.

After the initial feasibility assessment is done, many clients ask us to optimize their ultrasonic process and estimate the potential commercial-scale production rate. This is commonly a two or three-step procedure:

Step 1. Laboratory-scale studies aimed at optimizing basic process parameters, such as components ratios, ultrasonic amplitude, specific reactor residence time, static pressure, temperature, etc. This step is normally done in a batch or small-volume flow-through mode, utilizing a conventional ultrasonic horn (CH) with and output tip diameter of 13 -15 mm. Electric power consumption during this step is commonly 100 - 150 W.

Step 2. Pilot semi-industrial scale study during which all optimized parameters are retained, while the size of the ultrasonic horn and reactor chamber is increased, thereby increasing the flow-through rate. Since the scale-up is accomplished without changing any of the parameters optimized in step 1, the product quality is expected to remain unchanged. This step is normally done in a flow-through mode, utilizing a Half-Wave or Full-Wave Barbell Horn (HBH or FBH) with an output tip diameter of 30 - 35 mm. The goal of this step is to determine the exact scale-up factor between the lab and the pilot setting and to ensure that the quality of the product is unchanged. For most processes the scale-up factor turns out to be between 8 and 12 which means that approximately 8 to 12 times more product is produced per unit of time. Electric power consumption commonly also goes up by a similar factor and reaches approximately 900 - 1200 W.

Step 3. The results obtained during Step 2 can normally be used to predict the scale-up factor that will be achieved when the process is transferred to the plant floor. However, it is sometimes necessary to run a full-scale study to ensure that this prediction is in fact accurate. This verification is done by further increasing the horn (HBH or FBH) and the reactor chamber sizes, commonly resulting in a productivity rate (and electrical power consumption) increase by an additional factor of about 3 - 4.

Based on the above, for an average process an overall per-processor production rate scale-up factor of 25 – 50 can be expected when transferring the process from lab to industrial scale. An example of process optimization and commercial-scale production rate estimation study is given in a separate document.

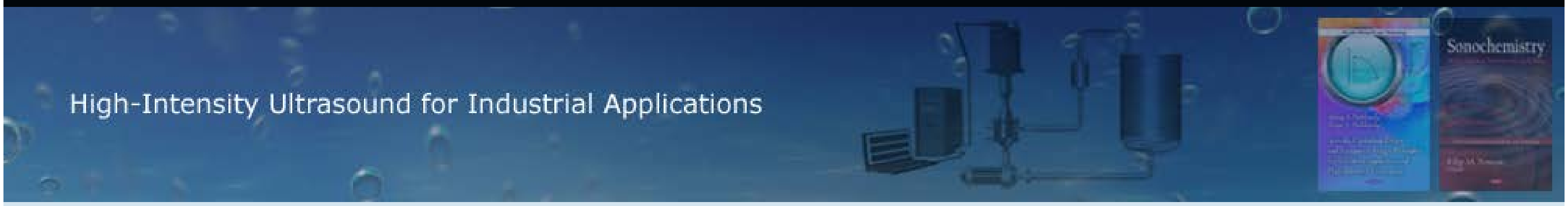

Home → Services → Service Project Example - Translucent Nanoemulsion for Food Industry

SERVICE PROJECT EXAMPLE - TRANSLUCENT NANOEMULSION FOR FOOD INDUSTRY

This project consisted of two main steps: 1. lab study aimed at optimizing the formulation and ultrasonic processing conditions for the production of a non-toxic, translucent nanoemulsion of soybean oil in water and 2. transferring the process from lab to pilot scale using BHUT, determining the production rate scale-up factor, and estimating the potential industrial-scale production rate.

The nanoemulsions were produced using ISM's 1.2 kW laboratory/bench-scale ultrasonic liquid processor, operating in the flow-through and batch modes. High-purity soybean oil, Tween 80 and Span 80 were purchased from Sigma-Aldrich, St. Louis, MO. The ingredients were initially pre-mixed using a magnetic stirrer at 500 rpm for 2 min. Mean oil droplet sizes (MDS) were measured using Beckman Coulter N4 Plus Particle Size Analyzer.

LABORATORY-SCALE EXPERIMENTS

A set of lab experiments was carried out in order to optimize the nanoemulsion's formulation and ultrasonic processing parameters: processing rate, vibration amplitude, power requirement. The requested concentration of oil was 10%. Tween 80 and Span 80 surfactants were chosen due to their Generally Recognized As Safe (GRAS) FDA status. Lab experiments were conducted using the processor fitted with a conventional converging ultrasonic horn (CH), having an output tip diameter of 15 mm. For the nanoemulsion to be translucent, its MDS had to be below 100 nm.

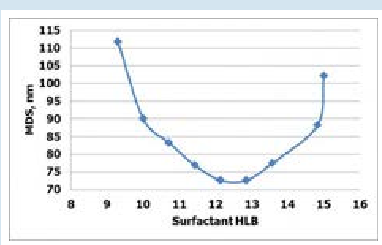

Dependence of MDS on Surfactant HLB

These experiments were conducted in a batch mode using an 80 ml glass beaker inserted into an ice bath. The ultrasonic amplitude was 90 microns. Concentrations of Tween 80 and Span 80 were varied from 10% of Tween 80 and 0% of Span 80 (HLB=15) to 4.67% of Tween 80 and 5.33% of Span 80 (HLB=9.3). Batch sizes were 50 ml and processing times were 5 min (processing rate of 10 ml/min). Minimum MDS was achieved at HLB of about 12 – 13. At these values, the resulting nanoemulsions were sufficiently translucent, with MDS falling to about 73 nm. Based on these results, all further experiments were carried using the following formulation: 10 % soybean oil, 8 % Tween 80, 2 % Span 80 (HLB = 12.86), and 80 % water.

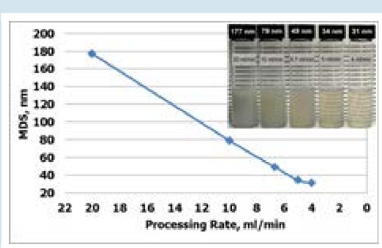

Dependence of MDS on Processing Rate

The effect of the processing rate on MDS was investigated next. These experiments were conducted in a flow-through mode using the same CH, operating at the same amplitude, placed in a small reactor chamber. A series of 50 ml samples of the working liquid were re-circulated through the reactor chamber for 2.5 min, 5 min, 7.5 min, 10 min and 12.5 min, resulting in processing rates of 20 ml/min, 10 ml/min, 6.7 ml/min, 5 ml/min and 4 ml/min. MDS decreased as the processing rate was lowered, falling to 31 nm when the rate was 4 ml/min. The nanoemulsion became increasingly translucent as the droplet size decreased. Since the product nanoemulsion was intended by our client to be used in a diluted formulation, the degree of clarity achieved at the processing rate of 10 ml/min was determined to be sufficient.

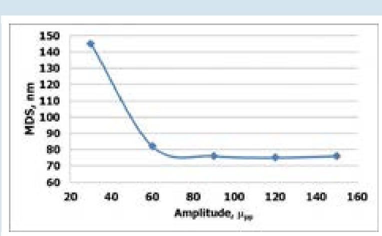

Dependence of MDS on Ultrasonic Amplitude

The next part of the study was to investigate the effect of the ultrasonic amplitude on MDS. These experiments were conducted in the flow-through mode at the processing rate of 10 ml/min. Based on the results of these experiments, the ultrasonic amplitude of 90 microns was selected for the production of this nanoemulsion. It is important to point out that all presented data is self-consistent: MDS of about 75 nm is consistently obtained at the processing rate of 10 ml/min and the ultrasonic amplitude of 90 microns, for both batch and flow-through setups.

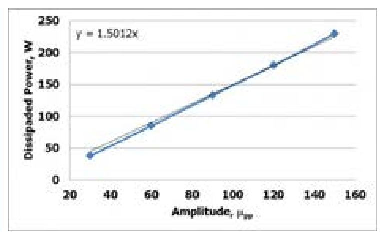

Power Requirement Versus Amplitude

In preparation for the pilot-scale studies, the dependence of power requirement on the ultrasonic amplitude delivered to the liquid was also investigated. These tests were carried out in the flow-through mode. The results show a nearly linear dependence on the amplitude, with power draw of 130 W at the amplitude of 90 microns.

Summary of Lab Experiments' Results

The results of the laboratory experiments were, therefore, as follows: 1. Surfactant HLB = 12.86, 2. Processing rate = 10 ml/min, 3. Ultrasonic amplitude = 90 microns, 4. Power requirement (15 mm horn output diameter) = 130 W.

PILOT-SCALE EXPERIMENTS

An estimation of the scale-up factor was first made based on the following considerations. The common converging horn (CH) with the output tip of 15 mm in diameter creates one active cavitation zone under the tip. The radiating area of this horn is, therefore, 1.8 cm^2. A Half-wave Barbell horn (HBH) with the output tip diameter of 35 mm (used in pilot-scale studies) creates two active cavitation zones, one under and one above its output section. The total radiating area of this horn is, therefore, approximately 19.2 cm^2. Therefore, if the ultrasonic amplitude produced by both horns is similar, the size of the cavitation zone is about 10 times greater for the HBH than for the CH. Therefore, a factor of approximately 10 increase in the processing rate and power requirement was expected.

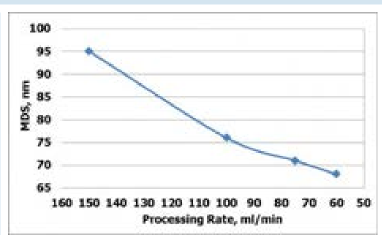

Dependence of MDS on Processing Rate After Scaleup

Pilot-scale experiments were conducted in the flow-through mode and utilized an HBH, having an output section diameter of 35 mm. The ultrasonic amplitude was maintained at 90 microns. A series of 300 ml samples of the working liquid were re-circulated through the reactor chamber for 2 min, 3 min, 4 min and 5 min, resulting in processing rates of 150 ml/min, 100 ml/min, 75 ml/min, and 60 ml/min. The closest MDS match to the final nanoemulsion obtained during lab experiments was achieved at the processing rate of 100 ml/min. This corresponded to the scale-up factor of about 10, as anticipated. The power draw was approximately 1,150 W, which is consistent with the fact that the same ultrasonic amplitude was now radiated via an area about 10 times greater than in the lab setup.

CONCLUSIONS

Formulation and ultrasonic processing conditions optimization for the production of a non-toxic, translucent nanoemulsion of soybean oil in water for the use in the food industry was carried out. Laboratory-scale results were obtained using ISM's 1.2 kW laboratory/bench-scale ultrasonic liquid processor equipped with a CH, having the output diameter of 15 mm. The optimized processing rate was 10 ml/min, the ultrasonic amplitude was 90 microns, and the power requirement was 130 W.

The process was then successfully transferred to a pilot-scale flow-through setup using the same processor equipped with an HBH, having the output section diameter of 35 mm. The scale-up factor was approximately 10, resulting in the pilot-scale processing rate of 100 ml/min at the amplitude of 90 microns. The power requirement at this scale was 1,150 W. By extension, it was concluded that a further scale-up factor of approximately 3.5 can be obtained by transferring this process to a full industrial scale using a processor capable of providing 4 kW of power and equipped with an HBH, having the output section diameter of 65 mm, thereby achieving the production rate of 350 ml/min (21 L/hour) per processor. It is important to point out that the process described here was among the most challenging, as it involved extremely small droplet sizes. Nanoemulsions requiring MDS on the order of 200 - 300 nm can commonly be produced 5 to 10 times faster.

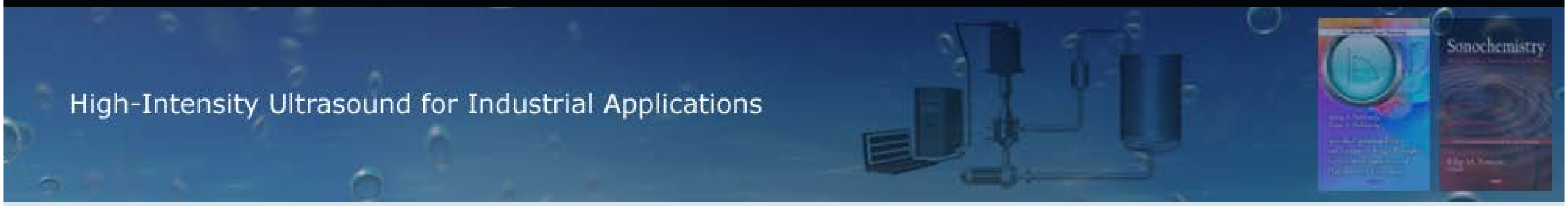

COSMETIC AND DERMATOLOGICAL

- **Translucent Oil-in-Water Nanoemulsions**

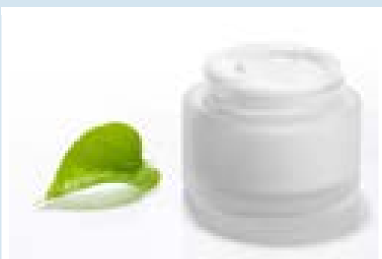

BACKGROUND

The ability of high-power ultrasound to make nanomaterials, such as nanoemulsions, nanocrystal dispersions and liposomes, makes it invaluable for producing a wide variety of cosmetic products, including sunscreens, creams, lotions, moisturisers, shampoos, conditioners, makeup, etc.

In cosmetics and dermatological industry, nanomaterial-based products are mainly used 1) as delivery systems for active lipophilic compounds and drugs and 2) as UV blockers. The application as delivery systems enables cosmetic products to transport active agents and drugs through the skin, giving the products important therapeutic properties ranging from enhanced skin hydration to anti-inflammatory, anti-oxidant, anti-aging and hair loss preventive. In addition, it is possible to design the products to release the actives in a slow and controlled manner, thereby extending their effects (for example, for long-acting therapy or slow perfume release). The application of nanomaterials as UV blockers mainly takes advantage of UV filtering properties of titanium dioxide ($TiO2$) and zinc oxide (ZnO) nanosuspensions. These metal oxide particles are commonly used in sunscreens and moisturizers. Breaking down or dispersing the particles down to the nanometer scale (about 200 nm) ensures that, unlike in traditional sunscreens based on larger particles, much higher degree of translucency is achieved along with better absorption by the skin and enhanced rheological properties. Polymeric nanoparticles are also sometimes used for this application.

PRODUCTION WITH HIGH-AMPLITUDE ULTRASOUND

Industrial Sonomechanics, LLC (ISM), offers bench and industrial-scale high-power ultrasonic processors for the production of nanomaterials. The processors are based on our patented Barbell Horn Ultrasonic Technology (BHUT), which, as explained below, makes it possible to directly implement laboratory accomplishments in a production environment, guaranteeing reproducible and predictable results at any scale.

Very high ultrasonic amplitudes are required for efficient particle size reduction. The necessary shear forces are created by ultrasonic cavitation, which produces violently and asymmetrically imploding vacuum bubbles and causes micro-jets that disperse and break up crystals, agglomerates and oil droplets down to the nanometer scale. Known for many decades, this effect of high-amplitude ultrasound has been extensively studied and successfully used in laboratory-scale research. However, prior to the introduction of BHUT, none of the existing ultrasonic liquid processors could generate the required amplitudes on the industrial scale. Commercial implementation of high-power ultrasound has, therefore, been limited to processes for which low-amplitudes are sufficient (cleaning, simple deagglomeration, mixing, macro-emulsification, etc.).

Why ISM's Ultrasonic Technology?

Conventional high-power ultrasonic technology inherently forces all processes to run either at a small scale and high amplitude or a large scale and low amplitude. ISM has successfully overcome this limitation by developing BHUT, which permits constructing industrial-scale ultrasonic processors able to operate at extremely high amplitudes. The processors are directly scalable and can be used in the commercial production of high-quality nanomaterials for the cosmetics and dermatological industry. Our equipment is compact and relatively low-cost, needs little technical support, includes very few wetted parts, generally requires no special pre-treatment of precursors, and is potentially self-sterilizing due to antibacterial properties of high-intensity ultrasound.

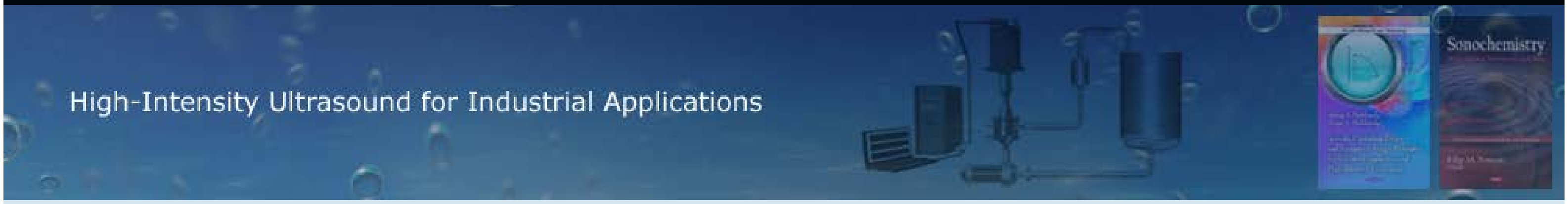

TRANSLUCENT OIL-IN-WATER NANOEMULSIONS

BACKGROUND

Cosmetic and dermatological industries use nanomaterials, such as nanoemulsion and nanocrystals, as delivery systems for active lipophilic compounds and drugs. Translucent nanoemulsions are a special class of nanoemulsions that have extremely small droplet sizes (below 100 nm) and narrow droplet size distributions. These materials have special properties, including optical translucency, low viscosity and long term kinetic stability. Due to their extremely small droplet sizes and very large dispersed phase surface-to-volume ratios, translucent oil-in-water nanoemulsions are especially attractive for cosmetics, ophthalmological and dermatological industries, as they are readily absorbed by the skin, easily sterilized by filtration, and can deliver exceptionally high concentrations of active oil-soluble substances.

Due to similarity in appearance, translucent nanoemulsions are sometimes confused with microemulsions, which belong to another class of stable (thermodynamically) and optically clear colloidal systems. Microemulsions are spontaneously formed by “solubilizing” oil molecules with a mixture of surfactants, co-surfactants and co-solvents. The required surfactant concentration in a microemulsion is several times higher than that in a translucent nanoemulsion and significantly exceeds the concentration of the dispersed phase (generally, oil). Because of many undesirable side-effects caused by surfactants, this is disadvantageous or prohibitive for many applications. In addition, stability of microemulsions is easily compromised by dilution, heating or changing pH levels.

PRODUCTION WITH HIGH-AMPLITUDE ULTRASOUND

Industrial Sonomechanics, LLC (ISM), offers bench and industrial-scale high-power ultrasonic processors for the production of translucent nanoemulsions. The processors are based on our patented Barbell Horn Ultrasonic Technology (BHUT), which, as explained below, makes it possible to directly implement laboratory accomplishments in a production environment, guaranteeing reproducible and predictable results at any scale.

Very high ultrasonic amplitudes are required for the efficient production of translucent nanoemulsions. The necessary shear forces are created by ultrasonic cavitation, which produces violently and asymmetrically imploding vacuum bubbles and causes micro-jets that break up the original oil droplets down to sizes below 100 nanometers. Known for many decades, this effect of high-amplitude ultrasound has been extensively studied and successfully used in laboratory-scale research. However, prior to the introduction of BHUT, none of the existing ultrasonic liquid processors could generate the required amplitudes on the industrial scale. Commercial implementation of high-power ultrasound has, therefore, been limited to processes for which low-amplitudes are sufficient (cleaning, simple deagglomeration, mixing, macro-emulsification, etc.).

Why ISM's Ultrasonic Technology?

Conventional high-power ultrasonic technology inherently forces all processes to run either at a small scale and high amplitude or a large scale and low amplitude. ISM has successfully overcome this limitation by developing BHUT, which permits constructing industrial-scale ultrasonic processors able to operate at extremely high amplitudes. The processors are directly scalable and can be used in the commercial production of high-quality translucent nanoemulsions for the cosmetics and dermatological industry. Our equipment is compact and relatively low-cost, needs little technical support, includes very few wetted parts, generally requires no special pre-treatment of precursors, and is potentially self-sterilizing due to antibacterial properties of high-intensity ultrasound.

Examples of Produced Translucent Nanoemulsions

Target nanoemulsion parameters were: soybean oil content - 10 %; surfactant concentration - 6%, mean droplet size (MDS) - 75 – 80 nm. The ingredients were pre-mixed using a magnetic stirrer at 500 rpm for 2 min. MDS values were measured using Beckman Coulter N4 Plus Particle Size Analyzer.

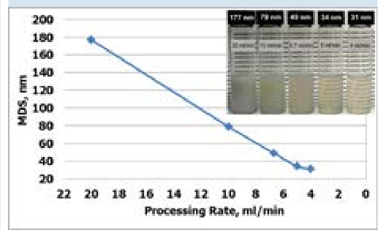

Lab Scale: Nanoemulsions were first prepared using ISM's 1200 W flow-through ultrasonic reactor system operating in a laboratory-scale configuration. This setup utilized a common horn (CH) and a small reactor chamber. The horn's output diameter was 15 mm and its operation amplitude was 90 microns. Nanoemulsion samples were prepared at the processing rates of 20, 10, 6.7, 5, and 4 ml/min. MDS decreased as the processing rate was lowered, and the nanoemulsion became increasingly translucent. Target MDS was achieved at the processing rate of 10 ml/min. The acoustic power deposition under these conditions was 130 W.

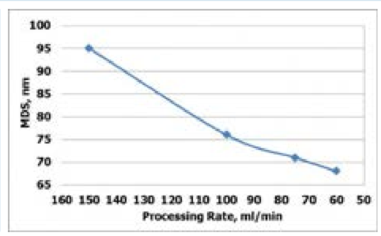

Pilot Scale: The process was subsequently upgraded to pilot scale by switching to a Half-wave Barbell horn (HBH) and using a larger reactor chamber. The horn's output diameter was 35 mm and its operation amplitude was 90 microns, same as in the previous lab experiment. Nanoemulsion samples were prepared at the processing rates of 150, 100, 75, and 60 ml/min. The results presented on the left show that the closest match to target parameters in terms of the final required MDS was obtained at the processing rate of 100 ml/min. This corresponds to a scale-up factor of 10. The acoustic power deposition in this case was 1,150 W, which is consistent with the obtained scale-up factor.

This process may be further scaled up by using ISM's 2400 W industrial-scale ultrasonic processor system equipped with a larger HBH and/or by using a series multi-reactor arrangement. Ultrasound is a simple and effective technique for producing translucent nanoemulsions. With the use of BHUT, the process is directly scalable, making it possible to implement in an industrial production environment.

The data presented above was collected in collaboration with Allied Innovative Systems, LLC (ALLIS).

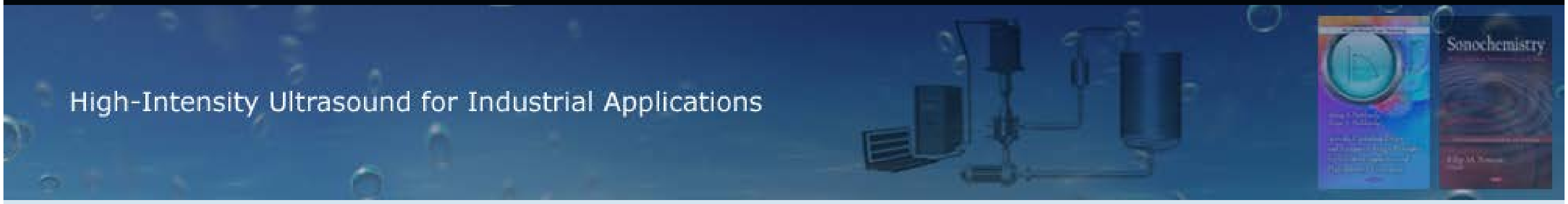

EXTRACTION AND TRANSESTERIFICATION OF MIRCOALGAL OIL

BACKGROUND

Biodiesel is a renewable, domestic and environmentally friendly fuel with a potential of becoming a broadly accepted substitute for petrodiesel. Its widespread implementation is, however, currently hindered by excessive costs of production and limited availability of feedstock oils.

Microalgae

Microalgae is one of the few sources of feedstock oil that can meet the existing demand. The major challenge, however, has been the high cost of recovering the oil from the microalgae prior to converting it into biodiesel. The most commonly used method involves mechanical cell disruption followed by hexane extraction. This approach has significant drawbacks when applied on a commercial scale because it involves a complicated and energy-intensive hexane distillation step. Furthermore, large quantities of hexane escape into the atmosphere, which contributes to air pollution and has significant replacement costs.

A promising method called "in-situ transesterification" allows to completely eliminate the oil extraction and refining steps from the biodiesel production process. Instead, the oil is extracted directly into methanol (or ethanol) premixed with a catalyst, where it simultaneously undergoes transesterification and becomes converted to biodiesel. In-situ transesterification has been tried on various oil-bearing materials, including microalgae, yielding promising results. Furthermore, laboratory studies have shown that in-situ transesterification of microalgal oil benefits from exposing the reaction mixture to ultrasound.

ULTRASONIC EXTRACTION AND TRANSESTERIFICATION

Biodiesel production involves two processes: oil extraction and transesterification, both of which are greatly accelerated by high-amplitude ultrasound. Acoustic cavitation created by ultrasound tremendously facilitates solvent access through cell walls and promotes oil extraction. It also provides very efficient mixing of oil and alcohol, which speeds up the phase transfer-limited transesterification reaction. These effects occur due to the mechanical action of ultrasonic cavitation, which produces violently and asymmetrically imploding bubbles and causes micro-jets that pierce cell walls.

WHY ISM ULTRASONIC TECHNOLOGY?

Laboratory studies show that high ultrasonic amplitudes, on the order of 70 - 120 microns peak-to-peak (below, microns), are necessary to maximize the efficiency of ultrasound-mediated extraction and transesterification. Conventional high-power ultrasonic technology, however, inherently forces all processes to run either at a small scale and high amplitude or a large scale and low amplitude, not allowing for the possibility of implementing high amplitudes on industrial scale. Consequentially, scaling up a traditional ultrasonic system is always associated with a reduction in ultrasonic amplitudes, decreasing the resulting shear forces and sacrificing process efficiencies.

Industrial Sonomechanics, LLC, (ISM) has successfully overcome the aforementioned limitation by developing Barbell Horn Ultrasonic Technology (BHUT), which permits constructing industrial ultrasonic systems able to operate at extremely high ultrasonic amplitudes (up to about 200 microns). The output tip areas of the incorporated Barbell horns and the resulting productivity rates of the systems are more than 10 times higher than those of any conventional ultrasonic device operating at high amplitudes. Any laboratory study can, therefore, be directly implemented on the industrial scale, without lowering ultrasonic amplitudes or changing any other optimized process parameters.

EVALUATION EXPERIMENTS CONDUCTED BY ISM

In order to assess the feasibility of industrial-scale ultrasonic microalgal oil extraction and biodiesel production, ISM conducted a set of evaluation experiments. All experiments were run in a batch mode and utilized ISM's 1200 W bench-scale ultrasonic system.

Conventional and Barbell Horn Setups

The system comprised an ultrasonic generator, a piezoelectric transducer and either a conventional converging ultrasonic horn with an output tip diameter of 15.7 mm or a Barbell horn with a tip diameter of 35 mm. The ultrasound exposure cycles were 3 minutes for both setups. The ultrasonic amplitudes provided by the converging horn and the Barbell horn were the same - 70 microns. However, since the diameter of the Barbell horn was 2.23 times larger, its output area was 5 times larger, and, therefore, this horn could process 5 times more material during the same amount of time.

This comparison was done to demonstrate the ability of Barbell horns to directly scale up laboratory processes. Dry microalgae was used as the feedstock. The extraction and transesterification medium was dry ethanol.

Other Extraction Methods

In addition, the experiments were repeated using mechanical homogenization with a high-speed laboratory stirrer. Dry microalgae was used as the feedstock. The extraction and transesterification medium was dry ethanol. The exposure cycle for this experiment was also 3 minutes.

Yield baseline (shown below as 100 %) was established by standard laboratory extraction and transesterification techniques (automatic soxhlet extraction/transesterification). These techniques, although very lengthy, provide close to maximum possible yields, and are, therefore, useful for making comparisons with other methods.

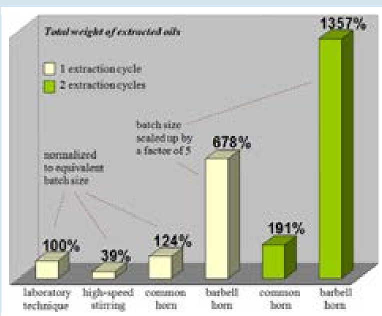

Results of Extraction Experiements

As shown in the figure on the left, high-amplitude ultrasound-assisted extraction provided much higher yields than high-speed stirring and was even more efficient than the lengthy automatic soxhlet extraction (laboratory technique).

Two extraction cycles into the same solvent were possible, without losing the process efficiency (data shown in green).

The use of the Barbell horn permitted a factor-of-five scale up of the ultrasonic extraction process also without any loss in the efficiency.

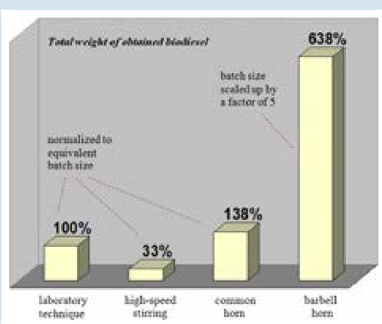

Results of In-Situ Transesterification Experiements

High-amplitude ultrasound-assisted in-situ transesterification was also more efficient than that assisted by high-speed stirring and the laboratory technique.

The use of the Barbell horn permitted a factor-of-five scale up of the ultrasonic in-situ transesterification process without any loss in the efficiency.

DISCUSSION

The data presented above show that high-intensity ultrasonic exposure affords very high extraction and in-situ transesterification efficiency, which greatly exceeds mechanical homogenization and is even more efficient than lengthy standard laboratory techniques. The data also suggest that it is possible to reuse the alcohol practically without any loss of extraction efficiency by running multiple extraction cycles prior to transesterification, where at the end of each cycle the used-up algae is filtered out and replaced with fresh material. During the last extraction cycle, when sufficient concentration of the oils is built up in the mix, a catalyst may be added to initiate the transesterification reaction.

In addition, our ability to use BHUT to directly scale up ultrasonic processes has been demonstrated, achieving, in this case, approximately a factor of 5 increase in the extraction and in-situ transesterification rates compared which traditional converging horn ultrasonic technology.

No systematic process conditions optimization (ultrasonic amplitude, pressure, exposure time, etc.) was attempted in the described evaluation experiments. Optimization is necessary in order to be able to calculate the method's energy balance and evaluate its commercial potential.

ENERGY EFFICIENCY ESTIMATION

Industrial implementation of microalgal oil in-situ transesterification should be preceded by a thorough flow-through laboratory study aimed at optimizing all process parameters and evaluating the energy balance. The key ultrasonic exposure parameters are: ultrasonic amplitude, static pressure and exposure time. Once these conditions are established, BHUT will permit a direct scale up from laboratory to industrial size without changing any of the identified parameters, with the exception of the ultrasonic reactor volume and the associated total liquid processing capacity.

Based on our previous experience with similar processes, for in-situ transesterification we estimate the optimum flow rate through our 2400 W industrial ultrasonic system to be 10 liters per minute (l/min). If the working liquid mixture has about 20 % of microalgae, of which approximately

50% by weight is extracted and converted into biodiesel, the total productivity rate of the system with respect of the final product will be approximately 1 l/min.

Power consumption of our industrial-scale system is 2400 W. It is, therefore, estimated that the process will require 2.4 kWh to produce 60 L of biodiesel. This means that 300 L (78 gallons) of biodiesel will be produced for about $1 worth of electricity. The average cost of residential electricity of 11¢/kWh in the U.S. in December 2008 was used in this calculation.

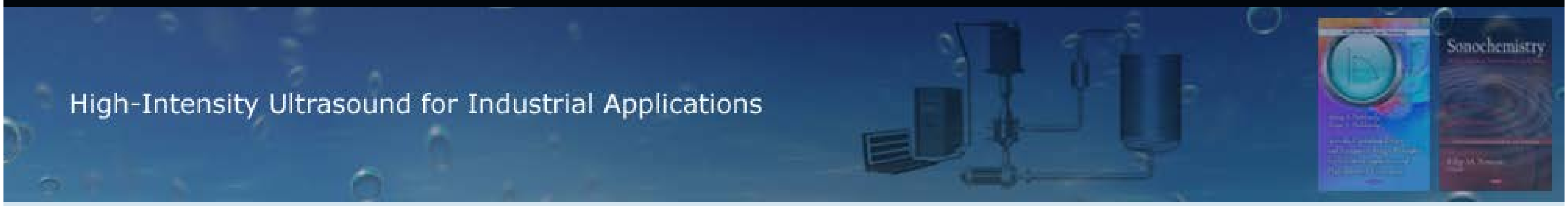

Home → Technical Resources → Videos

VIDEOS

Ultrasonic Dispersion of Carbon Black in Water, 750 ml Batch

This video shows ultrasonic dispersion of a small amount carbon black in a medium-size batch of water. The process was carried out with a 1.2 kW bench-scale ultrasonic reactor equipped with a Full-wave Barbell Horn (FBH), produced by Industrial Sonomechanics, LLC (ISM). The ultrasonic amplitude during the process was 100 microns. The process can be directly scaled up by using ISM's industrial ultrasonic processors at the same operating conditions. All ISM's ultrasonic reactors can be used in a flow-through mode in order to ensure continuous production. Unlike other ultrasonic systems, our processors are able to generate high amplitudes and extremely intense ultrasonic cavitation even when using large-diameter industrial-scale ultrasonic horns and flow-through reactor chambers.

Ultrasonic Degassing of Heavy Industrial Gear Oil

Degassing of high-viscosity oils by conventional methods can be challenging. Ultrasonic degassing is very useful in this case. Ultrasonic removal of air bubbles from heavy industrial gear oil is illustrated in this video. The experiment was conducted with Industrial Sonomechanics' 1200 W ultrasonic system.

Ultrasonic Removal of Air Bubbles from Epoxy Resin

When epoxy resin is mixed, air bubbles are inadvertently introduced and must be removed. Ultrasonic degassing technique can be very useful in this case, as shown in this video. Ultrasonic removal of air bubbles from premixed epoxy resin is illustrated in this video. The experiment was conducted with a 1200 W ultrasonic reactor system produced by Industrial Sonomechanics, LLC.

> Next Page

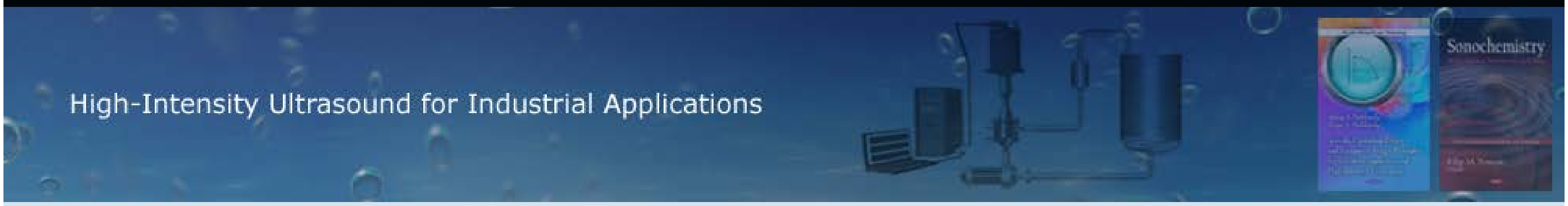

BOOKS

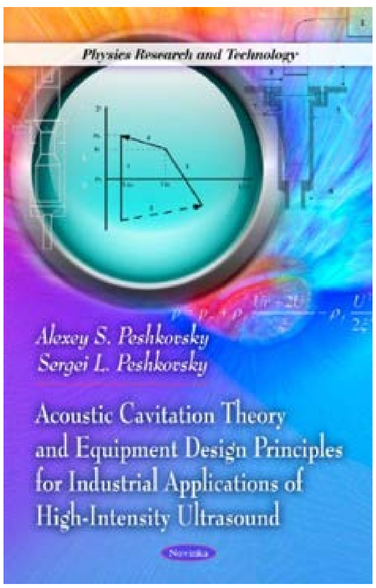

ACOUSTIC CAVITATION THEORY AND EQUIPMENT DESIGN PRINCIPLES FOR INDUSTRIAL APPLICATIONS OF HIGH-INTENSITY ULTRASOUND (Physics Research and Technology) [Paperback]

Alexey Peshkovsky, Sergei Peshkovsky, Paperback: 60 pages, Publisher: Nova Science Pub Inc (October 31, 2010), ISBN-10: 1617610933

Abstract

A multitude of useful physical and chemical processes promoted by ultrasonic cavitation have been described in laboratory studies. Industrial-scale implementation of the high-intensity ultrasound has, however, been hindered by several technological limitations, making it difficult to directly scale up the ultrasonic systems in order to transfer the results of the laboratory studies to the plant floor. High-capacity flow-through ultrasonic reactor systems required for commercial-scale processing of liquids can only be properly designed if the energy parameters of the cavitation region are correctly evaluated. Conditions which must be fulfilled to ensure an effective and continuous operation of an ultrasonic reactor system are provided in this book.

Book is available at [Amazon.com]

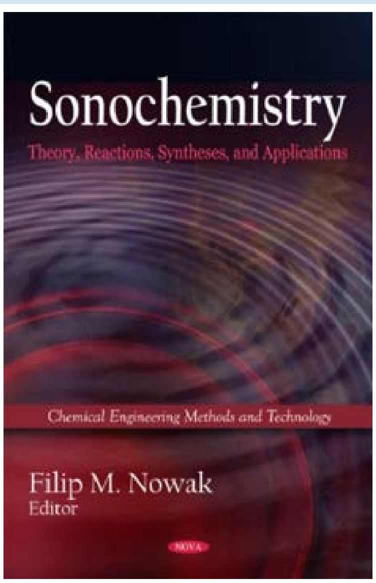

INDUSTRIAL-SCALE PROCESSING OF LIQUIDS BY HIGH-INTENSITY ACOUSTIC CAVITATION: THE UNDERLYING THEORY AND ULTRASONIC EQUIPMENT DESIGN PRINCIPLES [Hardcover]

Alexey Peshkovsky, Sergei Peshkovsky, Chapter 2 in "Sonochemistry Theory, Reactions, Syntheses and Applications", Publisher: Nova Science Pub Inc (October, 2010), ISBN-10: 1617286524

Abstract

A multitude of useful physical and chemical processes promoted by ultrasonic cavitation have been described in laboratory studies. Industrial-scale implementation of high-intensity ultrasound has, however, been hindered by several technological limitations, making it difficult to directly scale up ultrasonic systems in order to transfer the results of the laboratory studies to the plant floor. High-capacity flow-through ultrasonic reactor systems required for commercial-scale processing of liquids can only be properly designed if all energy parameters of the cavitation region are correctly evaluated. Conditions which must be fulfilled to ensure effective and continuous operation of an ultrasonic reactor system are provided in this chapter, followed by a detailed description of "shockwave model of acoustic cavitation", which shows how ultrasonic energy is absorbed in the cavitation region, owing to the formation of a spherical micro-shock wave inside each vapor-gas bubble, and makes it possible to explain some newly discovered properties of acoustic cavitation that occur at extremely high intensities of ultrasound. After the theoretical background is laid out, fundamental practical aspects of industrial-scale ultrasonic equipment design are provided.

Book is available at [Amazon.com]

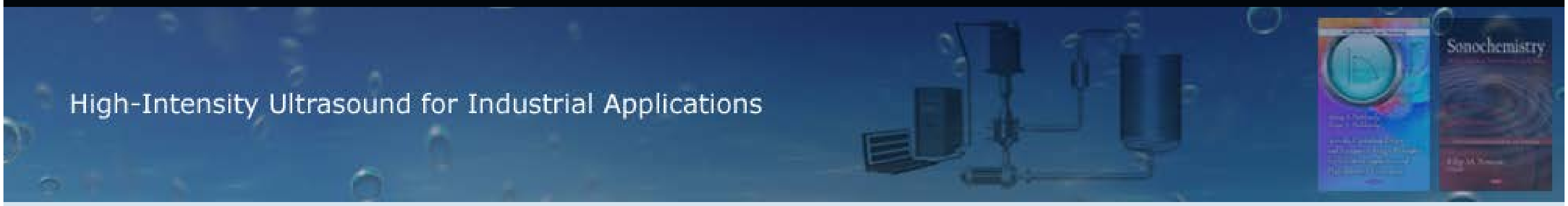

Home → Technical Resources → Peer-Reviewed Publications

PEER-REVIEWED PUBLICATIONS

SHOCK-WAVE MODEL OF ACOUSTIC CAVITATION

Sergei Peshkovsky, Alexey Peshkovsky, Ultrasonics Sonochemistry, Volume 15, Issue 4, April 2008, Pages 618-628

Abstract

Shock-wave model of liquid cavitation due to an acoustic wave was developed, showing how the primary energy of an acoustic radiator is absorbed in the cavitation region owing to the formation of spherical shock-waves inside each gas bubble. The model is based on the concept of a hypothetical spatial wave moving through the cavitation region. It permits using the classical system of Rankine–Hugoniot equations to calculate the total energy absorbed in the cavitation region. Additionally, the model makes it possible to explain some newly discovered properties of acoustic cavitation that occur at extremely high oscillatory velocities of the radiators, at which the mode of bubble oscillation changes and the bubble behavior approaches that of an empty Rayleigh cavity. Experimental verification of the proposed model was conducted using an acoustic calorimeter with a set of barbell horns. The maximum amplitude of the oscillatory velocity of the horns' radiating surfaces was 17 m/s. Static pressure in the calorimeter was varied in the range from 1 to 5 bars. The experimental data and the results of the calculations according to the proposed model were in good agreement. Simple algebraic expressions that follow from the model can be used for engineering calculations of the energy parameters of the ultrasonic radiators used in sonochemical reactors.

Complete document is available in PDF format:

MATCHING A TRANSDUCER TO WATER AT CAVITATION - ACOUSTIC HORN DESIGN PRINCIPLES

Sergei Peshkovsky, Alexey Peshkovsky, Ultrasonics Sonochemistry Volume 14, Issue 3, March 2007, Pages 314-322

Abstract

High-power ultrasound for several decades has been an integral part of many industrial processes conducted in aqueous solutions. Maximizing the transfer efficiency of the acoustic energy between electromechanical transducers and water at cavitation is crucial when designing industrial ultrasonic reactors with large active volumes. This can be achieved by matching the acoustic impedances of transducers to water at cavitation using appropriately designed ultrasonic horns. In the present work, a set of criteria characterizing the matching capabilities of ultrasonic horns is developed. It is shown that none of the commonly used tapered-shape horns can achieve the necessary conditions. An analytical method for designing five-element acoustic horns with the desirable matching properties is introduced, and five novel types of such horns, most suitable for practical applications, are proposed. An evaluation of the horns' performance is presented in a set of experiments, demonstrating the validity of the developed theoretical methodology. Power transfer efficiency increase by almost an order of magnitude is shown to be possible with the presented horn designs, as compared to those traditionally utilized.

Complete document is available in PDF format:

High-Intensity Ultrasound for Industrial Applications

DOWNLOADS

Ultrasonic Processor Manuals

1200 W Air-Cooled Ultrasonic Liquid Processor:

Software Help

Generator Control Software Help:

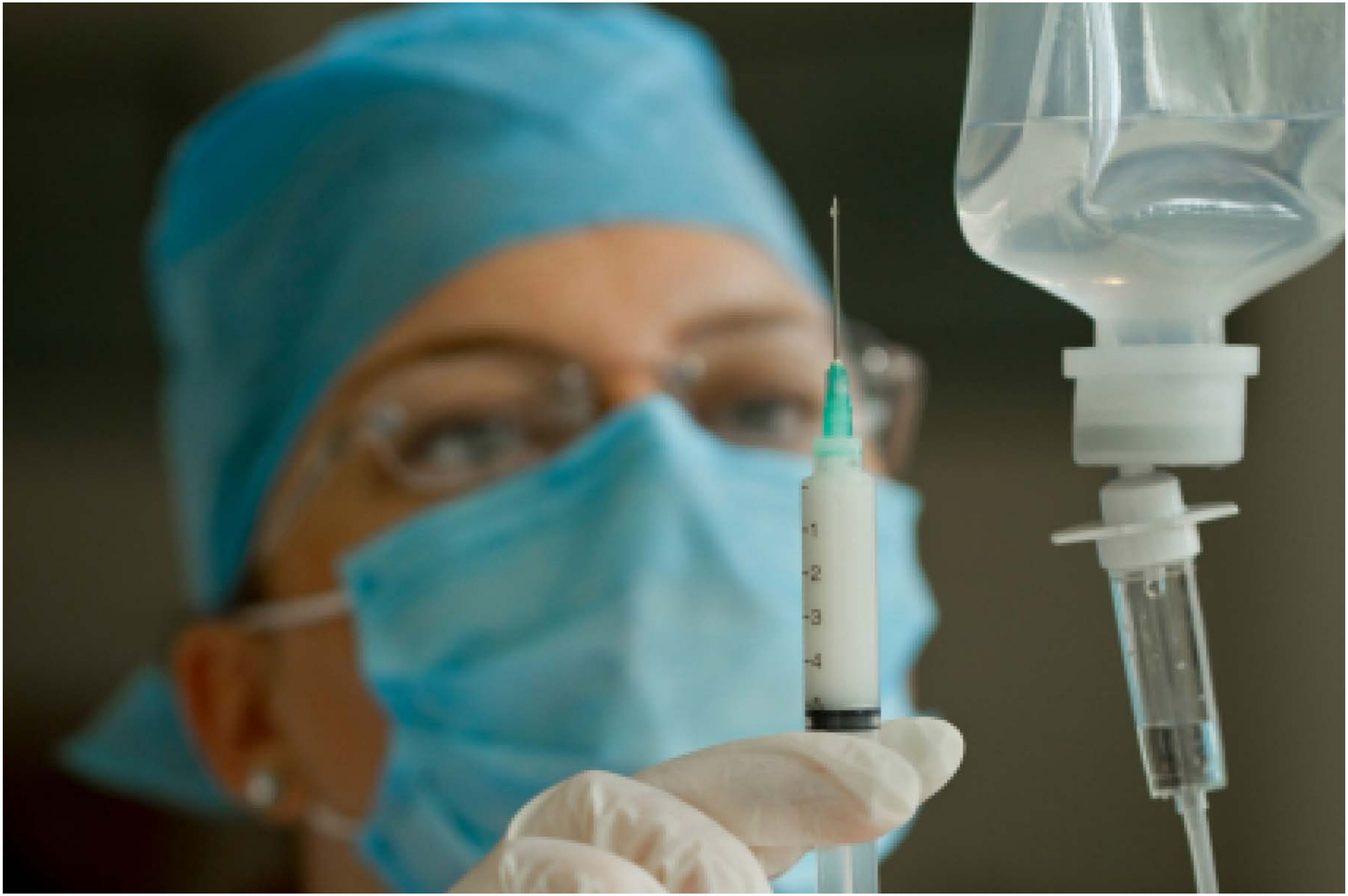

Number of passes	Ultrasonic amplitude (μ_{pp})	SLS, MDS (nm)	DLS, MDS (nm)	$PFAT_5$ (%)
1	75	319.7		
3	75	308.7		
5	75	200.2	199.23	0.024
5	**25**		527.7	0.364

Table 1. $PFAT_5$ is percentage (volume-weighted) of oil droplets > 5 μm, determined by LE/SPOS, MDS is mean droplet size (intensity-weighted) determined by Static (SLS) and Dynamic Light Scattering (DLS). Color coding refers to pass and fail, according to USP recommendations.

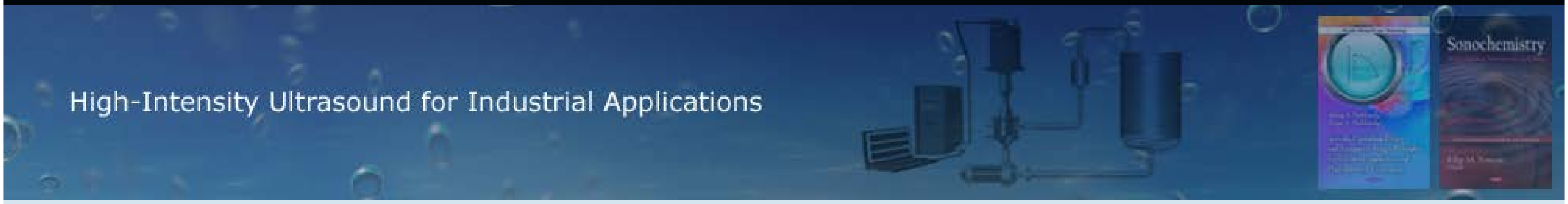

ULTRASONIC SYSTEMS

OVERVIEW

Industrial Sonomechanics, LLC, (ISM) offers bench and commercial-scale ultrasonic liquid processors (also known as ultrasonic homogenizers and sonochemical reactors) able to provide very high ultrasonic amplitudes and cavitation intensities. Application examples include: production of nanoemulsions, nanocrystals and wax nanoparticles for pharmaceutical, cosmetic, food, ink, paint, coating, wood treatment, metalworking, nanocomposite, pesticide, and fuel industries, extraction of oil from algae, production of biofuels, crude oil desulphurization, degassing, cell disruption, polymer and epoxy processing, and more.

ISM's ultrasonic processors are based on Barbell Horn Ultrasonic Technology (BHUT), which makes it possible to implement high-amplitude ultrasound on any scale, form laboratory to industrial, guaranteeing reproducible and predictable results. The processors utilize patented ultrasonic reactor chambers and provide very uniform ultrasonic treatment with no bypass.

HIGH-EFFICIENCY ULTRASONIC LIQUID PROCESSORS

1200 W Processor with Air-Cooled Transducer

1200 W bench-scale ultrasonic processor system is designed for batch and flow-through process investigations and small-scale production. The system operates at the frequency of approximately 20 kHz. Barbell horns used in this system have output tip diameters of up to 35 mm and can provide stable operation at output amplitudes up to 120 microns in aqueous loads at a normal pressure, corresponding to acoustic power intensities up to 80 W/cm^2. This gives investigators a wide range of experimental conditions to determine optimal parameters for even the most challenging ultrasonic processes. The system can be used for small-scale production.

2400 W Processor with Air-Cooled Transducer

2400 W industrial-scale ultrasonic processor system is designed for high-volume continuous-mode commercial production. The system operates at the frequency of approximately 20 kHz. Barbell horns used in this system have large output tip diameters (Ø) and provide very high output amplitudes (A) and output power densities (Pd). For example, for FBH-type horns the following combinations are possible (water up to the nodal point, at 1 bar and 25 ºC):

Ø = 50 mm, A = 120 microns, Pd = 80 W/cm^2;
Ø = 60 mm, A = 85 microns, Pd = 55 W/cm^2;
Ø = 70 mm, A = 60 microns, Pd = 35 W/cm^2.

Other types of Barbell horns can be used as well. These amplitudes and power densities are extremely high and are unprecedented for industrial-scale systems, which are commonly restricted to ultrasonic amplitudes below 25 microns and power densities below 10 W/cm^2. ISM's Barbell Horn Ultrasonic Technology (BHUT) utilized in this processor makes it possible to implement even the most challenging ultrasonic processes in the commercial environment.

SPECIAL-REQUEST ULTRASONIC LIQUID PROCESSORS

1000 W Processor with Water-Cooled Transducer

1000 W (output power) bench-top water-cooled ultrasonic system is a "special request" unit, designed for batch and flow-through process investigations and small-scale production. The system operates at the frequency of approximately 22 kHz. FBH-type Barbell horns used in this system have output tip diameters up to 35 mm and can provide stable operation at output amplitudes up to 75 microns in aqueous loads at a normal pressure, corresponding to acoustic power intensities up to 50 W/cm^2. The system is based on a water-cooled magnetostrictive transducer.

2000 W Processor with Water-Cooled Transducer

2000 W (output power) industrial water-cooled ultrasonic system is a "special request" unit, designed for flow-through or batch production on a commercial scale. The system operates at the frequency of approximately 18 kHz. FBH-type Barbell horns used in this system have output tip diameters of 60 mm, with larger diameters (up to 75 mm) available upon request. These horns can provide stable operation at output amplitudes up to 85 microns in aqueous loads at a normal pressure, corresponding to acoustic power intensities up to 55 W/cm^2. The system is able to directly reproduce any laboratory or bench-scale process optimization study in a commercial production environment and is based on a water-cooled magnetostrictive transducer.

Sample type	SLS, MDS (nm)	DLS, MDS (nm)	$PFAT_5$ (%)
Emulsion 1	215	**190**	**0.007**
Emulsion 1+ ZnPC	210	**177**	**0.001**
Emulsion 2	60		
Emulsion 2+ ZnPC	84	**70**	**0.026**
Liposomes	101		

$PFAT_5$ is the percentage (volume-weighted) of oil droplets > 5 μm, determined by LE/SPOS, MDS is the mean droplet size (intensity-weighted) determined by Static (SLS) and Dynamic Light Scattering (DLS).

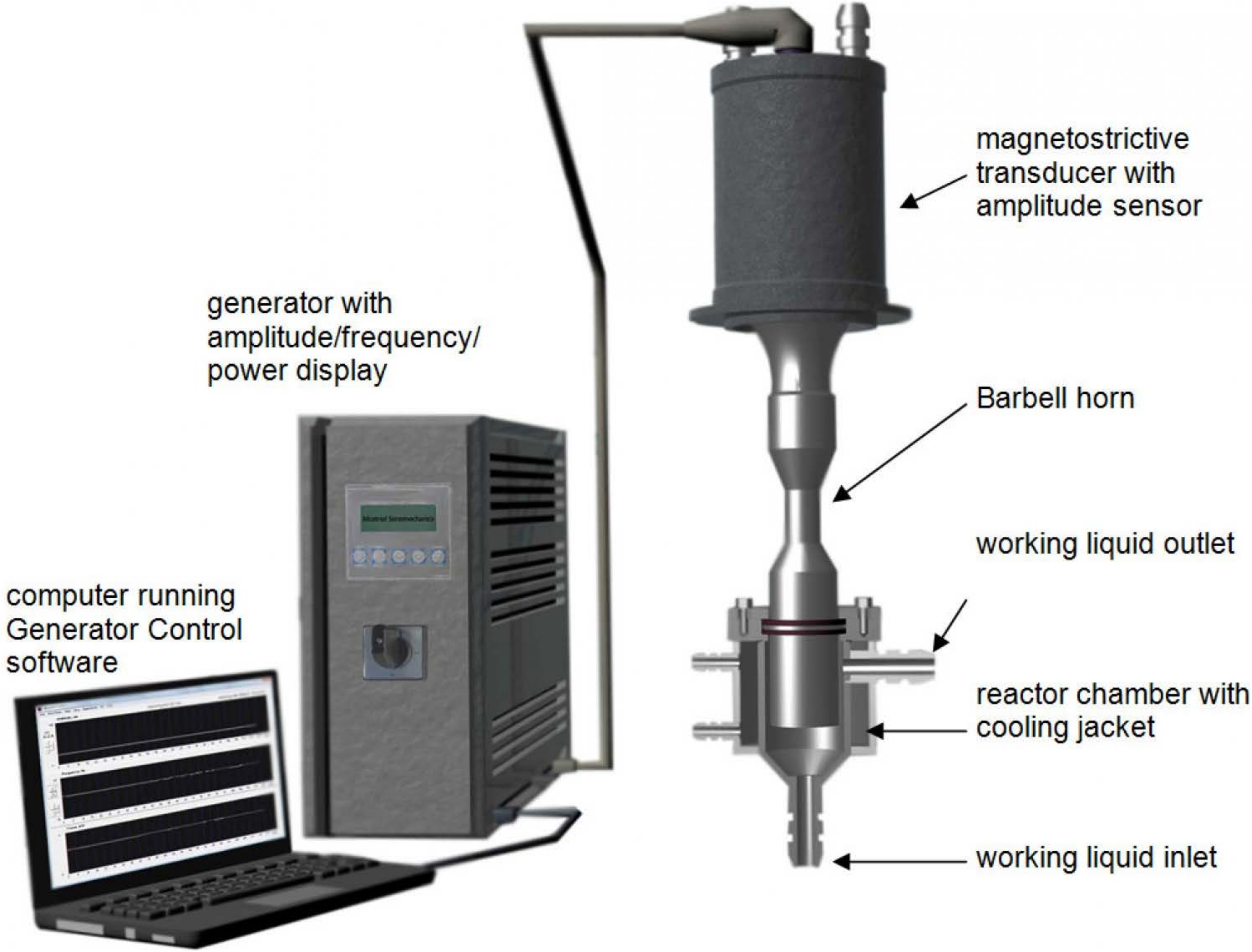
magnetostrictive
transducer with
amplitude sensor
generator with
amplitude/frequency/
power display
Barbell horn
working liquid outlet
computer running
Generator Control
software
reactor chamber with
cooling jacket
working liquid inlet


1
2
3

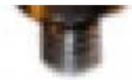

http://sonomechanics.com/files/ultrasonic_systems/1000_w_water_cooled/m_804185693.jpg[11.04.2012 18:20:18]

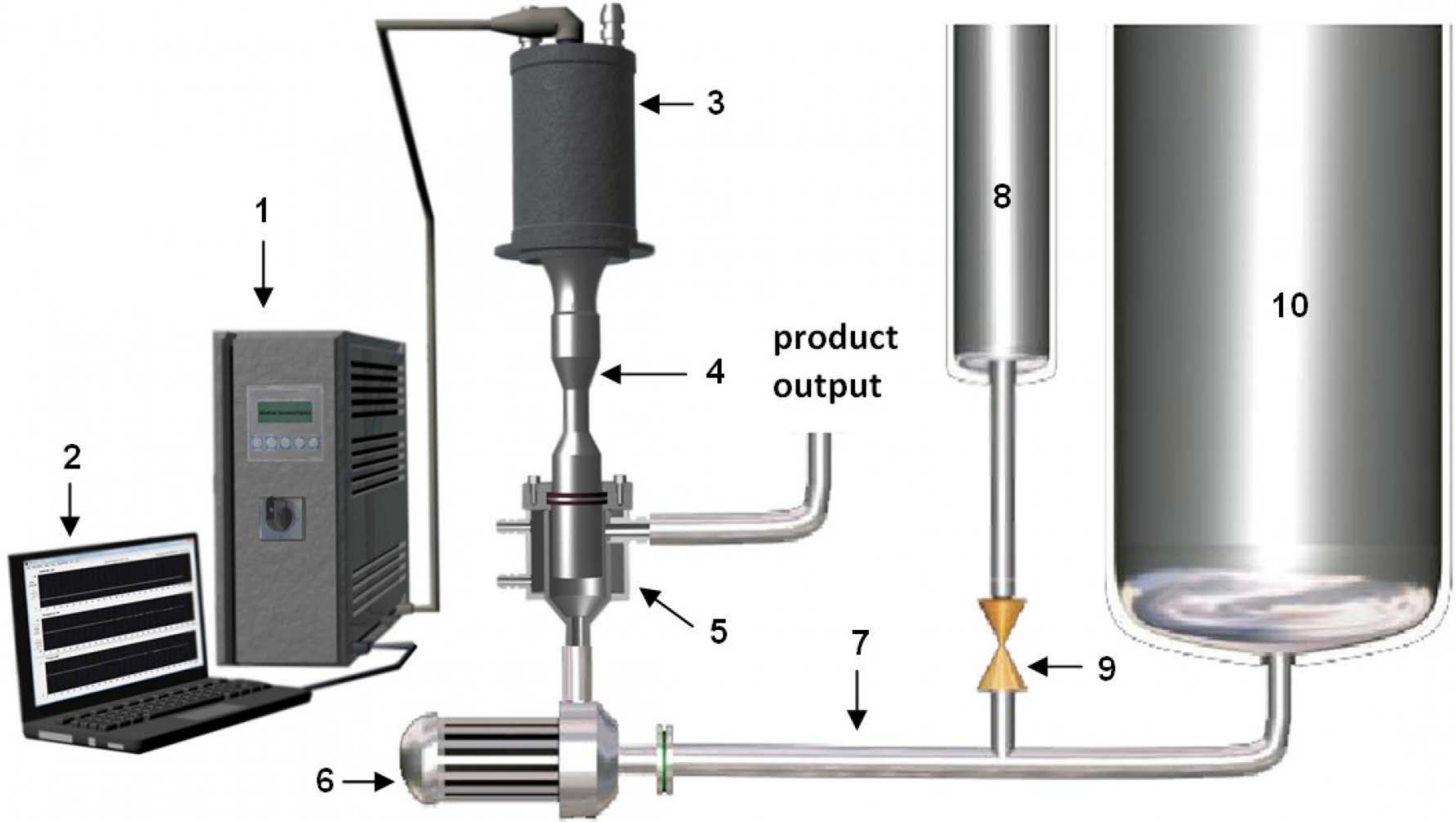

1
2
3
4
5
6
7
8
9
10
product
output

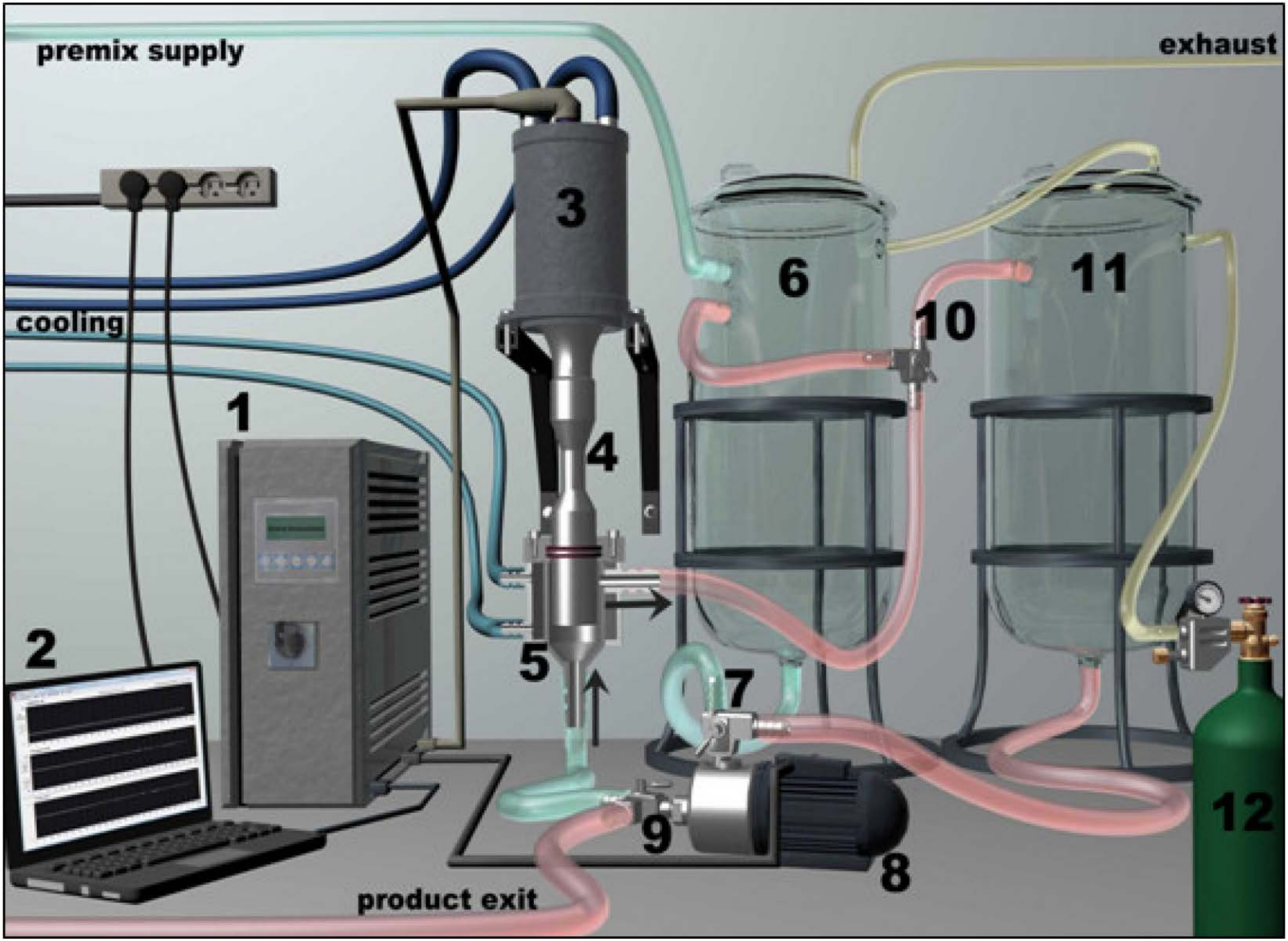
premix supply
exhaust
cooling
product exit
1
2
3
4
5
6
7
8
9
10
11
12

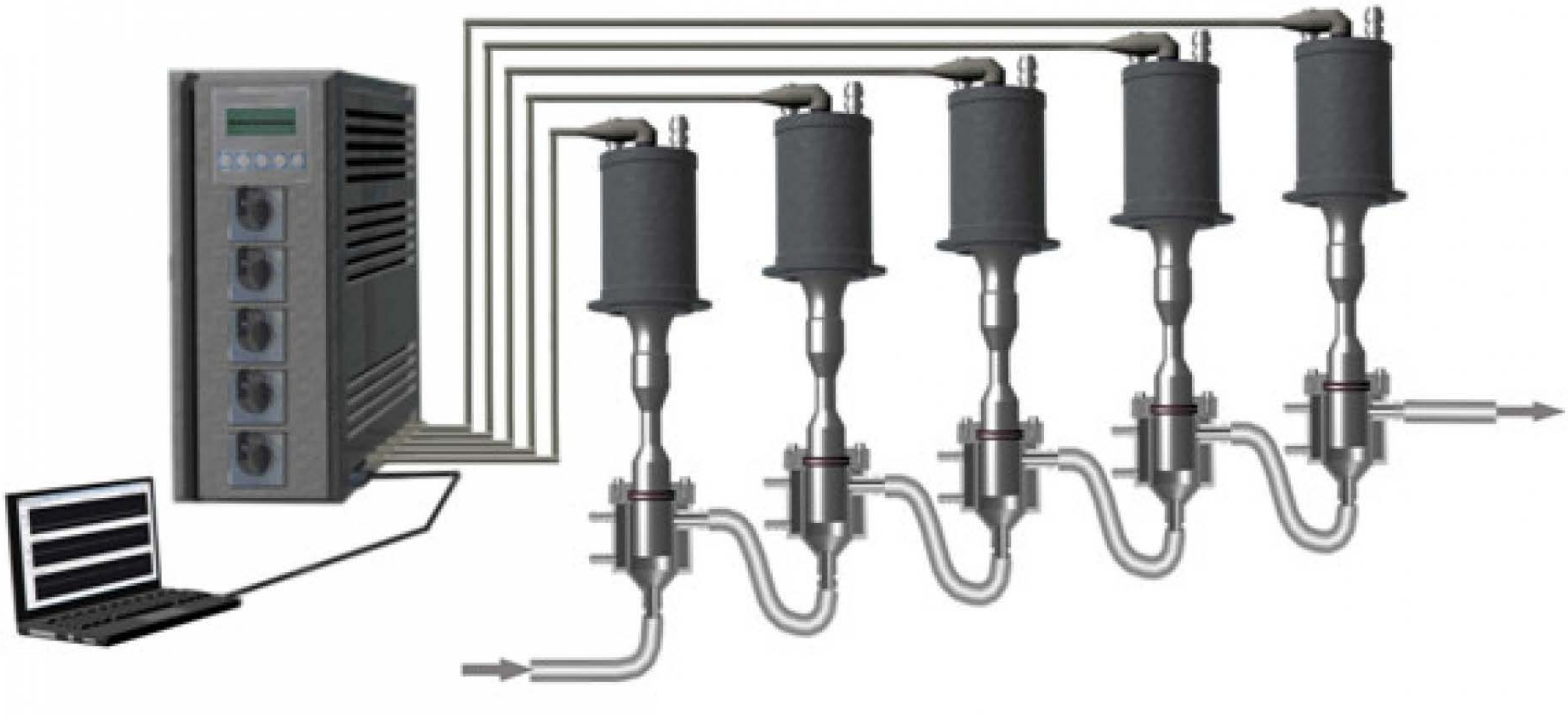

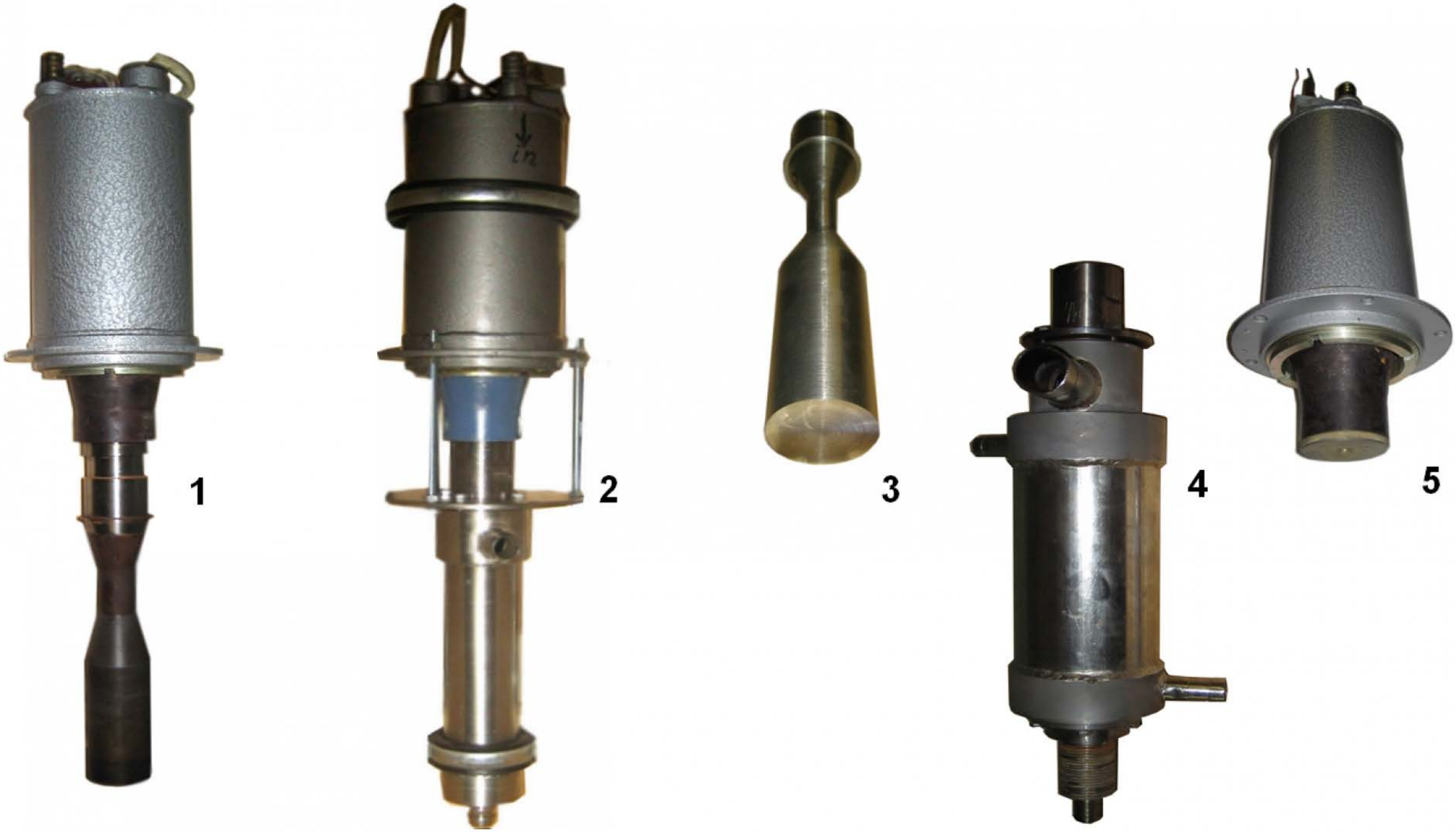
1
2
3
4
5


1
2
3
4
5

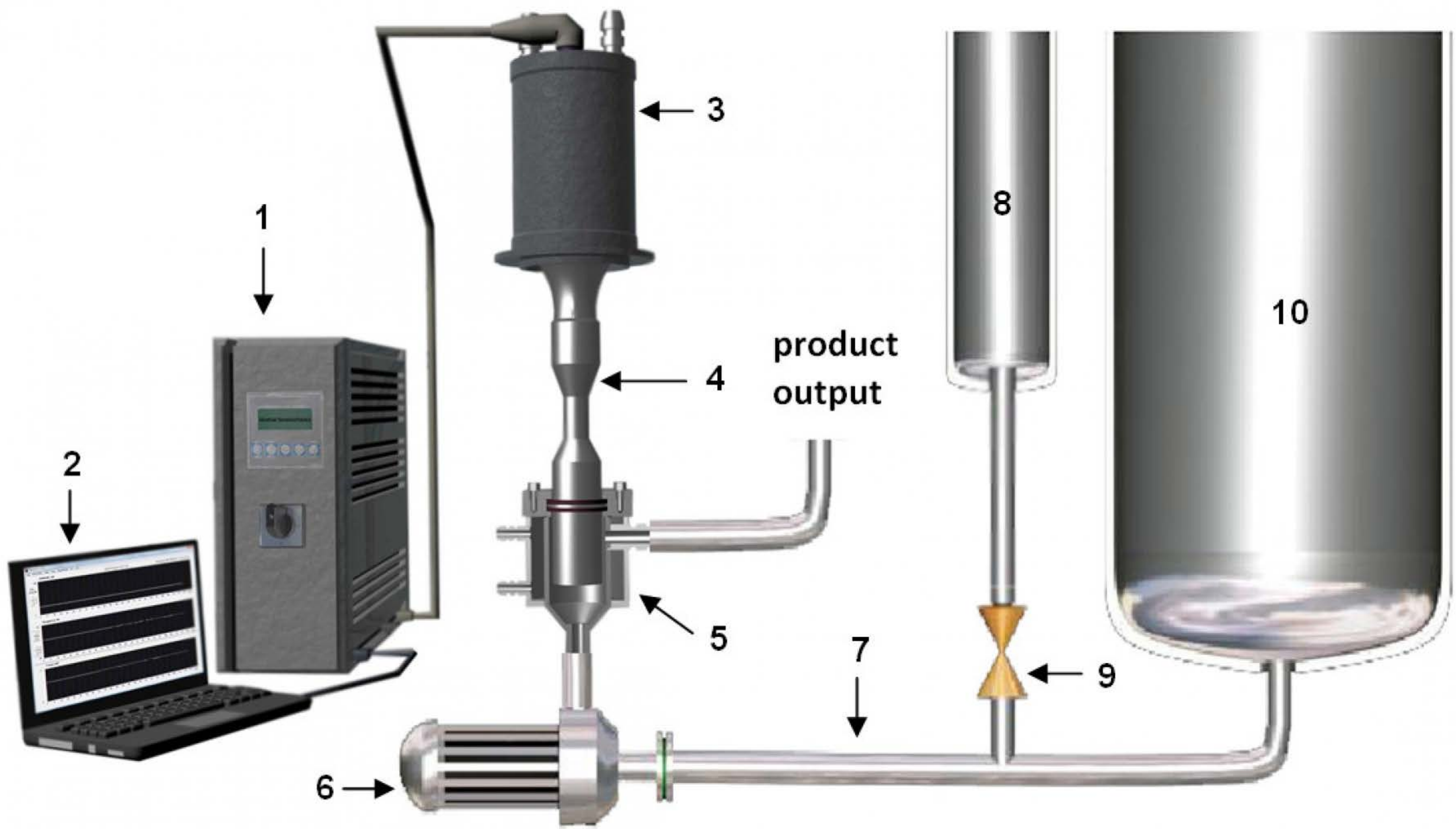
1
2
3
4
product
output
5
6
7
8
9
10


1
2
3
4
5

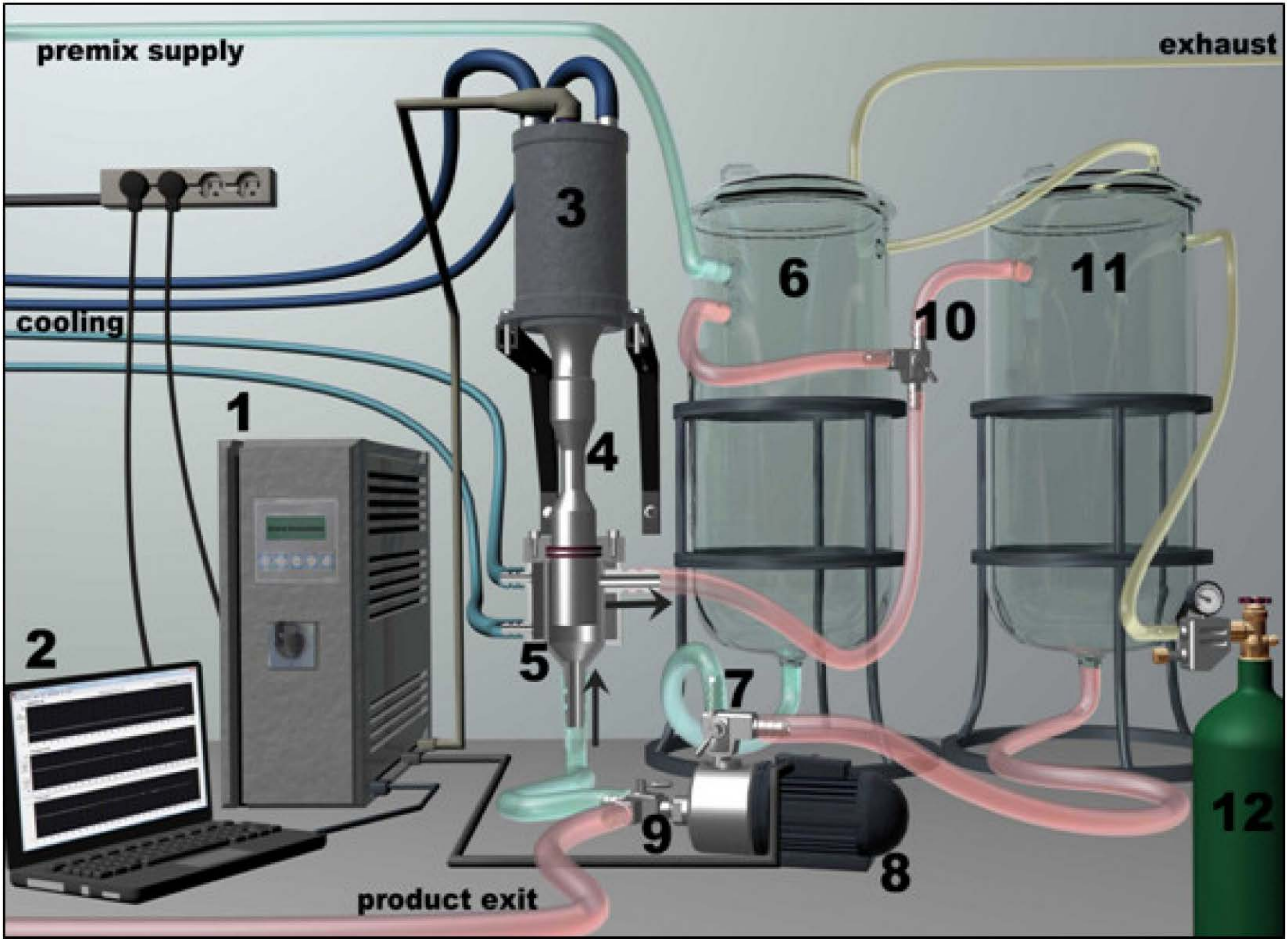
premix supply
exhaust
3
6
11
cooling
10
1
4
2
5
7
12
9
8
product exit

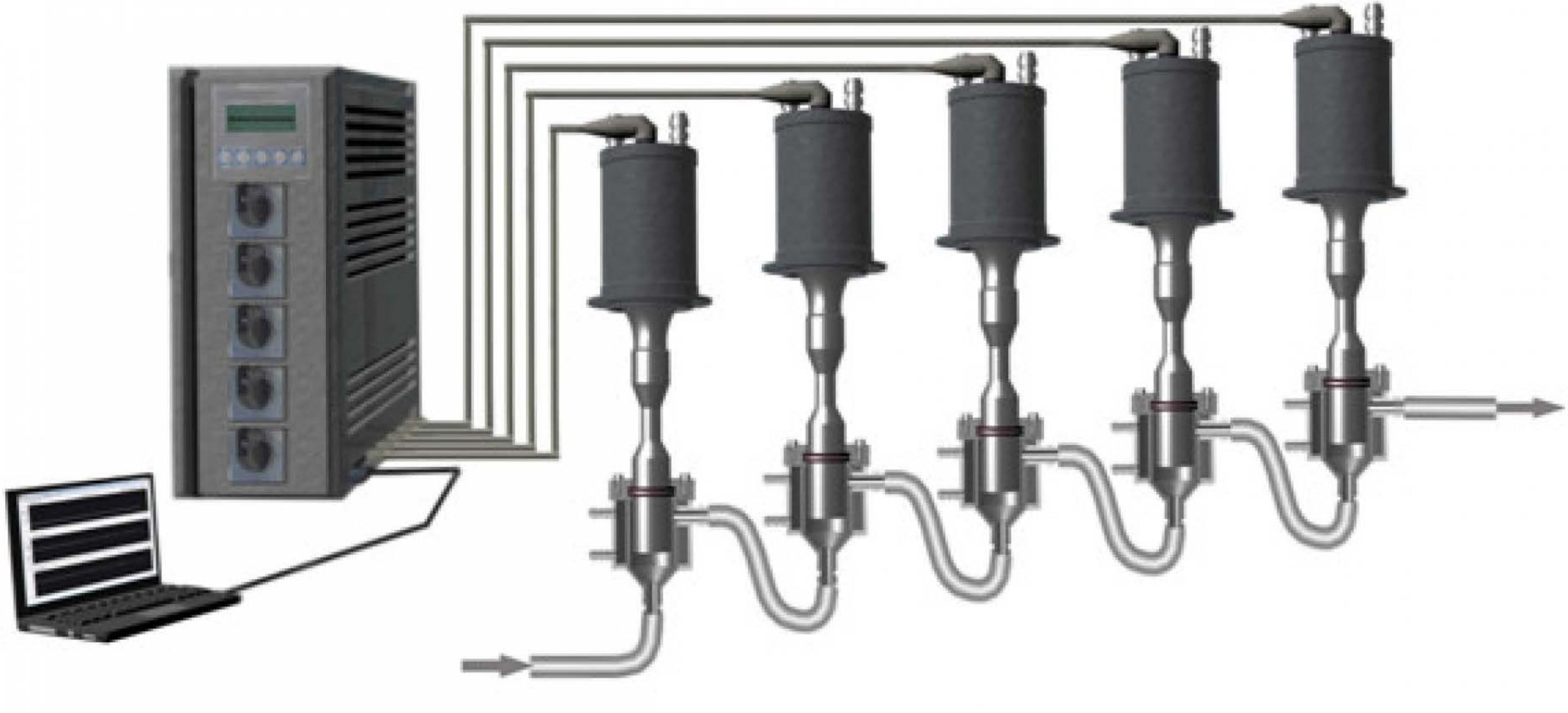

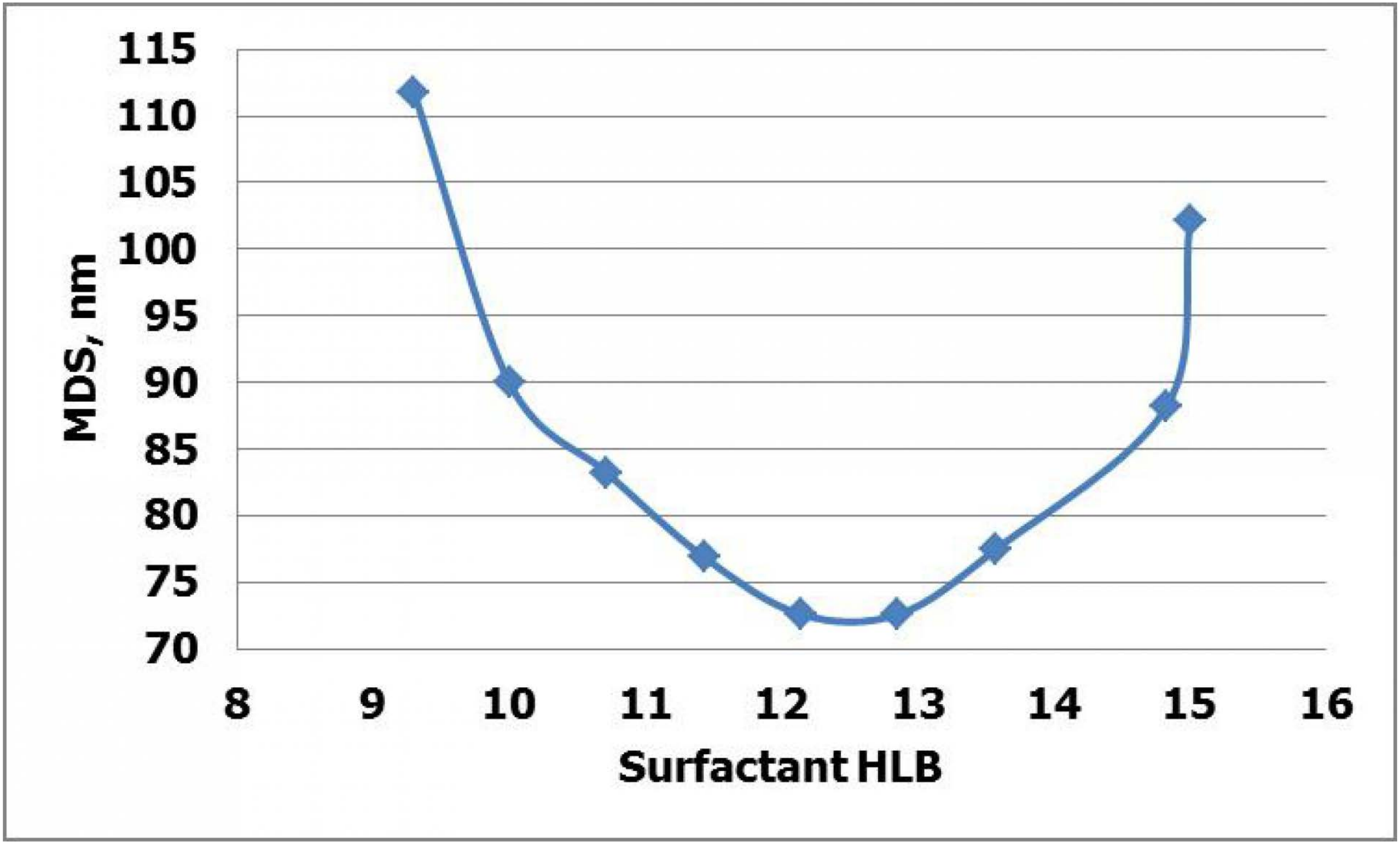
115
110
105
100
95
90
85
80
75
70
MDS, nm
8
9
10
11
12
13
14
15
16
Surfactant HLB

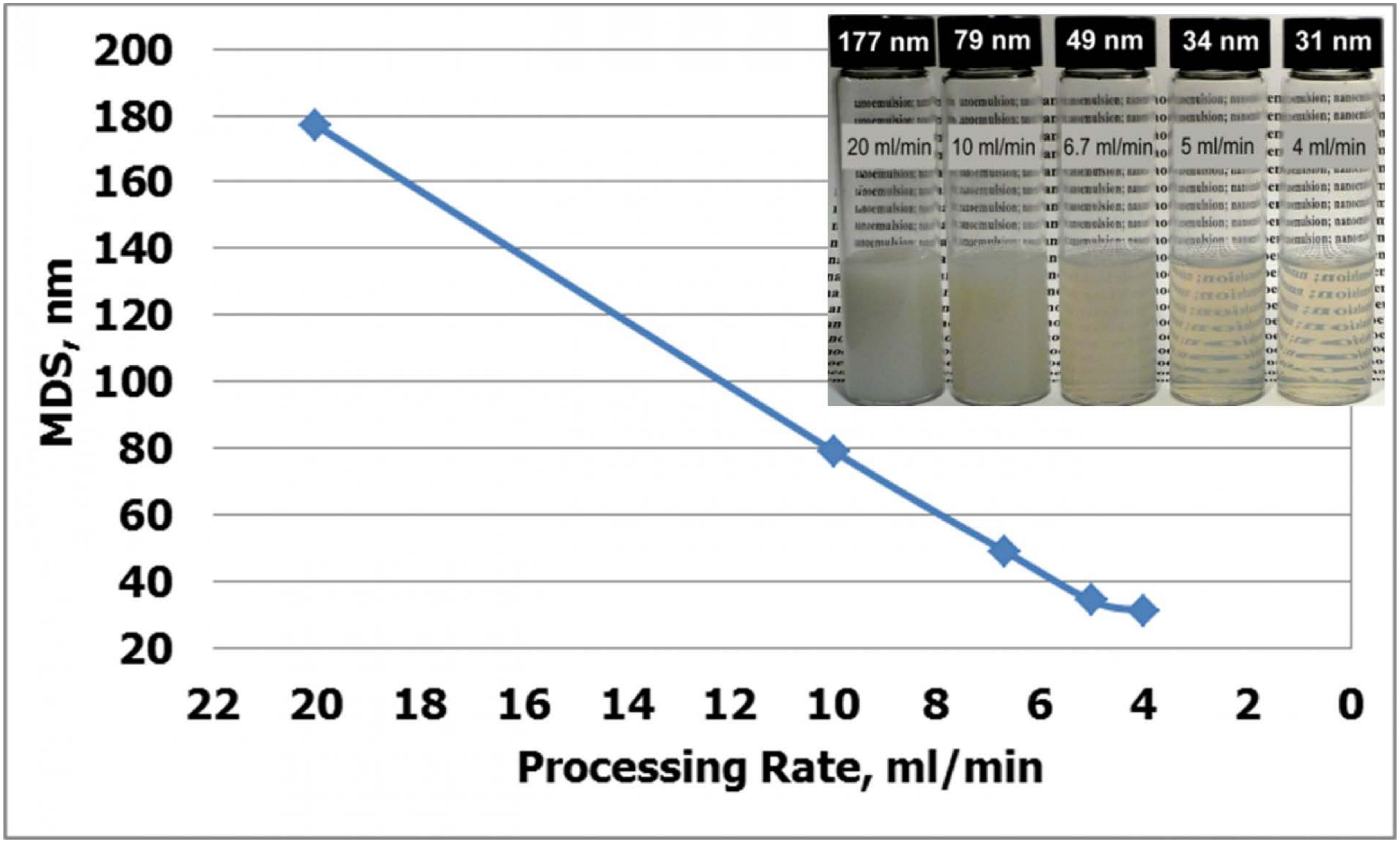
177 nm
79 nm
49 nm
34 nm
31 nm
20 ml/min
10 ml/min
6.7 ml/min
5 ml/min
4 ml/min
MDS, nm
200
180
160
140
120
100
80
60
40
20
22
20
18
16
14
12
10
8
6
4
2
0
Processing Rate, ml/min

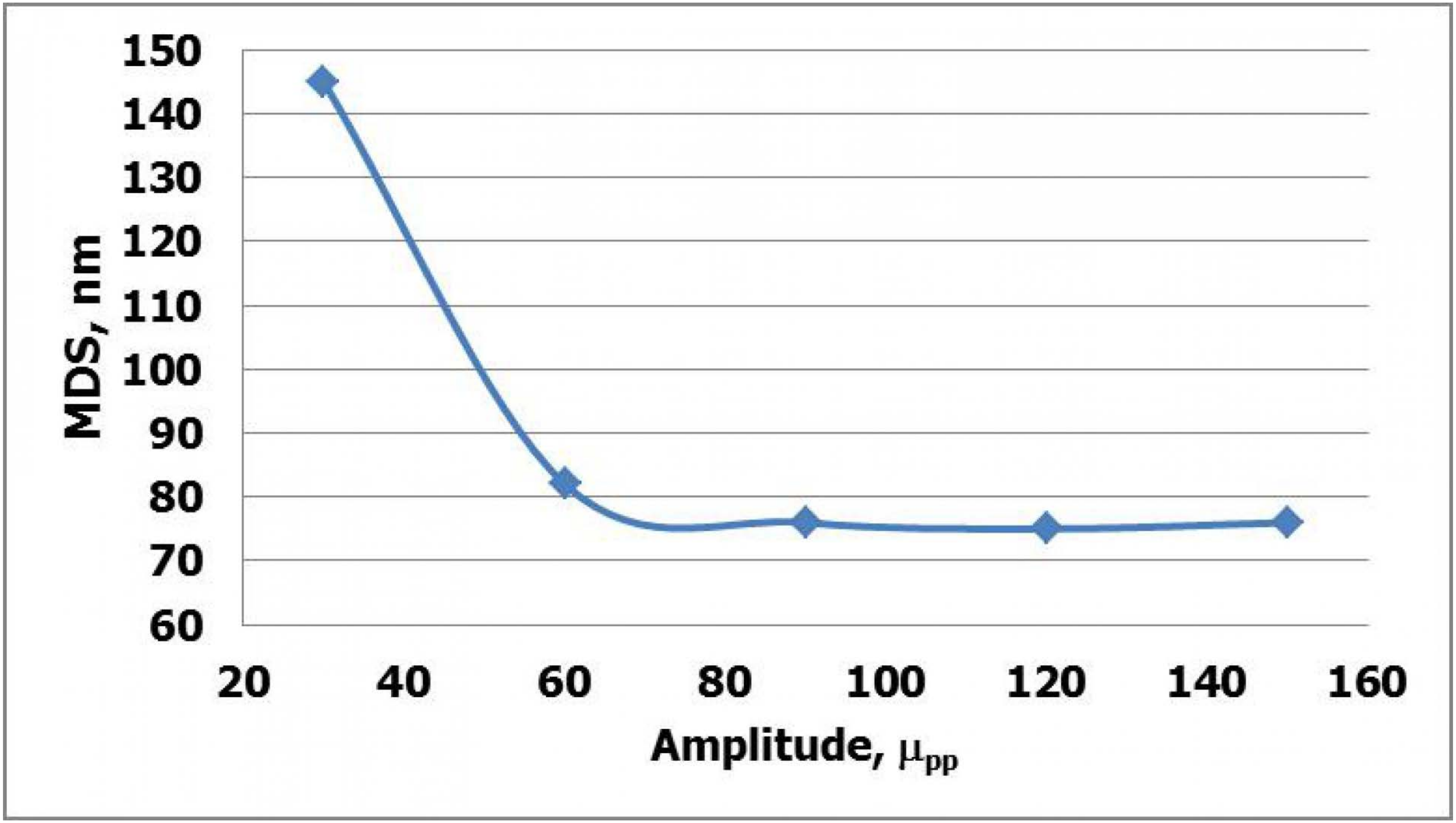
MDS, nm
150
140
130
120
110
100
90
80
70
60
20
40
60
80
100
120
140
160
Amplitude, μpp

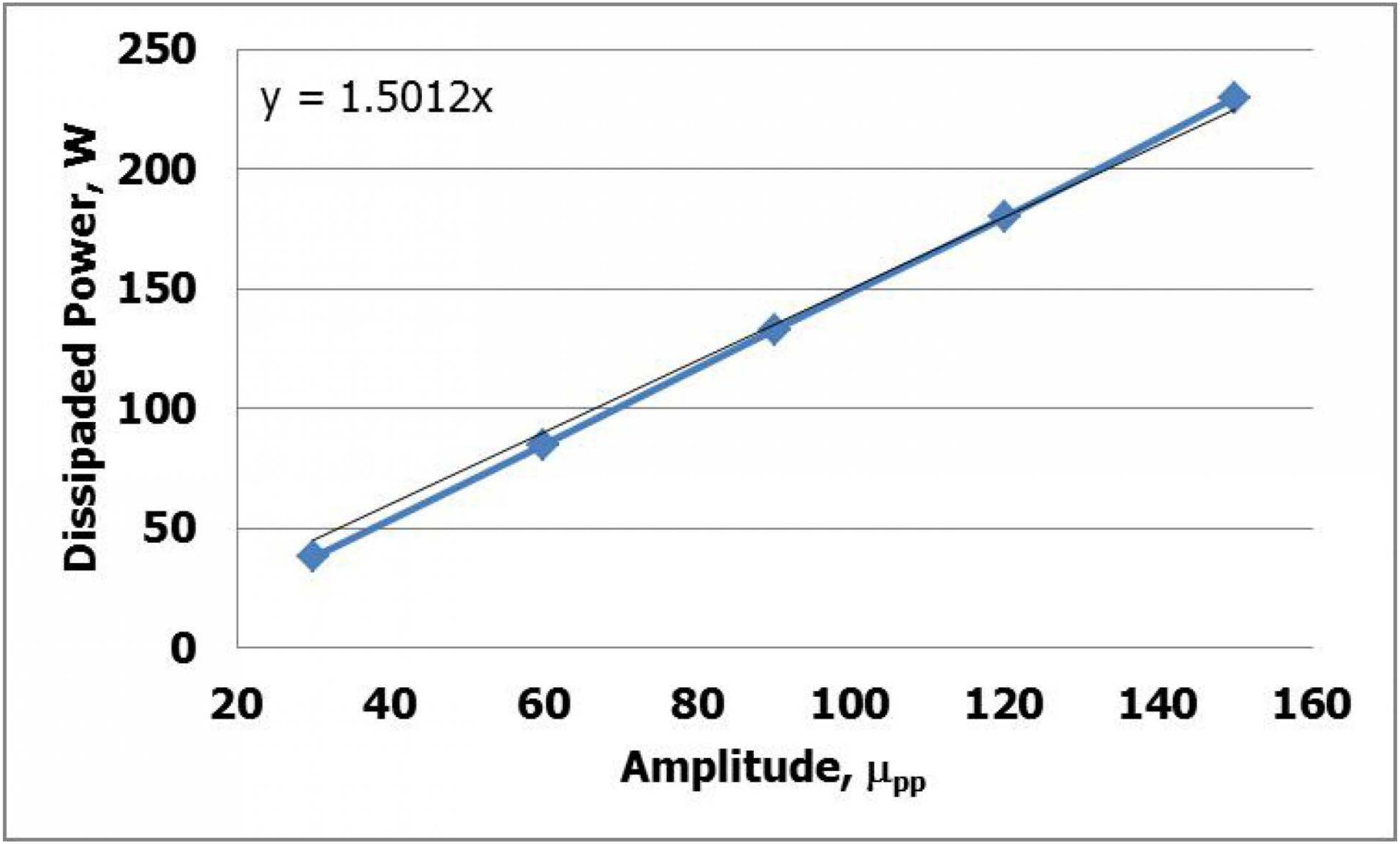

y = 1.5012x
Dissipaded Power, W
250
200
150
100
50
0
20
40
60
80
100
120
140
160
Amplitude, μ_{pp}

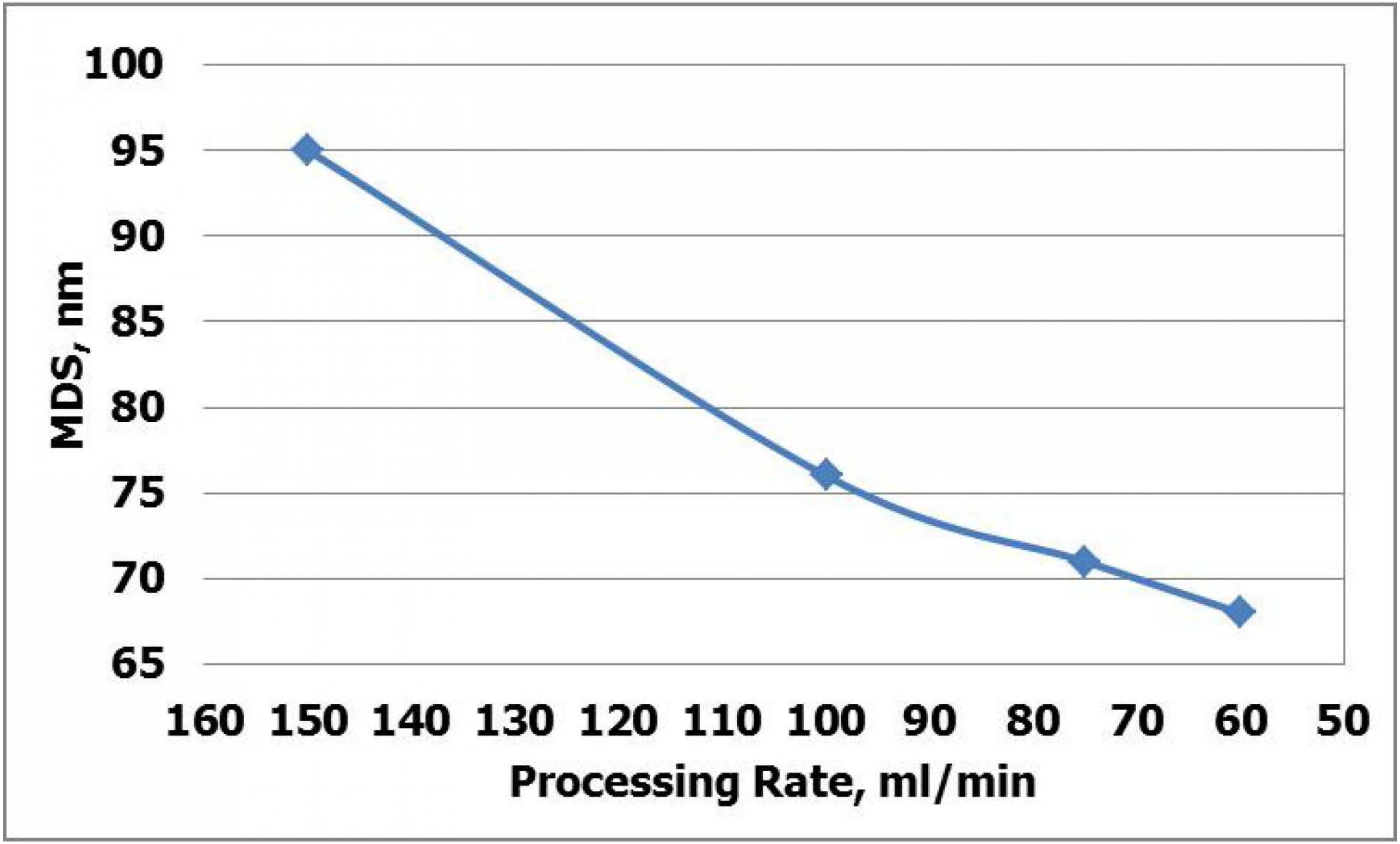
100
95
90
85
80
75
70
65
MDS, nm
160 150 140 130 120 110 100 90 80 70 60 50
Processing Rate, ml/min

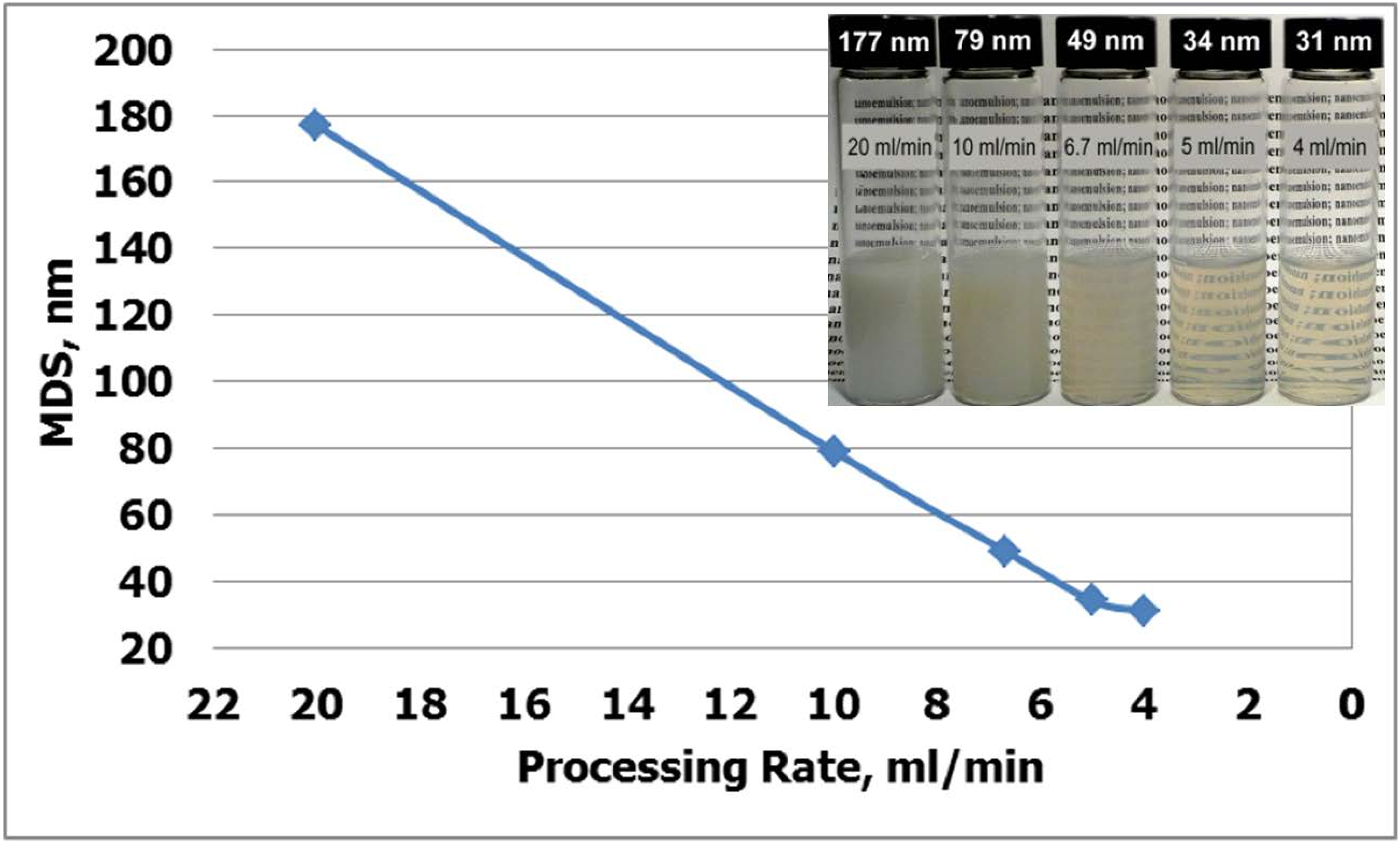

200
180
160
140
120
100
80
60
40
20
MDS, nm
22
20
18
16
14
12
10
8
6
4
2
0
Processing Rate, ml/min
177 nm
79 nm
49 nm
34 nm
31 nm
20 ml/min
10 ml/min
6.7 ml/min
5 ml/min
4 ml/min

Ultrasound-assisted micro-algal oil extraction/transesterification setups are shown, utilizing a conventional horn (left) and Barbell horn (right) both operating at the amplitude of 70 microns.

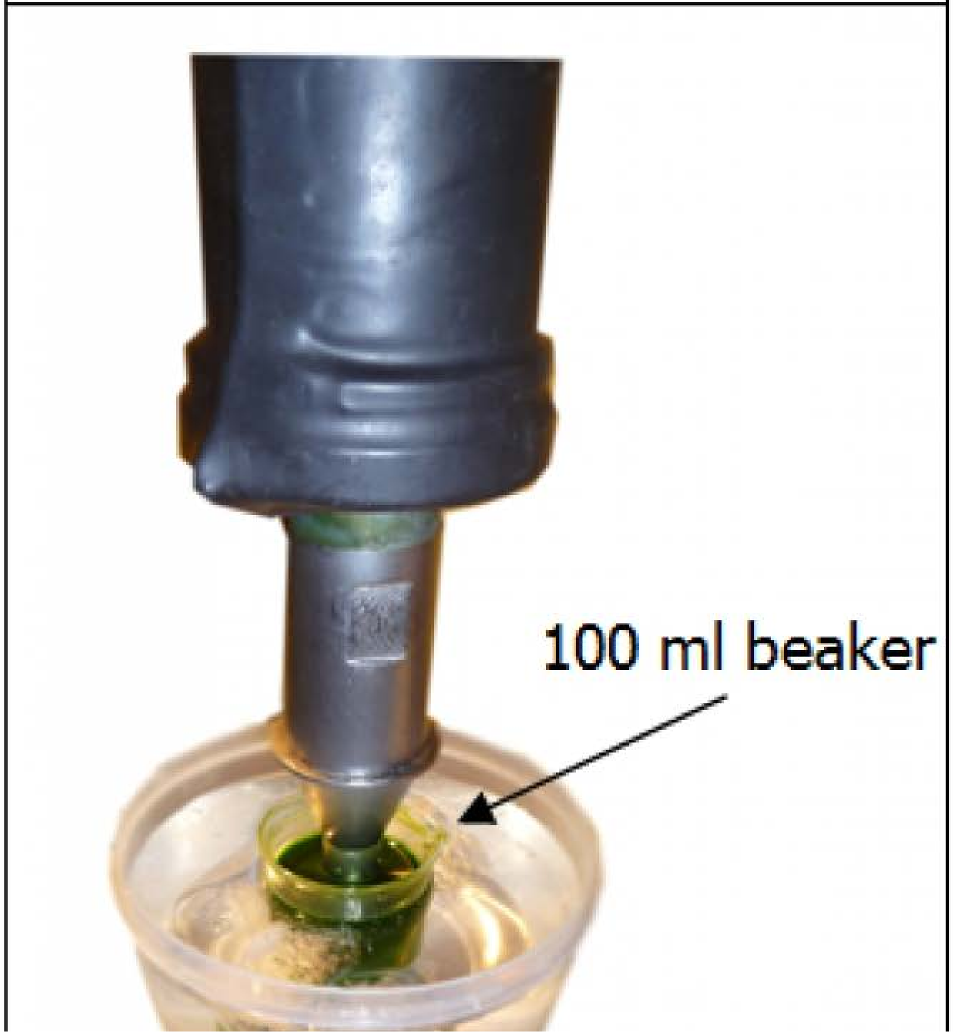

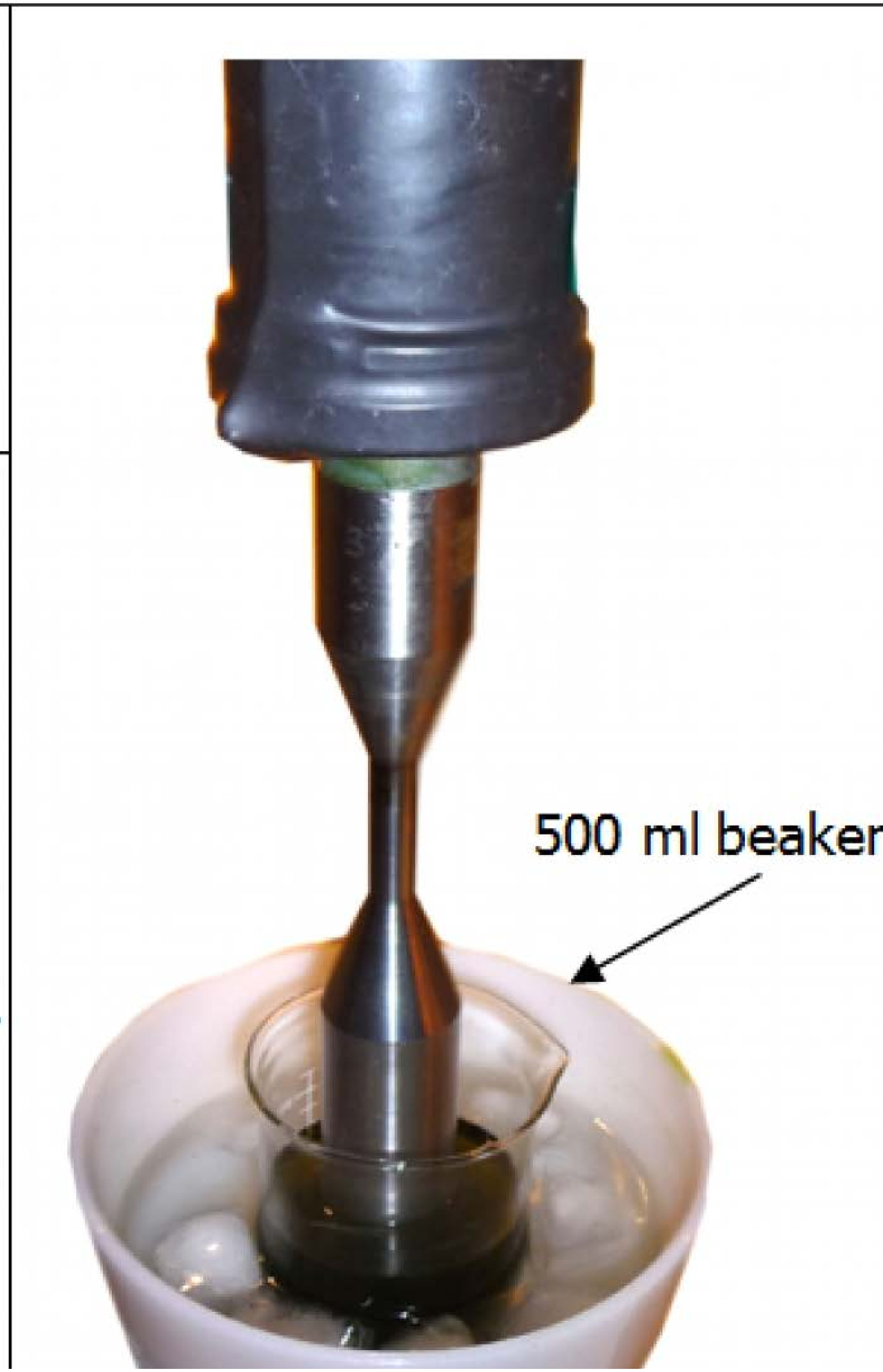

 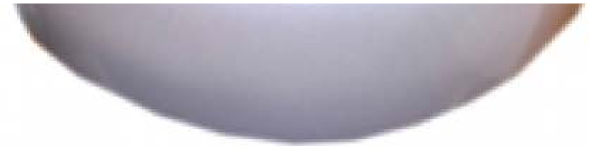

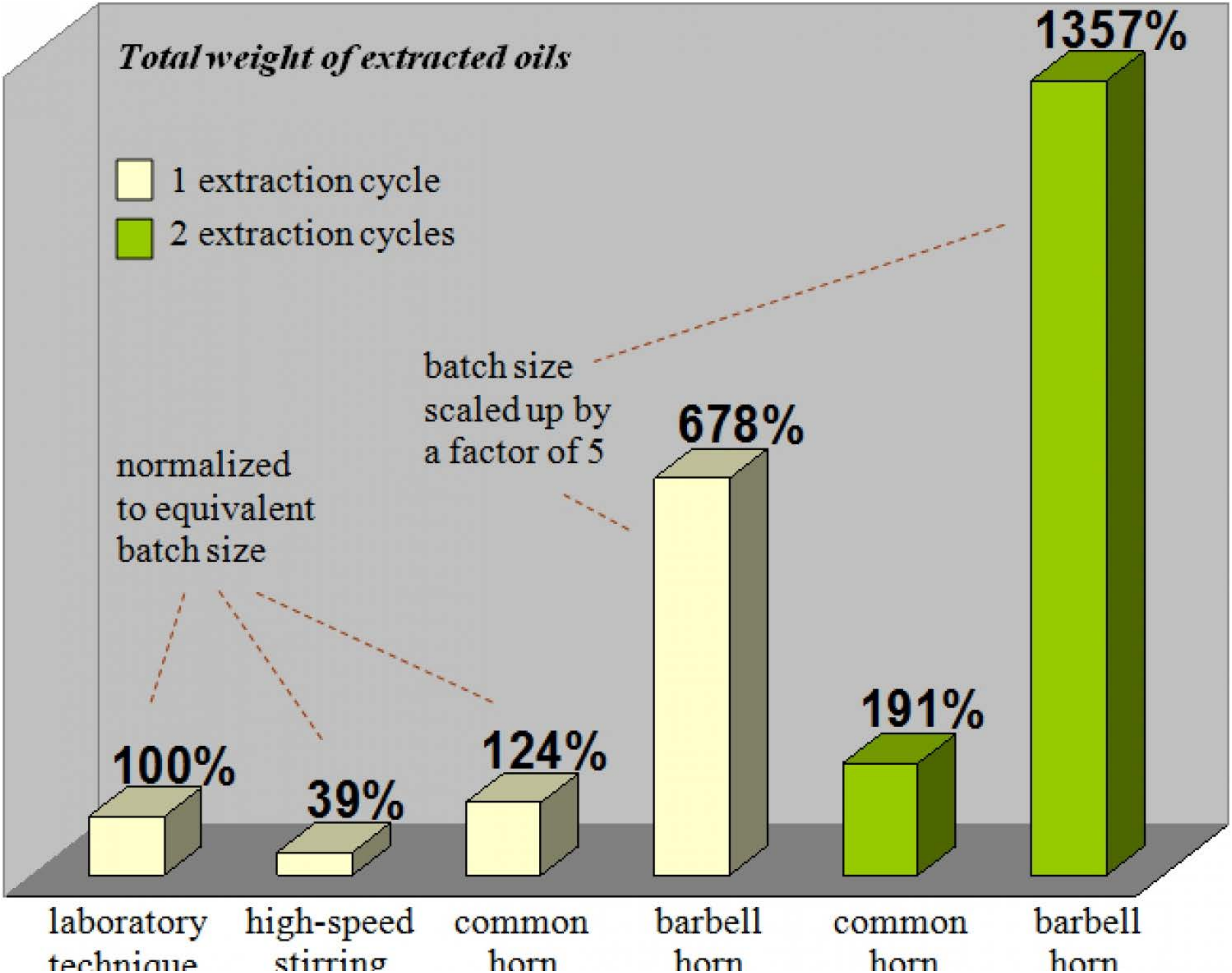
Total weight of extracted oils
1 extraction cycle
2 extraction cycles
batch size
scaled up by
a factor of 5
normalized
to equivalent
batch size
100%
39%
124%
678%
191%
1357%
laboratory
high-speed
common
barbell
common
barbell

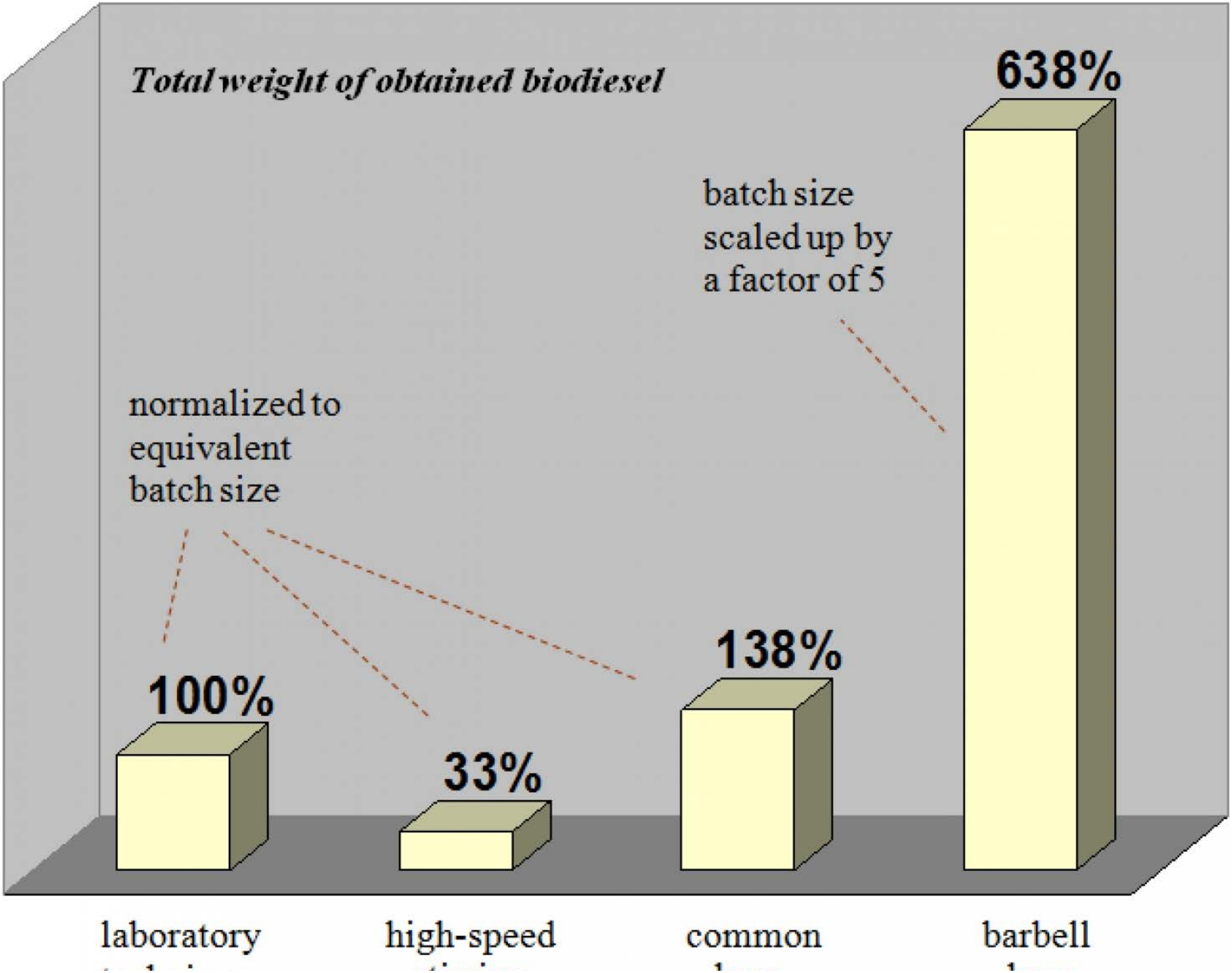
Total weight of obtained biodiesel
638%
batch size
scaled up by
a factor of 5
normalized to
equivalent
batch size
138%
100%
33%
laboratory
high-speed
common
barbell

technique	stirring	horn	horn

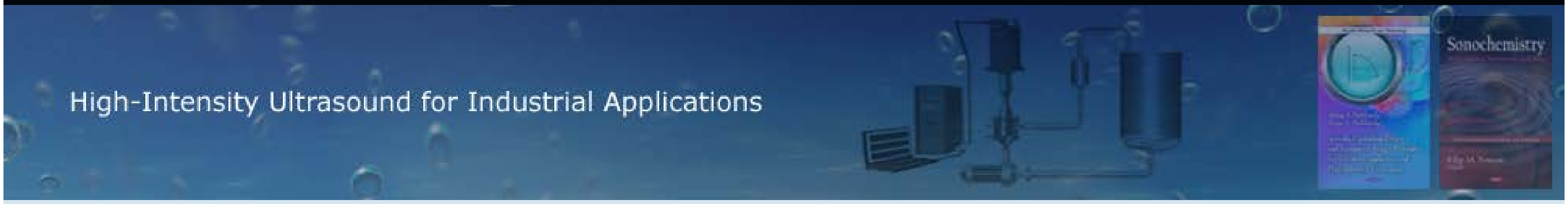

VIDEOS

Ultrasonic Cavitation in Water Produced by FBH, tip Ø = 75 mm

This video shows ultrasonic cavitation in water produced by a Full-wave Barbell Horn (output tip diameter = 75 mm) at a range of vibration amplitudes (from 10 to 150 microns). Unlike all other types of ultrasound horns, Barbell Horns (US Patent # 7156201) are capable of providing high vibration amplitudes and having large output tip diameters simultaneously, thereby allowing to implement high-intensity ultrasonic processes in the production environment. Most of the parts used in this demonstration were manufactured by Märkisches Werk Halver, according to ISM's intellectual property license.

Water in Diesel Nanoemulsion Prepared by High-Intensity Ultrasound

Nano-emulsification of water in oil has been carried out using a 1200 W ultrasonic system manufactured by Industrial Sonomechanics, LLC. A common converging ultrasonic horn (tip diameter 15.6 mm) was used in the first part of the video, producing 40 ml of the nano-emulsion. A Full-wave Barbell horn (tip diameter 35 mm) was used in the second part of the video, allowing to scale up the volume of the formulation by a factor of 5, thereby producing 200 ml of the nano-emulsion. The ultrasonic amplitude delivered by both horns was 60 microns.

Ultrasonic Cavitation in Water Produced by HBHO, tip Ø = 35 mm

This video shows ultrasonic cavitation in water produced by Industral Sonomechanics' 1200 W ultrasonic processor equipped with a Half-wave Barbell Horn with an Opening (HBHO). Ultrasonic amplitudes of 30 and 100 microns were used. Unlike other ultrasonic processor systems, ISM's processors are able to generate high-intensity ultrasonic cavitation when using large-diameter industrial-scale ultrasonic horns and reactors. ISM's Barbell ultrasonic horns are capable of providing high vibration amplitudes and having large output tip diameters simultaneously.

Previous Page < > Next Page

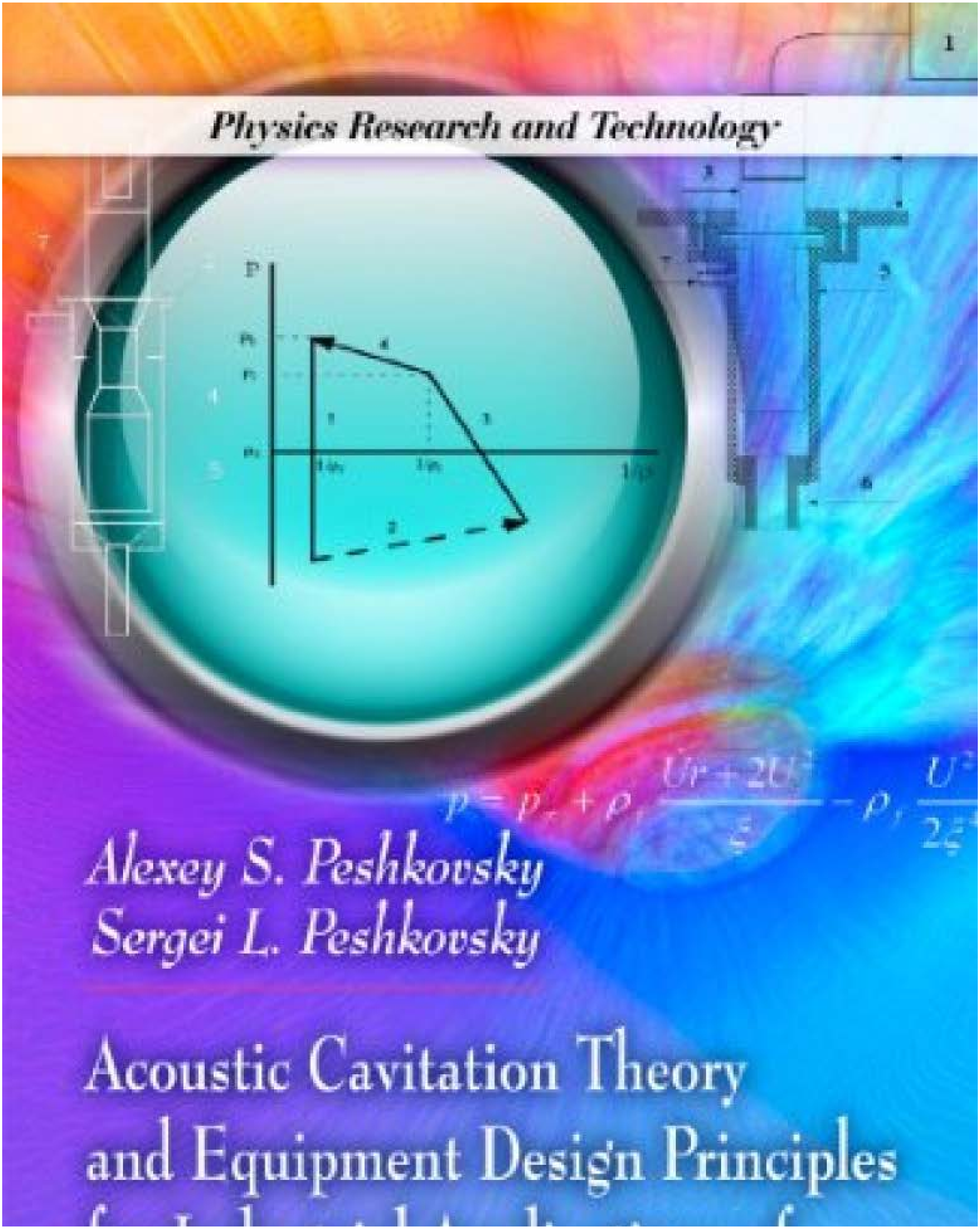
Physics Research and Technology
Alexey S. Peshkovsky
Sergei L. Peshkovsky
Acoustic Cavitation Theory
and Equipment Design Principles


for Industrial Applications of
High-Intensity Ultrasound
Novinka

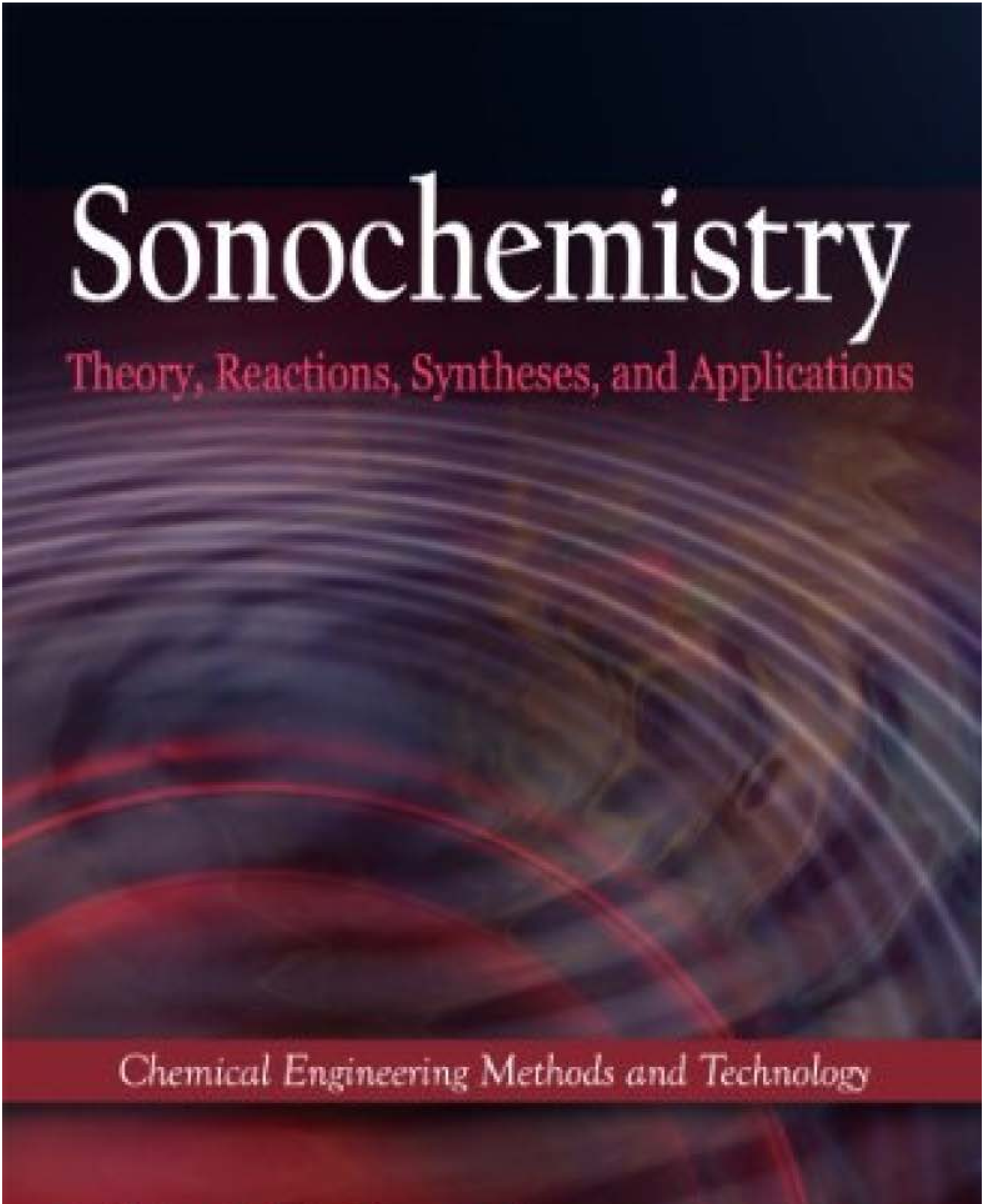
Sonochemistry
Theory, Reactions, Syntheses, and Applications
Chemical Engineering Methods and Technology

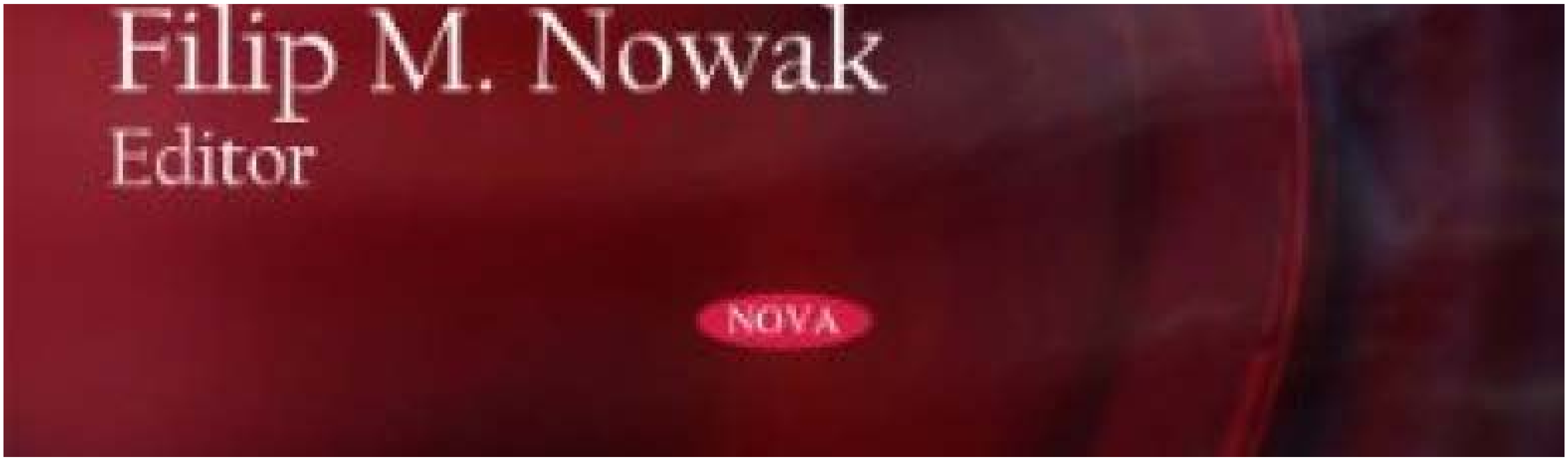
Filip M. Nowak
Editor
NOVA

Available online at www.sciencedirect.com

ScienceDirect

Ultrasonics Sonochemistry 15 (2008) 618–628

Ultrasonics SONOCHEMISTRY

www.elsevier.com/locate/ultsonch

Shock-wave model of acoustic cavitation

Sergei L. Peshkovsky, Alexey S. Peshkovsky *

Industrial Sonomechanics, LLC, 1505 St. Nicholas Ave., Suite 5B, New York, NY 10033, USA

Received 8 December 2006; received in revised form 5 July 2007; accepted 22 July 2007
Available online 7 August 2007

Abstract

Shock-wave model of liquid cavitation due to an acoustic wave was developed, showing how the primary energy of an acoustic radiator is absorbed in the cavitation region owing to the formation of spherical shock-waves inside each gas bubble. The model is based on the concept of a hypothetical spatial wave moving through the cavitation region. It permits using the classical system of Rankine–Hugoniot equations to calculate the total energy absorbed in the cavitation region. Additionally, the model makes it possible to explain some newly discovered properties of acoustic cavitation that occur at extremely high oscillatory velocities of the radiators, at which the mode of bubble oscillation changes and the bubble behavior approaches that of an empty Rayleigh cavity. Experimental verification of the proposed model was conducted using an acoustic calorimeter with a set of barbell horns. The maximum amplitude of the oscillatory velocity of the horns' radiating surfaces was 17 m/s. Static pressure in the calorimeter was varied in the range from 1 to 5 bars. The experimental data and the results of the calculations according to the proposed model were in good agreement. Simple algebraic expressions that follow from the model can be used for engineering calculations of the energy parameters of the ultrasonic radiators used in sonochemical reactors.

PACS: 43.35+d

Keywords: Acoustic cavitation; Acoustic wave; Cavitation bubble; Shock-wave; Shock-wave theory; Acoustic horn; Ultrasonic cavitation; Ultrasonic radiator; Ultrasonics

1. Introduction

In the design and calculation of powerful ultrasonic sources for sonochemical reactors, it is necessary to know the exact value of the intensity of the acoustic energy radiated into the working liquid. This information is usually obtained experimentally because no adequate physical model of acoustic cavitation that would allow one to obtain such data through calculation so far exists. The development of an adequate model of acoustic cavitation, although of great importance, has in the past been severely restricted by considerable mathematical difficulties connected with the necessity of finding numerical solutions of nonlinear equations describing the cavitation region (the visible region of large cavitation bubble population) [1]. Direct analytical solutions of these equations in different approximations do not give practical results suitable for the design of ultrasonic equipment [2,3].

Current literature on acoustic cavitation mainly tends to involve numerical models of spatio-temporal characteristics of the cavitation region [4–6]. Large number of theoretical acoustic cavitation models has been developed along with the corresponding methods of numerical analysis of such models. Further computer simulation-based investigations of acoustic cavitation have also been proposed, involving complex nonlinear physicomathematical models and including many aspects of spatial movement of cavitation bubbles in an acoustic field, spatial distribution of the characteristics of these fields in a liquid, interaction between the bubbles themselves, properties of acoustical flow, etc. [7–10]. Water is most frequently used for the experimental verification of such theoretical models.

* Corresponding author. Tel.: +1 (646) 267 2890.
E-mail address: alexey@sonomechanics.com (A.S. Peshkovsky).

doi:10.1016/j.ultsonch.2007.07.006

Available online at www.sciencedirect.com
ScienceDirect
ELSEVIER
Ultrasonics Sonochemistry 14 (2007) 314–322
Ultrasonics SONOCHEMISTRY
www.elsevier.com/locate/ultsonch

Matching a transducer to water at cavitation: Acoustic horn design principles

Sergei L. Peshkovsky, Alexey S. Peshkovsky *

Industrial Sonomechanics, LLC, 1505 St. Nicholas Avenue #5B, New York, NY 10033, USA

Received 14 February 2006; received in revised form 6 June 2006; accepted 1 July 2006
Available online 14 August 2006

Abstract

High-power ultrasound for several decades has been an integral part of many industrial processes conducted in aqueous solutions. Maximizing the transfer efficiency of the acoustic energy between electromechanical transducers and water at cavitation is crucial when designing industrial ultrasonic reactors with large active volumes. This can be achieved by matching the acoustic impedances of transducers to water at cavitation using appropriately designed ultrasonic horns. In the present work, a set of criteria characterizing the matching capabilities of ultrasonic horns is developed. It is shown that none of the commonly used tapered-shape horns can achieve the necessary conditions. An analytical method for designing five-element acoustic horns with the desirable matching properties is introduced, and five novel types of such horns, most suitable for practical applications, are proposed. An evaluation of the horns' performance is presented in a set of experiments, demonstrating the validity of the developed theoretical methodology. Power transfer efficiency increase by almost an order of magnitude is shown to be possible with the presented horn designs, as compared to those traditionally utilized.

Keywords: Ultrasonic rod horns; Electromechanical transducers; Acoustic impedance matching; Ultrasonic power transference; Acoustic energy transference; Acoustic horns; Industrial ultrasonic reactors; Sonochemistry; Industrial processes in liquids; Cavitation

1. Introduction

High-power ultrasound for several decades has been an integral part of many industrial processes conducted in weak aqueous solutions, such as cleaning, extraction, homogenizing, emulsification, sonochemistry, pollutant destruction, etc. [1–3]. These ultrasound-aided (macrosonics) processes are based on the effect of acoustic cavitation induced in water during intensive ultrasonic treatment. The electromechanical transducers used to convert the high frequency electric power into the ultrasonic power cannot, however, directly provide the necessary amplitudes of longitudinal ultrasonic vibrations to induce cavitation. Acoustic rod horns connected to the transducers are, therefore, used to amplify the vibration amplitude. Commonly used acoustic horns have tapered shapes, such as conical, exponential, catenoidal, stepped, or more complex, and converge in the direction of the loads [3–5]. Although widely used, these horns suffer from an important limitation: they are incapable of providing matching between the transducers and the liquid loads, leading to an inefficient acoustic power transmission.

It is well known that for an optimal operation of an ultrasonic horn system, the maximum cross-sectional dimension of any portion of the resonant horn or transducer cannot exceed, approximately, a quarter-wavelength of the corresponding longitudinal acoustic wave at the horn's resonance frequency [6]. Consequently, a convergent horn with a maximal allowed base-width always ends up having a working tip dimension that is smaller than this limitation. The final size of the tip depends on the gain factor of the horn, and becomes reduced as the gain factor

* Corresponding author.

E-mail address: alexey@sonomechanics.com (A.S. Peshkovsky).

increases. This is problematic when the abovementioned

doi:10.1016/j.ultsonch.2006.07.003

Available online at www.sciencedirect.com
ScienceDirect
Ultrasonics Sonochemistry 15 (2008) 618–628
Ultrasonics SONOCHEMISTRY
www.elsevier.com/locate/ultsonch

Shock-wave model of acoustic cavitation

Sergei L. Peshkovsky, Alexey S. Peshkovsky *

Industrial Sonomechanics, LLC, 1505 St. Nicholas Ave., Suite 5B, New York, NY 10033, USA

Received 8 December 2006; received in revised form 5 July 2007; accepted 22 July 2007
Available online 7 August 2007

Abstract

Shock-wave model of liquid cavitation due to an acoustic wave was developed, showing how the primary energy of an acoustic radiator is absorbed in the cavitation region owing to the formation of spherical shock-waves inside each gas bubble. The model is based on the concept of a hypothetical spatial wave moving through the cavitation region. It permits using the classical system of Rankine–Hugoniot equations to calculate the total energy absorbed in the cavitation region. Additionally, the model makes it possible to explain some newly discovered properties of acoustic cavitation that occur at extremely high oscillatory velocities of the radiators, at which the mode of bubble oscillation changes and the bubble behavior approaches that of an empty Rayleigh cavity. Experimental verification of the proposed model was conducted using an acoustic calorimeter with a set of barbell horns. The maximum amplitude of the oscillatory velocity of the horns' radiating surfaces was 17 m/s. Static pressure in the calorimeter was varied in the range from 1 to 5 bars. The experimental data and the results of the calculations according to the proposed model were in good agreement. Simple algebraic expressions that follow from the model can be used for engineering calculations of the energy parameters of the ultrasonic radiators used in sonochemical reactors.

PACS: 43.35+d

Keywords: Acoustic cavitation; Acoustic wave; Cavitation bubble; Shock-wave; Shock-wave theory; Acoustic horn; Ultrasonic cavitation; Ultrasonic radiator; Ultrasonics

1. Introduction

In the design and calculation of powerful ultrasonic sources for sonochemical reactors, it is necessary to know the exact value of the intensity of the acoustic energy radiated into the working liquid. This information is usually obtained experimentally because no adequate physical model of acoustic cavitation that would allow one to obtain such data through calculation so far exists. The development of an adequate model of acoustic cavitation, although of great importance, has in the past been severely restricted by considerable mathematical difficulties connected with the necessity of finding numerical solutions of nonlinear equations describing the cavitation region (the visible region of large cavitation bubble population) [1]. Direct analytical solutions of these equations in different approximations do not give practical results suitable for the design of ultrasonic equipment [2,3].

Current literature on acoustic cavitation mainly tends to involve numerical models of spatio-temporal characteristics of the cavitation region [4–6]. Large number of theoretical acoustic cavitation models has been developed along with the corresponding methods of numerical analysis of such models. Further computer simulation-based investigations of acoustic cavitation have also been proposed, involving complex nonlinear physicomathematical models and including many aspects of spatial movement of cavitation bubbles in an acoustic field, spatial distribution of the characteristics of these fields in a liquid, interaction between the bubbles themselves, properties of acoustical flow, etc. [7–10]. Water is most frequently used for the experimental verification of such theoretical models.

* Corresponding author. Tel.: +1 (646) 267 2890.
E-mail address: alexey@sonomechanics.com (A.S. Peshkovsky).

1350-4177/$ - see front matter
doi:10.1016/j.ultsonch.2007.07.006

No adequate explanation of the mechanism by which dissipation of the primary acoustic energy of a radiator occurs in a liquid at cavitation is, however, available from the literature. Additionally, no theoretical method permitting to calculate this energy in a manner adequate to the available experimental data currently exists. Meanwhile, the exact knowledge of the mechanisms by which the heating of a liquid in the presence of a cavitation-inducing acoustic wave occurs is quite important not only for the understanding of the related sonochemical processes, but also for the practical design parameter calculations that would permit constructing improved high-capacity ultrasonic radiators and reactors.

1.1. Visual observations of acoustic cavitation

Several authors provided common [11], high-speed [12] and stereoscopic high-speed [13] photographs of the cavitation region, obtained in the presence of relatively low-intensity acoustic fields. At these conditions, the cavitation region is located some distance away from the radiating surface and has a typical pattern similar to that of an electrical discharge.

Photographs of the cavitation region formed by powerful ultrasonic radiators have also been provided [14,15]. The diameters of the radiating surfaces of the radiators were greater than the sound wavelengths in the given liquid at the working frequencies. In these cases, plane acoustic waves are radiated into the liquid. The photographs show that at relatively low acoustic radiation intensity, the cavitation region is also located some distance away from the radiating surface, has an irregular pattern and is composed of thread-like collection of cavitation bubbles. As the radiation intensity goes up, however, the cavitation region approaches the radiating surface and grows in size. When the intensity reaches the value of, approximately, 1.5 W/cm^2, the cavitation region "sits" on the radiating surface and its shape becomes regular, resembling an upside-down circular cone. The so-called "cone bubble structure" begins to form. Further radiation intensity increases have little effect on the shape and position of the cone bubble structure. The photographs in the abovementioned studies show that at high radiation intensity the cone bubble structure is in contact with the radiating surface. Ref. [16] provides photographs of the radiating surface of a metal radiator which was utilized for a period of time to create high-intensity cavitation in a liquid. The surface of the radiator contains clear traces of metal degradation due to cavitation.

Therefore, it can be concluded with certainty that at high radiation intensities, acoustic cavitation starts at the surface of the acoustic radiator. This location in the liquid is known, according to theory, to have the lowest value of tensile strength due to the constant presence of adsorbed gas inclusions at the metal surface [2].

However, at low radiation intensities just above the cavitation threshold, the cavitation region in always formed at a significant distance away from the radiating surface, which contradicts the abovementioned theory. Clearly, the tensile strength of the liquid at any location away from the metal surface should be higher than near it, since the concentration of the preexisting bubbles (inceptions) that "weaken" the liquid at that location should diminish with time.

1.2. Justification for the shock-wave approach

At low radiation intensity, harmonic acoustic wave is not yet capable of inducing cavitation even at the weakest location in the liquid near the radiating surface. Formation of cavitation away from the radiating surface in this case can be explained by the effect of the increase of the planar acoustic wave front steepness during its propagation through a liquid. As a result of such increase, at some location in the liquid a discontinuity in the wave profile is formed. Since such discontinuity is physically not possible in a continuous media, a shock-wave with a steep front is formed as a result. This effect has to do with the acoustic radiation-induced nonlinearity of the compressible media properties and is very well known and documented [17].

This explanation, however, seems contradictory to the common shock-wave theory, since the attainable amplitude of vibration velocity of the radiating surface is always much lower than the speed of sound in the pure liquid and, therefore, the necessary conditions for the creation of such a discontinuity in the wave profile are not fulfilled. The explanation may, nevertheless, still be valid due to the following two considerations. It is well known that during propagation of an acoustic wave of slightly lower intensity than the cavitation threshold, an ensemble of tiny bubbles is formed in the liquid. This occurs due to the so-called "rectified diffusion" [2]. It is also well known that the speed of sound in a liquid containing gas bubbles is significantly lower than that in a pure liquid [18,19], and, under certain conditions, it may become similar to the amplitude of vibration velocity of the radiating surface.

It may, therefore, be considered that the bubbles formed in an acoustic wave due to rectified diffusion help forming a discontinuity in the profile of the acoustic wave at a location away from the radiating surface by significantly lowering the sound speed in the liquid. Further, at the location of the discontinuity in the acoustic wave, these tiny bubbles begin to undergo such rapid nonlinear movements that they loose dynamic stability and, consequentially, rapidly multiply forming the cavitation region.

The abovementioned observations and analysis formed the basis of the shock-wave model of acoustic cavitation described in this work. The model shows how the primary energy of an acoustic radiator causing the cavitation of liquid is absorbed in the cavitation region owing to the formation of spherical shock-waves inside each cavitation bubble. Calculation of the total energy absorbed in the cavitation region using the concept of a hypothetical spatial wave moving through the cavitation region is possible with this model using the classical system of the Rankine–

Hugoniot equations. Additionally, the proposed model makes it possible to explain some newly discovered properties of acoustic cavitation of water that occur at extremely high oscillatory velocities of the radiating surfaces.

2. Theory

Let us assume that an acoustic radiator emitting a plane-wave is used to generate cavitation in a liquid. The diameter of the radiator's output surface is comparable with the length of the acoustic wave in the liquid at the given frequency of vibrations. The frequency of the acoustic radiator vibrations should be considered to be much lower than the resonance frequency of the cavitation bubbles. We assume that the liquid always contains an equilibrium concentration of dissolved gas as well as some cavitation nuclei (tiny spherical bubbles filled with the gas) and, consequentially, the liquid possesses no tensile strength during rarefaction caused by the acoustic waves. As, for example, is indicated in Ref. [2], water that has not been purified of gas inclusions ruptures at the negative acoustic pressure of, approximately, 1 bar. The density of the liquid with the tiny cavitation nuclei is taken to be equal to the density of the pure liquid, ρ_f. Surface tension of the liquid and the presence of stable (non-cavitational) gas bubbles are neglected. Thus, within the framework of the model, only the so-called low-frequency transient gas cavitation is considered. We, additionally, assume the liquid to be non-viscous, non-compressible and non-volatile.

Let us represent acoustic cavitation in the liquid as a sequence of the following events. When an acoustic rarefaction wave of certain amplitude passes through a volume of the liquid, an explosive growth of cavitation nuclei occurs, leading to the formation of the gas-filled cavitation bubbles. Possible parameters of such rarefaction wave are described, for example, in [20]. A mixture of the spherical bubbles and the liquid is, therefore, formed. The gas dissolved in the volume of the liquid passes inside the free space formed by the bubbles. The density of the liquid, therefore, drops. At this point, the bubbles are so small, as compared with the acoustic wavelength, that the liquid/bubble mixture can be considered a continuous medium. The rarefaction wave phase is followed by a compression wave phase, whose passage results in a collapse of all gas bubbles, restoring the density of the liquid to ρ_f. The reverse diffusion of the gas back into the liquid during compression is insignificant and should be ignored. This particular stage of acoustic cavitation completes the total cavitation cycle and is further considered here in great detail, since it is this stage that is mainly responsible for the sonochemical effects of acoustic cavitation.

2.1. Oscillations of a single gas bubble

The problem of the liquid motion during the compression of an empty spherical bubble in liquid was solved by Rayleigh (see reviews [2,3]). On the basis of this solution and Ref. [17], the instantaneous pressure distribution in the liquid can be written as

$$p = p_\infty + \rho_f \frac{\dot{U}r + 2U^2}{\xi} - \rho_f \frac{U^2}{2\xi^4}. \tag{1}$$

Here, p_∞ is the pressure in the liquid at infinity, U is the velocity of the bubble boundary (wall), $\xi = R/r$, r is the current bubble radius, and R is the current radial coordinate. For the boundary of a gas-filled bubble at $\xi = 1$, the following equality must be met:

$$p_g = p_\infty + \rho_f\left(\dot{U}r + \frac{3}{2}U^2\right). \tag{2}$$

Here, p_g is the gas pressure in the bubble. This expression is the well-known Noltingk–Neppiras equation (see reviews [2,3]).

For an empty bubble, taking $p_g = 0$ and $p_\infty = p_0$, integration of Eq. (2) gives Rayleigh's equations for the velocity of the bubble wall movement and the time of the bubble collapse:

$$\begin{aligned} u^2 &= \frac{2p_0}{3\rho_f}\left(\frac{r_{in}^3}{r^3} - 1\right), \\ \tau &= 0.915 r_{in}\left(\frac{\rho_f}{p_0}\right)^{0.5}. \end{aligned} \tag{3}$$

Here, p_0 is the static pressure, and r_{in} is the initial bubble radius.

From Eqs. (1) and (2), an expression for the instantaneous distribution of the pressure in liquid during the compression of a gas-filled bubble can be obtained:

$$p = p_\infty\left(1 - \frac{1}{\xi}\right) + \frac{p_g}{\xi} + \frac{\rho_f U^2}{2}\left(\frac{1}{\xi} - \frac{1}{\xi^4}\right). \tag{4}$$

Let us single out a spherical liquid volume that includes a gas bubble. The gas bubble/surrounding liquid system has a certain acoustic compressibility, which determines the velocity of the propagation of small perturbations or the velocity of sound in this volume. Using the linearized form of the Noltingk–Neppiras equation, one can obtain an expression for the velocity of sound in such a system, as it was done, for example, in the work [18]. The velocity of sound, with the abovementioned assumptions taken into account, is determined using the following expression:

$$c = \left(\frac{p_g}{\rho_f \alpha(1-\alpha)}\right)^{0.5}. \tag{5}$$

Here, α is the volumetric gas concentration in the singled-out liquid volume that includes a gas bubble. From Eq. (5) it can be seen that the velocity of sound at a given gas pressure in the bubble has a minimum at $\alpha = 0.5$. For example, at $p_g = 1$ bar the minimum velocity of sound $c_{min} = 20$ m/s. It should also be noted that the velocity of sound in the range $0.4 < \alpha < 0.6$ changes little.

A gas bubble is formed during the half-period of the liquid rarefaction in the acoustic wave. Under the abovementioned assumptions, this occurs at the moment when the pressure in the liquid near the wall of a cavitation nucleus decreases to zero, i.e. the negative acoustic pressure is equal to p_0. At that point, the gas pressure in the formed bubble is also very small. Further, during the subsequent period of increase in the acoustic pressure, the bubble is compressed, and the gas pressure in it also increases. During the subsequent compression half-period, in the singled-out liquid volume near the gas bubble wall a spherical flow in the direction of the bubble center is formed, which is described by Eq. (4). From Eq. (5) it is seen that the velocity of sound for the singled-out system gas bubble/surrounding liquid depends on the gas pressure in the bubble p_g and the value of coordinate ξ, along which the boundary of the singled-out volume passes. If we start reducing the singled-out volume, while the radius of the bubble and the gas pressure in it are constant, the velocity of sound in this system will fall to a certain limit and then will grow again. This means that in the considered spherical volume near the moving wall of the bubble, there is a critical spherical region, where the sound velocity, $c_{\min}$, is at the minimum at a given gas pressure in the bubble, p_g. The position of this region is determined from the condition $0.4 < \alpha < 0.6$. It is located close to the bubble wall in the coordinate range $1.18 < \xi < 1.35$. For the simplicity of further analysis of Eq. (4), it is taken that the velocity of the flow of the liquid particles in the critical region is equal to the velocity of the bubble wall movement, U.

In the model being considered, it is assumed that when the gas bubble/surrounding liquid system is compressed by the external pressure, p_∞, the velocity of the flow of the liquid particles in the critical region near the bubble wall increases to such a degree that at a certain gas pressure in the bubble, p_g, it reaches the minimum velocity of sound in the system under consideration, i.e. $U = c_{\min}$.

At a ratio of the initial radius of an empty bubble to its current radius, $r_{in}/r = 2$, and static pressure, $p_0 = 1$ bar, the value of $U \approx 21$ m/s reached according to Eq. (3) is indeed close to $c_{\min} = 20$ m/s.

Let us represent the pressure at infinity as a sum of the static and the acoustic (excessive) pressures, $p_\infty = p_0 + p'_\infty$ and transform Eq. (4) taking into account that $U = c_{\min}$:

$$p = (p_0 + p'_\infty)\left(1 - \frac{1}{\xi}\right) + \frac{p_g}{\xi} + 2p_g\left(\frac{1}{\xi} - \frac{1}{\xi^4}\right). \tag{6}$$

This expression describes the extreme condition of equilibrium of the system. Eq. (6) shows that during compression of the flowing liquid, in the vicinity of the gas bubble a pressure impulse is formed, which is stationary with respect to the bubble wall. The amplitude of the excess pressure in this impulse is $p - p_0 = 1.4p_g + 0.5\delta p'_\infty$, where $\delta p'_\infty = (p'_\infty - p_0)$. This value is reached at the coordinate $\xi \approx 2$ located upstream from the critical region. As we show below, the quantity, $\delta p'_\infty$, does not need to be considered for small oscillation velocities of acoustic radiators.

When the velocity of the bubble wall motion exceeds the minimum velocity of sound, $U > c_{\min}$, the equilibrium state described by Eq. (6) becomes destroyed, and the pressure in the liquid at the bubble wall downstream from the critical region decreases to p_0. The velocity of the bubble wall movement also reduces because the driving pressure difference decreases. At the same moment, the excessive pressure amplitude in the impulse increases stepwise up to the value $p - p_0 = 1.4p_0 + 0.5\delta p'_\infty$, since the boundary condition in Eq. (2) is changed and the pressure near the bubble wall becomes $p_g = p_0$. This occurs because the bubble pressure signal does not penetrate upstream from the bubble wall when $U > c_{\min}$.

Due to destruction of the dynamic equilibrium (retardation of a part of the flow), the pressure impulse located in the liquid upstream from the critical section disintegrates and begins to move relative to the bubble boundary in the form of a converging spherical wave. The supposed instantaneous distribution of excessive pressure in the impulse near the gas bubble wall at $U = c_{\min}$ is shown in Fig. 1.

Phenomena similar in essence are observed during the breakup of arbitrary pressure discontinuity in a gas, during hydraulic impact, and during the flow of gases and gas–liquid mixtures through nozzles. See, for example, the works [5,6], as well as the studies on Laval nozzles and water hammers.

In accordance with the assumed form of pressure distribution in a converging spherical wave shown in Fig. 1, the excessive pressure at the bubble wall first increases smoothly up to the value of $p - p_0 = 1.4p_g + 0.5\delta p'_\infty$, and, accordingly, the gas pressure inside the bubble increases smoothly (isothermally) as well. Then, when an abrupt excess pressure jump (up to the value of $p - p_0 = 1.4p_0 + 0.5\delta p'_\infty$) approaches the bubble wall, a spherical shock-wave is formed in the gas inside the bubble. The pressure jump itself, evidently, is equal to $1.4(p_0 - p_g)$. After focusing in the center of the gas bubble, the spherical shock-wave is reflected, and the bubble "explodes" from the

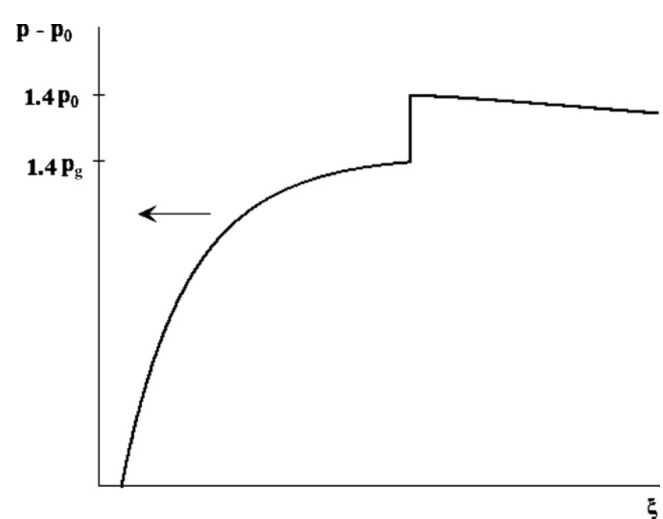

Fig. 1. Instantaneous distribution of the excessive pressure in the liquid near the cavitation bubble wall at $U > c_{\min}$ is shown. The quantity $\delta p'_\infty$ is not taken into account.

inside, breaking up into small fragments. The collapse of the gas bubble or, more precisely, its shock destruction occurs. Gas pressure and temperature inside the bubble during the focusing and the subsequent reflection of the shock-wave reach very large, albeit theoretically restricted, values [17]. When the collapse of the gas bubble is completed, its small fragments are left in the singled-out liquid volume, which are equal in size to the original cavitation nuclei, and the density of the singled-out liquid volume becomes close to the initial liquid density, ρ_f. As we show below, when the oscillation velocities of the ultrasonic radiators reach very high values, cavitation may follow a different mechanism, which does not involve breaking the gas bubbles up into small fragments, but rather exhibits bubble behavior approaching that of an empty Rayleigh cavity.

This approach permits easily eliminating a seemingly clear contradiction that follows from the Noltingk–Neppiras equation: how can a gas-filled bubble implode with a very high rate if the gas pressure inside the bubble during compression rapidly increases, while the rate of the gas diffusion from the bubble, according to [2,3], is negligible. In the proposed model, the gas bubble does not implode in the literal sense of the word, but is destroyed by a spherical shock-wave reflected after focusing in its center. The presence of a well-known phenomena accompanying acoustic cavitation, such as sonoluminescence, erosion and dispersion of solids, emulsification of liquids, etcetera, can be well explained from this point of view. Additionally, the mechanism of the dissipation of the primary acoustic energy during the liquid cavitation becomes clear. This is the mechanism of the heating of a compressible medium in a shock-wave, which is well described in the literature (see, for example, [17]).

2.2. Cavitation region

During the rarefaction of a liquid in an acoustic wave, a mixture of a great number of spherical gas bubbles with the liquid (cavitation region) is formed. Let us call this gas–liquid mixture present in the cavitation region, the "continuum". In the previous section, the course of events during the collapse of a single bubble in some small volume of liquid was described. To extend these events over the entire continuum, a transition to spatial description is necessary. At that, the results of this transition must depend neither on the dimensions and the form of the continuum itself nor on the sizes and the spatial distribution of the bubbles in it.

During the compression stage, an acoustic radiator creates a pressure impulse in the liquid beyond the continuum in the form of a plane acoustic wave. Since the velocity of sound in the continuum is finite, the collapse of a multitude of gas bubbles located arbitrarily in the continuum must also occur simultaneously only in some narrow layer, as the impulse of the acoustic pressure approaches it, i.e. it must have a wave character. In the current model representation, the result of the superposition of many spherical shock-waves, which are formed near each gas bubble during its collapse in a narrow layer of the continuum, is a spatial wave (SW) moving through the continuum. Such a representation is the most exact and visual way of extending the events occurring during a single gas bubble collapse, over the entire continuum.

In the real situation, the cavitation region in a liquid may take very complex, branched shapes. The spatial distribution of bubbles in the region also may be quite non-uniform and the sizes of the bubbles may vary. When the transition to the presented spatial description of cavitation is made, for the results to be independent of the shape of the cavitation region as well as of the spatial distribution and the sizes of the bubbles, in our fundamental equations we will further utilize hypothetical physical parameters related to the cavitation region as a whole. In other words, instead of operating with local values of density, changes in internal energy and so on, we will use the values averaged over the whole cavitation region. As demonstrated below, these values disappear when further modifications of the fundamental equations are made.

The experimental investigations of acoustic cavitation described below conducted for the verification of the presented model were carried out using calorimetry of the entire environment and, therefore, provide only the spatially averaged values due to a relatively high thermal conductivity of the liquid. Therefore, the final purpose of the calculations following this model is the determination of a cumulative value of the changes in the internal energy of the environment, as a result of acoustic cavitation.

The spatial wave (SW) described above has a bore wave-like character, however, the continuum density and pressure inside the SW front change stepwise. This occurs because the cavitation bubbles collapse inside its front, following the process outlined in Section 2.1. The presence of such a wave is the final stage of acoustic cavitation, within one cycle of the continuum rarefaction–compression. In other words, according to the model, it is assumed that the collapse of the gas bubbles occurs inside a relatively narrow front of a hypothetical SW, being formed and moving through the continuum in each compression half-period of an acoustic radiator.

The width of the SW front, inside which the collapse of the bubbles and the change of the continuum density occur, can be estimated as the product of the empty bubble collapse time, according to Eq. (3) and the wave front movement velocity with respect to the continuum, $h = c\tau$. A rough estimate for the wave front movement velocity can be made using expression (5). Then, at $\alpha = 0.1$ (taken from the literature data [20] and characteristic for the initial stage of acoustic cavitation) we obtain $h \approx 3r_{in}$. According to the estimation performed in the work [2], the maximum radius of a gas bubble in water does not exceed 2×10^{-4} m, since larger bubbles rapidly rise to the surface. Hence, the value is: $h \leqslant 6 \times 10^{-4}$ m, which is smaller than the dimensions of the continuum itself by many orders of magnitude. Thus, the specified wave has a front that is very narrow relative to the dimensions of the entire continuum. Getting over this barrier, therefore, the physical parameters of the continuum change stepwise.

It is necessary, further, to establish a relation between the continuum parameters ahead of and behind the SW front, as well as the relationship between these parameters and the oscillatory velocity of an acoustic radiator. It is important to note that the velocity of the specified wave can be lower than the velocity of sound in the continuum.

The SW moving through the continuum is not only a physical abstraction used for the construction of the model, but can, apparently, exists in reality. In this case, however, we are not faced with an ordinary shock-wave, which arises in a compressible continuum when the piston movement velocity is higher than the sound velocity in the continuum. Such shock-waves in a gas–liquid suspension obtained by bubbling a gas through a liquid are described in detail in literature [18]. Here, it is assumed that in a gas–liquid suspension formed as a result of the liquid rarefaction in an acoustic wave, another type of bore wave-like shock-waves may exist, which is associated with the radial movement of the liquid in the vicinity of each bubble.

It is well known that when a jump (discontinuity) of a physical quantity arises in a compressible continuum, a solution should be sought using the general conservation laws in the form of the Rankine–Hugoniot equations [17]. These equations reflect the ratios of the steady-state physical parameters of the compressible continuum before and after the passage of the shock-wave front. Additionally, there appears a possibility to analytically calculate the values of important parameters, without considering in detail the transient processes inside the SW front, which are connected with the complex kinetics of a collapsing gas bubble.

Let us introduce the following designations: p_h is the pressure in the liquid phase of the continuum near the bubble wall after the SW passage; p_l, $\rho_l = \rho_f(1 - \alpha_l)$, α_l are, respectively, the pressure in the liquid phase of the continuum near the bubble wall, the density and the volumetric gas content of the continuum before the SW passage. A scheme of the continuum flow is presented in Fig. 2. It is assumed that a SW moves through the continuum, and that the gas bubbles collapse inside the narrow front of this wave. Also shown in this figure is the supposed pressure profile in the continuum.

Fig. 3 shows the supposed processes occurring in one cycle of the acoustic cavitation of liquid. The pressure in the liquid phase of the continuum near the gas bubble wall in an arbitrary state is plotted on the ordinate, and the continuum specific volume is plotted on the abscissa. Line 1 represents the rarefaction of the continuum with cavitation nuclei in an acoustic wave. Line 2 represents a nonlinear process of the growth of cavitation bubbles in the rarefaction wave. Line 3 represents a preliminary compression of the continuum in an acoustic wave (for a single gas bubble, this corresponds to a rise in the gas pressure in the bubble on the smooth section of a converging spherical wave, as described in Section 2.1). Line 4 represents the continuum's transition from one state to the other when the SW passes (for a single gas bubble, this corresponds to a rise in the gas pressure in the bubble on the steep section of a converging spherical wave, as described in Section 2.1). In this scheme, it is assumed in advance that the velocity of the SW movement through the continuum can be lower than the sound velocity in the continuum itself ahead of SW. Additionally, the SW front itself serves as a source of the acoustic wave, propagating forward in the direction of the shock-wave movement. In this connection, there is a preliminary compression of the continuum, and line 4 begins above the abscissa axis.

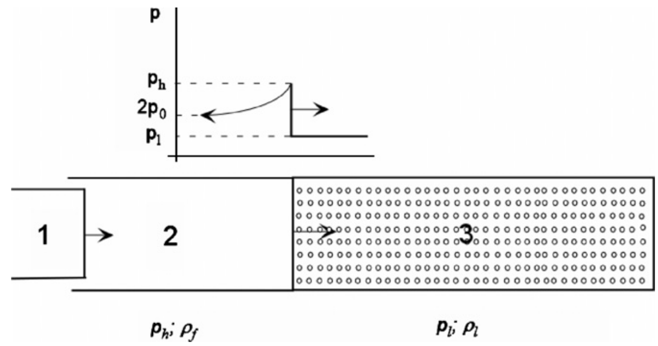

Fig. 2. Schematic of the continuum's flow during compression is shown (1 – acoustic radiator, 2 – flow region after the SW passage, 3 – flow region before the SW passage).

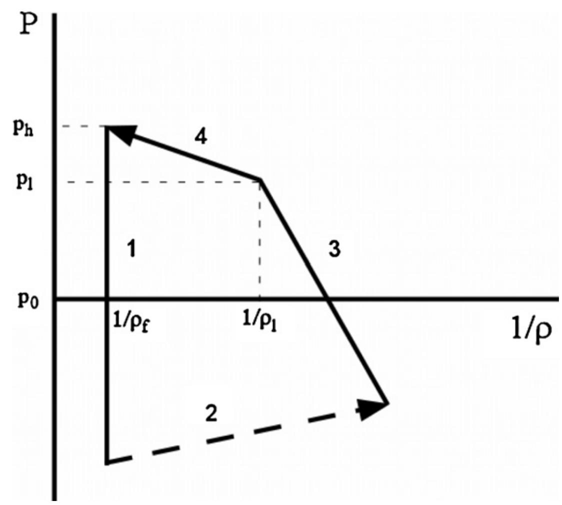

Fig. 3. Processes occurring during acoustic cavitation are illustrated. Line 1 represents the rarefaction of the continuum with cavitation nuclei in an acoustic wave, line 2 represents a nonlinear process of the growth of cavitation bubbles in the rarefaction wave, line 3 represents a preliminary compression of the continuum in an acoustic precursor wave, line 4 represents the continuum transition from one state to the other when the SW passes.

This kind of an acoustic wave is called a precursor. The precursor does not cause the collapse and disintegration of the bubbles because of a small value of its amplitude. Similar representations are used for initially loose or porous environment. In such environment, during the compression phase, the shock-wave front is formed only due to the parameters of the compression process itself since this environment tends to change the specific volume of pores (cavities) abruptly (stepwise) under pressure [22–24].

Let us introduce the following additional designations: $p_\mathrm{l} = p_0 + p'_\mathrm{l}, p_\mathrm{h} = p_0 + p'_\mathrm{h}$; p'_l and p'_h are the excessive pressures in the liquid phase of the continuum near the bubble wall before and after the SW passage, respectively; u_l and u_h are the continuum flow velocities relative to SW before and after its passage, respectively; e_l and e_h are the specific internal energy of the continuum before and after the SW passage, respectively; v is the current oscillatory velocity of an acoustic radiator; v_t is the critical oscillatory velocity of an acoustic radiator, which corresponds to the cavitation onset (cavitation threshold). Note that a stepwise increase in the continuum density from ρ_l to ρ_f at the SW front corresponds to a change in pressure from p_l to p_h. The relative movement of the liquid and the gas bubbles is neglected.

Let us now write the system of conservation equations (Rankine–Hugoniot equations) for the continuum parameters on both sides of the SW front:

$$\begin{aligned}
&\rho_\mathrm{l} u_\mathrm{l} = \rho_\mathrm{f} u_\mathrm{h},\\
&p'_\mathrm{l} + \rho_\mathrm{l} u_\mathrm{l}^2 = p'_\mathrm{h} + \rho_\mathrm{f} u_\mathrm{h}^2,\\
&\frac{p_0 + p'_\mathrm{l}}{\rho_\mathrm{l}} + \frac{u_\mathrm{l}^2}{2} + e_\mathrm{l} = \frac{p_0 + p'_\mathrm{h}}{\rho_\mathrm{f}} + \frac{u_\mathrm{h}^2}{2} + e_\mathrm{h},\\
&v - v_\mathrm{t} = u_\mathrm{l} - u_\mathrm{h}.
\end{aligned} \tag{7}$$

The fourth equation of system (7) shows that a change in the continuum's movement velocity getting over the SW front is equal to the excessive oscillatory velocity of an acoustic radiator, which exceeds the critical value, v_t.

This system of equations can be transformed to the following form:

$$\begin{aligned}
&I = \frac{(2p_0 + p'_\mathrm{l} + p'_\mathrm{h})}{2}(v - v_\mathrm{t}),\\
&\eta_\mathrm{l} = \frac{(v - v_\mathrm{t})^2}{p'_\mathrm{h} - p'_\mathrm{l}}.
\end{aligned} \tag{8}$$

Here, $I = (e_\mathrm{h} - e_\mathrm{l})\rho_\mathrm{f} u_\mathrm{h}$ is the flux density of the energy dissipated inside the SW as a consequence of the dissipation processes related to the bubble collapse and $\eta_\mathrm{l} = \alpha_\mathrm{l}/\rho_\mathrm{l}$ is the volume of all cavitation bubbles per unit mass of the liquid phase of the continuum before the SW passage.

The average flux density of the acoustic energy (acoustic energy intensity) absorbed in one acoustic wave period can be presented in the following way:

$$I_\mathrm{a} = \frac{\omega}{2\pi}\int_0^{\pi/\omega} |I\sin(\omega t)|\mathrm{d}t = I/\pi. \tag{9}$$

3. Setup of the equations for the experimental verification

To experimentally verify resulting Eq. (8), it is necessary to determine the values of p'_h, p'_l, η_l and v_t.

3.1. Small oscillatory velocities of acoustic radiator

From Eq. (6) and the analysis given in Section 2.1, it follows that the maximum excessive pressure at the SW front is equal to $p'_\mathrm{h} = 1.4p_0 + \delta p'_\infty$. As mentioned above, the liquid utilized for the construction of the theoretical model, does not possesses tensile strength during rarefaction. Consequentially, the explosive growth of the cavitation nuclei and their conversion into gas bubbles in the rarefaction wave takes place at the negative pressure equal to the static pressure, $p'_\infty = p_0$. It is possible to assume that for small oscillation velocities of the acoustic radiator near the cavitation threshold a symmetry of acoustic pressure amplitudes during the half-periods of compression and rarefaction is conserved. Consequentially, in this case, $\delta p'_\infty = 0$ and $p'_\mathrm{h} = 1.4p_0$. It will be shown below that for large radiator oscillatory velocities it is no longer possible to ignore the quantity $\delta p'_\infty$. Note that the value of $p'_\mathrm{h} \approx 1.4p_0$ actually corresponds to the threshold of water cavitation, at least, in its initial stage. This fact was experimentally established in [21].

Above, it was assumed that during the rarefaction of a liquid in an acoustic wave, all gas dissolved in a unit volume of the liquid passes into the bubbles formed in this volume. The oscillations of the gas bubbles before the onset of their collapse are isothermal, and the mass of the gas in them does not change. From the analysis of Eq. (6) given in Section 2.1, it follows that $p'_\mathrm{l} = 1.4p_\mathrm{g}$, hence, the condition $p_0\eta_0 = 0.71p'_\mathrm{l}\eta_\mathrm{l}$ must be met. Here, η_0 is the equilibrium volume of gas dissolved in a unit mass of the liquid at the pressure, p_0.

The quantity v_t is the critical oscillatory velocity of an acoustic radiator, which corresponds to the cavitation threshold. In view of the conditions described above, one can assume that for a plane acoustic wave, $(v_\mathrm{t})_\mathrm{rms} = 0.71p'_\infty/\rho_\mathrm{f}c_\mathrm{f} = 0.71p_0/\rho_\mathrm{f}c_\mathrm{f}$.

It should be borne in mind that the value of v_t in each particular experimental case can be different from the specified theoretical value. This is connected with the fact that the practical value of v_t depends on a large number of different parameters of liquid (physical nature, purity degree, gas content, volatility, sample preparation history, etc.). Besides, v_t also depends on the conditions of the conducted measurements (frequency of ultrasound, degree of isolation from external radiation, temperature, etc.).

From the second equation of system (8) we obtain:

$$p'_\mathrm{l} = \frac{1.4p_0^2\eta_0}{\eta_0 p_0 + 1.42(v - v_\mathrm{t})^2_\mathrm{rms}}. \tag{10}$$

Now from the first equation of system (8) in view of Eqs. (9) and (10) we obtain the final equation for the average flux density of the acoustic energy (intensity of acoustic energy) absorbed in the cavitation region:

$$I_\mathrm{a} = 0.76p_0\left[1 + \frac{0.41p_0\eta_0}{\eta_0 p_0 + 1.42(v - v_\mathrm{t})^2_\mathrm{rms}}\right](v - v_\mathrm{t})_\mathrm{rms}. \tag{11}$$

For the initial stage of acoustic cavitation, at a small value of $(v - v_t)_{\rm rms}$, the final equation is as follows:

$$\frac{I_a}{p_0} = 1.07(v - v_t)_{\rm rms}. \tag{12}$$

It is important to point out that in Eqs. (11) and (12) the quantities related to the spatial distribution of gas bubbles in the continuum and their size, as well as the form and shape of the continuum itself are not present.

3.2. High oscillatory velocities of acoustic radiator

From the main system of Eq. (7), one can obtain the expression for the SW velocity relative to the unperturbed continuum, $u_l = [(p'_h - p'_l)/\rho_f\alpha(1-\alpha)]^{0.5}$. The ratio of u_l to the sound velocity, c, in the continuum according to Eq. (5), using Eq. (10) and taking into account that $p_g = 0.71p'_l$, can be written as

$$\frac{u_l}{c} = \left(\frac{p'_h - p'_l}{p_g}\right)^{0.5} = \left(\frac{2(v - v_t)^2_{\rm rms}}{p_0\eta_0}\right)^{0.5}. \tag{13}$$

From this expression, it is seen that at $(v - v_t)_{\rm rms} \geqslant 1$ m/s, the SW movement must become supersonic, making it a real shock-wave in the classical sense. When the SW movement is supersonic, a precursor is absent because it is absorbed by the faster shock-wave. The density and the pressure of the gas inside the bubbles in this case are initially small since they are not compressed beforehand by the precursor. From the analysis of Eq. (10), it is seen that at $(v - v_t)_{\rm rms} > 3$ m/s the gas pressure in such bubbles becomes approximately an order of magnitude lower than the static pressure, p_0, and continues to decrease. A spherical shock-wave in rarefied gas inside such a bubble is not formed and, accordingly, the bubble does not break up into small fragments as a result of the collapse. The behavior of the bubble becomes close to the behavior of an empty Rayleigh cavity.

It is also important to keep in mind that the minimum width of the shock-wave front in a gas is on the order of the molecule free path [17]. At a normal density of the gas, this distance is about 10^{-7} m. With a decreasing gas density, this distance increases proportionally and becomes close to the characteristic size of the bubble itself 10^{-5} m. Under these conditions, a spherical shock-wave inside the bubble cannot be formed, and the bubble is compressed like a Rayleigh cavity.

At the final stage of the collapse of the bubble, the gas pressure in it increases to such a degree that it can hold back the liquid's pressure. At that, the pressure and temperature of the compressed gas can reach very high values (theoretically unrestricted under the assumptions of this model [17]). In this case, at the excess pressure, $p'_h = 1.4p_0$, the continuum behind the SW is a gas–liquid suspension with some density $\rho_h = \rho_f(1 - \alpha_h)$. If the conditions identified in the beginning of Section 2, assumed for the construction of the model, are to be met, the continuum behind the front of SW is additionally compressed by the acoustic radiator until density ρ_f is reached. This corresponds to a pressure increase at the SW front up to the value of $p'_h = 1.4p_0 + \delta p'_\infty = 1.4p_0 + 0.5c_h^2\delta\rho = 1.4p_0 + 0.5c_h^2\rho_f\alpha_h$, where $\delta\rho = \rho_f - \rho_h = \rho_f\alpha_h$ is the additional increase in the continuum's density behind the SW front, necessary to reach the quantity ρ_f, and c_h is the speed of sound in the gas–liquid suspension with density ρ_h. For high oscillatory velocities of acoustic radiator similar to the sound speed in the continuum, $p'_h = 1.4p_0 + \rho_f\alpha_h v^2_{\rm rms}$, since in this case it can be taken that $c^2 = 2v^2_{\rm rms}$.

The value of v_t is neglected. Since $\delta p'_\infty$ should be taken into account only at high v and the second term of Eq. (11), which corresponds to the excessive pressure p'_l, is negligible, we leave it unchanged. Let us now write Eq. (11) in the final form in view of Eq. (9):

$$I_a = 0.76p_0\left[1 + \frac{0.41\eta_0 p_0}{\eta_0 p_0 + 1.42(v - v_t)^2_{\rm rms}} + \frac{0.29\rho_f\alpha_h v^2_{\rm rms}}{p_0}\right](v - v_t)_{\rm rms}. \tag{14}$$

4. Interpretation of the experimental results provided in Ref. [21]

A large series of experiments aimed at studying acoustic cavitation of water at low oscillatory velocities of acoustic radiator is presented in the work [21]. Experiments were conducted in degassed water with the concentration of the dissolved air equal to 30% of the nominal concentration in the equilibrium state at the room temperature and the normal static pressure.

For the interpretation of these data, let us introduce the following designations: $\sum I_a = 0.5(p'_h)^2\gamma = p_0^2\gamma$ is the total intensity of the acoustic energy radiated into water; $I_{a0} = 0.5(p'_h)^2\gamma_f = p_0^2\gamma_f$ is the intensity of the acoustic energy propagating beyond the bounds of the cavitation region. Here, γ is the specific acoustic radiation admittance of the continuum, $\gamma_f = 1/\rho_f c_f$. The difference of these intensities is the intensity of the acoustic energy absorbed in the cavitation region. Thus, when compared with the theoretical results of the given model, the experimental values of γ for each oscillatory velocity obtained in [21] were recalculated by the following expression:

$$\frac{I_a}{p_0} = (\gamma - \gamma_f)p_0. \tag{15}$$

In representing the data of the work [21], the values of $(v_t)_{\rm rms}$ were determined directly from the experimental plots of this work at the point of characteristic inflection.

5. Experimental setup

To measure the acoustic energy absorbed in a cavitating liquid at an increased static pressure p_0, an acoustic calorimeter described in [25] was used. The operating frequency of the magnetostrictive transducer was 17.8 kHz. Acoustic radiators were a set of the barbell horns with equal-size radiation surfaces, which were designed using the method described in [25]. The radiating surfaces' diameters were 60 mm and thus provided the generation of plane acoustic waves in water at the given frequency. The oscillatory velocity of the acoustic radiators reached very high values. The highest oscillatory velocity amplitude achieved in the experiments was $v = 17$ m/s. Static pressure in the calorimeter was produced with compressed nitrogen. Settled tap water at 20 °C was used. The static pressure, p_0, varied in the range of 1.0–5.0 bar; the water density, $\rho_f = 998$ kg/m^{-3}; sound velocity in the water, $c_f = 1500$ m/s; the volume of air dissolved in unit mass of water, $\eta_0 = 2.2 \times 10^{-5}$ m^3/kg. Each experimental point shown on the plots was obtained as a mean value of 10 measurements.

6. Experimental results

Experimental data for small oscillatory velocities of an acoustic radiator, v, and different static pressures, p_0, are shown in Fig. 4. The values of v_t used in the treatment of these experimental data were calculated from the expression $(v_t)_{rms} = 0.707 p_0/\rho_f c_f$ for different static pressures. Also shown in this figure are the experimental data from [21] for ultrasound frequencies of 19 and 28 kHz, closest to the frequency 17.8 kHz used in the present work, which are interpreted by Eq. (15). The values of the cavitation threshold obtained from the corresponding plots of [21] for both frequencies $(v_t)_{rms} = 0.08$ m/s. Fig. 4 also shows the theoretical lines calculated from Eqs. (11) and (12), which are represented by the solid and the dotted lines, respectively.

A good agreement between the theoretical lines themselves and the experimental data with these lines at small values of v can be clearly seen. With increasing $(v - v_t)_{rms} > 0.2$ m/s, the experimental points diverge from the straight line plotted from Eq. (12) and approach the line plotted from Eq. (11).

Fig. 5 shows the experimental results for all oscillatory velocities of the acoustic radiator, v, which were used in the experiments at normal static pressure, $p_0 = 1$ bar. Also shown in this figure are the theoretical lines plotted from Eqs. (11) and (14). From Fig. 5 it is seen that at intermediate values of v the experimental points are located near practically coincident lines plotted from Eqs. (11) and (14), which are represented by the dotted and solid lines, respectively.

At high oscillatory velocities, $(v - v_t)_{rms} > 3$ m/s, the specified theoretical relationships diverge, and the experimental points are located according to a more general relationship (14) at $\alpha_h = 0.4$. It can be seen that the theoretical and the experimental data are in good agreement up to the highest values of the oscillatory velocity, v.

A spread of the experimental points on the curve in Fig. 5 in the region $2\ \text{m/s} < (v - v_t)_{rms} < 3$ m/s is also observed. Here, the beginning of the divergence of the theoretical curves 1 and 2 is observed as well. These phenomena are, apparently, associated with the establishment of the supersonic regime of the SW movement and a considerable decrease in the gas pressure in the bubbles. The indication of the possibility of the supersonic regime of radiation at acoustic cavitation was first made in the work [26]. The phenomenon itself was called the second threshold of acoustic cavitation. The region located over the second threshold at $(v - v_t)_{rms} > 3$ m/s was called the region of acoustic supercavitation. The closest related known phenomenon is called hydrodynamic supercavitation and is described, for example, in [27].

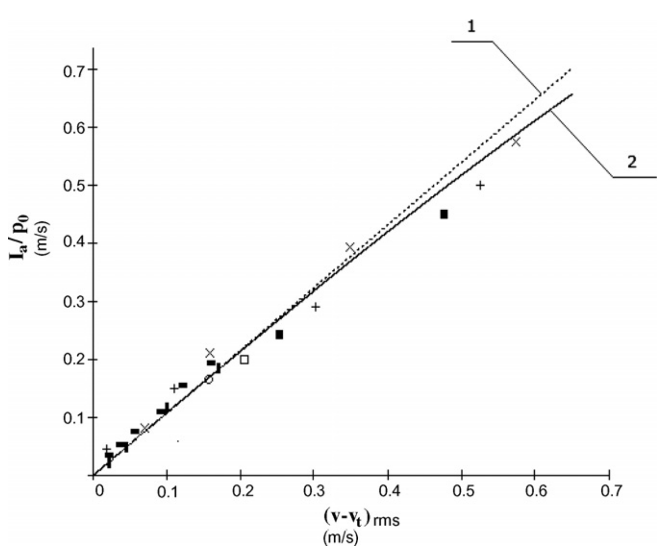

Fig. 4. Intensity of acoustic energy absorbed in water at cavitation is shown as a function of the excessive oscillatory velocity of an acoustic radiator for pressures of × – 1 bar, + – 2 bar, ■ – 3 bar, □ – 4 bar, ○ – 5 bar, at frequencies of ▌ – 28 kHz and ▬ – 19 kHz from the work [21]. Line 1 is plotted from Eq. (12); line 2 is plotted from Eq. (11).

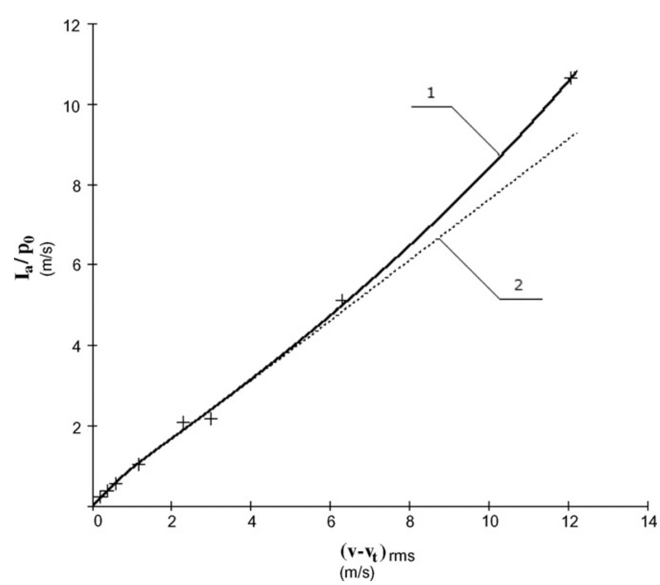

Fig. 5. Intensity of acoustic energy absorbed in water at cavitation is shown as a function of the excessive oscillatory velocity of an acoustic radiator. Line 1 is plotted from Eq. (14); line 2 is plotted from Eq. (11).

Since, as the stated theory assumes, at supercavitation the spherical shock-wave is not formed in the gas inside the bubbles, at oscillatory velocities $(v - v_t)_{rms} > 3$ m/s the characteristic changes of the secondary effects of cavitation, which are used in the sonochemical technology, must be observed.

An experimental verification of this effect was conducted by observing the cavitation-induced ultrasonic dispersion of solid particles. During the experimental setup, it was assumed that the transition to the supercavitation regime should in some way be reflected in the manner in which the dispersion occurs. The experimental study was conducted during the ultrasonic dispersion of graphite particles with the initial size 200–250 μm in settled tap water under normal conditions. To avoid any possible influence of the reactor geometry on the results of the measurements, the acoustic calorimeter described above was used as an apparatus for dispersing. For the analysis of the relative transparency of the obtained dispersions, the degree of the light absorption (at the wavelength of 420 nm) in them was measured using a photo-colorimeter. From the measurement results presented in Fig. 6 in relative units, it can be seen that the obtained curve reaches a maximum and then discontinues at $2.5\ \text{m/s} < (v - v_t)_{rms} < 3$ m/s. A subsequent smooth rise of this curve in the supercavitation region is also observed, which is most likely associated with the intense acoustic streaming, rather than with the effect of cavitation itself.

In the literature, it is indicated that the chemical action of acoustic cavitation, which is determined, for instance, from the rate of the free iodine release from the aqueous solution of potassium iodide, first increases to a certain limit with the increasing cavitation intensity and then abruptly decreases. See, for example, review [28]. In the work [25] it is experimentally shown that a rise in the rate

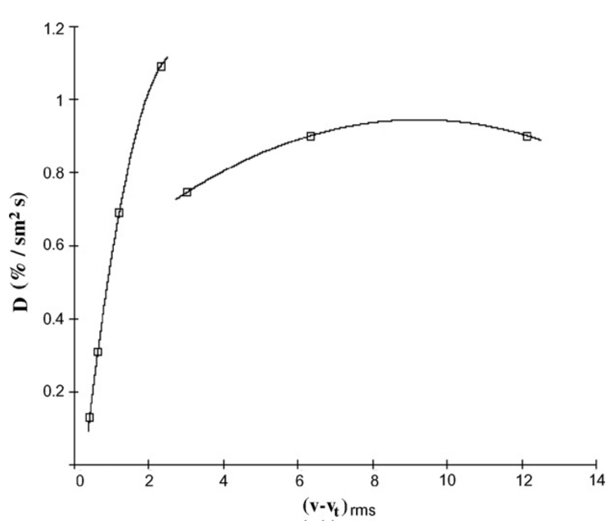

Fig. 6. Dispersing effect of acoustic cavitation (dispersion of graphite powder in water) determined by the degree of the 420 nm wavelength light absorption is illustrated as a function of the excessive oscillatory velocity of an acoustic radiator.

of the release of the free iodine continues up to very high intensities of cavitation. The process rate dependence on the intensity of cavitation simply has a deep discontinuity at the transition to the supercavitation regime, which is analogous to that observed in Fig. 6. With a further increase in the radiator oscillatory velocity, the rise in the rate of the free iodine release continues.

It appears that it is in the acoustic supercavitation region where the achievement of the highest possible temperatures during the compression of the rarefied gas inside the bubble oscillating as a Rayleigh cavity can be expected. Pressure at the bubble wall at the moment of focusing theoretically approaches infinitely high values because the gas compression is exerted by the moving dense bubble wall acting as a spherical plunger, rather than by a spherical acoustic wave [17]. In the same region, the highest intensities of the cavitation-induced sonochemical processes occurring at high temperatures may be observed. At the same time, processes connected with erosion, dispersion of solids and the like can be inhibited in the supercavitation region.

7. Conclusions

The proposed shock-wave model of acoustic cavitation reflects real events occurring in water at cavitation since calculations based on the equations that follow from the model are in good agreement with the results of the experiments. The presented experimental data extend to the region of super-high oscillatory velocities of an acoustic radiator and agree well with the theoretical model. The model makes it possible to obtain the resulting equation for the calculations of the energy absorbed by liquids during cavitation without having to consider in detail all the complex processes of the absorption of the acoustic energy, which are connected with the nonlinear oscillations of the gas bubbles during their collapse.

Within the framework of this model, the existence of a transition from the subsonic regime of acoustic cavitation to the supersonic regime is predicted. The possibility of a change in the character of the oscillations of a cavitation bubble at high values of v is theoretically shown. The conducted experimental studies confirm such a possibility.

Simple algebraic expressions that follow from the proposed model can be used in practical engineering calculations for designing powerful ultrasonic waveguide systems for sonochemical reactors following, for example, the methodology described in the work [25].

References

[1] T.G. Leinghton, Ultrason. Sonochem. 2 (1995) 123.
[2] H.G. Flynn, in: W.P. Mason (Ed.), Physical Acoustics, Methods and Devices, Part B, vol. 1, Acad. Press, 1964.
[3] M.S. Plesset, A. Prosperitty, Ann. Rev. Fluid Mech. 9 (1977) 145.
[4] W. Lauterborn, C.-D. Ohl, Ultrason. Sonochem. 4 (1997) 65.
[5] J.-L. Laborde, A. Hita, J.-P. Caltagirone, A. Gerard, Ultrasonics 38 (2000) 297.

[6] G. Servant, J.L. Laborde, A. Hita, J.P. Caltagirine, A. Gerard, Ultrason. Sonochem. 8 (2001) 163.
[7] G. Servant, J.-L. Laborde, A. Hita, J.-P. Caltagirone, A. Gerard, Ultrason. Sonochem. 10 (2003) 347.
[8] W. Lauterborn, T. Kurz, R. Geisler, D. Schanz, O. Lindau, Ultrason. Sonochem. 14 (2007) 484.
[9] R. Mettin, Ph. Koch, W. Lauterborn, D. Krefting, Modeling acoustic cavitation with bubble redistribution. In: Sixth International Symposium on Cavitation CAV2006, Wageningen, The Netherlands, September 2006.
[10] J. Klima, A. Frias-Ferrer, J. Gonzalez-Garsia, J. Ludvik, V. Saez, J. Iniesta, Ultrason. Sonochem. 14 (2007) 19.
[11] R. Mettin, S. Luther, C.-D. Ohl, W. Lauterborn, Ultrason. Sonochem. 6 (1999) 25.
[12] S. Luther, R. Mettin, P. Koch, W. Lauterborn, Ultrason. Sonochem. 8 (2001) 159.
[13] J. Appel, P. Koch, R. Mettin, D. Krefting, W. Lauterborn, Ultrason. Sonochem. 11 (2004) 39.
[14] A. Moussatov, C. Granger, B. Dubus, Ultrason. Sonochem. 10 (2003) 191.
[15] A. Moussatov, R. Mettin, C. Granger, T. Tervo, B. Dubus, W. Lauterborn, WCU 2003, Paris, September 7–10, 2003.
[16] P. Diodati, G. Giannini, Ultrason. Sonochem. 8 (2001) 49.
[17] Ya. B. Zel'dovich, Yu. P. Raizer, Physics of Shock Waves and High-Temperature Hydrodynamic Phenomena, Acad. Press, New York, 1966.
[18] L. Van Vijngaarden, Annual Review of Fluid Mechanics, vol. 4, Annual Review Inc., Palo Alto, 1972, p. 369.
[19] R.A. Thuraisingham, Ultrasonics 36 (1998) 767.
[20] L.D. Rosenberg (Ed.), High-Intensity Ultrasonic Fields, Plenum Press, New York, 1971.
[21] K. Fukushima, J. Saneyoshi, Y. Kikuchi, in: Y. Kikuchi (Ed.), Ultrasonic Transducers, Corona Publ. Co., Tokyo, 1969.
[22] M.G. Salvadory, R. Skalak, P. Weidlinger, New York Acad. Sci., Div. Eng. 2 (21) (1959) 427.
[23] W. Herrmann, J. Appl. Phys. 40 (1969) 2490.
[24] A.D. Resnyansky, N.K. Bourne, J. Appl. Phys. 95 (2004) 1760.
[25] S.L. Peshkovsky, A.S. Peshkovsky, Ultrason. Sonochem. 14 (2007) 314.
[26] N.B. Brandt, A.D. Yakovlev, S.L. Peshkovsky, Russ. Tech. Phys. Lett. 1 (10) (1975) 460.
[27] R.T. Knapp, J.W. Daily, F.G. Hammitt, Cavitation, New York, 1970.
[28] T.J. Mason, Ultrason. Sonochem. 7 (2000) 145.

Available online at www.sciencedirect.com

ScienceDirect

ELSEVIER

Ultrasonics Sonochemistry 14 (2007) 314–322

Ultrasonics SONOCHEMISTRY

www.elsevier.com/locate/ultsonch

Matching a transducer to water at cavitation: Acoustic horn design principles

Sergei L. Peshkovsky, Alexey S. Peshkovsky *

Industrial Sonomechanics, LLC, 1505 St. Nicholas Avenue #5B, New York, NY 10033, USA

Received 14 February 2006; received in revised form 6 June 2006; accepted 1 July 2006
Available online 14 August 2006

Abstract

High-power ultrasound for several decades has been an integral part of many industrial processes conducted in aqueous solutions. Maximizing the transfer efficiency of the acoustic energy between electromechanical transducers and water at cavitation is crucial when designing industrial ultrasonic reactors with large active volumes. This can be achieved by matching the acoustic impedances of transducers to water at cavitation using appropriately designed ultrasonic horns. In the present work, a set of criteria characterizing the matching capabilities of ultrasonic horns is developed. It is shown that none of the commonly used tapered-shape horns can achieve the necessary conditions. An analytical method for designing five-element acoustic horns with the desirable matching properties is introduced, and five novel types of such horns, most suitable for practical applications, are proposed. An evaluation of the horns' performance is presented in a set of experiments, demonstrating the validity of the developed theoretical methodology. Power transfer efficiency increase by almost an order of magnitude is shown to be possible with the presented horn designs, as compared to those traditionally utilized.

Keywords: Ultrasonic rod horns; Electromechanical transducers; Acoustic impedance matching; Ultrasonic power transference; Acoustic energy transference; Acoustic horns; Industrial ultrasonic reactors; Sonochemistry; Industrial processes in liquids; Cavitation

1. Introduction

High-power ultrasound for several decades has been an integral part of many industrial processes conducted in weak aqueous solutions, such as cleaning, extraction, homogenizing, emulsification, sonochemistry, pollutant destruction, etc. [1–3]. These ultrasound-aided (macrosonics) processes are based on the effect of acoustic cavitation induced in water during intensive ultrasonic treatment. The electromechanical transducers used to convert the high frequency electric power into the ultrasonic power cannot, however, directly provide the necessary amplitudes of longitudinal ultrasonic vibrations to induce cavitation. Acoustic rod horns connected to the transducers are, therefore, used to amplify the vibration amplitude. Commonly used acoustic horns have tapered shapes, such as conical, exponential, catenoidal, stepped, or more complex, and converge in the direction of the loads [3–5]. Although widely used, these horns suffer from an important limitation: they are incapable of providing matching between the transducers and the liquid loads, leading to an inefficient acoustic power transmission.

It is well known that for an optimal operation of an ultrasonic horn system, the maximum cross-sectional dimension of any portion of the resonant horn or transducer cannot exceed, approximately, a quarter-wavelength of the corresponding longitudinal acoustic wave at the horn's resonance frequency [6]. Consequently, a convergent horn with a maximal allowed base-width always ends up having a working tip dimension that is smaller than this limitation. The final size of the tip depends on the gain factor of the horn, and becomes reduced as the gain factor increases. This is problematic when the abovementioned

* Corresponding author.
E-mail address: alexey@sonomechanics.com (A.S. Peshkovsky).

1350-4177/$ - see front matter © 2006 Elsevier B.V. All rights reserved.
doi:10.1016/j.ultsonch.2006.07.003

processes are carried out on an industrial scale, since a deposition of substantial acoustic power is needed to create acoustic cavitation in large volumes of liquid. While using the converging horns permits increasing the specific acoustic power (or vibration amplitude) radiated by the electromechanical transducer into the load quite effectively, it is impossible to achieve the technologically necessary levels of total radiated acoustic power, since the cross-sectional area of the horn tip in contact with the load is small. Therefore, it is intuitive that the use of the convergent horns does not permit transferring all available power of an acoustic transducer into a load.

In actual practice a technique that is frequently attempted to circumvent this limitation is the use of a convergent horn with an extension in the form of a small disk at the end. This horn, however, usually works inadequately because when a disk of arbitrary dimensions is connected to a horn, the resonance frequency and the vibration amplitude conditions change dramatically, in comparison with the calculated values, and the horn's behavior becomes difficult to predict. Complicated experimental fitting of the parameters is then required for each horn. Additionally, the fatigue strength of the disk joint is low, which diminishes the horn's reliability and lifetime of operation. Rod horns connected to planar resonant systems, such as large discs or planes are also sometimes used [7]. Another solution attempted in the past was to develop an alternative reactor design with an incorporated converging horn [3].

In this manuscript we introduce novel design principles used for the development of a completely novel family of acoustic horns, whose shapes permit achieving high gain factors and large output surfaces simultaneously. These horns can be designed to accurately match an ultrasonic source to a liquid load at cavitation, maximizing the transference of the available acoustic energy into the load and creating a large cavitation volume. The devices are easy to machine and have well-isolated axial resonances and uniform output amplitudes, as shown in the experimental section.

2. Criteria for matching a magnetostrictive transducer to water at cavitation

Under the most convenient approximation, which is, nevertheless, quite suitable for the engineering calculations, the highest specific acoustic power that a well (perfectly) cooled resonant magnetostrictive transducer can transmit into a load is limited by two main factors – the magnetostrictive stress saturation, τ_m (the maximal mechanical stress achievable due to the magnetostrictive effect for a given transducer material), and the maximum allowed oscillatory velocity, limited by the fatigue strength of the transducer material, V_m, such that [8]

$$\begin{aligned} \tau_m &= e_m E \phi_1 \\ V_m &= \sigma_m \phi_2 / \rho c \end{aligned} \tag{1}$$

where e_m is the deformation amplitude associated with τ_m, E is Young's modulus, ϕ_1 and ϕ_2 are the coefficients that take into account the features of the transducer construction [4,8], σ_m is the stress amplitude of the material fatigue strength, ρ is the transducer material's density, and c is the thin-wire speed of sound in the material. The highest specific power radiated under conditions of perfect matching between the transducer and the load is represented by the quantity

$$W_m = 0.5 \tau_m V_m \tag{2}$$

Let us now consider the criteria, upon which an ultrasonic horn should be designed in order to achieve a matching condition between a transducer and a given load. As an acoustic load of the transducer, water at cavitation will be further considered as the most common and experimentally studied load encountered in technological applications of ultrasound. It should be noted that the acoustic load under consideration, water at cavitation, has a purely active character [9], and, therefore, is appropriately described by the term "acoustic resistivity", r_w. Practically, this means that virtually all of the acoustic energy deposited into water at cavitation is converted into heat [10]. Under the term "matching" we will further mean supplying an electromechanical transducer with a multi-element ultrasonic horn possessing a gain factor, $G \gg 1$ (G is defined as a ratio of the output to input oscillatory velocities, V/V_m), which allows the transference of a maximum of the available acoustic power of the transducer, W_m, into the load.

Specific acoustic power, W_1, generated in a purely active load by the longitudinal vibrations of an acoustic rod horn with an output oscillatory velocity, V, is represented by

$$W_1 = 0.5 r_w V^2 \tag{3}$$

Taking $W_m = W_1$ as a matching condition, we obtain

$$\frac{\tau_m}{r_w V} = G N^2 \tag{4}$$

where $N^2 = S_{out}/S_{in}$, S_{in} and S_{out} are, respectively, the input and the output cross-sections of the acoustic horn, while S_{in} is taken to be equal to the output cross-section of the electromechanical transducer, S_t (please see Fig. 1). The left-hand side of Eq. (4) reflects the degree of underloading of an acoustic transducer, and the right-hand side describes matching capabilities of an acoustic horn.

For a resonant system matched to an acoustic load, the traveling-wave factor can be presented as the ratio of the

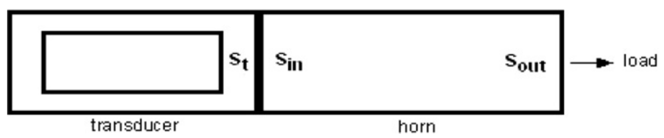

Fig. 1. General schematic is shown, describing matching between an electromechanical transducer and a load achieved by using an acoustic rod horn of an arbitrary shape. S_{in} and S_{out} are, respectively, the input and the output cross-sections of the acoustic horn; S_t is the output cross-section of the electromechanical transducer.

maximum energy radiated into the load to the maximum energy stored in the transducer in the form of a standing acoustic wave

$$k_t = \frac{\tau_m V_m}{\rho c V_m^2} = \frac{\tau_m}{\sigma_m \phi_2} \tag{5}$$

For the common magnetostrictive materials, τ_m is much smaller then σ_m, and, therefore, $k_t \ll 1$. This means that a standing-wave mode in the transducer matched to the load is always present. In addition, since the considered acoustic load has an active character, the resonance dimensions of the transducer and the horn are preserved.

From experimental studies [9] it is known that during the radiation of ultrasound into water at cavitation, the relationship $r_w V = \sqrt{2}P_0$, where P_0 is the hydrostatic pressure of water, remains, roughly, constant. Therefore, the following can be written:

$$\frac{\tau_m}{r_w V} = \frac{e_m E \phi_1}{\sqrt{2}P_0} \tag{6}$$

It is seen from Eq. (6) that the degree of the under-loading of an acoustic transducer depends only on the characteristics of the transducer itself and the hydrostatic pressure of water. For most common magnetostrictive materials, the calculated values of $\tau_m/r_w V$ are between 15 and 44. In this calculation, the values of $P_0 = 10^5\ \mathrm{N/m^2}$ and $\phi_1 = 0.45$ were assumed.

Industrial acoustic transducers, generally, have their nominal electrical power W_e, efficiency factor η and output oscillatory velocity V_n specified. The practical degree of the under-loading for such industrial magnetostrictive transducers can be, therefore, characterized by the relationship $2\eta W_e/r_w V V_n S_t$, having assumed that $W_m = \eta W_e/S_t$. The practical values of the degree of under-loading obtained from this expression are much lower than the corresponding theoretical limits for the magnetostrictive materials themselves, and for most models fall in the range between 3 and 5.

It is important to point out that in the case of piezoelectric transducers the highest achievable level of specific acoustic power is practically restricted by the electrical resilience of the entire apparatus, rather than by the properties of the piezoelectric material itself. The limiting value of maximal electric power is, generally, available from the transducer supplier and can also be used in this expression for the evaluation of the practical degree of under-loading of the industrial piezoelectric transducers.

It is less evident how to use the right-hand side of Eq. (4), which reflects the matching capabilities of a horn. The point to emphasize is that in spite of a variety of types and shapes of the acoustic horns known from the literature and used in practice, none exist, for which the relationship $GN^2 > 1$, when $G > 1$, would hold true. It is, therefore, clear that in order to be able to match ultrasonic transducers to water at cavitation, it is necessary to develop new types of acoustic horns that would meet the matching criterion, $GN^2 > 1$.

3. Five-element matching horns

3.1. Design principles

The theory of acoustic horns is based on the problem of longitudinal vibrations of multi-element rods that have cylindrical elements and elements of variable cross-sections [11]. We will consider only the horns of axially symmetric shapes. Other types of horns (for example, wedge-shaped) can be considered in an analogous way. In the current work we will restrict the discussion to the five-element horns, although no theoretical restriction for the number of elements exists.

We assume that during the passage of the stress waves through a horn, the wave front remains planar, while the stresses are uniformly distributed over the horn's cross-section. This assumption limits us to the thin horns, whose resonance lengths significantly exceed their diameters. For all practical purposes, it is sufficient to require that the maximum cross-sectional dimension of any portion of a resonant horn not exceed, approximately, a quarter-wavelength of the corresponding thin wire acoustic wave at the horn's resonance frequency [6].

The schematic and the designation of parameters for a general case of a five-element rod horn are given in Fig. 2, where two possible situations are presented: a horn with $d_1/d_3 > 1$ is shown by the solid line; a horn with $d_1/d_3 < 1$ is shown by the dotted line. Under the assumed approximation, the problem is reduced to one-dimension, and it is limited to the consideration of elements with variable cross-section of only conical shape. For a steady-state mode, the equation of vibrations for displacements, u, takes the following form:

$$u'' + \frac{1}{S}S'u' + k^2 u = 0 \tag{7}$$

where $k = \omega/c$ is the wave number, $\omega = 2\pi f$ is the angular frequency of vibrations, and f is the frequency of vibrations.

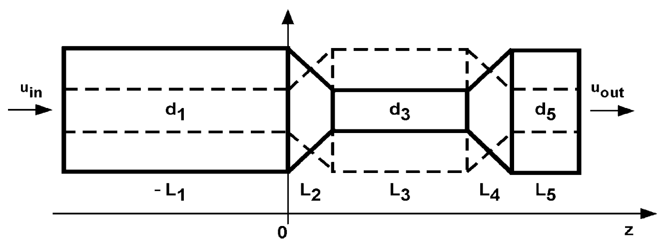

Fig. 2. Schematic defining the parameters of a five-element matching horn is shown. The horn having $d_1/d_3 > 1$ is shown by a solid line, and the horn with $d_1/d_3 < 1$ is shown by a dotted line. Parameters L_1–L_5 correspond to the lengths of each element.

The solutions of Eq. (7) for each of the horn's elements can be written as

$$\begin{aligned}
&u_1 = A_1\cos kz + B_1\sin kz; \quad -L_1 < z < 0\\
&u_2 = F(A_2\cos kz + B_2\sin kz); \quad 0 < z < L_2\\
&u_3 = A_3\cos kz + B_3\sin kz; \quad L_2 < z < L_2 + L_3\\
&u_4 = F(A_4\cos kz + B_4\sin kz); \quad L_2 + L_3 < z < L_2 + L_3 + L_4\\
&u_5 = A_5\cos kz + B_5\sin kz; \quad L_2 + L_3 + L_4 < z < L_2 + L_3 + L_4 + L_5
\end{aligned} \tag{8}$$

Then, using the boundary conditions for the horn's element, we obtain the system of equations for displacements, u, and strains, u'.

$$\begin{aligned}
&\text{At } z = -L_1,\ u_1 = u_{\text{in}},\ ES_1u_1' = -F_{\text{in}},\ F_{\text{in}} = 0\\
&A_1\cos kL_1 - B_1\sin kL_1 = u_{\text{in}};\\
&EkS_1(A_1\sin kL_1 + B_1\cos kL_1) = -F_{\text{in}}\\
&\text{At } z = 0,\ u_2 = u_1,\ u_2' = u_1'\\
&FA_2 = A_1; \quad F'A_2 + FB_2k = kB_1;\\
&\alpha = (d_1 - d_3)/L_2d_1;\\
&F = 2/d_1; \quad F' = F\alpha\\
&\text{At } z = L_2,\ u_3 = u_2,\ u_3' = u_2'\\
&A_3\cos kL_2 + B_3\sin kL_2 = F(A_2\cos kL_2 + B_2\sin kL_2);\\
&-kA_3\sin kL_2 + kB_3\cos kL_2\\
&\quad = (F'B_2 - FkA_2)\sin kL_2 + (F'A_2 + FkB_2)\cos kL_2;\\
&\alpha = (d_1 - d_3)/L_2d_1;\\
&F = 2/d_3; \quad F' = -F/(L_2 - 1/\alpha)\\
&\text{At } z = L_2 + L_3,\ u_4 = u_3,\ u_4' = u_3'\\
&F[A_4\cos k(L_2 + L_3) + B_4\sin k(L_2 + L_3)]\\
&\quad = A_3\cos k(L_2 + L_3) + B_3\sin k(L_2 + L_3);\\
&(F'B_4 - FkA_4)\sin k(L_2 + L_3) + (F'A_4 + FkB_4)\cos k(L_2 + L_3)\\
&\quad = -kA_3\sin k(L_2 + L_3) + kB_3\cos k(L_2 + L_3);\\
&\alpha = (d_3 - d_5)/L_4d_3; \quad F = 2/d_3; \quad F' = F\alpha\\
&\text{At } z = L_2 + L_3 + L_4,\ u_5 = u_4,\ u_5' = u_4'\\
&A_5\cos k(L_2 + L_3 + L_4) + B_5\sin k(L_2 + L_3 + L_4)\\
&\quad = F[A_4\cos k(L_2 + L_3 + L_4) + B_4\sin k(L_2 + L_3 + L_4)];\\
&-kA_5\sin k(L_2 + L_3 + L_4) + kB_5\cos k(L_2 + L_3 + L_4)\\
&\quad = (F'B_4 - FkA_4)\sin k(L_2 + L_3 + L_4)\\
&\qquad + (F'A_4 + FkB_4)\cos k(L_2 + L_3 + L_4);\\
&\alpha = (d_3 - d_5)/L_4d_3; \quad F = 2/d_5; \quad F' = -F/(L_4 - 1/\alpha)\\
&\text{At } z = L_2 + L_3 + L_4 + L_5,\ u_5 = u_{\text{out}},\ u_5' = 0\\
&A_5\cos k(L_2 + L_3 + L_4 + L_5) + B_5\sin k(L_2 + L_3 + L_4 + L_5) = u_{\text{out}};\\
&-A_5\sin k(L_2 + L_3 + L_4 + L_5) + B_5\cos k(L_2 + L_3 + L_4 + L_5) = 0
\end{aligned} \tag{9}$$

The gain factor of the horn can be expressed as

$$G = \left|\frac{u_{\text{out}}}{u_{\text{in}}}\right| = \left|\frac{A_5\cos k(L_2 + L_3 + L_4 + L_5) + B_5\sin k(L_2 + L_3 + L_4 + L_5)}{A_1\cos kL_1 - B_1\sin kL_1}\right| \tag{10}$$

where $F = 2/d_n$, d_n is the diameter of the corresponding cylindrical element of the horn, A_n and B_n are the constant coefficients for the corresponding elements of the horn, L_n is the length of the corresponding element of the horn, n is the order number of the horn element, α is the cone index of the horn element with variable cross-section, u_{in} and u_{out} are the amplitudes of displacements at the horn input and output, respectively. The boundary conditions for the force acting on the horn's input, $F_{\text{in}} = 0$, and for the strain at the horn output, $u_5' = 0$, in this system of equations indicate that the horn has a total resonance length and does not have an acoustic load.

From the system of equation (9), one can obtain all necessary characteristics of a five-element horn: lengths and diameters of the elements, gain factor, distribution of vibration amplitudes, and distribution strains along the horn. From this system of equations, it is also easy to obtain solutions for any horns with conical elements (for example, with a number elements smaller than five). Horns with other shapes of the variable cross-section elements (for example, with exponential or catenoidal elements) can be considered in an analogous way, taking into account the variation of sound velocity in such elements.

3.2. Analysis of five-element horns

To solve the system of Eq. (9) and to present results in a convenient graphical form, a computer program has been written that allows all the indicated above characteristics of five-element horns to be obtained in real time for subsequent analysis. The input parameters are: operating frequency of the horn, acoustic properties and fatigue strength of the horn material, and the diameter-to-length ratios of the horn elements.

Out of all variety of possible types of five-element horns, let us consider the five horns that are most suitable for practical applications. For the convenience of a comparison of horn parameters, we further assume $N = d_1/d_5 = 1$. Fig. 3 shows a conical–cylindrical matching horn and its design parameters. This is the simplest degenerate horn with $L_1 = 0$. Such a horn has low matching capabilities, the maximum value being $GN^2 \approx 3$.

Fig. 4 shows a step matching horn and its design parameters. The maximum value of the matching capability of this horn is $GN^2 \approx 4$. Both horns considered above can be used to match industrial acoustic transducers of low power for exciting relatively low amplitudes of ultrasonic vibrations in the load. Their small resonance dimensions convenient for construction should be particularly noted.

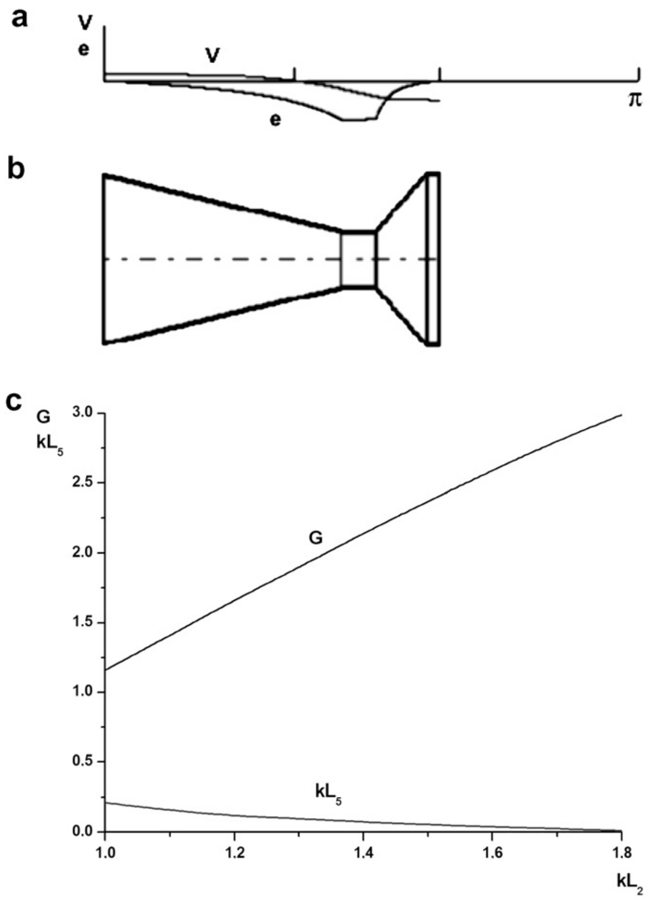

Fig. 3. Conical–cylindrical horn is shown with $d_1 = d_5$; $d_1/d_3 = 3.0$; $kL_1 = 0$; $kL_3 = 0.2$; $kL_4 = 0.3$, along with (a) the distribution of the oscillatory velocity, V, and strain, e, along the horn; (b) drawing of the horn; (c) plot of the distribution of the horn's parameters.

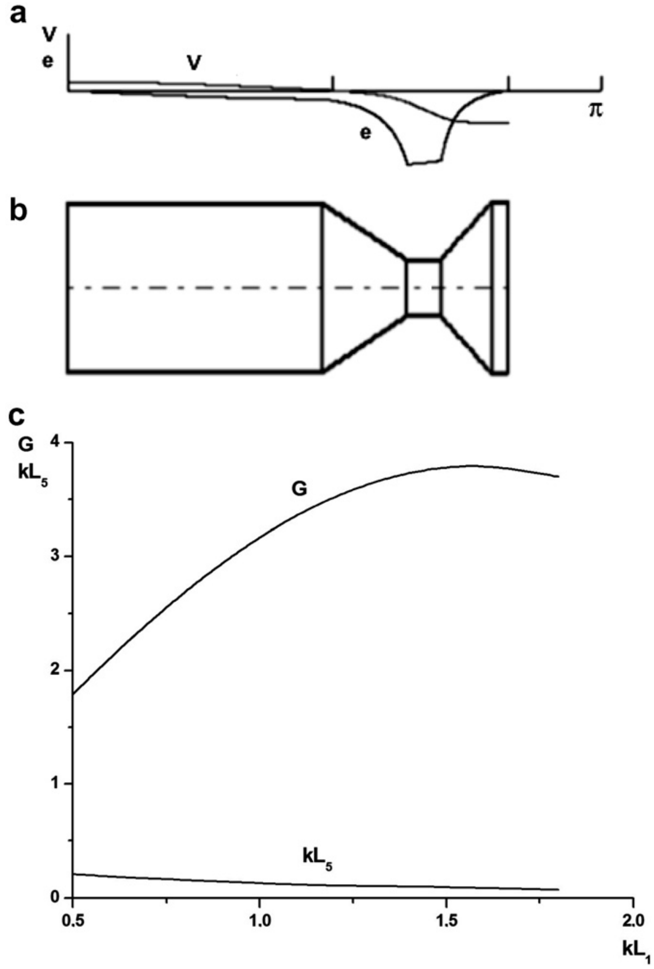

Fig. 4. Stepped horn is shown with $d_1 = d_5$; $d_1/d_3 = 3.0$; $kL_1 = 0.5$; $kL_3 = 0.2$; $kL_4 = 0.3$, along with (a) the distribution of the oscillatory velocity, V, and strain, e, along the horn; (b) drawing of the horn; (c) plot of the distribution of the horn's parameters.

A barrel-shaped matching horn and its design parameters are shown in Fig. 5. This horn is quite promising for the matching of acoustic transducers of small cross dimensions or for the use as a booster. The maximum value of its matching capabilities at the given parameters is $GN^2 \approx 8$. It should be borne in mind that the diameter of the horn's heavy section, d_3, under the considered approximation must not exceed about a quarter of the length of acoustic wave.

Fig. 6 shows a spool-shaped matching horn and its design parameters. This horn is atypical because its main radiating surface is lateral, and it mainly radiates a cylindrical wave into the load, as opposed to a plane wave radiated by other matching horns. Given a symmetric form of the horn, the gain factor is always equal to 1, the node of displacements is located in the middle, and lateral surfaces move in anti-phase. When using lateral radiation, the horn's matching capabilities are quite high since there are no limitations on the overall length. Such horn connected into a sequential string can radiate a cylindrical wave of high total power into the load and produce a well-developed cavitation region of a large volume.

Above, we have considered the horns whose lengths were less than or close to half the length of the acoustic wave in the rod, the so-called half-wave horns. The system of Eq. (9) also allows one to obtain solutions for full-wave horns. One of such horns intended for the radiation of a plane acoustic wave of a very high power into water is a barbell-shaped horn shown in Fig. 7. Its design parameters, as a function of d_1/d_3, are presented in Fig. 7(c). The matching capabilities of the barbell-shaped horn can reach the values of $GN^2 = 20$ or more. Such horn is very promising for the matching of high-power acoustic transducers that have large cross dimensions. For example, the highest design power radiated into the water at cavitation by this horn, made of titanium alloy, taking into account the fatigue strength limitations and limitations on output diameter under normal hydrostatic pressure, is about 5 kW at a frequency of 20 kHz. This value of the power of the acoustic radiation is close to the theoretically attainable maximum under the given conditions for any metallic rod horn. An expression for the theoretically attainable maximum power of acoustic radiation deposited into water under cavitation at a given frequency and electrostatic pressure, $W = P_0 V_m S_m$, can be obtained based on expressions 2 and 3,

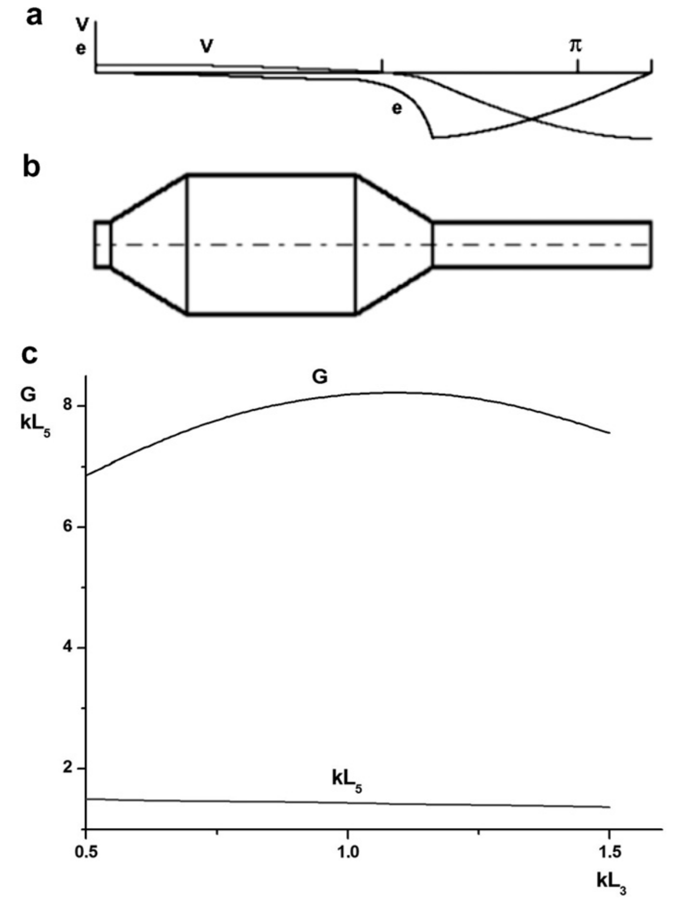

Fig. 5. Barrel horn is shown with $d_1 = d_5$; $d_3/d_1 = 3.0$; $kL_1 = 0.1$; $kL_2 = kL_4 = 0.5$, along with (a) the distribution of the oscillatory velocity, V, and strain, e, along the horn; (b) drawing of the horn; (c) plot of the distribution of the horn's parameters.

taking into account that $r_w V = \sqrt{2} P_0$. Here, S_m is the maximum possible area of the circular output surface of the acoustic horn, whose diameter is restricted by the quarter-wavelength condition mentioned above. The maximum achievable oscillation velocity, V_m, for best titanium alloys used as horn materials reaches, approximately, 10–15 m/s.

Due to the significant potential of the barbell-shaped horn for the industrial applications of ultrasound, we provide its exact parameters in Table 1. These parameters are convenient for the use during practical calculations.

3.3. Frequency characteristics of five-element horns

The knowledge of the frequency characteristics of an acoustic horn is very important when choosing the type of a matching horn for specific conditions of its excitation (type of an ultrasonic generator) and operation (properties of an acoustic load). These characteristics, according to (8), can be obtained by calculation in the form of a frequency dependence of the horn's input resistance. If losses are ignored, the expression for the input resistance of a five-element horn can be derived from the system of equation (9), assuming $z = F_{in}/j\omega u_{in}$. Taking $z_0 = EkS_{in}/\omega$, one can write

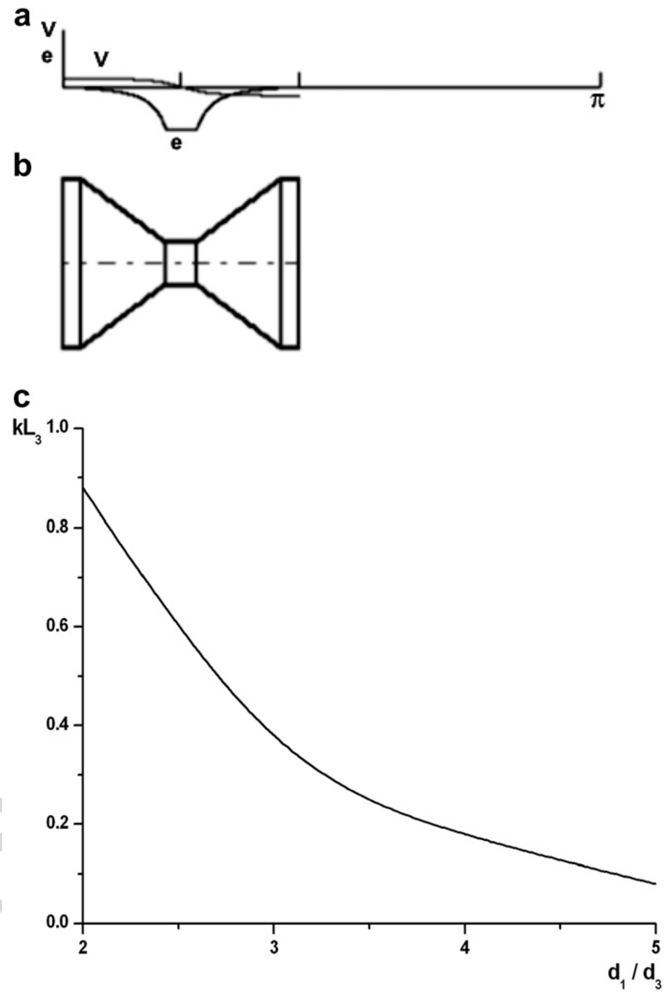

Fig. 6. Symmetrical spool-shaped horn is shown with $d_1 = d_5$; $kL_1 = kL_5 = 0.1$; $kL_3 = kL_4 = 0.5$, along with (a) the distribution of the oscillatory velocity, V, and strain, e, along the horn; (b) drawing of the horn; (c) plot of the distribution of the horn's parameters.

$$\frac{z}{z_0} = \frac{j(A_1 \sin kL_1 + B_1 \cos kL_1)}{A_1 \cos kL_1 - B_1 \sin kL_1} \tag{11}$$

The values of $|z/z_0|$ for the five-element horns considered above were calculated at a small change in the current frequency f, as compared with the horn natural frequency f_r, so that $(f_r - f)/f_r = 0.02$. Table 2 gives the values of $|z/z_0|$ obtained at the frequency, f, for the horns shown in Figs. 3–7 with similar gain factors, $G \approx 3$ (with the exception of the horn in Fig. 6). For comparison, the table also gives the values of $|z/z_0|$ for two resonant cylindrical rods that have characteristic lengths $kL = \pi$ and $kL = 2\pi$. It is evident that the presented values of $|z/z_0|$ characterize the rate of change in the horn's input resistance with a change in the frequency of excitation or the parameters of the acoustic load.

From Table 2 it is seen that the horn shown in Fig. 6 has the lowest frequency dependence of the input resistance. It is most suitable for the use in a sequentially connected string of such horns for the radiation of a cylindrical wave into the load. In this case, the low dependence of the horn input resistance on frequency is a positive property because when

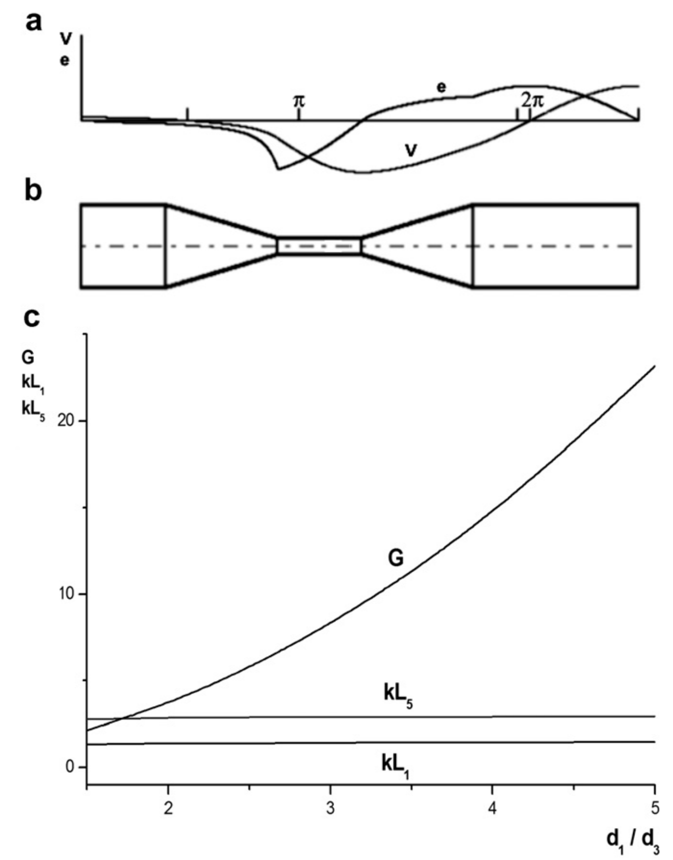

Fig. 7. Barbell-shaped horn is shown with $d_1 = d_5$; $kL_1 = kL_3$; $kL_2 = kL_4 = 0.5$, along with (a) the distribution of the oscillatory velocity, V, and strain, e, along the horn; (b) drawing of the horn; (c) plot of the distribution of the horn's parameters.

Table 1
Parameters convenient for practical calculations of barbell-shaped horns are provided

N	G	kL_1	kL_2	kL_5
1.5	2.176	1.383	0.405	2.853
2.0	3.527	1.290	0.693	2.725
2.5	4.918	1.245	0.916	2.640
3.0	6.285	1.224	1.099	2.574
3.5	7.597	1.216	1.253	2.519
4.0	8.834	1.215	1.386	2.470
4.5	9.987	1.217	1.504	2.426
5.0	11.049	1.222	1.609	2.384

Table 2
Values of $|z/z_0|$ obtained at the frequency, f, for the horns shown in Figs. 3–7 with similar gain factors, $G \approx 3$ (with the exception of the horn in Fig. 6), are provided. For comparison, the values of $|z/z_0|$ for two resonant cylindrical rods that have characteristic lengths, $kL = \pi$ and $kL = 2\pi$, are also given

Horn type	Cylinder $kL = \pi$	Cylinder $kL = 2\pi$	Fig. 3	Fig. 4	Fig. 5	Fig. 6	Fig. 7
$\lvert z/z_0 \rvert$	0.063	0.126	0.09	0.14	0.345	0.024	0.67

several horns are connected in series, the analogous total dependence for the string will be also low. For horns with a gain factor greater than unity, the lowest dependence of the input resistance on frequency is displayed by the horn shown in Fig. 3. The barbell-shaped full-wave horn is characterized by an abrupt dependence of input resistance on frequency. In this case, the positive feature is that a small error in dimensions during manufacturing of the horn has little influence on its resonance frequency. The horn can also reliably operate regardless of changes in its characteristic length, for example, if the reactive component of the acoustic impedance of the load changes. However, it should be noted that a barbell-shaped horn, due to the large diameter of its output surface, produces a plane wave in water at cavitation, during the radiation of which the reactive component of radiation impedance is virtually absent.

4. Experimental

For the experimental verification of the described horn design principles we have chosen the barbell-shaped horn, shown in Fig. 7. Direct calorimetric measurement of acoustic energy transmitted by this horn into water at cavitation was selected as a method of this horn's performance evaluation. The measurements of the acoustic energy absorbed in the cavitation region were conducted with the apparatus shown in Fig. 8. Settled tap water at a temperature of 20 °C

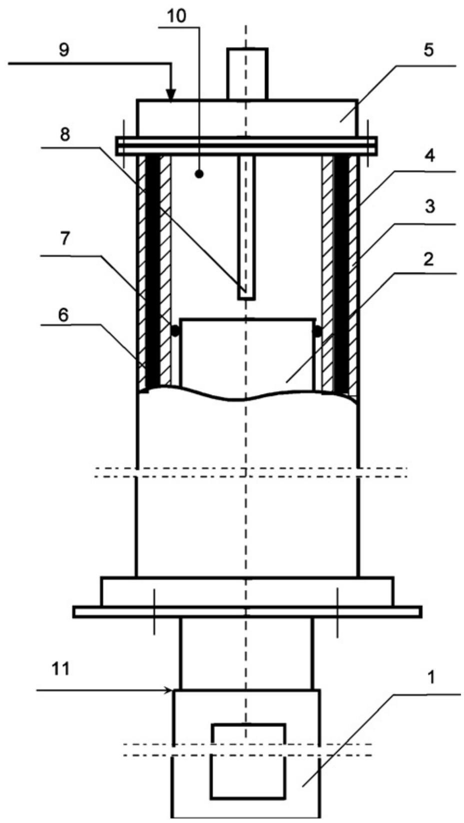

Fig. 8. Schematic of acoustic calorimeter is presented. 1 – magnetostrictive transducer, 2 – replaceable horn-radiator, 3 – external wall of calorimeter, 4 – heat insulation gasket, 5 – cover with porous sound-absorber, 6 – internal wall of calorimeter, 7 – sealing ring, 8 – set of thermocouples, 9 – gas supply, 10 – microphone, 11 – point of control over amplitude of transducer vibrations.

was used. The apparatus was based on an acoustic radiator consisting of a titanium horn connected to a magnetostrictive transducer, which operated at the resonance frequency of 17.8 kHz. The working power of the ultrasonic generator coupled to the magnetostrictive transducer was 5 kW. The oscillation amplitude of the magnetostrictive transducer was kept constant in all experiments at 1.67 m/s (rms). It was measured by placing a magnetic ring with an inductive coil on the transducer next to its output surface. Voltage was created in the coil as the transducer oscillated. The amplitude of this voltage corresponded to the oscillation amplitude and was measured by an oscilloscope. Prior calibration of this device was performed, in which the vibration amplitude was measured directly by a microscope.

A set of replaceable barbell-shaped horns was constructed to provide the necessary stepped change in the amplitude of the oscillatory velocity of the output end in contact with water. The set consisted of nine such horns with different gain factors (greater or smaller than unity), all of which had equal input and output diameters of 60 mm. Maximum oscillation velocity of some of these horns reached very large values, close to maximum theoretically possible for the best titanium alloys. Greatest achieved oscillation velocity was 12 m/s (rms). Therefore, maximum gain factor for the set was 7.2.

Static pressure in the calorimeter was produced with compressed nitrogen. The measurements of the resulting temperature of water were performed using a set of thermocouples. A change in the temperature of water during ultrasonic treatment was not more than 2–5 °C.

Fig. 9 shows an experimentally obtained plot of the specific acoustic power absorbed in the cavitation area, as a function of the oscillatory velocity of the horns' output radiating surfaces, at a static pressure of 1 bar. For the purpose of the measurement precision evaluation, data from Ref. [9] is also provided in the figure for the acoustic radiation frequency of 19 kHz and the static pressure of 1 bar. The figure shows that the experimental data obtained in this work in the small oscillation velocity range corresponds very well to the data from Ref. [9]. Unfortunately, for large vibration velocities, no literature data was found. Performance verification of the horns with different gain factors conducted during the experiments showed that all of them possessed resonance and gain characteristics well corresponding to the theoretically predicted values. In no case was it necessary to make any adjustments to the horns after they were originally machined.

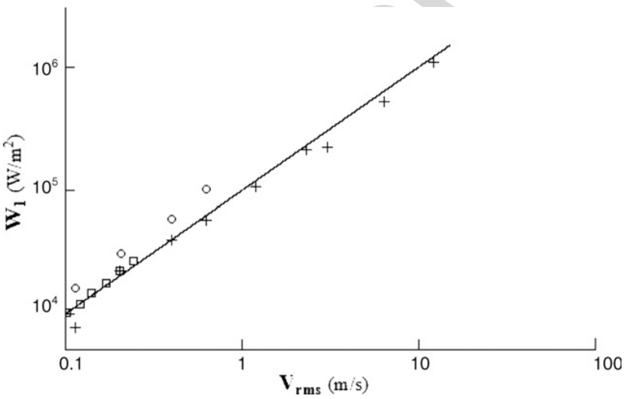

Fig. 9. Dependence of the intensity of the acoustic energy absorbed in the cavitation area is presented as a function of the oscillation velocity of the horns' output surfaces for a set of nine horns with different gain factors (+ are the data points from this work for the load pressure of 1 bar, ○ are the data points from this work for the load pressure of 2 bars, □ are the data points from Ref. [9]).

Fig. 9 additionally shows a curve corresponding to the Eq. (3), $W_1 = 0.5 r_w V^2 = r_w V_{\mathrm{rms}}^2 = P_0 V_{\mathrm{rms}}$. The fact that the experimental data follows the curve very well shows that the relationship, $r_w V = \sqrt{2} P_0$, suggested in Ref. [9] and verified there for the small oscillation velocities, is maintained also for the significantly larger oscillation velocities. Thus, it has been experimentally proven that the matching between our barbell-shaped acoustic horns and water at cavitation truly takes place, in accordance with the theory presented above, for all possible oscillation velocities of the horns' output surfaces.

To demonstrate the effect of the elevated static pressure, Fig. 9 also shows the experimental data corresponding to the static pressure of 2 bars. It is clearly seen that increasing the pressure augments the absorbed acoustic energy in the cavitation area.

The region of the specific power with the values above 10^5 W/m^2 is very little studied, especially from the technological standpoint. The reason for this, from our perspective, is that the traditional cone-shaped horns, widely used in ultrasonic technology, are incapable of providing a large total radiation power, since their oscillation amplitudes are inversely proportional to the areas of their output surfaces. At large gain factors, the output surface area becomes very small, which complicates the development of sonochemical reactors capable of processing significant volumes of liquids. Thus, for example, a traditional stepped horn having an input diameter of 60 mm and a gain factor of 7.2 has the output diameter of, approximately, 20 mm. Therefore, at the maximum experimentally achieved specific power of 10^6 W/m^2, this stepped horn is capable of depositing not more than 300 W into its liquid load. Our barbell-shaped horn, used in the experiments presented in this section, on the other hand, delivers, approximately, 2.7 kW of total power, providing a power transfer efficiency increase by almost an order of magnitude.

A well-known method, described in detail in Ref. [12], was used for the experimental verification of the chemical activity in the cavitation area. The chemical activity level was determined by monitoring the oxidation reaction of KI in aqueous solution, resulting in the formation of free iodine. The obtained data is presented in Fig. 10. It can be clearly seen that the specific (divided by the horn's output surface area) rate of the concentration of the free iodine formation in the cavitation volume increases with the augmented intensity of the acoustic radiation. Total

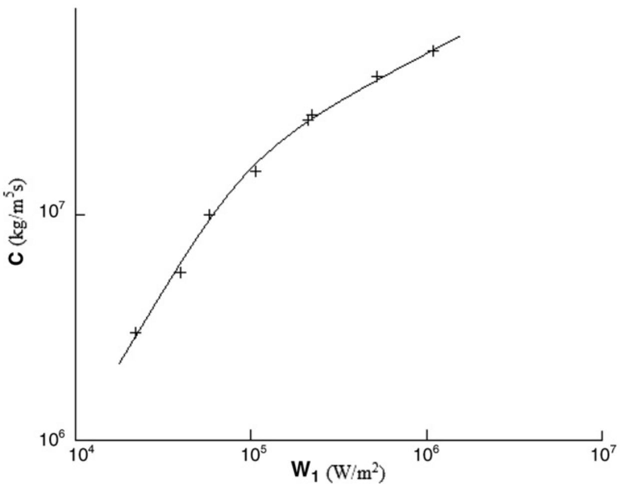

Fig. 10. Dependence of the specific (divided by the horn's output surface area) rate of the concentration of the free iodine formation in the cavitation volume is shown as a function of the intensity of the absorbed acoustic radiation.

increase of the concentration of the reduced iodine at maximum intensity of acoustic radiation of 10^6 W/m^2 reaches 1.5×10^5 kg/m^3 s.

5. Conclusions

Matching an ultrasonic transducer to a liquid load is a matter of choosing the matching horn that ensures the expression (4) at a given gain factor G, and of subsequent calculation of its resonance dimensions with the use of the system of Eq. (9). As stated above, when matching to an active acoustic load with $k_t \ll 1$, the standing acoustic wave in the transducer and in the horn is not disturbed, and their resonance dimensions do not change. The most powerful horn, from the designs described above, is the barbell-shaped horn, which was chosen for the experimental investigations. During the experiments, performance evaluation of a set of such horns with different gain factors showed that all of them had the resonance and the gain factor characteristics that corresponded very well to those predicted theoretically. It was also experimentally verified that matching of the acoustic horns with water at cavitation, according to the theory described above, is truly established for all possible values of the output oscillation velocities of the horns.

It should be noted that matching an acoustic transducer to a load using an acoustic horn is not the only possible method of matching. Another powerful matching factor, which results from the specific properties of water at cavitation, is hydrostatic pressure P_0, according to the expression (6) and the experimental results presented here. It was also previously theoretically demonstrated that an increase in the load's hydrostatic pressure leads to an augmentation of the intensity of acoustic radiation [13], further resulting in an increase in the technological effectiveness of cavitation. It is evident that the best results are obtained when these two matching techniques are used jointly.

In conclusion, we would like to point out that our barbell-shaped horns also perform well in low-viscosity non-aqueous liquids and solutions, and permit building very effective sonochemical reactors for conducting experiments with these systems. This makes the described technology very attractive for the studies involving secondary effects of cavitation, such as sonoluminescence and sonofusion [14,15], which have been receiving a lot of attention recently.

References

[1] A. Shoh, IEEE Trans. Sonics Ultrasonics su-22 (1975) 60.
[2] T.J. Mason, Ultrason. Sonochem. 10 (2003) 175.
[3] U.S. Bhirud, P.R. Gogate, A.M. Wilhelm, A.B. Pandit, Ultrason. Sonochem. 11 (2004) 143.
[4] E. Eisner, in: W.P. Mason (Ed.), Methods and Devices, Part B, vol. 1, Academic Press, New York, 1964.
[5] S. Sherrit, S.A. Askins, M. Gradziol, B.P. Dolgin, X.B.Z. Chang, Y. Bar-Cohen, in: Proceedings of the SPIE Smart Structures Conference, San Diego, CA 4701, Paper No. 34, 2002.
[6] J.W. Rayleigh (Strutt), The Theory of Sound, New York, 1945.
[7] A. Gallego-Juárez, G. Rodríguez-Corral, E. Riera-Franco de Sarabia, C. Campos-Pozuelo, F. Vázquez-Martínez, V.M. Acosta-Aparicio, Ultrasonics 38 (2000) 331.
[8] Y. Kikuchi, in: Y. Kikuchi (Ed.), Ultrasonic Transducers, Corona Publ. Co., Tokyo, 1969.
[9] K. Fukushima, J. Saneyoshi, Y. Kikuchi, Ultrasonic Transducers, in: Y. Kikuchi (Ed.), Corona Publ. Co., Tokyo, 1969.
[10] E.F. Neppiras, Ultrasonics 3 (1965) 9.
[11] L.G. Merkulov, A.B. Kharitinov, Sov. Phys. – Acoust. (1959) 183.
[12] Sin Pin Lin, J. Acoust. Soc. Am. 36 (1964) 5.
[13] L.D. Rosenberg (Ed.), High-intensity Ultrasonic Fields, Plenum Press, New York, 1971.
[14] R.P. Taleyarkhan, C.D. West, J.S. Cho, R.T. Lahey Jr., R.I. Nigmatulin, R.C. Block, Science 295 (2002) 1868.
[15] D.J. Flannigan, K.S. Suslick, Nature 434 (2005) 52.

1200 W ULTRASONIC LIQUID PROCESSOR

USER'S MANUAL

Notice of Liability:

Patent Protection:

This ultrasonic equipment is manufactured under one or more of the following: International Patent Application PCT/US2008/068697 and US Patent 7,156,201.

Section 1

Introduction

Contents

General User Information

Read This Manual First

Before operating your ultrasonic processor, read this User's Manual to become familiar with the equipment. This will ensure correct and safe operation. The manual is organized to allow you to learn how to safely operate this processor. The examples given are chosen for their simplicity to illustrate basic operation concepts.

Notes, Cautions and Warnings

Throughout this manual we use NOTES to provide information that is important for the successful application and understanding of the product.

In addition, we use special notices to make you aware of safety considerations. These are the CAUTION and WARNING blocks as shown here. They have important information that, if ignored, could have increasingly severe outcomes. These statements help you to identify and avoid hazards and recognize the consequences. One of three different symbols also accompany the CAUTION and WARNING blocks to indicate whether the notice pertains to a condition or practice, an electrical safety issue or an operator protection issue.

NOTE
Note statements provide additional information or highlight procedures.

CAUTION
Caution statements identify conditions or practices that could result in damage to the equipment or other property.

WARNING
Warning statements point out conditions or practices that could result in personal injury or loss of life.

Batch Mode Processor Schematic

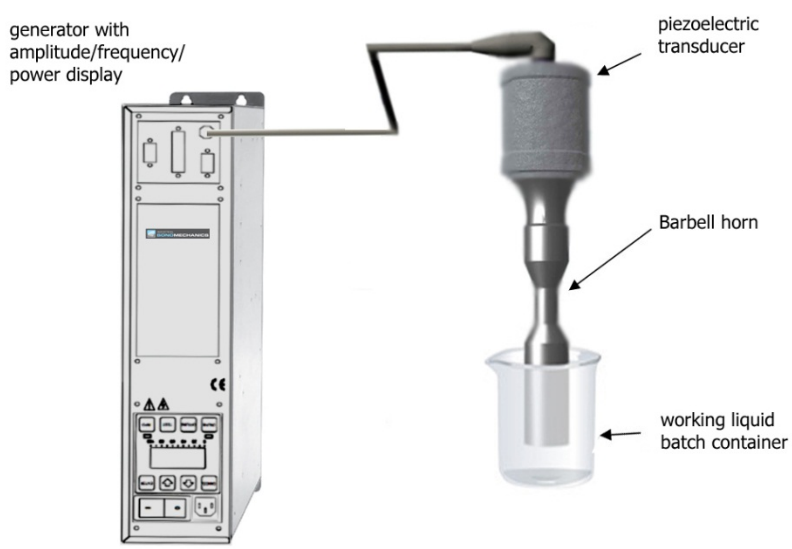

Figure 1 - 1. Schematic of the ultrasonic processor is illustrated in its batch mode configuration. Ultrasonic generator excites vibrations in the piezoelectric transducer, which are subsequently amplified by the Barbell horn. The horn delivers the ultrasonic energy to the liquid, contained in the beaker. The liquid may be cooled by using an ice bath or a water-cooled jacketed beaker.

Flow-Through Mode Processor Schematic

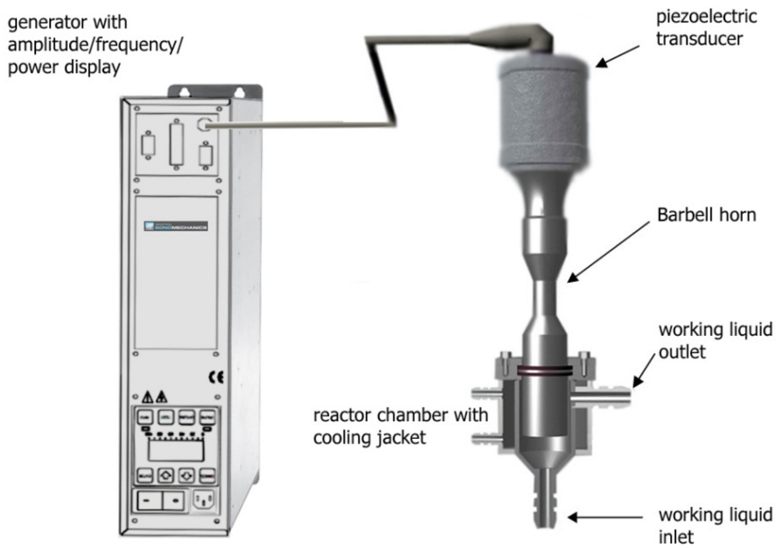

Figure 1 - 2. Schematic of the ultrasonic processor is illustrated in its flow-through mode configuration. Ultrasonic electric generator excites vibrations in the piezoelectric transducer, which are subsequently amplified by the Barbell horn. The horn delivers the ultrasonic energy to the liquid, flowing through the reactor chamber. The reactor chamber may include a cooling jacket. The working liquid inlet and outlet valves may be designed to enable adjustable, pressurized flow through the ultrasonic reactor chamber. The system can be configured to operate under pressures of up to 3 atmospheres.

CAUTION

The piezoelectric transducer must be cooled with forced air, supplied through the connection at the top (not shown in this schematic). The air must be filtered, dry and not warmer than 30 ^{0}C (86 ^{0}F). The air flow rate must be at least 0.5 m^{3}/min (18 cfm). Operating the unit without the cooling air may irreversibly damage the transducer and is strictly prohibited.

Generator Overview

This product has rugged internal ultrasonic generator circuitry and ensures a continuous resonant frequency lock during operation. The LCD display can be used to change the factory default ultrasonic settings for the drive signal phase delay angle, starting frequency and ramp-up or ramp-down parameters. This enables users to modify the generator performance to meet a wide variety of ultrasonic processing requirements. The generator's compact size allows multiple units to be placed into an industrial equipment cabinet. This generator includes an RFI line filter that passes strict CE test specifications for global applications.

Key Generator Features

- **Compact Enclosure Size** means that a very small footprint is required for the horizontal bench-top configuration. It is also available in a vertical back–plate mount configuration. 220/240VAC systems - come in a low profile (3.5”) compact enclosure. 110/120VAC systems - come in a high profile (5.25”) enclosure.
- **Pulse Width Modulation** incorporates circuitry giving the generator the ability to efficiently change the output amplitude.
- **Linear Ramp Soft-Start** circuitry allows the transducer/horn to be brought to operating amplitude smoothly, minimizing start-up surges and abnormal stress to the transducer, horn and generator.
- **Automatic Tuning** tracks the resonant frequency of the acoustic stack (transducer/horn assembly) and adjusts the generator output frequency to match it. This eliminates the need to manually tune the generator.
- **Line Voltage Regulation** automatically maintains constant amplitude regardless of line voltage deviation. The available output power is maintained with any voltage input within the specified range. This provides consistent system performance regardless of line voltage fluctuations. It also eliminates the need for bulky, external constant-voltage transformers.
- **Load Regulation** provides constant ultrasound amplitude automatically regardless of power draw. The ultrasonic output amplitude level is held to within ±1%.
- **High Line-Voltage Power Supply** means that 220/240VAC systems will operate worldwide at the local high line voltage level, whether it is 200VAC @ 60Hz in Japan, 240VAC @ 50Hz in Europe or 208VAC @ 60Hz in the United States. There are no internal transformer taps to change for world-wide operation.
- **Flow-Through Cooling Tunnel** with a high-performance heat-sink and thermostatically controlled fan reduces thermal gradients and increases component life.
- **AC Power Inrush** protection reduces electrical stress on the internal components by protecting them from AC power start-up transient current surges.
- **Multiple Electronic Overload** protection circuits prevent instantaneous component failure in the event of extreme output overload conditions.
- **CE Certification** means that the system meets the required European standards to be sold and used in Europe.

Section 2

Health and Safety

General Considerations

Please observe these health and safety recommendations for safe, efficient, and injury-free operation of your equipment. A typical system consists of a generator, remote button switch, connecting cables, and the probe assembly, which includes the transducer and horn.

- **Proper Installation** - Operate system components only after they are properly installed and checked.
- **No Unauthorized Modifications** - Do not modify your system in any way unless authorized to do so by the manufacturer. Unauthorized modifications may cause injury to the operator and/or equipment damage. In addition, unauthorized modifications will void the equipment warranty.
- **Keep the Cover On** - Do not remove any equipment cover unless specifically directed to do so by the manufacturer. The generator produces hazardous electrical voltages which could cause injury.
- **Grounded Electrical Power** - Operate this equipment only with a properly grounded electrical connection. (See *Electrical Safety*, and the grounding instructions below.)
- **Comply with Regulations** - You may be required to add accessories to bring the system into compliance with applicable OSHA regulations for machine guarding and noise exposure.

IMPORTANT

Never operate the generator with the cover off. This is an unsafe practice and may cause injury.

CAUTION

Parts sometimes vibrate at audible frequencies. Wear ear protection to reduce annoying or uncomfortable sounds. In addition, sound absorbing materials, enclosures or sound deflectors may be installed to reduce the noise level.

Electrical Safety

Domestic and International Power Grounding

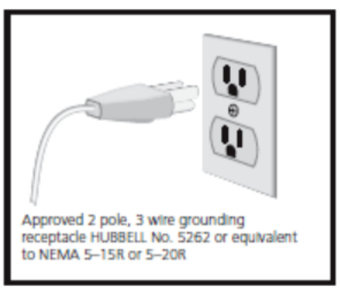

For safety, this product has a three-wire, grounding-type power cord. Figure 2 - 1 illustrates the appropriate electrical outlet to use with the power cord that is included with 120 V rated generators shipped to North America.

Figure 2 - 1. Example of 120 Volt, Grounded, 3-Prong Receptacle

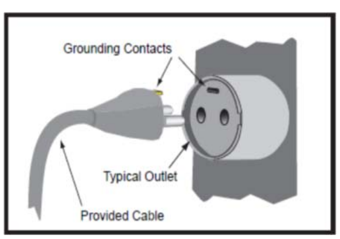

The power cable normally provided for international use is compatible with the power outlet used in many Continental European countries (Refer to Figure 2 - 2.)

Figure 2 - 2. International 220/240V Grounding

CAUTION

If you have a two-prong electrical receptacle, we strongly recommend that you replace it with a properly grounded three-prong type. Have a qualified electrician replace it following the National Electric Code and any local codes and ordinances that apply.

CAUTION

If there is any question about the grounding of your receptacle, have it checked by a qualified electrician. Do not cut off the power cord grounding prong, or alter the plug in any way. If an extension cord is needed, use a three-wire cord that is in good condition. The cord should have an adequate power rating to do the job safely. It must be plugged into a grounded receptacle. Do not use a two-wire extension cord with this product.

SECTION 3

Generator Installation

Unpacking

Carefully open your shipping container, and make sure it contains the items shown on the shipping documents. Inspect all items, and report any damage immediately.

Placing

Vertical Panel Mount Chassis

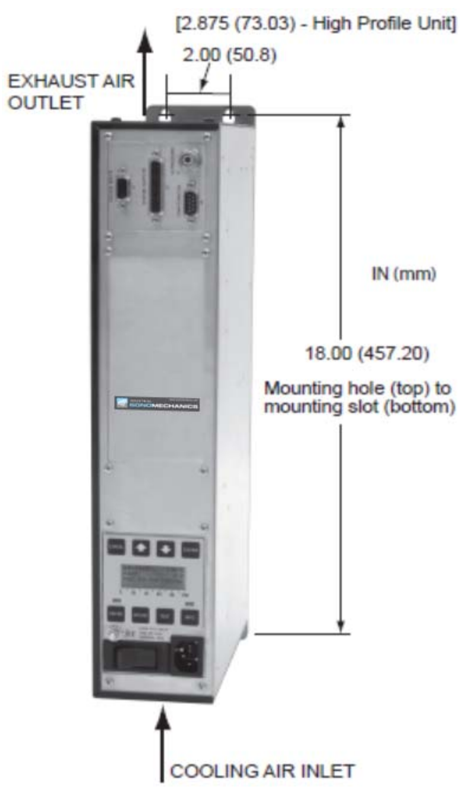

Make certain the generator placement and cable routing allow for easy access and that they do not interfere with normal operation. The operator should have unobstructed access to any control switches and should have a clear view of the LCD panel, and generator status LEDs.

Hang the generator securely by the upper and lower holes in the mounting panel with its control panel easily accessible as shown in Figure 3-1. Allow at least 5 inches (13 cm) of space on the top and bottom of the generator chassis for air circulation. If the generator is installed inside an enclosure with a front door, be sure to allow at least 3 inches (8 cm) clearance behind the door for the system cables.

CAUTION

Allow 5 inches for air ventilation at the cooling air inlet and at the exhaust air outlet. The fan draws in fresh air to cool the internal components, reduce thermal gradients and increase component life.

Figure 3 - 1. Vertical Panel Mount Chassis Placement (Low profile unit shown with optional panel mounting plate.)

Horizontal Panel Mount Chassis

Generator placement and cable routing should permit easy access and not interfere with normal system operation. Allow at least 5 inches (13 cm) of space on both ends of the generator chassis for air circulation. Allow a 3 inch space (8 cm) in the front of the chassis for cable clearance.

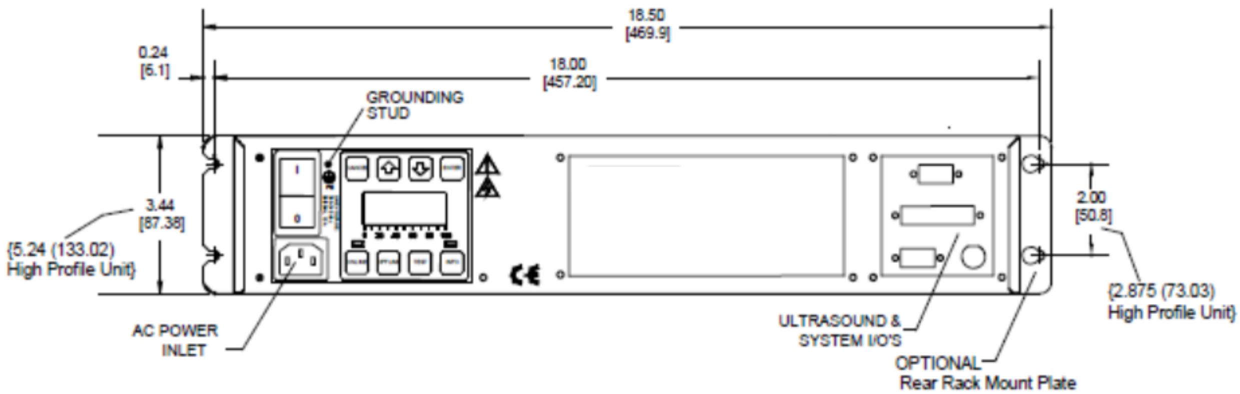

Figure 3 - 2. Horizontal Panel Mount Chassis (low profile unit shown with optional rear rack mount plate)

RFI Grounding

In addition to the safety considerations previously mentioned, proper grounding at the generator power cord is essential for the effective suppression of electrical noise or RFI (Radio Frequency Interference). Every ultrasonic generator contains a RFI filter which blocks noise on the AC power line from entering the system control circuitry. This filter also prevents ultrasonic frequency noise from being fed back into the AC power line. In order for the RFI filter to operate properly, it is necessary to correctly ground the system. Run a grounding wire from the ground stud connection (see Figure 3 - 2) to the nearest grounded metal pipe or equivalent earth ground, and secure it with a ground clamp.

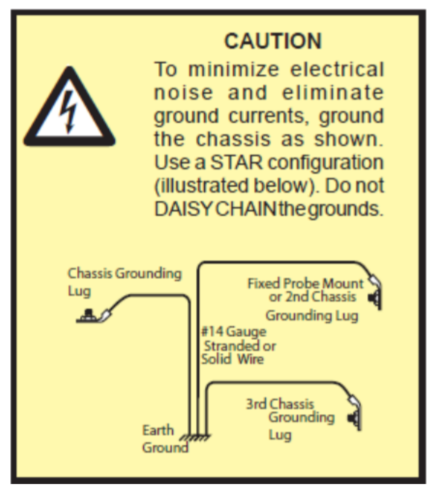

Connecting Cables (Quick Start Guide)

The connections are the same for both the vertical and horizontal generator configurations. However, the panel location of the connectors differs between the two chassis styles. Details about the various system connectors are covered in Section 4.

Power Cords

The 3-wire grounding AC line cords supplied with the standard generators are matched to the ultrasonic output power rating and the continent of specified use.

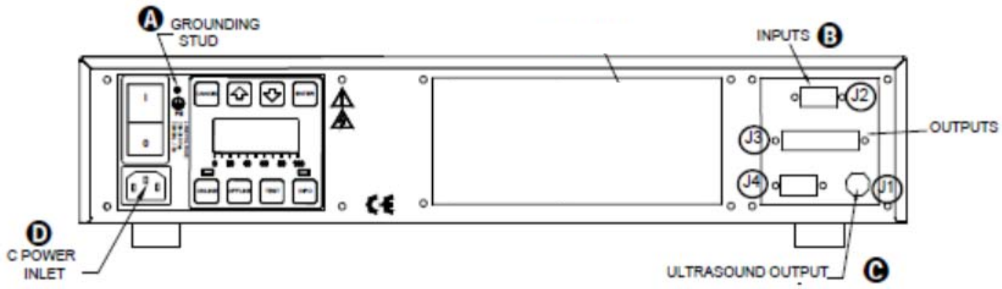

Figure 3 - 3. Horizontal Bench Generator

> **NOTE**
> Horizontal bench generator is shown for reference. Vertically mounted units use the same connections, but those connections have a different orientation. (See Figure 4-1.)

Connecting System Cables – Standard Transducer

(See Figure 3 - 3 for connection locations.)

Step 1. Ground the generator chassis using the supplied 14 - Gauge wire - attaching it to the grounding stud.
A in Figure 3 - 3.

Step 2. Attach the included cable with remote button switch to the generator's input HD - 15 connector, J2 on the I/O panel.
B in Figure 3 - 3.

Step 3. Attach the high voltage coax cable from the transducer to the ultrasound output connector J1.
C in Figure 3 - 3.

Step 4. Power cords with an IEC connector are always supplied with bench chassis style and 240 V rated generators. Connect the AC power cord to the generator IEC power inlet connector, and plug the other end into an approved AC outlet. 120 V rated systems have permanently mounted power cords.
D in Figure 3 - 3.

Connecting System Cables – Handheld Transducer

(See Figure 3 - 3 for connection locations.)

Step 1. Ground the generator chassis using the supplied 14 - Gauge wire - attaching it to the grounding stud.
A in Figure 3 - 3.

Step 2. Attach the handheld transducer's HD-15 system input connector to the generator's input HD - 15 connector, J2 on the I/O panel.
B in Figure 3 - 3.

Step 3. Attach the high voltage coax cable from the transducer to the ultrasound output connector J1.
C in Figure 3 - 3.

Step 4. Power cords with an IEC connector are always supplied with bench chassis style and 240 V rated generators. Connect the AC power cord to the generator IEC power inlet connector, and plug the other end into an approved AC outlet. 120 V rated systems have permanently mounted power cords.
D in Figure 3 - 3.

SECTION 4

Generator Connections

Panel Layout Overview

Vertical Panel Mount Chassis

This section provides an overview of the vertical panel mount chassis panel layout, which includes panel areas dedicated to various standard system functions and options. Figure 4 - 1 illustrates the panel layout for a vertical panel mount chassis.

AC Power Inlet Panel

A IEC Power Inlet Connector – Attaches to an IEC style power cord. 120 V rated systems have permanently mounted power cords.

B Power Switch / Circuit Breaker – Used to switch system power **ON** and **OFF**.

C Chassis Ground Stud – Chassis connection for a protective earth ground.

System Status Control Panel and Display

D **INFO** Key.

E System Operating Mode Keys and Status LEDs.

F Power Output Level Scale.

G 4 - line LCD Display.

H Display Control Keys.

Section 5 provides descriptions of these basic user controls and status LEDs.

J Blank Panel.

System I/O Panel

K System Input Connector – Connections for system control input signals

L System Output Connector – Connections for system status output signals

M Ultrasound Output Connector – Coaxial high voltage connection to ultrasonic transducer

N Configuration Port Connector – Digital control port to modify system parameters

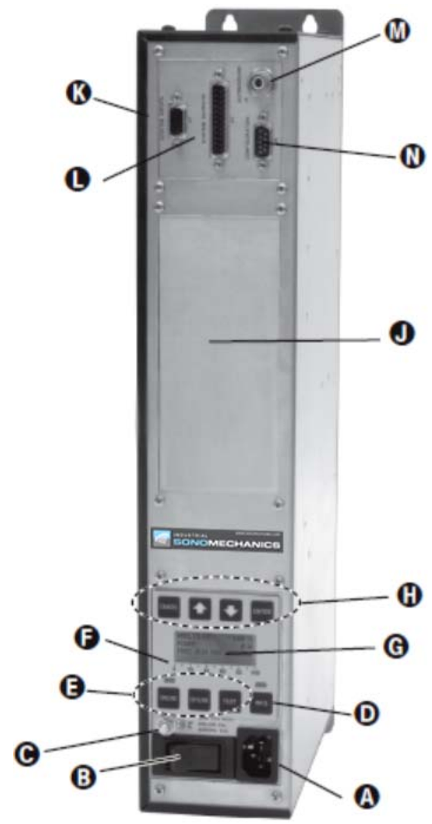

Figure 4 – 1. Panel Layout - Vertical Panel Mount Generator

AC Power Inlet Panel

The standard AC power inlet panel is described in this section.

IEC AC Power Inlet Connector

The IEC AC power inlet connector mounted on the system AC power inlet panel requires a properly configured IEC compliant power cord, which enables worldwide system operation by simply changing the power cord.

Low profile systems are equipped with a 10 Amp rated IEC inlet connector. The high profile systems include a 16/20 ampere rated IEC inlet connector.

An appropriately rated power cord must be securely attached to the system’s IEC inlet connector. If the correct power cord configuration is not included with the system for the local AC power outlet at your location, an appropriate IEC power cord should be available from a local electrical parts supplier.

Power Switch/Circuit Breaker

The power switch/circuit breaker has a rocker type actuator switch that will activate or deactivate the AC power to the system. The power **ON** position is marked with the internationally recognized **I** symbol, the power **OFF** position is marked with the **0** symbol. This power switch also integrates an appropriately sized over-current protection circuit breaker function in the generator.

If an over-current condition trips the circuit breaker, it will automatically switch to the **OFF** position. If the overload current that caused the circuit breaker to trip is due to a transient condition, the circuit breaker can be reset by switching the actuator back to the **ON** position. If when resetting the circuit breaker after it has tripped, it immediately trips again, there is likely an internal system malfunction, and the generator will require service.

Do not repeatedly try to reset the circuit breaker. If it trips, this will only cause more damage to the generator.

Chassis Ground Stud

The chassis ground stud is used to attach a protective earth ground to the generator. This will aid in the suppression of electrical interference or radio frequency interference (RFI) that is common in an industrial environment. The chassis ground stud is **C** in Figure 4 - 1. Proper system grounding is discussed in Section 3.

Ultrasound Output Connector

The ultrasound output connector used with all standard generators is a high voltage (5000V) coaxial style SHV-BNC connector. This connector provides superior shielding of electrical noise, compared to other types of connectors. The ultrasound output connector mates with fully shielded coaxial ultrasound cables that are secured with a simple and reliable quarter-turn bayonet style attachment mechanism.

Figure 4 – 2. Ultrasound Output Connector

CAUTION

The ultrasonic output from this connector (that drives the attached ultrasonic load) is a very high AC voltage. At high power levels this can exceed 2 amperes of current and must be securely terminated via the ultrasound cable for safe operation. Use original equipment manufacturer ultrasound cables for safe and reliable system operation. Improperly assembled ultrasound cables can result in high voltage arcing and will destroy the ultrasound connectors.

Do not use your generator if there is any evidence of arcing (black carbon deposits) on either the ultrasound output connector or the ultrasound cable connectors.

SECTION 5

Generator Status and Controls

Control Panel and Display Overview

This section provides an overview of the control panel and display. The panel has two functions:
1) monitoring, using the LED status lights, and
2) display and control, using the Display Controls with the LCD display.
Figure 5-1 identifies the primary parts of the panel that are described in the pages that follow.

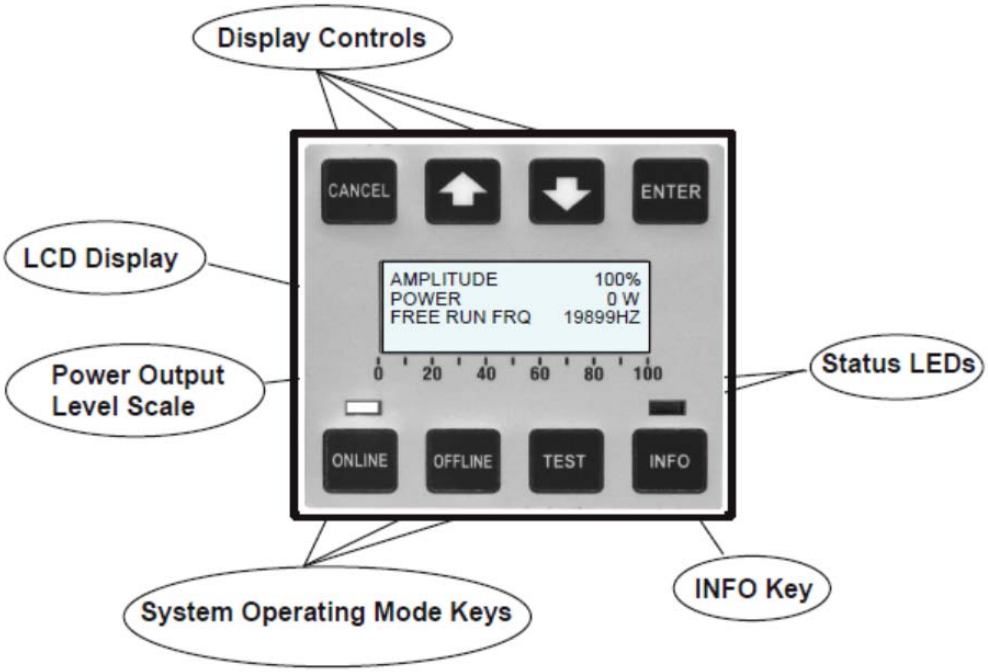

Figure 5 – 1. Control Panel and Display

Display Controls

The four keys on the top of the panel provide control for the LCD display.

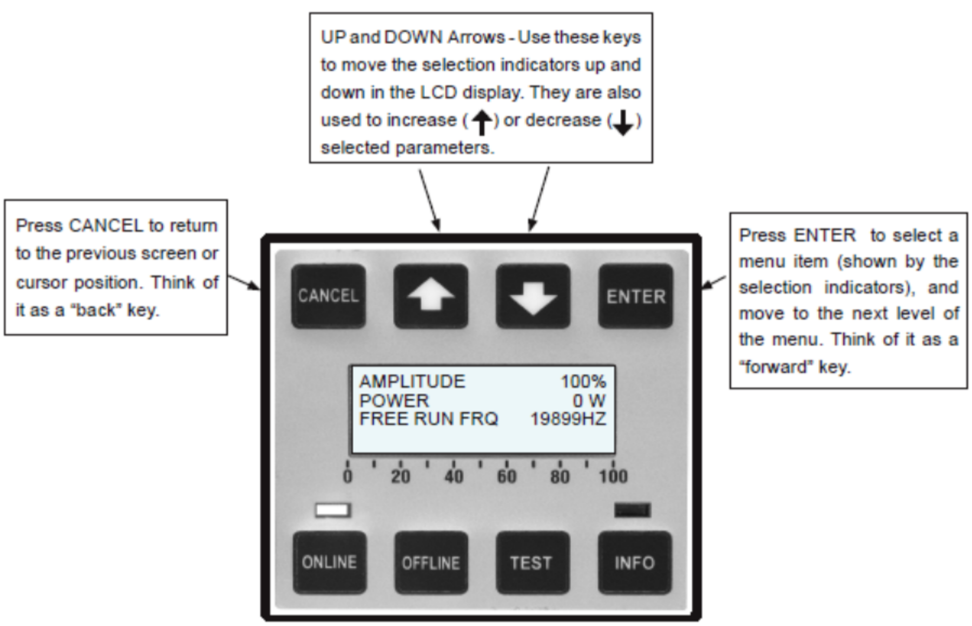

Figure 5 – 2. Control Panel Display Controls

LCD Display

The 4-line LCD display gives the operator a basic interface for generator monitoring and control. Figure 5 - 3 illustrates a typical view of the display just after the generator has been powered up.

Figure 5 – 3. Display After Power-up

Power Output Level Scale

Figure 5 - 4 shows what a display might show when the TEST key is pressed. In this example, the generator is producing an ultrasound signal at approximately 90% of its capacity.

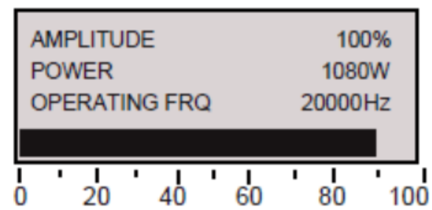

Figure 5 – 4. Power Output Level Scale

System Operating Mode Keys

The system operates in three basic modes: **ONLINE**, **OFFLINE**, and **TEST**.

Figure 5 - 5 shows the mode keys at the bottom of the control/display panel. Also note the location of the left and right status LEDs.

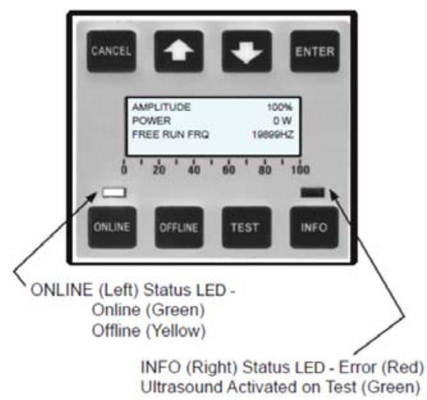

Figure 5 – 5. Operating Mode Keys and LEDs

ONLINE

Press the **ONLINE** key to operate in the online mode.

In this mode, ultrasound can be activated. The LED above the **ONLINE** key is GREEN when the generator is online.

OFFLINE

Press the **OFFLINE** key to operate in the offline mode. Select this mode during your process setup without ultrasound activated.

In the offline mode, ultrasound cannot be activated. The LED above the **ONLINE** key is YELLOW when the generator is offline.

TEST

Press the **TEST** key to operate in the test mode.

In this mode, ultrasound output will activate for the time that the **TEST** key is pressed. In test mode, the right status LED changes from being GRAY (Off) to GREEN. This mode is typically used when setting up an application. It is not normally used during an actual process.

NOTE

Use the test mode only when:
1) The ONLINE GREEN LED indicates that the generator is online, **and**
2) When the ultrasound output cable at J1 is connected to a probe/stack.

INFO Key

Press the **INFO** key.
Figure 5 - 6 shows what the **INFO** display looks like.

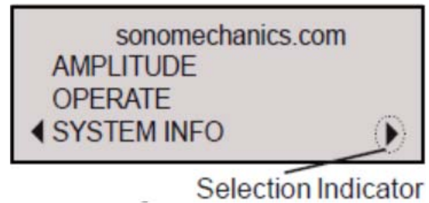

Figure 5 – 6. INFO Display

SYSTEM INFO

Select **SYSTEM INFO** (See the selection indicators shown in Figure 5 - 6.), and press **ENTER** to view:

- Firmware revision, and
- System identification including model number

See Figure 5 - 7 for a **SYSTEM INFO** example.

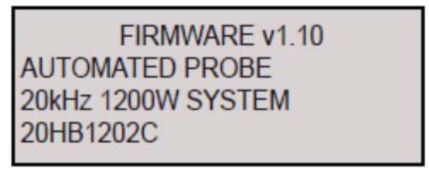

Figure 5 – 7. SYSTEM INFO Example Display

OPERATE

Select **OPERATE**, and press **ENTER** to view:

- Amplitude,
- Power, and
- Free Run Frequency

These values reflect what the parameters were during previous operation.

See Figure 5 - 8 for an example of the **OPERATE** display.

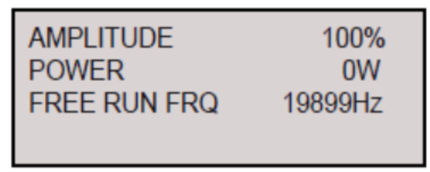

Figure 5 – 8. OPERATE Example Display

AMPLITUDE

Select **AMPLITUDE**, and press **ENTER** to view, and to change the amplitude setting.

Amplitude is a value with a minimum of 20% and a maximum of 100%.

See Figure 5 - 9 for an example of the **AMPLITUDE** display.

Use the **UP** and **DOWN** arrow keys to set the desired value.

Make the change, press **ENTER**, and **ENTRY ACCEPTED** will be displayed confirming that the change was made.

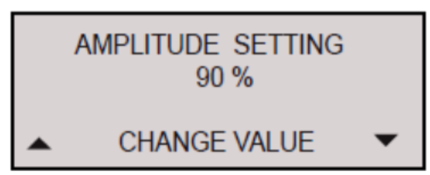

Figure 5 - 9. AMPLITUDE Example Display

NOTE

Pressing the UP arrow key when 100% is displayed will change the percentage to 20%.
Pressing the DOWN arrow key when 20% is displayed changes the percentage to 100%.

Status LEDs

Status LEDs provide operating status for system power, the system operating mode and system output status as described below:

INFO Status Indicator

(*On the panel's right side*)

GREEN = Generator ultrasound output is activated.

RED = Could be due to one of the three conditions listed below:

Red Fast Flashing (4 flashes per second) - Indicates an under or over voltage condition in the AC line voltage connected to the generator. If the proper voltage range is not maintained, a line voltage fault will inhibit system operation, and the **INFO** status indicator will flash approximately four times per second. This flashing may occur momentarily when the system power is switched off and does not indicate a problem or malfunction.

RED Slow Flashing (1 flash per second) - Indicates that the DC bus capacitors are not charged to the proper voltage level. This is a normal condition whenever the system is switched on. The DC bus capacitors will normally charge to the proper voltage level within 10 seconds. Then the **ONLINE** indicator should switch to a steady GREEN (if **ONLINE**), or YELLOW (if **OFFLINE**). If the slow flashing indication continues and does not stop, an internal problem is preventing the DC bus capacitors to charge to the proper voltage level. The system will require service, if this fault condition continues to flash and does not stop. Do not allow the system to operate in this fault condition for an extended period of time. There is likely a shorted internal component causing this type of fault condition, and some internal parts might get very hot as a result. If this fault occurs, switch the unit off, and return the generator for service.

Steady RED (No flashing) - Indicates that there is a problem with one of the DC voltage outputs on the system control power supply. If this fault condition occurs, switch off the system power, and return the generator for service.

ONLINE Status Indicator

(*On the panel's left side*)

GREEN = ONLINE

Generator ultrasound output is activated.

YELLOW = OFFLINE

Generator ultrasound output is deactivated.

Some system fault conditions will reset automatically. A system overload inhibits the ultrasound output when it occurs, but will automatically reset when the next ultrasound activation signal begins.

If an overtemperature condition is the cause of the fault indication, the fault condition will automatically reset when the system cools. Most other system fault conditions will not reset. In those cases the generator needs servicing.

SECTION 6

System Assembly, Testing and Operation

Ultrasonic Transducer

Ultrasonic transducers are devices used to convert electric energy coming from an ultrasonic generator into mechanical energy in the form of ultrasonic vibrations. Standard piezoelectric ultrasonic transducer supplied with the system is shown in Figure 6 - 1. Handheld version of this transducer is also available.

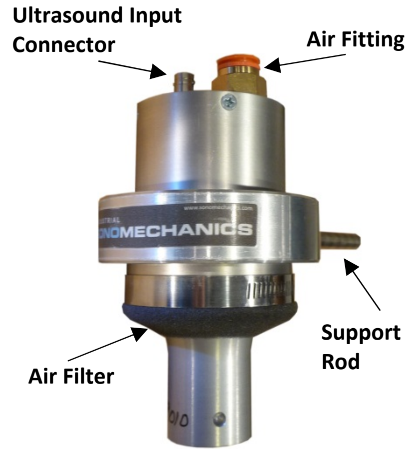

Figure 6 - 1. Piezoelectric Transducer

Air Fitting

In continuous duty operation, it is important to keep the transducer cool with flowing air. Use the air fitting to connect the cooling air source to the transducer. The cooling air must be filtered, dry and not warmer than 30 ^{0}C (86 ^{0}F). The air flow rate must be at least 0.5 m^3/min (18 cfm). Operating the unit without the cooling air may irreversibly damage the transducer and is strictly prohibited.

Air Filter

Round, 1/8" thick polyurethane foam filter with 60 pores per inch (ppi) is attached to the bottom of the transducer with a C-clamp in order to prevent any liquid from splashing into the transducer chassis through air outlet holes.

Support Rod

The support rod is screwed into the transducer chassis and is used for positioning the transducer in a clamp holder on a support stand.

Ultrasound Input Connector

The ultrasound input connector is a high voltage (5000V) coaxial style SHV-BNC connector. This connector provides superior shielding of electrical noise, compared to other types of connectors. The ultrasound input connector mates with fully shielded coaxial ultrasound cables that are secured with a simple and reliable quarter-turn bayonet style attachment mechanism.

CAUTION

The ultrasonic input through this connector (that drives the attached ultrasonic load) is a very high AC voltage. At high power levels this can exceed 2 amperes of current and must be securely terminated via the ultrasound cable for safe operation. Use original equipment ultrasound cables for safe and reliable system operation. Improperly assembled ultrasound cables can result in high voltage arcing and will destroy the ultrasound connectors.

Do not use your transducer if there is any evidence of arcing (black carbon deposits) on either the ultrasound output connector or the ultrasound cable connectors.

Ultrasonic Horn

Liquids exposed to high-intensity ultrasound undergo ultrasonic cavitation, which produces violently and asymmetrically imploding bubbles and causes micro-jets that create extreme mechanical shear forces. These forces are responsible for the well-known ability of ultrasound to facilitate many physical and chemical processes. In order to produce sufficient cavitation intensity, ultrasonic transducers are equipped with high-gain acoustic horns, which amplify the vibration amplitudes generated by the transducers and deliver the ultrasonic energy to working liquids.

CAUTION

NEVER clamp the horn in a vise. The resulting scratches or gouges in the surface are stress risers which may result in cracks.

Attaching the Mounting Stud to the Horn

1. Inspect the stud for cracks or damaged threads. Replace the stud if it is cracked or otherwise damaged.

2. Remove any foreign matter from the threaded stud and the mating hole.

3. Thread the mounting stud into the input* end of the horn and lightly tighten using an Allen wrench in the socket head of the mounting stud.

*Always assemble the mounting stud that mates the transducer and the horn to the input end of the horn first.

NOTE
Do not apply any grease to the stud threads or the tapped hole. This may cause the stud to loosen. If the stud wanders within the joint, it can vibrate, resulting in excessive heat. In some cases, this can melt the tooling material.

Attaching the Horn to the Transducer

1. Inspect all surfaces to be joined for stress cracks, chips, or gouges. Any of these irregularities will affect operation and could lead to further equipment damage.

2. Ensure that the mating surfaces of the two components are clean and smooth. These surfaces must make intimate contact for the mechanical energy to pass from one component to the next. Pitting or a buildup of old grease and dirt on a mating surface will interfere with the energy transfer and reduce the delivered power.

3. Make sure that the stud in the horn is tight. See the preceding mounting stud assembly instructions.

4. Remove any foreign matter from the threaded stud and mating hole.

5. Apply an extremely thin layer of a high temperature, high pressure silicon grease to the surface that mates with the horn. The grease will allow both surfaces to intimately mate and become acoustically transparent which improves the energy transfer. We recommend Dow–Corning #4 (or #111 as an alternate). If you cannot use silicon–based grease in your facility, petroleum–based grease may be used. However, it is likely to leave carbonaceous deposits on the surface, and require more frequent joint maintenance. Failure to follow these instructions may result in the mating surfaces bonding and difficulty removing the horn from the transducer.

6. Thread the components together and tighten to the following torque specifications: 420 In-lb (35 Ft-lb or 47.5 N-m). Use spanner wrenches on components with spanner wrench holes (we recommend the following spanner wrenches: for components with diameters 31 - 75 mm - Armstrong Tools, part # 34-358; 19 – 30 mm - Armstrong Tools, part # 34-354) or an open end wrench on components with wrench flats. See Figure 6 - 2 for the correct procedure. Be careful not to over-tighten.

CAUTION
Never leave a horn or booster assembly hand tight. Torque it to the proper specifications before proceeding. If the assembly is installed without being properly torqued down, the assembly may vibrate severely, damaging the mating surfaces and causing the generator to overload.

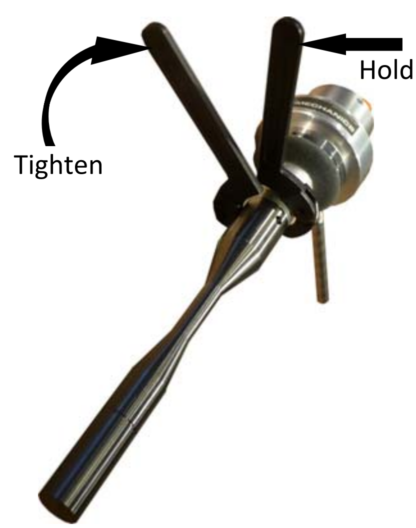

Figure 6 - 2. Transducer – Horn Assembly Procedure

Detaching the Horn from the Transducer

On all transducers and horns with spanner wrench holes, use only the correct size spanner wrenches to provide sufficient torque to loosen a joint. See Figure 6 - 3.

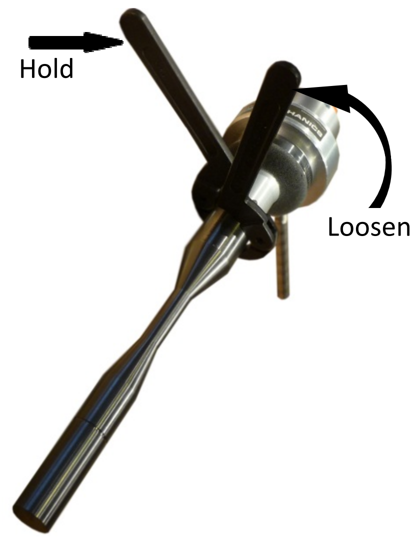

Figure 6 - 3. Transducer – Horn Disassembly Procedure

Removing the Mounting Stud from the Horn

Only use an Allen wrench of the correct size in the socket head's stud to remove the stud from the horn.

Testing the System

Step 1. Plug in the AC line cord to the correct AC power outlet.

Step 2. Connect the included cable with remote button switch to System Input Connector at the generator (**K** on Figure 4 – 1).

Step 3. Using the high-voltage coaxial cable, connect the ultrasound input connector at the transducer (Figure 6 – 1) to the ultrasound output connector at the generator (**M** on Figure 4 – 1). The horn should already be attached to the transducer.

Step 4. Insert the output tip of the ultrasonic horn into a liquid to the depth of at least 5 centimeters.

Step 5. Push the AC Breaker/Switch **A** to the **ON** position.

Step 6. The **INFO LED** on the panel **B** should flash **RED** for 5 – 10 seconds. Then, it turns off (GRAY), and the LED above **ONLINE C** turns GREEN (if **ONLINE**).

Step 7. **ONLINE/OFFLINE** Tests

a. Press the **OFFLINE** key. The LED status indicator **C** turns to YELLOW.

b. Press the **TEST** key. The ultrasound should not activate.

c. Press the **ONLINE** key. The **LED** status indicator **C** will be GREEN.

d. Press and hold the **TEST** key. Ultrasound should activate. The display shows amplitude, power and operating frequency. The segmented power bar graph should also appear. See the sample screen display - Figure 6 - 5. If you are using a handheld transducer, you may feel a slight vibration or sensation in your hand. This is normal. There should not be any loud or unusual noise.

e. Release the **TEST** key. Ultrasound will deactivate.

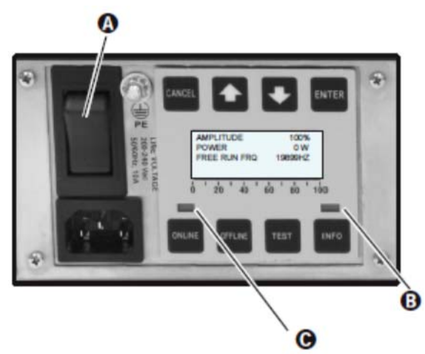

Figure 6 - 4. Control Panel at Startup

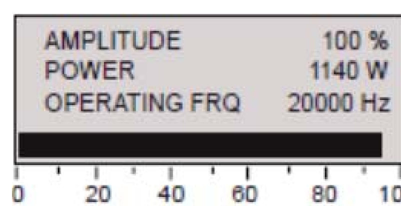

Figure 6 - 5. TEST Screen Display Sample

Running/Stopping the System

Running the System

Press the button on the remote button switch once. If you are using a handheld transducer, press the activation switch on its side. Ultrasound should activate. The display shows amplitude, power and operating frequency. The segmented power bar graph should also appear. See the sample screen display - Figure 6 - 5.

CAUTION

Any unusually loud noise from the trandsucer/horn indicates that they were improperly assembled

Stopping the System

Press the button on the remote button switch once again. If you are using a handheld transducer, release the activation switch on its side. Ultrasound will deactivate.

Alternatively, Press the **OFFLINE** key (**E** in Figure 6 - 6), and the ultrasound signal will deactivate.

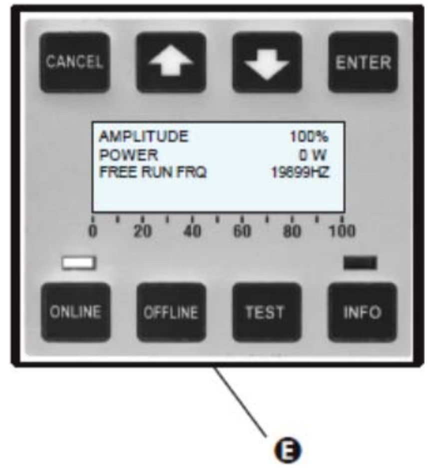

Figure 6 - 6. Stop Ultrasound Output

Reactor Chamber

During a flow-through ultrasonic process, it is important to make sure that all working liquid is directed through the active cavitation zone, otherwise inhomogeneous processing may occur, leading to a lower-quality product. A reactor chamber is utilized for this purpose. The chamber commonly includes a water-cooling jacket that helps maintain the temperature of the working liquid at the desired level. Figure 6 – 7 shows a Reactor Chamber - Half-wave Barbell Horn (HBH) Assembly drawing. Other types of Barbell horns, such as the Full-wave Barbell horn (FBH) or the Half-wave Barbell horn with an Opening (HBHO) may also be utilized with the same reactor chamber.

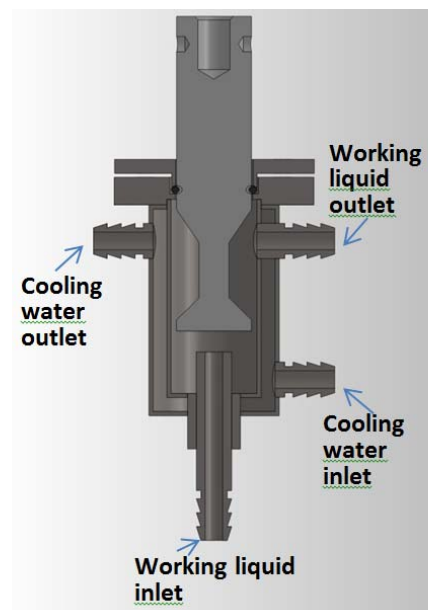

Figure 6 - 7. Reactor Chamber Assembled with a Half-wave Barbell Horn

Assembling the Reactor Chamber with a Barbell horn

Step 1. Assemble the transducer with the horn and secure by the side arm in a support stand.

Step 2. Insert six bolts with washers through the holes in the upper ring of the reactor chamber.

Step 3. Lift the upper ring (with the horn passing through its center opening) such that the ring is above the horn's nodal point.

Step 4. Place a rubber O-ring into the groove at the nodal point of the horn.

Step 5. Lift the reactor chamber (with the horn passing into its internal area) such that the bolts match up to the six threaded holes in the corresponding ring at the top of the chamber.

Step 6. Tighten the bolts evenly, maintaining the same tension on all sides.

Step 7. Provide separate support for the reactor chamber assembly. Its weight should NOT be supported by the O-ring at the horn.

Figure 6 - 8. Reactor Chamber – Horn Assembly Procedure

SECTION 7

Troubleshooting

No Ultrasonic Output

Transducer

Make sure that the high-voltage coaxial cable is connected to the transducer's ultrasound input connector (Figure 6 – 1) and the generator's ultrasound output connector (**M** on Figure 4 – 1). Also, make sure the horn and the transducer were properly assembled.

Cables

Make sure that both the high-voltage coaxial cable and the cable with remote button switch (or the handheld transducer's HD-15 input connector) are securely connected.

Place the generator **OFFLINE**, and check the coaxial cable for any signs of damage that may result in an open circuit preventing the cable from transmitting the generator-to-probe signal.

Generator

The generator will not produce an output signal when triggered if it is offline. Make sure that the **ONLINE** status LED is GREEN.

If the generator is **OFFLINE**, press the **ONLINE** key. See Figure 7 - 1.

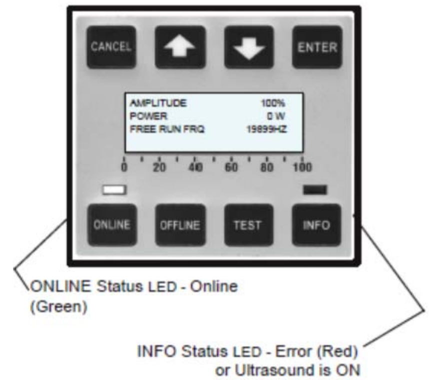

Figure 7 - 1. Status LEDs

INFO Status LED: RED

RED - Fault Condition

When the **INFO** status LED is RED (Figure 7 - 1) there is a fault condition.

Overloads

Overload - Frequency

There are two types of Overload-Frequency faults:

Frequency Failed, and *Frequency Lost.*

Other overloads are:

Overload - Peak, and **Overload - Average** (power above rating)

When an overload occurs, it will automatically reset when the next ultrasound activation signal begins.

If the condition persists, put the generator **OFFLINE** and:

1. Check the system: including cables, the transducer and the horn. Replace existing components with ones you know are reliable.

2. Press the **ONLINE** key to place the generator online, and see if the fault condition has been corrected.

Overtemperature

When the system overheats, there is an overtemperature condition that will cause the fault. When the system cools, the system automatically resets.

NOTE

Be sure to press the ENTER key to clear the fault message and the INFO status LED.

The System Latch Reset Input will only clear the Output I/O faults.

If a fault occurs while using the TEST key, the TEST key will not function again until the ENTER key has first been pressed (to clear the fault message).

SECTION 8

Generator Specifications

Drawings

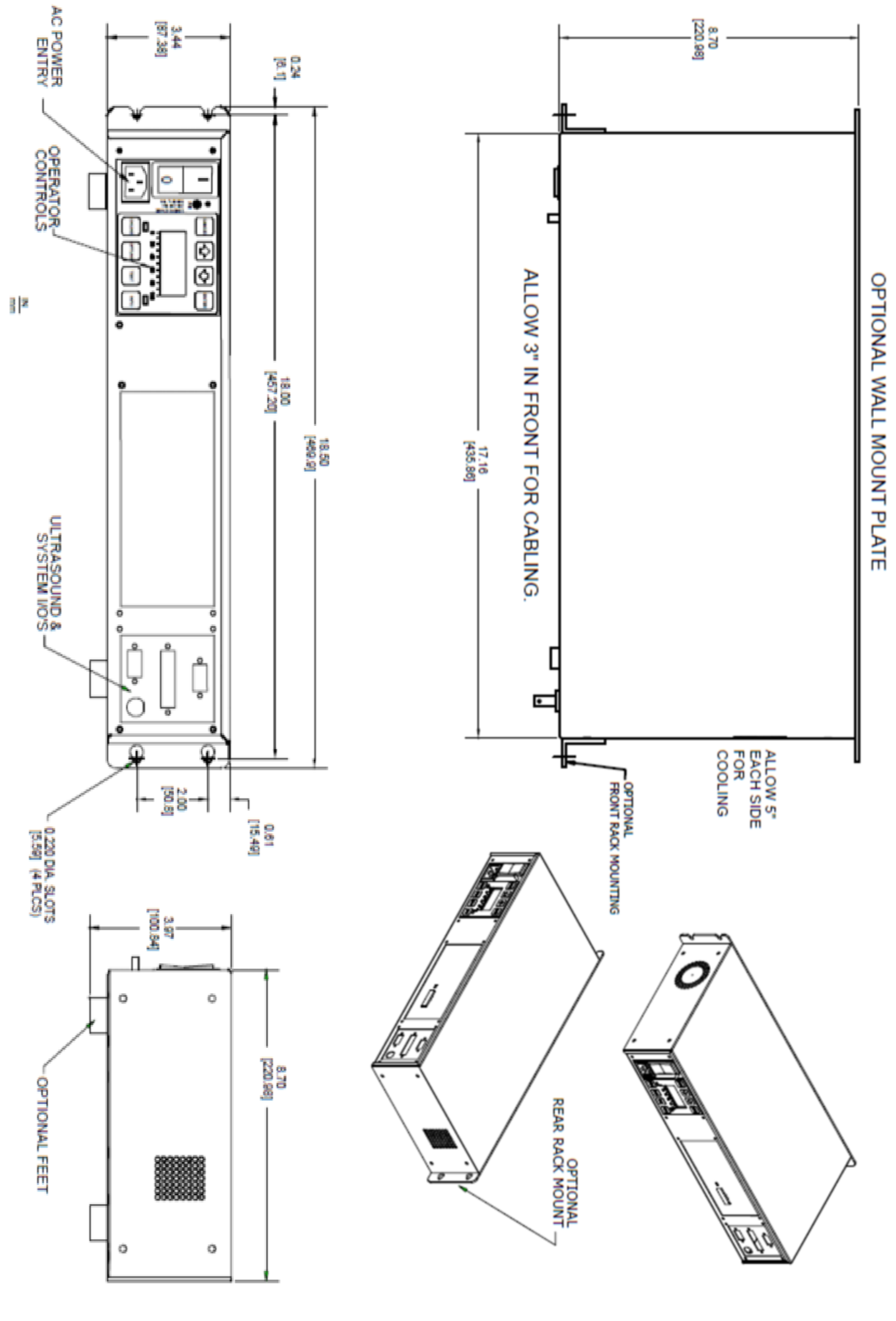

Figure 8 - 1. Low Profile Chassis Drawing

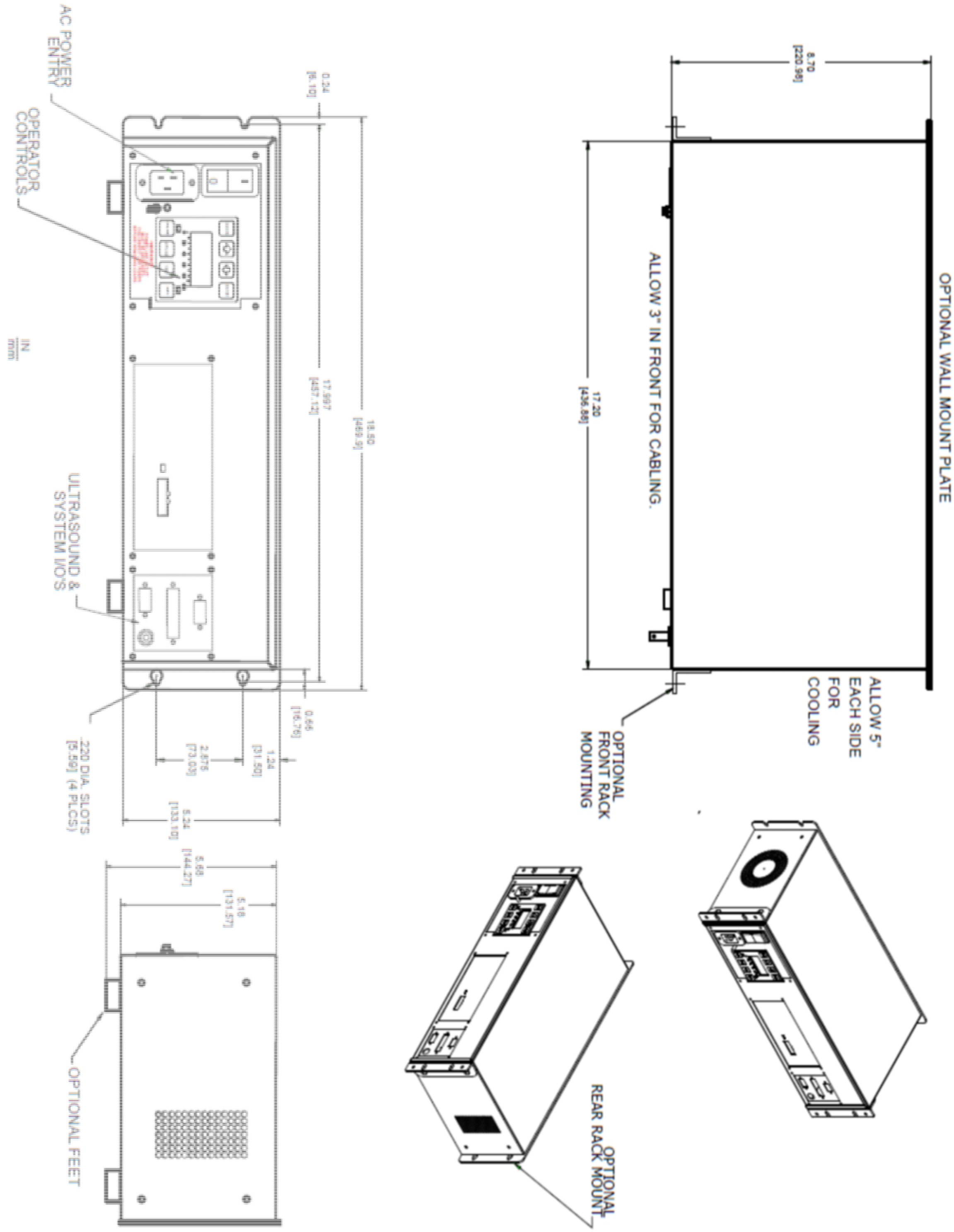

Figure 8 - 2. High Profile Chassis Drawing

Weight:

Low Profile Unit: 24 pounds (10.9 kg)
High Profile Unit : 30 pounds (13.6 kg)

Shipping: Add 5 pounds (2.3 kg) to unit weight for packing materials

AC Power Requirement:

Low Profile Unit: 200-240V 50/60 Hz @ 8 Amps
High Profile Unit : 100-120V 50/60 Hz @ 15 Amps

Operating Environment

Operate the generator within these guidelines:
Temperature: 40°F to 100°F (+5°C to +38°C)
Altitude: 15,000 ft (4572 m)
Air Particulates: Keep the equipment dry. Minimize exposure to moisture, dust, dirt, smoke and mold.
Humidity: 5% to 95% non-condensing @ +5°C to +30°C

Storage guidelines

(generator is not operating):
Temperature: - 4°F to 158°F (-20°C to +70°C)
Altitude: 40,000 ft (12,190 m)
Air Particulates: Keep the equipment dry. Minimize exposure to moisture, dust, dirt, smoke and mold.
Humidity: 5% to 95% non-condensing @ 0°C to +30°C

Regulatory Agency Compliance

FCC

The generator complies with the following Federal Communications Commission regulations.

• The limits for FCC measurement procedure MP-5, “Methods of Measurement of Radio Noise Emissions from ISM Equipment”, pursuant to FCC Title 47 Part 18 for Ultrasonic Equipment.

CE Marking

This mark on your equipment certifies that it meets the requirements of the EU (European Union) concerning interference causing equipment regulations. CE stands for Conformité Europeéne (European Conformity). The equipment complies with the following CE requirements.

• The EMC Directive 2004/108/EC
for Heavy Industrial —
EN 61000-6-4: 2001
EN 55011: 2003

EN 61000-6-2: 2001
EN61000–4–2
EN61000–4–3
EN61000–4–4
EN61000–4–5
EN61000–4–6
EN61000–4–8
EN61000–4–11

- The Low Voltage Directive 2006/95/EC.
- The Machinery Directive 2006/42/EC.

EN 60204: 2006
Safety of Machinery - Electrical Equipment of Machines Part 1: General Requirements.

Generator Control: Installation Instructions and Program Description

Table of Contents

Introduction

Generator Control program enables the recording of ultrasonic amplitude, vibration frequency and power consumption as a function of time during the operation of Ultrasonic Generator.

The program works under Windows 7, Windows XP or Windows Vista operating systems. Screen resolution not lower than 1200x800 pixels is recommended. True Color display setting is also recommended.

The program must be installed and run "as administrator". In Windows XP or Vista, this can be done by using the Administrator account. In Windows 7, the installation should be performed by right-clicking on "setup.exe" (see next section) and selecting "run as administrator”. When using the program, right-click on the GeneratorControlS icon and select "run as administrator”.

To begin

1. Install “plug and play” drivers of usb/com – port

In order to install the drivers, connect the included USB cable to the Ultrasonic Generator port, plug it into your computer's USB port and follow instructions. If the drivers are not installed automatically, they can be installed manually (the drivers can be found in the CDM 2.06 directory on the installation disk). After this step is done, a virtual serial port (COM port) will be created. The number of this port can be determined by right-clicking on the "Computer" icon, going to Properties, bringing up Device Manager and opening the link for the port. For example, if after opening the link you see “USB Serial Port (COM3), the port number is 3.

2. Install Generator Control program

The program is installed by clicking on "setup.exe” in "Package" directory. This step should be done “as administrator”. For example, in Windows 7 the installation is performed by right-clicking on "setup.exe" and selecting "run as administrator".

3. Start the program

The program is started by clicking on the "Generator ControlS.exe" file in the directory into which the program was installed or on its corresponding icon. If you see a warning message, “Invalid Port Number”, ignore it. After the program opens, input the correct port number into the box: “Port #”.

The program starts in the “Monitor” screen. This screen contains an ultrasonic amplitude indicator as well as three windows with Initial settings:

Rec.time – desired time of recording,

Port # - number of the usb/com computer port connected to Ultrasonic Generator,

Cr. Amp - minimum allowed ultrasonic amplitude for a given technological process. If the amplitude for some reason drops below this value, the indicator’s color turns from GREEN to RED.

Monitor screen also displays Recording Time and Recording Start Time.

Monitor screen buttons and tabs: File, Start, Stop, Pause, Read/Write and Help

File tab has the following menu items: Open, Save, Print and Exit.

Open – open previously recorded and saved data;
Save – save recorded data. The data is saved in a database located in "Results" folder in the main program directory;
Print – print the recorded data;
Exit – exit the program.
NOTE: File menu items (except Exit) are disabled when the words "Standby Mode" are displayed. In order to enable the menu items, "Stop" button should be pressed.

Start button – puts Ultrasonic Generator and the program in standby mode.

When this button is pressed, the words "Standby Mode" appear on the Monitor screen. When the Start/Stop button located on the front panel of Ultrasonic Generator is pressed, Generator Control starts to record the operating parameter data. The initial working frequency of Ultrasonic Generator is set to the value, R, which can be displayed on the Read/Write screen (see below).
NOTE: Starting Ultrasonic Generator by pressing the Start/Stop button on its front panel erases all unsaved data.

Pause button – puts the program in standby mode and stops Ultrasonic Generator and data recording.

If Ultrasonic Generator is subsequently started using the Start/Stop button on its front panel, it starts to operate at the operating frequency that was current when Pause was pressed.
NOTE: Starting Ultrasonic Generator by pressing the Start/Stop button on its front panel erases all unsaved data.

Stop button – stops Ultrasonic Generator and data recording.

Data recording also stops when Ultrasonic Generator is stopped using the Start/Stop button at its front panel. The recorded data remains on the Graphs screen and is available for analysis and storing in the database.

Read/Write – opens a screen permitting to request and display the values of variables from Ultrasonic Generator's control circuit board and, if necessary, to change these values (see the list of variables below).

The values of variables from Ultrasonic Generator's control circuit board can be requested and displayed by pressing the "Read" button. Three of these variables (R – starting frequency, Gn – horn gain, Amin – starting amplitude) can be changed by users. In order to change any of these variables, the corresponding field on the right-hand side of the screen (highlighted GREEN) is filled with the desired value, the box next to the field is checked and the "Write" button is pressed. The new setting is then written into the corresponding register of Ultrasonic Generator.

NOTE: If a 3-digid number is to be written into the Amin field, the number should be preceded by 0. For example, if the desired number is 300, the number 0300 should be written. The program will be closed if this rule is not observed.

NOTE: Writing the staring frequency parameter, R, takes about 10 - 20 seconds after the Write button is pressed. If this value is read before 20 seconds have passed, the value may be displayed incorrectly.

Pressing the Default Settings button retrieves and displays "factory" preset parameters.

The rest of the variables (highlighted RED) stored in the Ultrasonic Generator's controller cannot not be changed by users. Only Industrial Sonomechanics' personnel or users specifically authorized by Industrial Sonomechanics' personnel in writing may carry out this operation.

Graphs – opens the plotter screen.

If the graphs are not displayed correctly, resizing the Graphs window should be performed. Placing the mouse cursor over a line on a graph and pressing the left mouse button brings up information on the Amplitude, Frequency or Power and Time corresponding to this point on the graph. The point is marked with a red line marker.

Help – opens this manual.

List of variables on the Read/Write screen:

R – starting resonance frequency of the system (20 – 23 kHz);
J – frequency shift with respect to that identified by automatic frequency tracking algorithm;
As – starting amplitude during frequency scanning;
Ts – time between frequency auto-correction cycles;
Ba – amplitude sensor signal vertical offset coefficient;
Ka – amplitude sensor signal slope coefficient;
Gn – ultrasonic horn gain factor (0.1-9.9);
dF – downward frequency shift at the start of resonance frequency search;
dSCAN3 – step size during short frequency scan;
nSCAN3 – number of steps during short frequency scan;
MBAddress – device network address;
Baud Rate – information transfer rate (4.8 – code 159; 9.6 – code 207; 19.2 – code 231);
Amin – starting value of amplitude (when system is on resonance) in arbitrary units (> 255);
Amax – maximum value of amplitude in arbitrary units (< 3392).

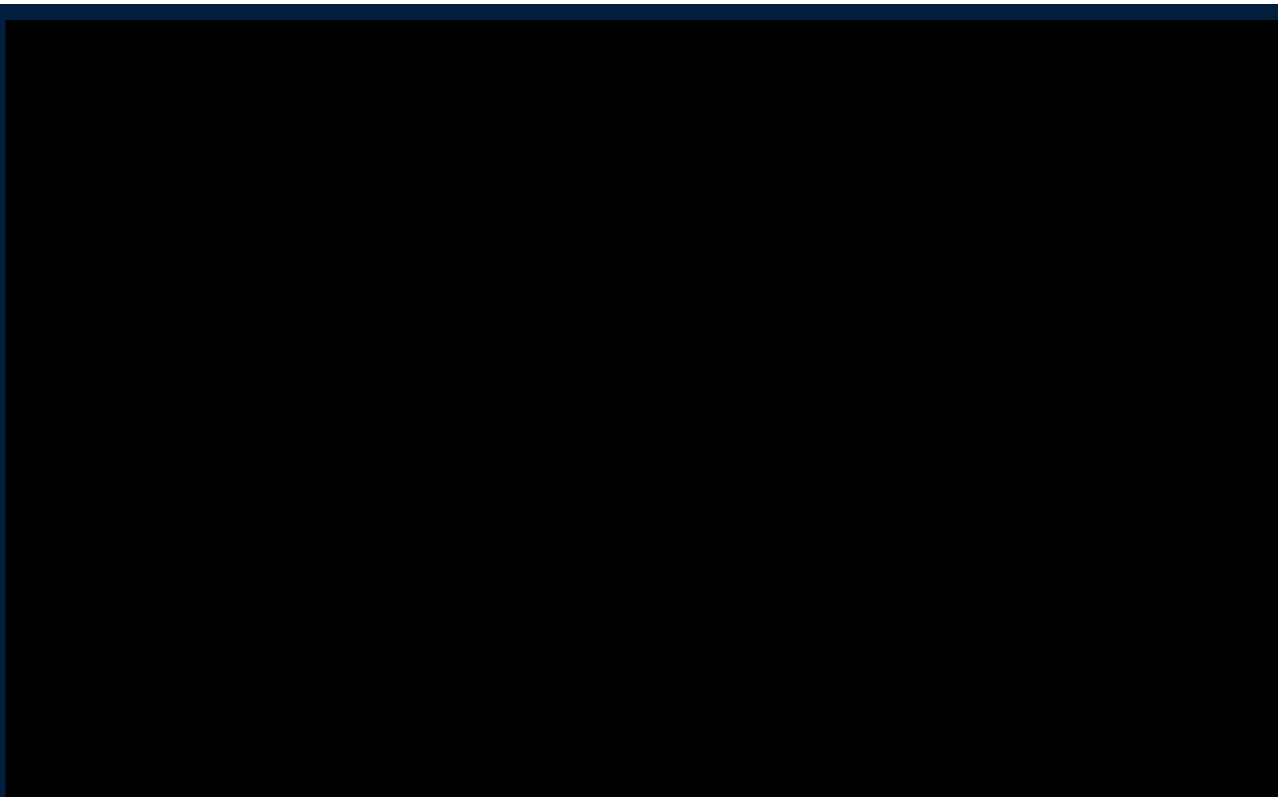

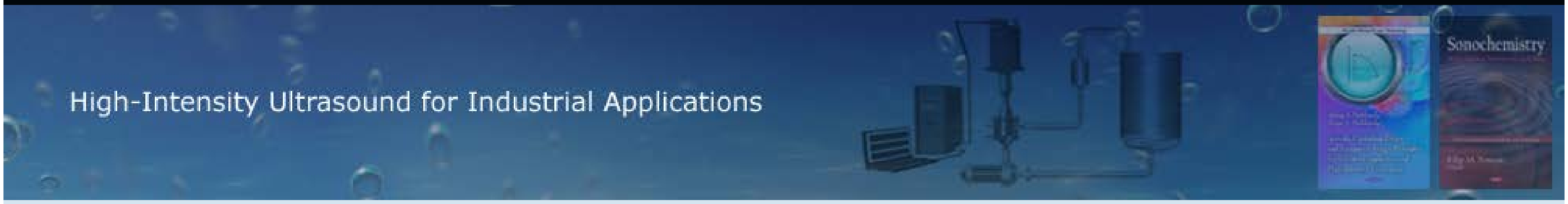

Home → Technical Resources → Videos

VIDEOS

Ultrasonic Dispersion of Carbon Black in Water, 750 ml Batch

This video shows ultrasonic dispersion of a small amount carbon black in a medium-size batch of water. The process was carried out with a 1.2 kW bench-scale ultrasonic reactor equipped with a Full-wave Barbell Horn (FBH), produced by Industrial Sonomechanics, LLC (ISM). The ultrasonic amplitude during the process was 100 microns. The process can be directly scaled up by using ISM's industrial ultrasonic processors at the same operating conditions. All ISM's ultrasonic reactors can be used in a flow-through mode in order to ensure continuous production. Unlike other ultrasonic systems, our processors are able to generate high amplitudes and extremely intense ultrasonic cavitation even when using large-diameter industrial-scale ultrasonic horns and flow-through reactor chambers.

Ultrasonic Degassing of Heavy Industrial Gear Oil

Degassing of high-viscosity oils by conventional methods can be challenging. Ultrasonic degassing is very useful in this case. Ultrasonic removal of air bubbles from heavy industrial gear oil is illustrated in this video. The experiment was conducted with Industrial Sonomechanics' 1200 W ultrasonic system.

Ultrasonic Removal of Air Bubbles from Epoxy Resin

When epoxy resin is mixed, air bubbles are inadvertently introduced and must be removed. Ultrasonic degassing technique can be very useful in this case, as shown in this video. Ultrasonic removal of air bubbles from premixed epoxy resin is illustrated in this video. The experiment was conducted with a 1200 W ultrasonic reactor system produced by Industrial Sonomechanics, LLC.

> Next Page

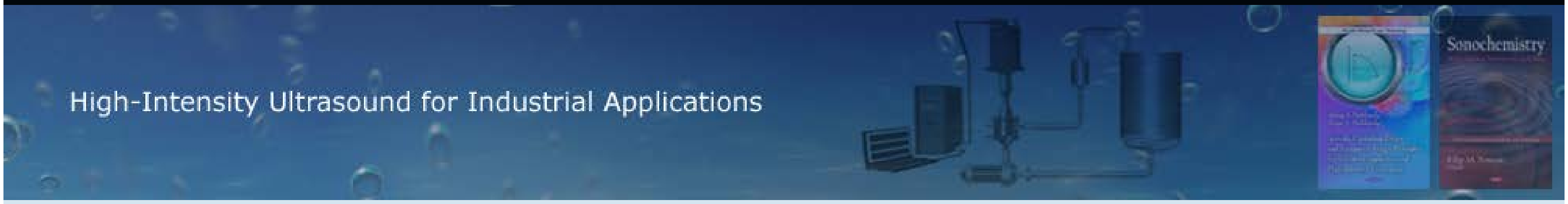

VIDEOS

Ultrasonic Dispersion of Carbon Black in Water, 10 Liter Batch

Ultrasonic dispersion of a small amount carbon black in a large batch of water is shown. The process was carried out with a 1200 W bench-scale ultrasonic reactor equipped with a Full-wave Barbell Horn (FBH), produced by Industrial Sonomechanics, LLC (ISM). The ultrasonic amplitude during the process was 100 microns. The process can be directly scaled up by using ISM's industrial ultrasonic processors at the same operating conditions. All ISM's ultrasonic reactors can be used in a flow-through mode in order to ensure continuous production. Unlike other ultrasonic systems, our processors are able to generate high amplitudes and extremely intense ultrasonic cavitation even when using large-diameter industrial-scale ultrasonic horns and flow-through reactor chambers.

Ultrasonic Cavitation in Water Produced by FBH, tip Ø = 35 mm

This video shows ultrasonic cavitation in water produced by a Barbell Horn (output diameter = 35 mm) operating at ultrasonic amplitudes of 25, 50, 75 and 100 microns. Unlike other types of ultrasound horns, Barbell Horns (US Patent # 7156201) are capable of providing high vibration amplitude gains and having large output tip diameters simultaneously, thereby allowing to directly transfer what can be accomplished in the laboratory to the plant floor. The video illustrates the operation of a 1200 W ultrasonic reactor system produced by Industrial Sonomechanics, LLC

Algae Oil Extraction Using High-Intensity Ultrasound

This video shows ultrasonic extraction of algae oil into water carried out using Industrial Sonomechanics' (ISM) Full-wave Barbell horn (output diameter = 65 mm, vibration amplitude = 100 microns). The experiment illustrates the operation of ISM's ultrasonic reactor system comprising: ultrasonic generator, magnetostrictive transducer, Full-wave Barbell horn, and flow-through reactor chamber.

Previous Page <